

UNCERTAINTY-OPTIMIZED PREDICTIVE TESTING

FOR A

NUCLEAR WASTE CONTAINER

by

ANDREW JOSEPH WOLFORD

B.N.E. Georgia Institute of Technology  
(1982)

B.A. Wittenberg University  
(1982)

SUBMITTED TO THE DEPARTMENT OF  
NUCLEAR ENGINEERING  
IN PARTIAL FULFILLMENT OF THE  
REQUIREMENTS FOR THE DEGREE OF

DOCTOR OF SCIENCE

at the

MASSACHUSETTS INSTITUTE OF TECHNOLOGY

January 1987

©Massachusetts Institute of Technology 1987

Signature of Author \_\_\_\_\_

Department of Nuclear Engineering  
January 21, 1987

Certified by \_\_\_\_\_

Dr. Norman C. Kasmussen, Thesis Supervisor  
McAfee Professor of Engineering

Certified by \_\_\_\_\_

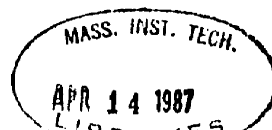
Dr. Ronald G. Ballinger, Thesis Supervisor  
Professor of Materials Science and Nuclear Engineering

Certified by \_\_\_\_\_

Dr. Ronald A. Christensen, Thesis Supervisor  
Research Affiliate and President, Entropy Ltd., Lincoln, MA

Accepted by \_\_\_\_\_

Dr. Allan F. Henry  
Chairman Departmental Graduate Committee



ARCHIVES

UNCERTAINTY-OPTIMIZED PREDICTIVE TESTING  
FOR A  
NUCLEAR WASTE CONTAINER

by  
ANDREW JOSEPH WOLFORD

Submitted to the Department of  
Nuclear Engineering on January 22, 1987  
in partial fulfillment for the degree of  
Doctor of Science In Nuclear Engineering

Abstract

Techniques of experiment design are developed specifically to address the large uncertainties accompanying 1000 year extrapolation of nuclear waste container penetration by general corrosion.

A methodology is developed which couples a parametric model of general corrosion, laboratory-obtained general corrosion data, and simulated, 'virtual' general corrosion data. Candidate experiments, represented by the simulated data, are investigated for their value in uncertainty reduction at extrapolated times. This methodology is automated in the form of a computer program named UNODEX, which evaluates each candidate experiment from the specified set. The program performs multiple sequential and cumulative evaluations of the candidate experiments to arrive at the optimized experiment design. The program also predicts the time-integrated penetration and uncertainty using predictions of the time-dependent waste container boundary conditions.

The UNODEX methodology is used to investigate waste container penetration and uncertainty as applied to the current salt repository design. Quantitative results are obtained which directly evaluate the role for accelerated life testing at expected conditions.

Thesis Supervisor: Dr. Norman C. Rasmussen

Title: McAfee Professor of Engineering

Thesis Supervisor: Dr Ronald G. Ballinger

Title: Professor of Materials Science and Nuclear Engineering

## Table of Contents

<b>ABSTRACT</b>	<b>2</b>
<b>DEDICATION</b>	<b>14</b>
<b>ACKNOWLEDGEMENTS</b>	<b>15</b>
<b>1. INTRODUCTION</b>	<b>18</b>
1.1 BACKGROUND	19
1.2 WASTE CONTAINER DEGRADATION MECHANISMS IN A SALT REPOSITORY	23
1.3 OUTLINE OF THE PRESENT WORK	24
<b>2. WASTE PACKAGE CONTAINER DEGRADATION MECHANISMS</b>	<b>26</b>
2.1 WASTE PACKAGE CONCEPTUAL DESIGN AND RATIONALE	26
2.2 A DESCRIPTION OF THE RECOMMENDED SALT REPOSITORY SITE	33
2.3 THE EXPECTED REPOSITORY ENVIRONMENT	36
2.3.1 Thermal Conditions	36
2.3.2 Water Availability at the Salt Repository Horizon	39
2.3.3 Stress Conditions	45
2.3.4 RADIATION ENVIRONMENT	51
2.4 WASTE CONTAINER DEGRADATION MECHANISMS	52
2.4.1 Macroscopic Mechanisms	53
2.4.1.1 General Corrosion	53
2.4.1.2 Pitting and Crevice Corrosion	62
2.4.2 Microscopic Mechanisms	66
2.4.2.1 Stress Corrosion Cracking	66
2.4.2.2 Hydrogen Embrittlement	70

2.5 SUMMARY	72
<b>3. DEVELOPMENT OF A METHODOLOGY TO SPECIFY UNCERTAINTY-OPTIMIZED EXPERIMENT DESIGNS</b>	<b>75</b>
3.1 TESTING REQUIREMENTS	75
3.1.1 Previous Work	76
3.1.1.1 Lifetime Distribution Approaches and Accelerated Life Testing	76
3.1.2 Summary	84
3.2 MAXIMUM LIKELIHOOD APPROACH TO UNCERTAINTY ESTIMATION	84
3.2.1 The Definition of Failure	85
3.2.2 Model Development as a Problem in Parameter Estimation	87
3.2.3 Extrapolation and Error Propagation	95
3.3 EXPERIMENT DESIGN: APPROACH	101
3.4 EXPERIMENT DESIGN: SIMULATION AND EVALUATION	106
3.4.1 Construction of the Experiment Sample Space	107
3.5 EXPERIMENT DESIGN: OPTIMIZATION	111
3.6 SUMMARY	113
<b>4. UNCERTAINTY-OPTIMIZED PREDICTIVE TESTING FOR A NUCLEAR WASTE CONTAINER</b>	<b>115</b>
4.1 THE EXPERIMENTAL DATA	115
4.1.1 Immersion General Corrosion Tests	116
4.1.2 Excess Salt Tests	120
4.1.2.1 Static Excess Salt Tests	121

4.1.2.2 Autoclave Static Excess Salt Tests	123
4.1.3 Assembly of the Database	124
4.2 DEVELOPMENT OF A MULTIVARIABLE MODEL FOR GENERAL CORROSION	130
4.2.1 Determination of the Principle Variables	131
4.2.1.1 Temperature	131
4.2.1.2 Dissolved Oxygen	134
4.2.1.3 Magnesium Concentration	134
4.2.1.4 Total Fraction of Water in the Test	136
4.2.1.5 Time	138
4.2.2 Comparison of Models Considered	140
4.2.3 Results of the Model	144
4.2.3.1 Specification of the In-Service Environment	144
4.2.3.2 Analysis of Waste Container Penetration and	148
Uncertainty	
4.3 DESIGN OF EXPERIMENTS FOR OPTIMAL UNCERTAINTY REDUCTION	158
4.3.1 Assignment of Uncertainty to the Virtual Data	158
4.3.1.1 Discussion of the Components of Uncertainty in	160
Predictive Modeling	
4.3.1.2 An Empirically-Consistent Model of Virtual Data	161
Error	
4.3.2 Specification of the Experiment Sample Space	164
4.3.3 Notation and Review of UNODEX	167
4.3.4 Validation of the Methodology	170

4.3.5 The Resequencing Frequency	175
4.3.6 Accelerated Life Testing and the First Point Uncertainty Reduction	177
4.3.7 Overall Trend in Uncertainty-Optimized Designs	185
4.3.7.1 Reference ESS	187
4.4 SUMMARY	191
<b>5. SUMMARY, CONCLUSIONS AND RECOMMENDATIONS FOR FUTURE STUDY</b>	<b>195</b>
5.1 INTRODUCTION	195
5.2 PURPOSE OF THE WORK	196
5.3 ASSESSMENT OF THE MODEL	198
5.4 ASSESSMENT OF THE EXPERIMENT DESIGN METHODOLOGY	199
5.5 ASSESSMENT OF THE RESULTS	203
5.6 CONCLUSIONS	207
5.7 RECOMMENDATIONS FOR FUTURE STUDY	207
<b>REFERENCES</b>	<b>209</b>
<b>A. List of Acronyms</b>	<b>218</b>
<b>B. Dataset Used for the Analysis of Waste Container General     Corrosion</b>	<b>220</b>
B.1 Description of the Data	221
B.2 File Listing	222
<b>C. THE UNODEX SYSTEM COMPUTER PROGRAM</b>	<b>227</b>
C.1 Users Documentation	228
C.1.1 Input to UNODEX	228

C.1.1.1 Sample Problem Input Deck	232
C.2 Program Source Listing	233
C.2.1 Annotated Sample Output from UNODEX	277

## List of Figures

<b>Figure 1-1:</b>	Location of the Deaf Smith County, Texas Potential Repository Site	21
<b>Figure 2-1:</b>	Schematic Cross Section of the Waste Package	27
<b>Figure 2-2:</b>	Conceptual Waste Package Design	29
<b>Figure 2-3:</b>	Stratigraphy of the Palo Duro Basin	35
<b>Figure 2-4:</b>	Thermal History of the Salt-Container Interface for the CSF(12PWR) Waste Package Design	38
<b>Figure 2-5:</b>	Midplane Container Boundary Stress	48
<b>Figure 2-6:</b>	Idealized Anodic Polarization Curve	57
<b>Figure 2-7:</b>	Composition Profile of Amakinite Layer	61
<b>Figure 2-8:</b>	Anodic Polarization Behavior of A216 Steel in Magnesium Solutions	69
<b>Figure 2-9:</b>	Potential-pH Diagram for Iron Including Cracking Regimes (After Ford [23])	71
<b>Figure 3-1:</b>	Test Requirements for Waste Containers Based on a Weibull Failure Model (after Thomas [54])	82
<b>Figure 3-2:</b>	Logic Diagram for Model Development	102
<b>Figure 3-3:</b>	Flowchart for Uncertainty-Optimized Experiment Design	108
<b>Figure 4-1:</b>	Schematic Diagram of the Autoclave Immersion General Corrosion Test System	118
<b>Figure 4-2:</b>	Schematic Diagram of the Static Excess Salt Test	122



System

<b>Figure 4-3:</b>	Schematic Diagram of the Autoclave Excess Salt Test System	125
<b>Figure 4-4:</b>	Temperature Dependence of the Corrosion Rate	133
<b>Figure 4-5:</b>	Dissolved Oxygen Dependence of the Corrosion Rate	135
<b>Figure 4-6:</b>	Corrosion Rate Dependence on Magnesium Concentration from [26]	137
<b>Figure 4-7:</b>	Water Content Dependence of the Corrosion Rate from [26]	139
<b>Figure 4-8:</b>	Uniform Penetration Time Dependence from [26]	141
<b>Figure 4-9:</b>	General Corrosion Container Penetration Reference in-service boundary conditions: Temperature profile as given in Table 4-5, O:0.05 ppm, Mg:0.05 w/o, W:0.05 w/f	149
<b>Figure 4-10:</b>	General Corrosion Container Penetration and Uncertainty Reference in-service boundary conditions: Temperature profile as given in Table 4-5, O:0.05 ppm, Mg:0.05 w/o, W:0.05 w/f	152
<b>Figure 4-11:</b>	General Corrosion Penetration and Uncertainty for Low Magnesium Brine Reference in-service boundary conditions: Temperature profile as given in Table 4-5, O:0.05 ppm, Mg:0.05 w/o, W:0.005 w/f	154
<b>Figure 4-12:</b>	General Corrosion Penetration and Uncertainty	156

Incorporating Brine Availability Cutoff at 200 Years Reference in-service boundary conditions: Temperature profile as given in Table 4-5, O:0.05 ppm, Mg:0.05 w/o, W:0.05 w/f up to 200 years

- Figure 4-13:** General Corrosion Penetration and Uncertainty for 159  
Commercial High Level Waste Temperature Profile  
Reference in-service boundary conditions:  
Temperature profile as given in Table 4-7, O:0.05  
ppm, Mg:0.05 w/o, W:0.05 w/f
- Figure 4-14:** Illustration of the Data Handling Steps in the 171  
UNODX Methodology
- Figure 4-15:** Uncertainty Reduction for the Validation Exercise 174  
ESS
- Figure 4-16:** Uncertainty Reduction for the Case of no 176  
Resequencing
- Figure 4-17:** Uncertainty Reduction with Resequencing at Points 178  
1, 2, 10, 125
- Figure 4-18:** Results of Uncertainty Reduction for the 180  
Reference ESS
- Figure 4-19:** First Point Uncertainty Reduction vs. Test 183  
Duration
- Figure 4-20:** Uncertainty Reduction Dependence on Test 184  
Temperature for Multivariable-Accelerated  
Experiments

<b>Figure 4-21:</b>	Uncertainty Reduction Dependence on Test Duration	186
	for Thermally-Accelerated Experiments	
<b>Figure 5-1:</b>	Response of First Point Uncertainty Reduction	206

## List of Tables

<b>Table 2-1:</b>	Reference Features of the CSF(12PWR) Waste Package	30
<b>Table 2-2:</b>	Container Material Composition and Mechanical Specifications	32
<b>Table 2-3:</b>	Ionic Compositions of Fluid Inclusion Brines in Halite (all concentrations in ppm)	44
<b>Table 3-1:</b>	Notation Used in Chapter 3	89
<b>Table 3-2:</b>	The Arrhenius and Eyring Rate Law Models	104
<b>Table 4-1:</b>	Test Conditions Summary for Data Generated by Immersion General Corrosion Tests	127
<b>Table 4-2:</b>	Test Conditions Summary for Data Generated by Static Excess Salt Corrosion Tests	128
<b>Table 4-3:</b>	Test Conditions Summary for Data Generated by Autoclave Excess Salt Corrosion Tests	129
<b>Table 4-4:</b>	Corrosion Rate Models Considered	143
<b>Table 4-5:</b>	Assumed In-Service Environmental Independent Variables	145
<b>Table 4-6:</b>	Maximum Likelihood Parameter Estimates for the Corrosion Rate Model	147
<b>Table 4-7:</b>	Container Boundary Temperatures for the Commercial High Level Waste Loading, 9.5 kW	157
<b>Table 4-8:</b>	Convergence Steps in Obtaining the Empirically-Consistent Model of Virtual Data Error	165

<b>Table 4-9:</b>	<b>Limiting Values for the Experiment Sample Space</b>	<b>168</b>
<b>Table 4-10:</b>	<b>Uncertainty-Optimized Design for the Validation Exercise</b>	<b>173</b>
<b>Table 4-11:</b>	<b>Tabulation of Uncertainty Reduction for the Reference ESS</b>	<b>181</b>
<b>Table 4-12:</b>	<b>The Uncertainty-Optimized Experiment Design for the Reference ESS</b>	<b>188</b>
<b>Table 4-13:</b>	<b>Oscillatory Nature of the Overall Trend in Uncertainty-Optimized Designs</b>	<b>192</b>

## DEDICATION

This doctoral dissertation, the culmination and apex of nine and a half years of formal education, is dedicated with love to my dear wife and supporter,

*Linda*

She was the one, for all those years, that saw my dreams along with me and worked as hard as I did to achieve them. Her courage, faith and strength have sustained our family through the difficult times of trial and her laughter and love have been my deepest joy. Without her encouragement this thesis would never have become a reality.

## ACKNOWLEDGEMENTS

Funding for this work was provided by subcontract E512-12000, between the Battelle Memorial Institute, acting through its Project Management Division, a prime contractor to the United States Department of Energy for its Civilian Radioactive Waste Management Program, Contract DE-AC02-83-CH10140, and the Massachusetts Institute of Technology. Much of this work was performed in residence at the Battelle Memorial Institute, hence the author is indebted to many people at both MIT and Battelle.

First, I wish to express my deepest gratitude to my co-advisors, Professor Norm Rasmussen and Professor Ron Ballinger. The combination of their unique talents provided the type of interdisciplinary advice invaluable to this type of research. Even more importantly, I am grateful to them for the confidence, encouragement and trust necessary to advise a student remotely.

This work would not have been possible without the dedicated help, expertise and computational resources of Ron Christensen and the staff of Entropy Limited. A very special acknowledgement, however, is due Ron, who became an inspiration, a co-worker, a friend and, in every sense of the word, a thesis supervisor to me in the pursuit of this research, thanks Ron!

I am very grateful for the many experiences at MIT, but in particular,

my close work with Professor Mike Driscoll and Professor Lawrence Lidsky will remain with me forever.

I express my deep thanks to John Haberman at Battelle Northwest Laboratories for furnishing some of the as yet unpublished corrosion data.

The perseverance of John Kircher, Dave Waite, Ralph Henricks and Charlie Nunn is gratefully acknowledged, for breaking new ground in bringing a graduate student into residence and dealing with all the unique financial and administrative aspects of my presence at Battelle. As well, I wish to thank my financial and administrative 'liaisons' at MIT, Bill Fitzgerald and Clare Egan, who many times represented my best interests relative to the MIT Bursar's Office, Payroll, Office of Sponsored Programs, Registrar's Office and Medical Departments.

Thanks to my office-mate, Bob Wilems, of Rogers and Associates Engineering Corporation, who as an employer taught me to appreciate the management of research, and as a friend encouraged my career goals.

Special thanks are due to my friends and colleagues at MIT and Battelle: Joe Borzekowski, Bruce Ching, Tom Downar, Ray Gamino, Bill Harper, Steve Maheras, Mike Manahan, Dave Petti, Arn Plummer, Ed Russell, Ralph Thomas and Bob Zellmer. I reserve warmest thanks for my special friend, Vesna Dimitrijevic.



As a son, I wish to express my warmest appreciation to my father, who instilled in me the courage to challenge myself and the love of learning. As a father, I wish to thank my young son Nathan, for giving me a reason to enjoy being an example.

And to my *entire* family: Mom, Dad, Barb, Grandpa and Grandma Gano, Marilyn, Frank, Kathy, Barbara, Marsha, Kate, Sharon, Frank, Mary, Marilyn and Tom, thank-you for understanding all the missed gatherings, nonexistent letters and phone calls and excuses in the name of graduate work.

My sincere gratitude goes to Frank Kruger and Barbara Lewis of the Systems Analysis Department, Brenda Napper of Text Processing and Mark Badillo of technical illustration for the typing and preparation of this manuscript.

---

Finally, I offer my ultimate thanks to GOD ALMIGHTY, who provided the only unfailing inspiration for this work, and will continue to do so for the innumerable researchers who follow me.

## 1. INTRODUCTION

"He that will not apply new remedies must expect new evils;  
for time is a great innovator"

- Sir Francis Bacon  
Essays II "Of Innovation"

The methodology presented herein for generating "uncertainty-optimized" experiment designs is motivated by and developed in the context of predicting nuclear waste container penetration by aqueous corrosion at long time extrapolations from sparse data. While this application is specific, the methodology is not, and it is anticipated to be a most useful approach to experiment design whenever knowledge in the form of a physical process model and relevant data are available to the experimental planner faced with significant extrapolation in time.

Uncertainty-optimized will be defined here to mean that the product experimental design, if performed, is expected to generate data which will have the most effective and greatest reduction in uncertainty at some desired extrapolated time value such as the design life of a long-lived component. The methodology developed herein is not a new approach to the formal, statistical design of experiments, but rather is a straightforward, nonclassical approach fundamentally rooted in the principles of decision analysis.

The product of this work, then, is a formal methodology which may be used by an experimental planner to design an "uncertainty-optimized" test matrix.

## 1.1 BACKGROUND

The Nuclear Waste Policy Act of 1982 [57] charges the U. S. Department of Energy with the responsibility of administering the nation's effort for ultimate disposal of High-Level radioactive Waste (HLW) in mined geologic repositories. The primary objective of this national program is to isolate existing and future high-level radioactive waste, generated by defense and commercial endeavors from the human environment. To meet this objective, the U. S. Department of Energy is conducting an extensive program to select three sites for the potential construction of a mined geologic repository, and to develop a facility design which will meet all relevant radiological protection requirements for public health and safety at each of these sites. Ultimately, the goal is to select the superior site from these three candidates.

The philosophy of geologic high-level waste isolation is based on (1) provision of an early radionuclide containment period by the various engineered barriers surrounding the waste, and, after release, (2) reliance on a very long radionuclide transport time to the biosphere by careful selection of a site which has very low groundwater flow rates.

Salt was first suggested as a suitable rock type for waste isolation

in 1957 by the National Academy of Sciences [42]. After more than 30 years site nomination activities of the U. S. Department of Energy [55] have recommended one salt (of three potential) site in Deaf Smith County, Texas. This location is in the panhandle of the state, in a geologic formation called the Permian Basin. This potential site is shown in Figure 1-1.

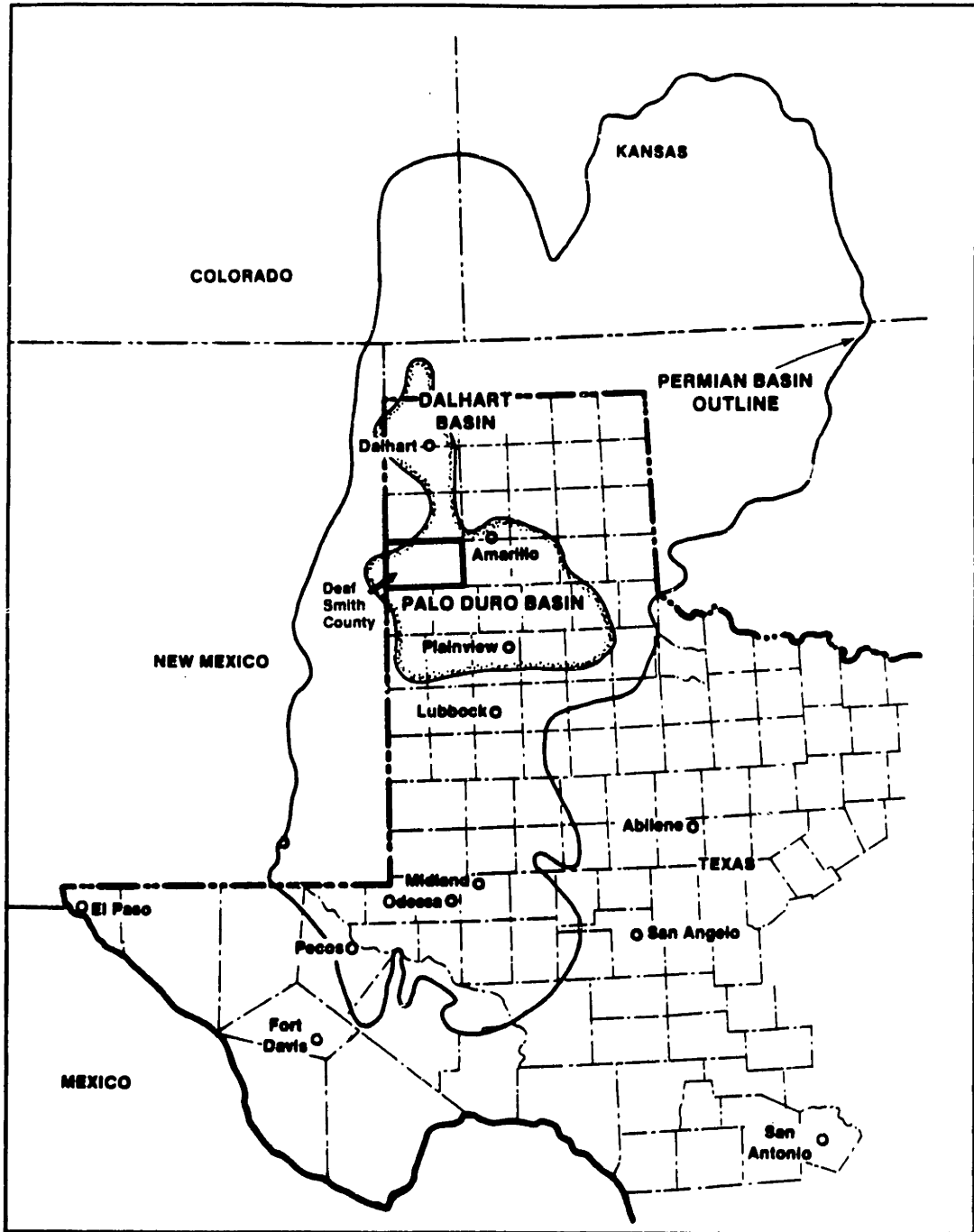
High-level waste will be disposed of by enclosing spent nuclear reactor fuel (or vitrified liquid defense wastes) in a handling canister, which will in turn be sealed within a thick-walled disposal container\*. The disposal container is the outermost sealed metallic vessel which encloses the waste.

Specific federal regulations [59, 58] and design requirements deriving from the Nuclear Waste Policy Act of 1982 [57] have indicated that the waste package is to provide the early radionuclide containment period of 300 to 1000 years. The current salt repository waste package conceptual design relies on a thick-walled consumable disposal container the function of which is to delay corrosion driven failure of the waste package. While designs may be made robust to the uncertainty in corrosion rates by increasing wall thickness, predictions of penetration at 1000 years validated by experimental measurements made over from 1 to

---

\*An equivalent yet obsolete term which has been used in earlier work to refer to this barrier is the "overpack".

Figure 1-1: Location of the Deaf Smith County, Texas Potential Repository Site



5 years will continue to be dominated by the uncertainty in the estimates at those long time extrapolations.

Recognizing the unique difficulties associated with validating performance predictions over time spans of a thousand years or greater, the U. S. Nuclear Regulatory Commission has adopted a qualitative "reasonable assurance" approach to waste isolation compliance, and committed to the use of data generated by accelerated testing:

For such long-term objectives and criteria, what is required is reasonable assurance, making allowance for the time period, hazards, and uncertainties involved....Demonstration of compliance with such objectives and criteria will involve the use of data from accelerated tests and predictive models that are supported by such measures as field and laboratory tests, monitoring data and natural analog studies [59].

There is much room for general improvement in the field of accelerated testing [7], and reliance on data of this type is likely to introduce new and significant sources of uncertainty in performance assessments. It would be useful at this time to develop the means of quantitatively estimating the "value" of data generated by means of at-condition and accelerated laboratory and *in situ* measurements, *a priori*, in terms of the reduction in estimate uncertainty at the (extrapolated) design life. This is the goal of the following work.

## 1.2 WASTE CONTAINER DEGRADATION MECHANISMS IN A SALT REPOSITORY

In any experimental investigation of mechanisms of degradation and/or failure, stated or not, there will be some mechanism which is expected to dominate the degradation process over all the others. Usually, the current understanding of the physical processes which drive this dominant mechanism has played a role in the design of the experiment. Generally, however, the role is often subtle, and not formalized enough so as to have become an experimental "strategy".

One goal of this work is to formalize a quantitative evaluation of potential experiments which will most effectively reduce the uncertainty in waste container life prediction. As a necessary first step toward that end, the relevant literature is surveyed to assess the plausible degradation mechanisms which could ultimately lead to a breach of the waste container in service. It is concluded, for the present application (that is, the current waste container design and the present understanding of the repository environment and its projected behavior), the mechanism of general corrosion is the most certain to prevail over the bulk of the package surface. Localized mechanisms such as pitting will likely not be severe, as the steels under investigation do not appear to support localized attack to any penetrations significantly greater than that due to general attack. Although investigators [61] have attempted to induce the mechanism of stress corrosion cracking in simulated repository environments and similar alloy-environment-stress

systems, no evidence of the phenomena has been observed. For this reason, the SCC mechanism has been eliminated from this thesis. And finally, with the weakest of substantiation, the hydrogen assisted failure mechanisms are also excluded from modeling considerations, pending further understanding and specification of the container weldment.

### 1.3 OUTLINE OF THE PRESENT WORK

By way of organization, the following structure serves to present this thesis. Chapter one is a general introduction to the problem, the simplified strategy of geologic nuclear waste disposal, the motivations which lead to containing the waste in a thick low carbon steel vessels and the uniqueness of making predictions in time, or forecasting, the container behavior and eventual demise.

Chapter two attempts to present a coherent description of the environment which is expected to challenge container integrity, once in service, and a thorough review of the literature for the relevant degradation mechanisms for present container designs.

Chapter three is the methods development section. In this chapter, the hypothesis, logic and approach of the formal methodology for the adaptive experiment design process is described.

Chapter four is the results section of the work, wherein the tools and



techniques are applied to the container life problem. Various assumptions are made and the resulting trends in experiment optimality, and "information value" are presented.

Chapter five, as in any thesis, is the overall summary of the work. As well this chapter contains all the authors own self criticism and hints for future readers. As well, there are several appendices of back matter not suitable, in one way or another, for the running text. These include a computer program listing and documentation, sample input and output and data employed in the studies of chapter four.

## 2. WASTE PACKAGE CONTAINER DEGRADATION MECHANISMS

### 2.1 WASTE PACKAGE CONCEPTUAL DESIGN AND RATIONALE

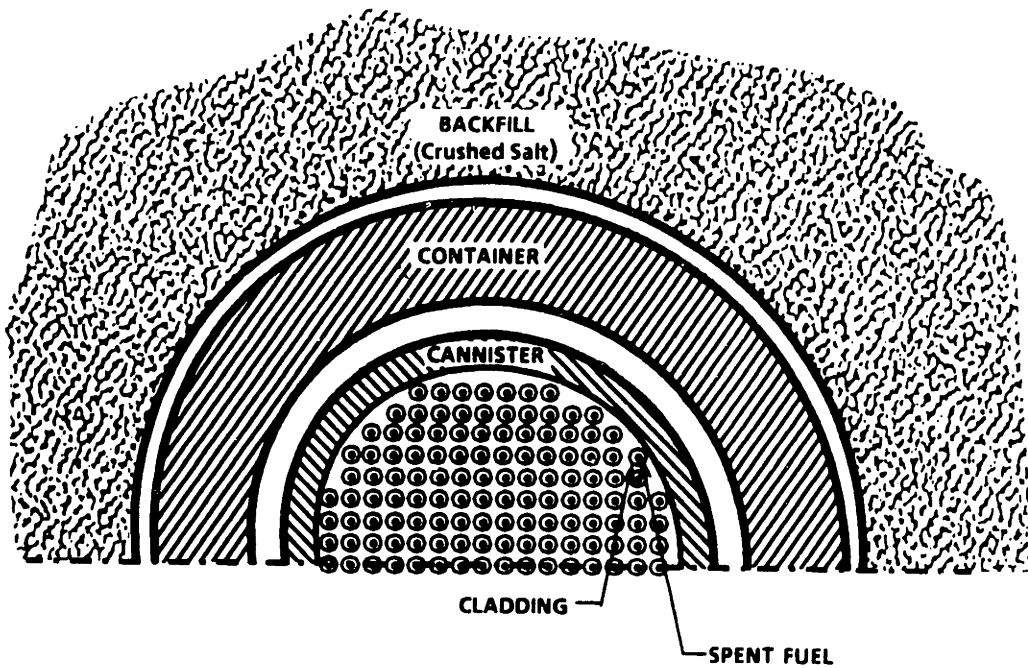
The reference waste package conceptual designs for a repository in salt are described in some detail in the Westinghouse report [63]. The basic features of the waste package design adopted here are repeated for completeness.

Current High-Level-Waste (HLW) isolation concepts in geologic media rely on (1) an early containment period sometimes called the thermal period, followed by a much longer period of rate-limited release to be provided by the engineered barrier system, and (2) a very long transport time (10,000 years) to the biosphere to be provided by the host rock media.

The major components of the engineered barrier system are the waste form, canister, container and backfill--which make up the waste package--and the excavated and structural systems of the underground facility and the materials used to seal them. The waste package is shown conceptually in cross section in Figure 2-1.

In the salt repository, there are no plans for a special backfill material different from the excavated salt, due to its low permeability. The container is therefore assigned a high level of responsibility for containment in the early thermal phase after permanent closure. This

Figure 2-1: Schematic Cross Section of the Waste Package



key allocation of performance to the container serves as a limit on the scope of this work and all efforts will be aimed at projections of container degradation.

Container designs differ slightly in dimension in order to accommodate the different waste form types. As the projected repository inventory fractions of commercial high level waste (CHLW), defense high level waste (DHLW), intact spent fuel (ISF) and consolidated spent fuel (CSF), continue to evolve in time, particularly increasing the anticipated CSF fraction, the CSF container with 12 Pressurized Water Reactor (PWR) assemblies as inventory is adopted for this work.

The disposal container is the outermost sealed metallic vessel the function of which is to delay corrosion-driven failure of the waste package. A conceptual waste package design is illustrated in Figure 2-2. This figure depicts a horizontally-emplaced disposal container which encloses the waste form and handling canister. An emplacement plug is shown sealing the borehole. Table 2-1 accompanies the design and presents the reference features of the CSF (12 PWR) package. Salt repository waste package designs to date have advocated a corrosion allowance concept. The basis of this concept is that in geologic formations the rate of dissolution of relatively low corrosion resistant (active) metals is limited by the oxygen reduction reaction. If this is indeed the case, adequate wall thickness may be incorporated in the

Figure 2-2: Conceptual Waste Package Design

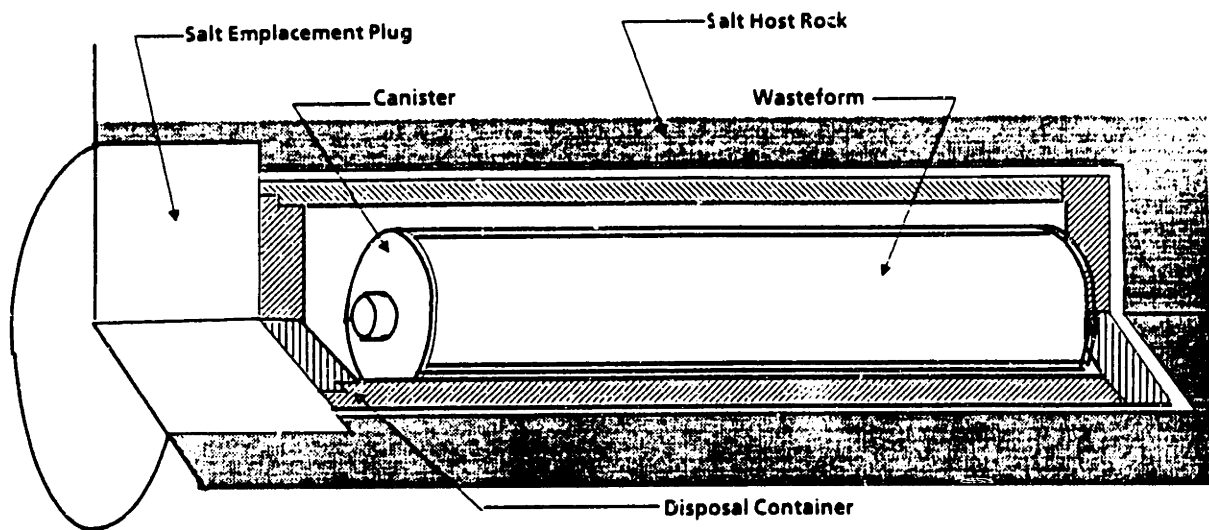


**Table 2-1: Reference Features of the CSF(12PWR) Waste Package**

---

---

Package Thermal Loading	6,600 kW
Package Inventory	5,532 kgU
Repository Areal Heat Loading	14.83 kW/Acre
Waste Form Diameter	62.0 cm
Waste Form Length	400.0 cm
Waste Form Weight	8,390 kg
Container Outside Diameter	84.5 cm
Container Wall Thickness	10.0 cm
Container Head Thickness	18.3 cm
Container Weight	9,250 kg
Total Package Weight	17,640 kg

---

---

disposal canister design. Specifically, a castable, fusion-weldable low-carbon steel, which is a slight modification of ASTM A216 grade WCA specification has been specified by the salt repository project [63, 61]. Table 2-2 presents composition and mechanical specifications for the A216 alloy and the recommended disposal container alloy [63]. The modifications reduce the carbon content and eliminate the normalizing heat treatment in an attempt to reduce the formation of martensite and hence vulnerability to hydrogen embrittlement and stress corrosion cracking in any weld heat affected zones.

It is intended, by choosing such a simple alloy for the primary metal barrier material that the alloy will preferentially degrade by the mechanism of general or uniform corrosion, with measurably lower tendency for localized and microscopic mechanisms of perforation such as pitting and environmentally assisted cracking, respectively. This is an assumption which must be supported by further experimental investigation, however.

Other selection criteria which have been considered in the choice of low strength low carbon steel for the container material are:

- **Strength Considerations.** The minimum yield strength for A216 steel is specified at 206 MPa. The ultimate tensile strength is roughly twice this. Maximum predicted stress at the Deaf Smith site is 17.9 MPa [55].
- **Suitability.** The data base on low carbon steels is the greatest of all iron alloys, perhaps greater than 100 years.

**Table 2-2: Container Material Composition and Mechanical Specifications**

	<u>Overpack Material</u>	<u>ASTM A 216 Grade WCA</u>
<b>Elements, %</b>		
Carbon, range	0.15 - 0.20 <sup>(1)</sup>	0.25 (max)
Manganese, range	0.90 <sup>(1)</sup> (max)	0.70 (max)
Silicon, max	0.30	0.60
Sulfur, max	0.65	0.045
Phosphorus, max	0.045	0.04
<b>Residual Elements</b>		
Copper, max	(1)	0.50
Nickel, max	(1)	0.50
Chromium, max	(1)	0.04
Molybdenum, max	(1)	0.25
Vanadium, max	(1)	0.03
Total of these residual elements, max	(1)	1.00
<b>Physicals</b>		
Ultimate Strength, MPa	415-585	415-585
Yield Point, MPa	205	205
Elongation in 2 in., %	22	24
Reduction of Area, %	30	35

(1) The total of these elements shall satisfy the following:

$$0.40 = C + \frac{Mn}{6} + \frac{Cr + Mo + V}{5} + \frac{Ni + Cu}{15}$$



**Table 2-2: Container Material Composition and Mechanical Specifications**

Although not directly relevant to the application of waste containers in brine environments, familiarity with this alloy and an available expertise helps to eliminate some of the more fundamental research required to rule out esoteric failure mechanisms.

- **Fabricability.** The alloy specification was developed as an easily castable, fusion-weldable material. This material should present a minimum of difficulty on both the thick-walled casting and remote closure welding operations.
- **Ductility.** Although not a primary attribute for fabrication, the selected material possesses sufficient ability to plastically deform so as to make it attractive in the event of a handling accident.
- **Availability.** Large production quantities of the alloy with significant quality control will be required. This should create no problem with the A216 alloy.
- **Strategic Materials.** In compliance with the siting guidelines [58], construction of the repository should not create any incentive for the future recovery of any material or resource employed and within it.
- **Cost Effectiveness.** As carbon steel is a very low cost alloy, the cost of the required material resources and fabrication are quite low. Given that the container is a thick-walled vessel, a large amount of raw material is required. Tradeoffs between a corrosion resistant alloy-clad reduced-thickness steel container were performed [63, 62].

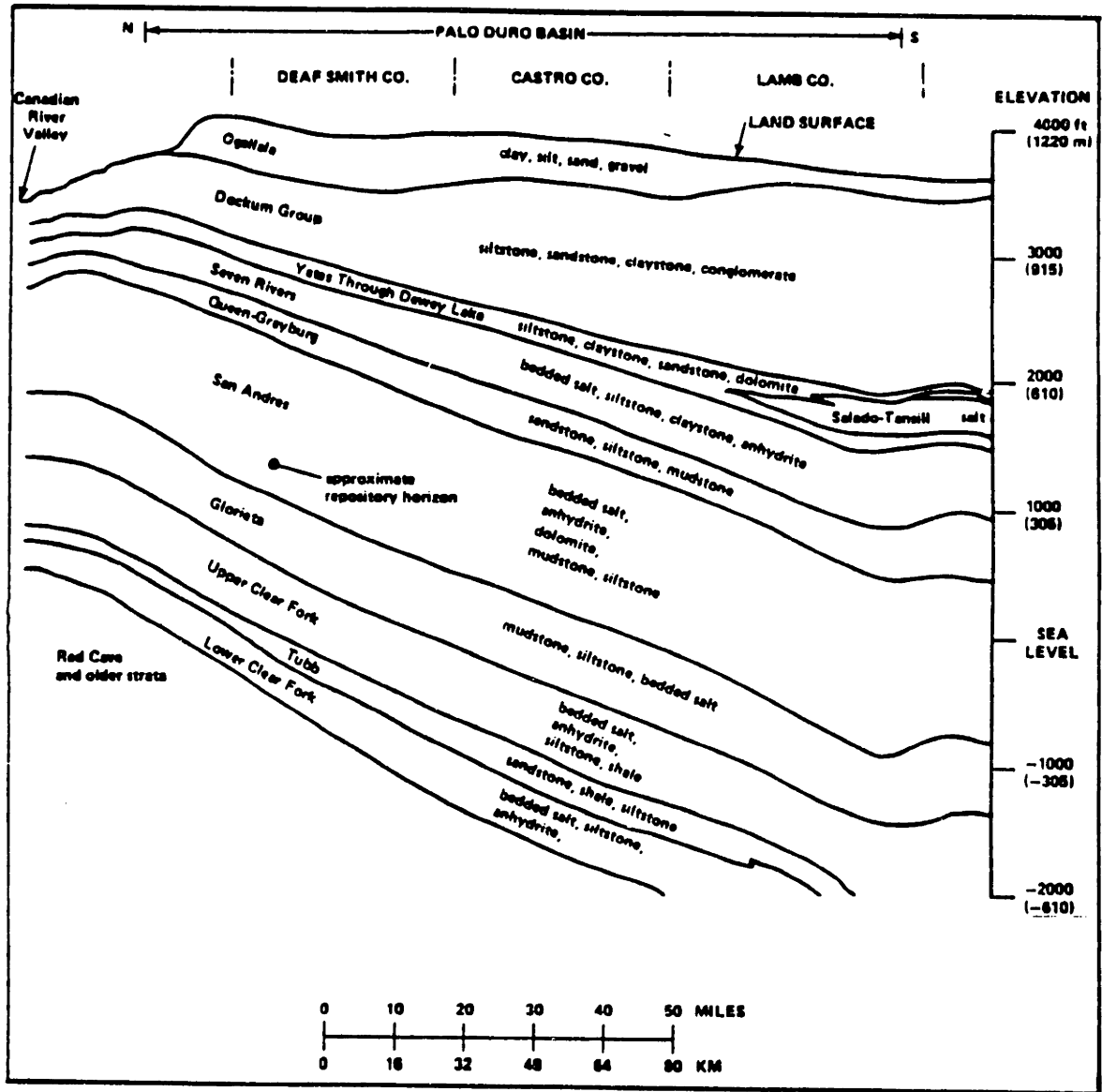
## 2.2 A DESCRIPTION OF THE RECOMMENDED SALT REPOSITORY SITE

The U. S. DOE has nominated the Deaf Smith County, Texas, bedded salt site for further characterization as a potential high level nuclear waste repository [55]. Figure 1-1 presents the geographic location. As indicated in the figure, the site is located in the Palo Duro Basin, a subunit of the larger Permian Basin. The repository host rock is a

thick layer (approximately 50 meters) of bedded salt within the Lower San Andreas Formation ranging from 700 to 760 meters depth from grade. This depth is referred to as the repository horizon. The Lower San Andreas Formation is subdivided into four layers called Units, and the repository horizon is located in Unit 4. The halite formations throughout the Palo Duro Basin are not pure bedded rock salt, but contain many impurities and interbeds. Hovorka et. al. [29], in compiling core data from 3 test wells near the Deaf Smith Site finds roughly 87 volume percent Halite, 4 percent anhydrite and 9 percent mudstone. In the 50.4 meter thickness of Unit 4, 86 distinct anhydrite beds were observed and more than 100 separate mudstone beds. The San Andreas is overlain by alternating sequences of sedimentary rocks and evaporites consisting primarily of sandstone, limestone, dolomite, shale and anhydrite as indicated in Figure 2-3.

There are three distinct hydrologic units of interest relative to the Deaf Smith Site. The uppermost unit is an unconfined aquifer which is in hydraulic communication with surface water. It is often called the High Plains aquifer, and is composed of the Ogallala aquifer and the Dockum groups. It is very extensive and underlies much of Texas and New Mexico. The repository horizon lies near the mid-depth of the middle unit, which is a large aquitard of some 800 meters in thickness. The deep unit is a brine aquifer composed of much older, fragmented rock.

Figure 2-3: Stratigraphy of the Palo Duro Basin



## 2.3 THE EXPECTED REPOSITORY ENVIRONMENT

### 2.3.1 Thermal Conditions

Reference repository conditions have been estimated and compiled by various authors both integral to and independent from the DOE program. The Reference Repository Conditions Interface Working Group [48] (RRC-IWG) have predicted a peak canister surface temperature occurring for a CHLW (25 kW/Acre, 2.16 kW/Package) salt repository of 260°C at 5 years after emplacement. For spent fuel (25 kW/Acre, 0.55 kW/Package) the thermal peak is 160°C at 50 years.

Workers at Brookhaven National Laboratory [50], under contract to the NRC have reviewed the near-field thermal environment. For an equivalent CHLW package design to that employed by the RRC-IWG they cite 264°C as the maximum expected canister surface temperature attained at 3 years post-emplacement.

Cunnane [13] has compiled available information for important factors in the waste package near field environment. Citing the work of McNulty [40], Cunnane indicates for a bedded salt formation the maximum salt-container interface temperature will be between 220°C and 230°C, at approximately 5 years after emplacement. The same analysis for the worst-case salt dome predicts the maximum interface temperature is just under 300°C. It is concluded in this work that the higher dome ambient temperature is the cause of greater peak surface temperatures.

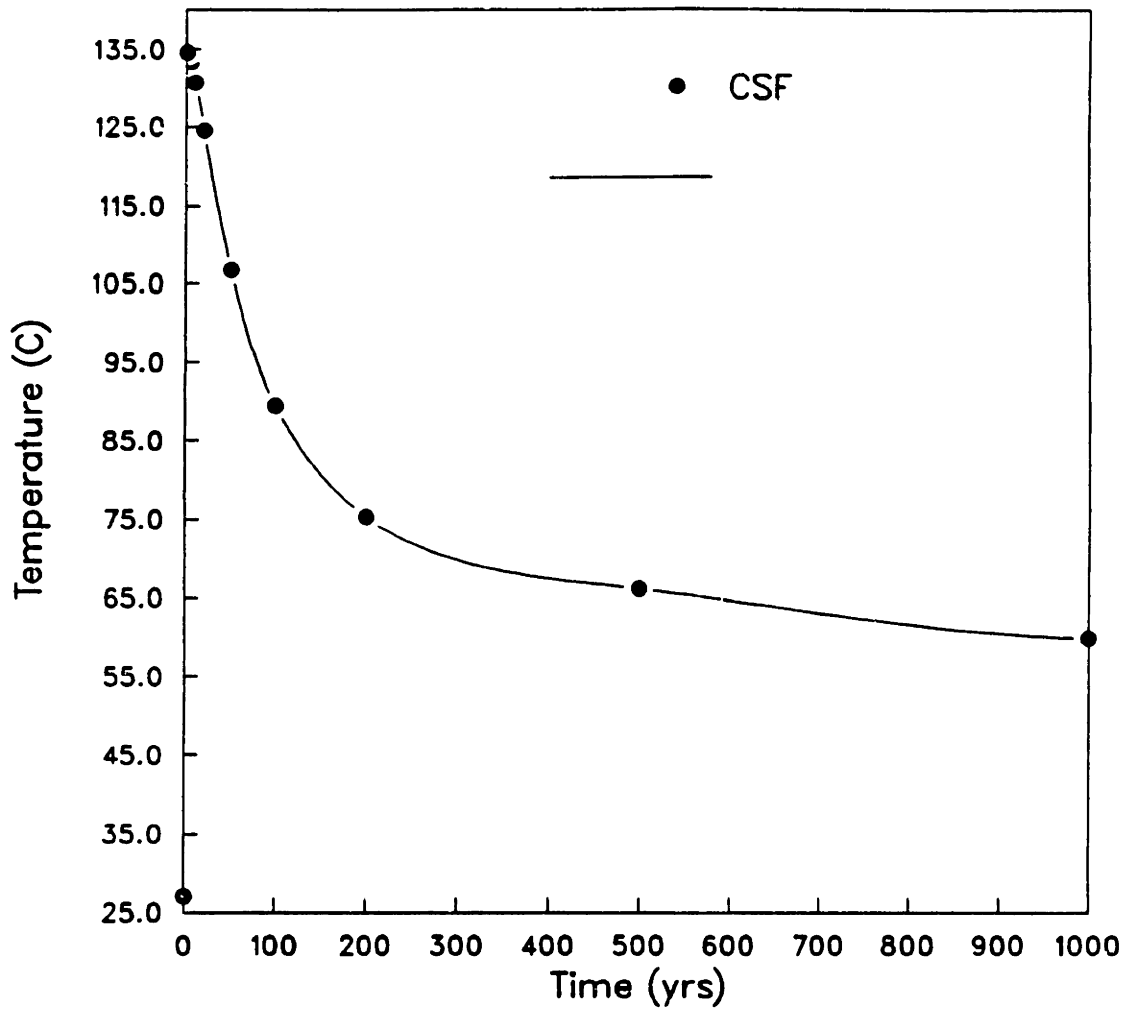
The above, predicted thermal conditions are in good agreement with one another. However, salt thermal conductivity values derive primarily from a single database which was established from a limited number of core samples taken from the Lower San Andreas halite formation. As well, the models used to make the above predictions are fairly simplistic treating the salt media surrounding the waste package as homogeneous and assuming axisymmetric heat transfer. McNulty [40] models the repository as an infinite array of heat sources while the others employ a unit cell approach. This modification tends to increase the interface temperature, however, it is offset by McNulty's use of a correction factor of 1.4 in scaling the laboratory-measured thermal conductivity to reflect realistic in-field values\*.

The above analyses employ a 10 year old CHLW package with a loading of approximately 2.2 kW and 10 year old spent fuel with a package loading of 550 W. Both areal heat loadings were 25 kW/Acre. Recent estimates more consistent with the CSF (12PWR) package and an updated areal heat load reflecting horizontal emplacement have been estimated by the Wurm, et. al. TEMP computer program [65]. The results are depicted in Figure 2-4. The peak temperature is 135°C between 3 and 4 years after emplacement.

---

\*Laboratory-measured thermal conductivities are lower than *in-situ* measurements, primarily due to stress relaxation upon removal of the salt core specimen.

Figure 2-4: Thermal History of the Salt-Container Interface for the CSF(12PWR) Waste Package Design



There is little reason to argue that the above predictions will be accompanied by significant uncertainty and that detailed *in situ* data will become a necessity in the future, yet a common theme is dictated by these analyses: the salt-container interface will be exposed to a time-at-temperature of greater than 100°C for nearly 100 years.

### 2.3.2 Water Availability at the Salt Repository Horizon

Natural salt formation can potentially contain three significant types of water sources, the significance of each is formation- and horizon-specific. These sources are:

- Intracrystalline fluid inclusions
- Fluids trapped within halite in grain boundaries
- Interbed water

The brines found as intracrystalline fluid inclusions are found to migrate up an applied thermal gradient. Early investigators, such as Anthony and Cline [1] postulate the migration mechanism is thermally-driven transport, in which brine inclusions become mobile by a process of dissolution and recrystallization at the hot and cold faces of the inclusion, respectively. More recently, Olander and others [43, 1] have suggested brine motion is under thermal control within the crystal, but upon reaching a grain boundary, is controlled by the effective pressure gradient and this fluid then remains confined to the intercrystalline space. This mechanism, thermomigration of halite brine inclusions has received the most attention to date and been the most extensively modeled source of water for waste package performance calculations.



Relatively little empirical data is available to support predictions of brine flow based on thermomigration. However, Jenks and Claiborne [32] have fit an analytical equation for the maximum rates of brine migration versus temperature. The equation relates brine inclusion velocity to temperature and local thermal gradient, thus:

$$\ln \frac{v}{\nabla T_{\infty}} = 0.0656 T - 0.6306 \quad (2.1)$$

Where:

$v \equiv$  Brine inclusion speed (cm/year)

$T \equiv$  Bulk temperature of the salt ( $^{\circ}C$ )

$\nabla T_{\infty} \equiv$  Bulk temperature gradient in the salt ( $^{\circ}C/cm$ )

Two models which treat the transport of brine inclusions in the waste package near field environment of a salt repository are the MIGRAIN computer program by Claiborne, et. al. [11] and the BRINEMIG computer program of McCauley and Raines [38]. Both of these models, developed from substantially the same set of working assumptions, avoid explicitly solving the fluid mass and momentum transport equations by evaluating the velocity field throughout the near field region from the phenomenological correlation given above as equation (2.1).

Of any reported analysis, the greatest brine accumulation has been estimated in work supportive of the Salt Repository Project's Draft Environmental Assessment (EA) task. Employing a site-specific temperature profile generated by the Wurm, et. al. TEMP [65] model, the BRINEMIG program predicts 850 liters per package will accumulate in 1000 years for a site located in the Permian Basin formation in Texas. In this analysis, the initial brine content of the site was intentionally overestimated by at least a factor of five. (It can be shown that the sensitivity of total brine accumulation is directly proportional to changes in initial brine content for simple models such as BRINEMIG).

Much lower total brine accumulations have been reported resulting from the MIGRAIN model, (8.50 liters per package [11]), owing to lower initial brine content in the host salt and lower package heat generation rates in the case problem input assumptions.

Sources of likely overestimation of brine accumulation above include assuming the midplane package temperature conditions prevail over the entire package and lack of accounting for the reduction in brine content of the host rock by evaporative processes during the preclosure (operational) phase, nor the time (delay) to resaturation.

Entrapped grain boundary fluids are the other source of included halite water. The transport of this fluid inventory is presumed to

behave as a flow system, under pressure control. Together intracrystalline fluid inclusions and grain boundary fluids in halite of the Deaf Smith County site have been found to contain from 0.1 to 0.8 weight percent water.

The most significant water source from clay minerals is the so called "interbed water", which is the fluid trapped between the sheetlike structures of the smectite clays. The smectite group of minerals are composed of two tetrahedral silica sheets with a central alumina octohedral sheet. The orientation of this sheetlike layer structure is such that there is a slight charge imbalance between the dissimilar silica and alumina units. The incorporation of polar molecules such as water then results in a more uniform electric field across layer boundaries. Hence, the smectites are noted for their ability to easily accommodate great amounts of water between layers. The maximum water content of Unit 4 mudstone (clay structures) is estimated to be 15 weight percent [18, 17]. It should be noted that the differential thermal analysis technique employed in the water release measurements cannot distinguish the small amount of (chemically bound) hydrated mineral water from the interlayer water.

A homogenized average brine content has been estimated by Means [41] by weighting the average halite brine content and average mudstone brine content with the Unit 4 estimates of halite and mudstone mass fractions

mentioned earlier. Results indicate 1.64 total weight percent water averaged over the entire repository horizon.

With regard to brine chemistry it has been found that those brines occurring as intracrystalline fluid inclusions - which possess significantly higher magnesium concentrations due to the greater solubility of the magnesium salts and reduced solubility of sodium chloride within the inclusion - are greatly more corrosive to ferritic steels [61]. Various compositions have been reported based on analyses of fluids prepared and collected in differing ways. Compositions of fluid inclusion brines are often interpreted based upon equilibrium seawater evaporation assumptions (the evaporative processes presumed to have formed the bedded salt structure). Deviations from those expected compositions are explained by participation, to varying degrees, of the inclusion brine in dolomitization\* and calcite precipitation reactions. Table 2-3 has been assembled from the various listed sources and presents significant ionic compositions of inclusion brines currently under study in the Salt Repository Program.

In a recent international workshop which was to assess the sources, chemistry and potential movement of brines in salt, participants generally agreed to the following conclusion [12]:

---

\*The dolomitization reaction is given by  $Mg^{++} + 2CaCO_3 \Rightarrow CaMg(CO_3)_2 + Ca^{++}$ . See, for example Berner, R. A., pp. 148-157 for further reading on the theories of sedimentary dolomite formation.

**Table 2-3: Ionic Compositions of Fluid Inclusion Brines in Halite  
(all concentrations in ppm)**

Ion	Seawater (1)	Dolomite (2)	Brine B (3)	PPB1 (4)	Brine A (5)	PPB 3 (6)	SSSS (7)
Na <sup>+</sup>	10,651	63,072	115,000	105,128	42,000	18,650	30,392
K <sup>+</sup>	380	4,024	15	33	30,000	8,441	6
Mg <sup>+2</sup>	1,272	15,048	10	115	35,000	42,765	21
Ca <sup>+2</sup>	400	10,104	900	1,333	600	11,817	904
Sr <sup>+2</sup>	13	--	15	30	5		
Cl <sup>-</sup>	18,890	160,720	175,000	163,248	190,000	168,810	45,040
SO <sub>4</sub> <sup>-2</sup>	884	376	3,500	2,735	3,500	129	2,088
HCO <sub>3</sub> <sup>-</sup>	146	--	10	26	700	--	25
Br <sup>-</sup>	65	--	400	27	400	1,929	--
BO <sub>3</sub> <sup>-3</sup>	--	--	10	--	1,200	--	--

- (1) Reference [B-4].
- (2) Brine 2 is an observed brine that has participated in dolomitization [C-4].
- (3) Brine B is a near-saturated predominantly NaCl brine representative of dissolved bedded salt from the WIPP site. [B-4].
- (4) Permian Basin Brine 1 (PBB1) is representative of dissolved bedded salt from the Deaf Smith Co. site, referred to as an intrusion brine [W-2].
- (5) Brine A is a representative inclusion brine from the WIPP site [B-4].
- (6) Permian Basin Brine 3 is a representative inclusion brine from the Deaf Smith Co. site [W-2].
- (7) Serrogate Site Specific Salt (SSSS) is a better attempt laboratory manufacture of Deaf Smith Co. bedded salt. It is improved over PBB1 by being saturated in NaCl at the test temperature of 150 C.

- Intracrystalline fluids are not the major source of water in the bedded formations under study, this is supported by:
  - Inclusions are unlikely to migrate through a grain boundary
  - A temperature gradient threshold exists, below which thermomigration ceases
- Darcy flow is the most probable mechanism for interbed fluid transport
- Compositions of brines resulting from brine-solid salt interaction at elevated thermal conditions are likely to be much more corrosive than those being employed in salt repository testing programs
- Composition of brines arriving at the waste container interface will likely be bounded by the composition and inclusion brine composition.

### 2.3.3 Stress Conditions

As currently understood there are five significant components contributing to the state-of-stress at the boundary of the disposal container: the overburden pressure which is essentially lithostatic, the hydraulic (brine) contact pressure, vapor and noncondensable gas pressure, thermal stress developed due to the waste form heat generation and residual stress resulting from fabrication. Of these five components, the first three are the least certain from a calculable standpoint, due to the uncertainty in long-term host rock thermomechanical response and brine availability at the interface.

Lithostatic pressure, also called overburden pressure, is site-

specific. For the candidate Deaf Smith County salt site in the Palo Duro basin the repository horizon is between 700 and 760 meters below grade. Initial lithostatic pressure at this depth is has been estimated between 13.8 and 17.9 MPa, vertically [20]. The latter estimate is inferred by direct integration of the density well log. Maxwell et. al. [37] have shown the total stress in the near-field salt is always compressive.

There will be a very short transient response in both the lithostatic loading of the container and the fluid (both gas and liquid) contact pressure. It has been estimated this transient will have a duration of less than one year after emplacement. The lithostatic temporal variations are due to the thermoelastic and mechanical response of the host rock salt. The response of the fluid, increased contact pressure, is due to the increased specific volume and increased vapor pressure of the entrapped brine. The salt will expand as it is subjected to the slow thermal pulse associated with fission product decay heat. As well, halite and clays both flow readily under stress. Creep deformation in the vicinity of the waste container is expected to consolidate the loosely packed material surrounding it and seal the borehole container interface.

Viscoplastic creep behavior has been investigated for relatively homogeneous bedded halite specimens. Investigators [5, 30] have found a

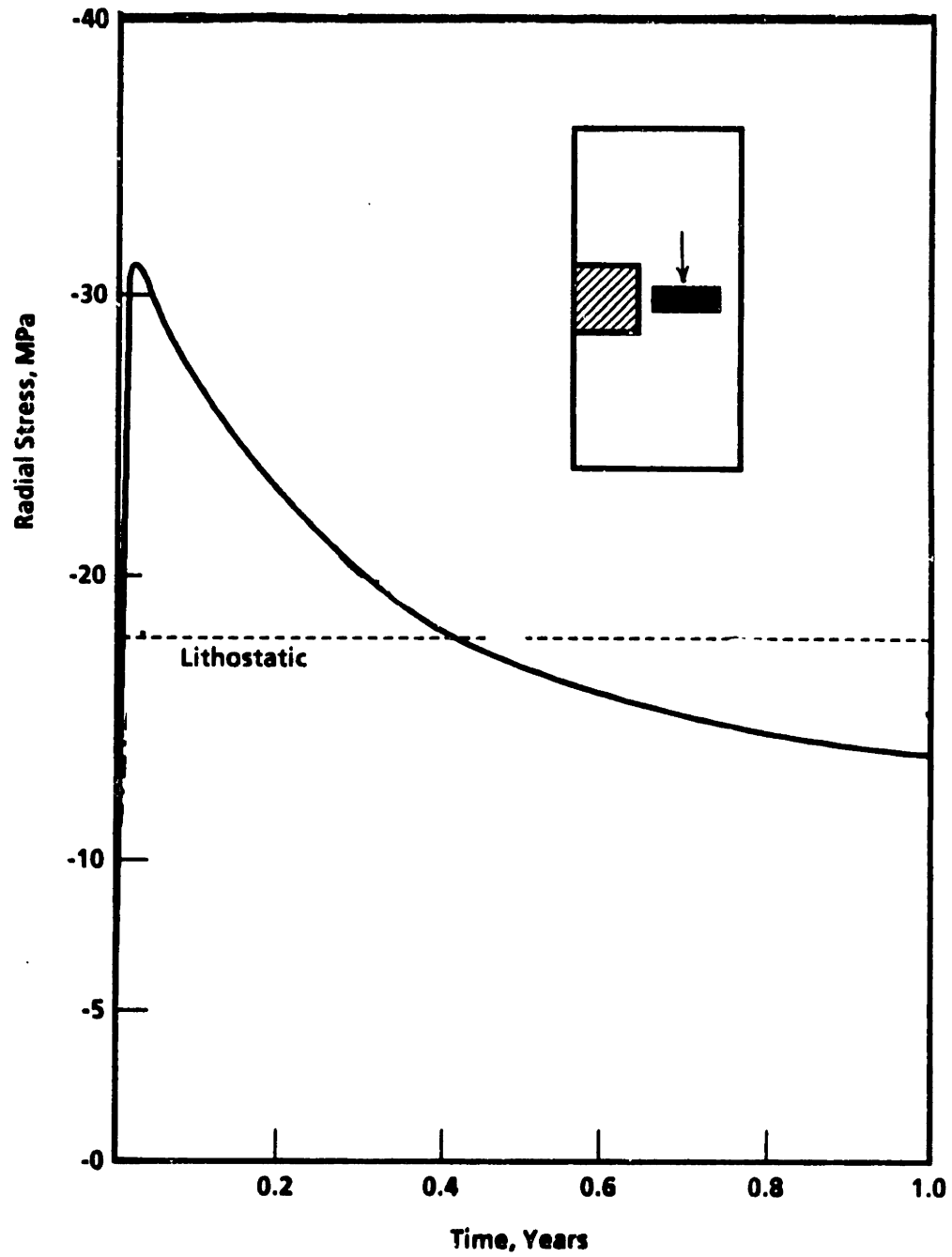
strong temperature dependence in the proposed constitutive creep rate law. Loken, et. al. [33] have analyzed the lithostatic response for a conceptual repository design with a two-dimensional finite element model of the near field. His findings indicate a short lived transient, due to creep closure in the first year, followed by a gradual approach to initial lithostatic for the lithostatic component of the total stress field. Loken's working assumptions imposed an initial lithostatic stress of 13.8 MPa.

Ghantous [25] has performed an updated evaluation of the thermomechanical repository response to the CSF(12PWR) horizontally-emplaced package design. Results are presented in Figure 2-5 Admittedly [55, p. 6-225], the peak values and decay histories of these stresses are currently poorly defined.

Brine contact pressure and gas and vapor pressures have not been estimated or analyzed in any detail. Potential contact pressures will depend upon (1) the inflow rate and quantity of brine arriving at the borehole-container interface, (2) the rate of creep closure, which determines when and how well sealed the borehole volume is and whether pressures will be relieved due to boiloff of the brine or if the vapor is trapped, and (3) generation of noncondensable gasses; most notably hydrogen from the hydrogen-iron redox reaction.



Figure 2-5: Midplane Container Boundary Stress



It has been pointed out in Section 2.3.2 that the state of knowledge of sources and especially of transport mechanisms for water in the repository environment are rudimentary. A determination of the brine pressure response would be very sensitive to the assumptions of fluid transport models. As well, constitutive laws have not been determined for the impure and heterogeneous bedded salt (and clay) of the Lower San Andres Unit 4 which results in uncertainty relative to the time of borehole closure and estimates of vapor pressures which could be supported by the borehole volume. Finally, corrosion kinetics at the container surface and rates of transport of hydrogen through halite and clay minerals will determine if the borehole volume can support large hydrogen vapor pressures, giving rise to significant container stresses.

In Loken's analysis mentioned above [33] the sum of these fluid pressure transient effects were simplistically accounted for by placing a 25% peak excess radial compressive stress and a 35% peak excess axial compressive stress limit on the transient response. This gave rise to a maximum normal axial stress of roughly 18.0 MPa, while lithostatic was considered 13.8 MPa.

Thermal stresses are expected to be an insignificant contribution relative to the uncertainty in current predictions, and as such have not been included in thermomechanical analyses. Estimated separately from other stress components, employing for carbon steel; a modulus of

elasticity of  $2.1 \times 10^5$  MPa, thermal expansion coefficient of  $1.1 \times 10^{-5}/^{\circ}\text{C}$ ,  $2.3 \text{ MPa}/^{\circ}\text{C}$  results. Considering that the maximum gradient established through the container is between 1 and  $2^{\circ}\text{C}$  [25], thermal stresses could conservatively contribute from 2 to 5 MPa to overall loading requirements.

Residual stresses are not generally included in the type of analyses presented thus far as it is necessary to know exactly what type of joining technique will be employed in the container design. If the container is to be welded as is indicated in the reference conceptual design [63], it is necessary to establish mechanical properties of the parent plate in the heat affected zone, the effect of any post-weld heat treatment or other stress relief treatment, and the properties of the filler material. McEvily [39] indicates that for butt-type welds in thin plates the stress field is most often compressive near the terminations of the weld (the free edges of the plates) and tensile at the mid-length and mid-depth of the bead. Thick plates behave much less predictably due to the interaction of strains generated in subsequent weld passes. The heating and cooling cycles which would be required of a thick multi-pass weld such as in the waste container can give rise to significant residual stresses, both tensile and compressive, in theory these may approach the yield strength.

#### 2.3.4 RADIATION ENVIRONMENT

Radiation in the waste package near field will be directly determined (and controlled) by design. There should be minimal difficulty associated with calculating the radiation field given the waste form isotopic inventories, geometry and spatial compositions of the salt and backfill materials. A formidable difficulty is encountered in attempting to model the radiation-assisted corrosion effects. Radiation can, in principle, assist corrosion mechanisms primarily via alteration of the electrolyte chemistry.

Fortunately, the radiation field will be significantly attenuated by the thick steel container. It has been suggested by Westerman, et. al. [61] that there is no observable radiation-induced effect on the general corrosion mechanism acting on low carbon steels in repository-like brines at dose rates of 2000 Rad/hour and below.

The results of Jansen, reported in the Deaf Smith Environmental Assessment [55, p. 6-221] indicate the maximum dose rate at the metal-salt interface is 21.2 rad/hour at emplacement for the CHLW package and 32 rad/hour considering the spent fuel source term. This dose rate decays an order of magnitude at some time before 100 years post burial.

## 2.4 WASTE CONTAINER DEGRADATION MECHANISMS

As has been reviewed earlier in section 2.1 the waste container is a barrier-type component which is functionally to contain its radionuclide inventory by complete enclosure. The container is a passive component from the standpoint that its sole purpose is to provide a time delay to natural geologic transport of the waste. It is doubtful that a waste container design based upon a corrosion allowance could demonstrate compliance with regulatory objectives with any degree of assurance should evidence of the potential for localized, small surface-area penetration (e.g. cracking, pitting) become manifest.

As will be postulated in the following development, the primary challenge to container integrity must be mechanical (e.g. buckling under failure stresses), after sufficient thinning due to general corrosion.

Site selection criteria require evidence to contraindicate past or expected future seismic activity, thereby ruling out the consideration of transient seismic loading of the container. Ruling out this type of loading does not eliminate the catastrophic failure modes linked with environmentally-assisted cracking or buckling under quasistatic loads.

For this review of potential mechanisms, the following categorization will be made. The term macroscopic mechanisms will be used to refer to the processes of bulk metal dissolution, those being general (or

uniform) corrosion, pitting, crevice and galvanic types of corrosion. Microscopic mechanisms will refer to those mechanisms which are operative at the microscopic material level and are nearly always associated catastrophic failure. These are the family of environmentally-assisted crack growth mechanisms to which hydrogen assisted failure (embrittlement) and stress corrosion cracking belong.

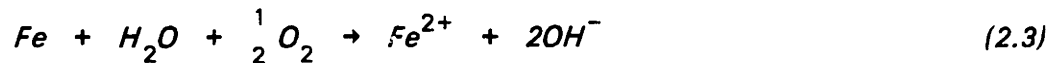
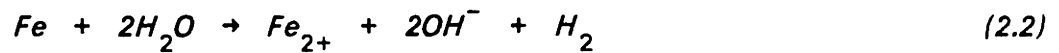
#### **2.4.1 Macroscopic Mechanisms**

It must be pointed out that conventional wisdom in materials selection for engineering projects would normally reject a low strength low carbon steel for application in an aggressive brine environment. However, predictable, general corrosion is being traded off against greater susceptibility to localized corrosive attack in the case of the salt repository project, due to the inordinately long design requirements and lack of active surveillance over the design life. It is for this reason that although the A216 alloy possesses a fairly comprehensive database, applications similar to the saliferrous environment of the candidate repository are few.

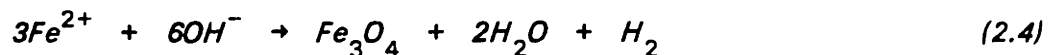
##### **2.4.1.1 General Corrosion**

General corrosion involves a reacting surface for which there is no distinct separation of the cathodic and anodic reactions. Both reactions proceed over the entire exposed metal surface. In neutral pH aqueous corrosion processes, the oxygen availability is nearly always the key factor controlling the rate of reaction [22].

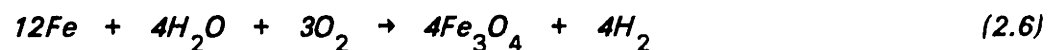
The simplest system of ferrous metal dissolution occurs when iron is exposed to a pure water electrolyte. In this case there are two possible reaction paths:



The first case, equation (2.2), holds under anoxic conditions, and the second when oxygen is present in stoichiometric excess. In most environments of interest the ferrous ion is not stable and the second reaction proceeds further by the Shikkor reaction:



It is illustrative to obtain the overall stoichiometry from equations (2.2) - (2.4), thus:



This is the classic presentation of the general corrosion of iron, and is very applicable to simple alloys of iron. The feature of interest here is that the thermodynamically stable oxide generated in both cases is magnetite,  $Fe_3O_4$ . Also, note that direct comparison between the

anoxic (2.5) and oxic (2.6) consumption of water may be made. That is, oxygen-free corrosion of iron requires four times the water as does corrosion in oxygen-excess conditions.

Passivation behavior occurs for numerous alloy-environment systems of interest in engineering applications. The passivation phenomena is observed as a marked decrease in surface reaction rate of an actively corroding metal in certain potential ranges due to the buildup of a protective oxide film. The film inhibits solution-metal contact. Decreases in reaction rate (which is observed as anodic current) of four to six orders of magnitude are common. The formation of a thin (of the order of 30 angstroms), thoroughly-hydrated adherent and protective surface film is implicated as the physical cause of the reduced reaction rate [22, p. 321].

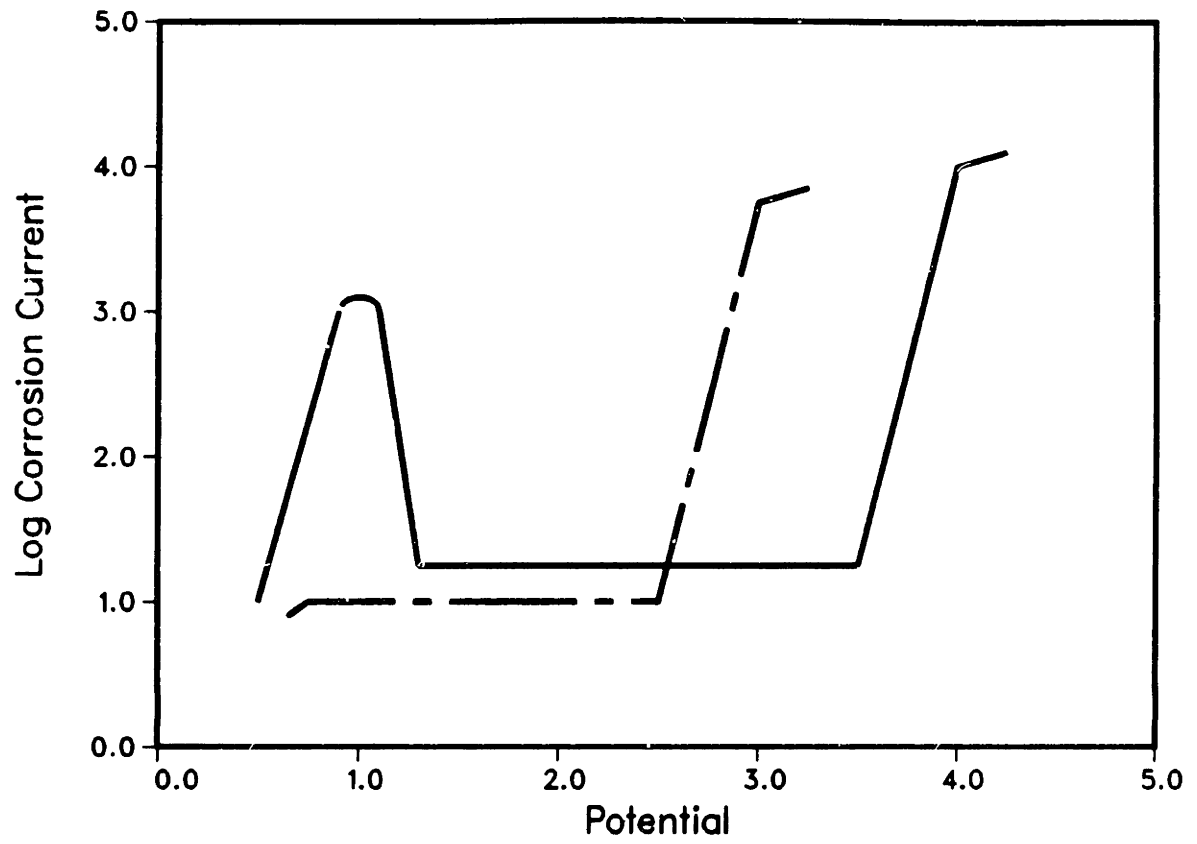
Some metals exhibit passivation-like behavior, though the above definition is not ostensibly met. The response may not be as pronounced, though it may still be appropriate to speak of a prepassive, passive and transpassive behavior. Carbon steel magnetite films are porous, reasonably conductive, do not generally contain water of hydration and grow to order-of-centimeter thicknesses. Of prime importance to an understanding of the protective nature of any film is a knowledge of the film composition, structure and relationship to the metal surface upon which it was formed.



Microscopic techniques are useful to identify structure and bulk crystal material properties of the oxide film grown on the metal surface. As well, since the formation and behavior of such films depend on the local thermodynamic state and local electric potential, investigations of these anodic films are also made via electrode kinetics techniques, such as measuring the anodic current response resulting from an externally controlled potential. An idealized anodic polarization curve is depicted in Figure 2-6. The solid line depicts pronounced active-passive behavior, while the chain dash line exemplifies a non-passivating metal. When the external potential is referenced to the reversible electrode potential (the potential at which infinitesimal current would begin to flow) it is called overvoltage and/or polarization.

Foley, et. al. [21] investigated the oxide films formed on iron foils *in situ* with transmission electron diffraction. In all instances the passive films contained gamma-Fe<sub>2</sub>O<sub>3</sub> (hematite). Films formed in the prepassive and transpassive (actively corroding) regions of the polarization curve contain the magnetite structure. The measurements were performed in 1N sulphuric acid, and two neutral aqueous environments - 0.1N sodium hydroxide and a buffered (pH=8.5) sodium borate-boric acid solution. In these instances magnetite growth definitively indicated active metal corrosion, even at the observed low corrosion rates.

Figure 2-6: Idealized Anodic Polarization Curve



Park and McDonald [45] report that the growth of porous magnetite films on carbon steels at 200°C and 250°C are parabolic in the early stages of corrosion and after long time obeys linear kinetics. In their particular investigation, a 0.998 M NaCl + 0.001 m FeCl<sub>2</sub> \* 4H<sub>2</sub>O solution was used. They conclude that the pores of the magnetite film contain an aggressive solution which is maintained by anion (Cl<sup>-</sup>) transport and cation (Fe<sup>2+</sup>) hydrolysis, which eventually reach limiting rates. Using an impedance technique they find that the external imposition of an anodic overvoltage results in an increased rate of corrosion, but the effect decreases with time owing to an increased fractional resistive loss of the overvoltage across the film as it thickens.

Bonnel, et. al. [4] also used an impedance technique to investigate mass transport of oxygen through the porous magnetite corrosion product layer formed on carbon steel in neutral chloride solutions. A rotating disk electrode was employed so as to separate the diffusional component of the oxygen reduction reaction from the total (mixed activation and diffusion controlled) oxygen reduction reaction. They report conclusive evidence providing direct proof of the occurrence of mass transport through porous films and that the overall corrosion reaction studied - carbon steel in neutral chloride media - is rate-limited by the reduction of oxygen under mixed charge transfer and mass transfer control. Dabosi, et. al. [14] support these conclusions in an extension of the same work.

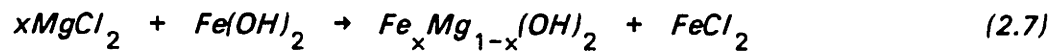
The above survey provides sound generalizations regarding the general corrosion of iron in neutral aqueous solutions. However, the brines present in salt repository environments are significantly more concentrated in dissolved solids, highly conductive and far more aggressive.

Westerman, et. al., [61] have performed an array of gravimetric corrosion tests of carbon steels in repository-like brines. Results to date overwhelmingly indicate severely (one hundredfold) greater corrosion rates for brines containing magnesium. In an attempt to address the correlation of high corrosion rates observed in high magnesium brines, a further series of gravimetric corrosion experiments was performed which varied the magnesium concentration from 0 to 1.7% by weight. These "excess salt tests" (which will be discussed further in Section 4.1.2.) provide significant evidence to support the magnesium concentration dependence of the steel corrosion rate, especially the A216 alloy.

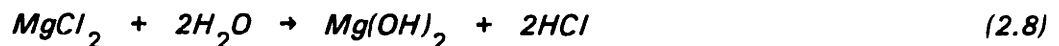
The unique feature of corrosion samples which have been subject to high magnesium brine corrosion is the formation of a thick (2 mm - on both surfaces of a 1.4 mm thick specimen) claylike layer not resembling magnetite. The deposit was not soluble at room temperatures, and resembled a hard clay. An X-ray diffraction spectra of the material corresponded to a complex iron-magnesium hydroxide,  $\text{Fe}_x\text{Mg}_{1-x}(\text{OH})_2$ . The

endpoint minerals for this mineral series are, for  $x=1$ ; ferrous hydroxide and for  $x=0$ ; brucite. The mineral name amakinite is used to refer to any fractional  $x$  greater than zero [19].

Since there is no thermodynamic data available for amakinite, reaction paths may only be postulated at this time. Peters and Kuhn [46] have proposed the following magnesium substitution reaction:



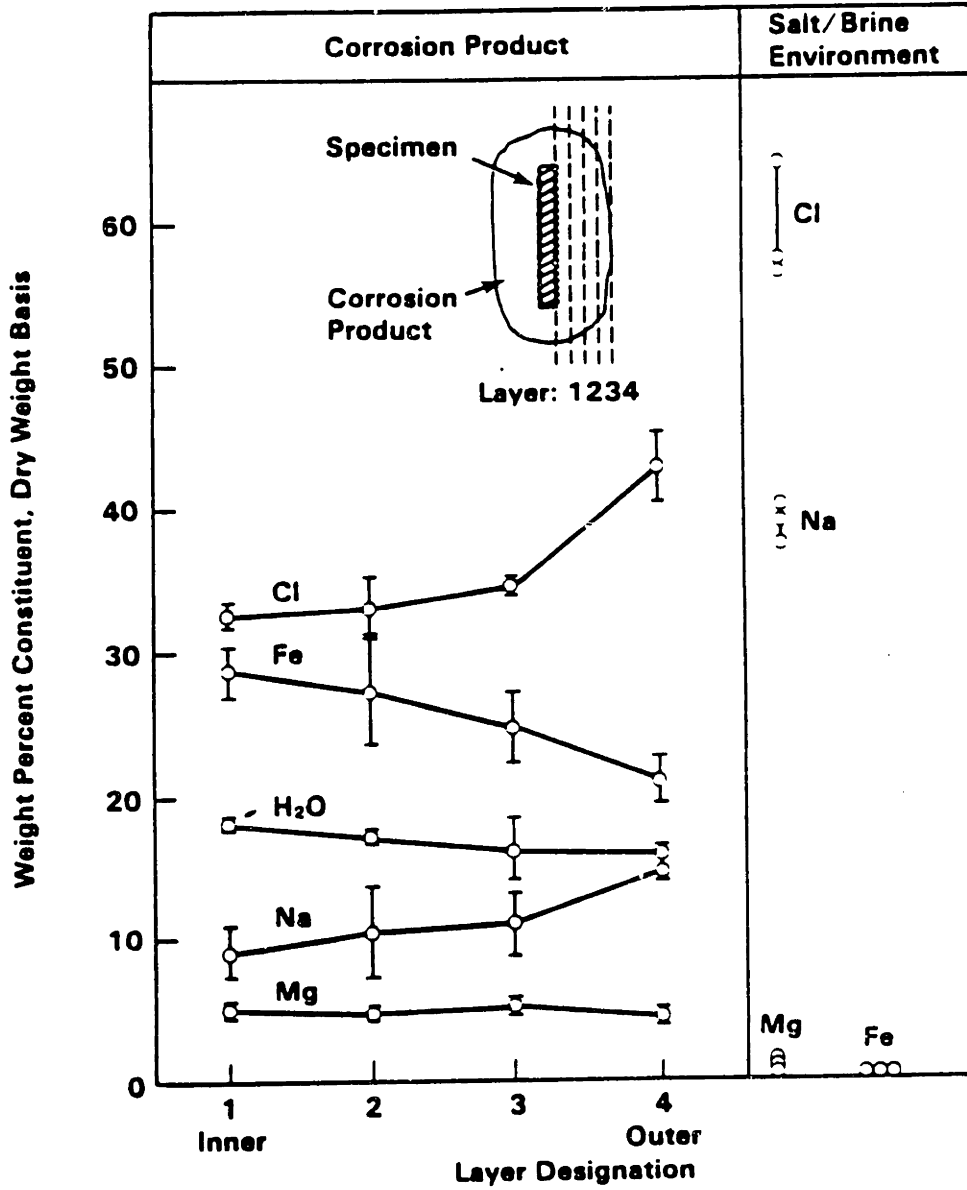
This reaction is consistent with the observed solution pH between 7 and 8 at test termination. If the reaction path involved a metal (magnesium) chloride hydrolysis step;



an observable pH drop would be expected. Peters and Kuhn also forward a plausible argument that hydrogen pressures observed in these tests (20 atm.) are at least an order of magnitude too low to stop the forward hydrogen evolution cathodic reaction (see equation (2.5) and (2.6)).

Westerman has also attempted to deduce the composition depth profile of the Amakinite layer by freezing and sectioning. These results are presented in Figure 2-7. Most notable is the uniform magnesium concentration profile and the slight increase in water content near the metal-layer interface.

Figure 2-7: Composition Profile of Amakinite Layer



Further confirmation of the aggressive nature of magnesium-rich solutions is indicated in the work of Pisigan and Singley [47] who after exploring the corrosion rates of mild steel in 22 different synthetic water compositions conclude that corrosion rates of the steels in waters containing significant (20-52 ppm) magnesium concentrations were relatively (50%) higher than the others.

The above early data on corrosion by high magnesium brines and amakinite formation is by no means sufficient to draw any conclusions regarding the reaction path, the kinetics or the long-term behavior of the product layer. However, the following observations are made based on the compiled literature:

- Amakinite formation appears to interrupt the normal magnetite formation from ferrous hydroxide by the Shikorr reaction
- Amakinite is not protective
- Active corrosion proceeds and is only slowed as the amakinite layer grows in thickness, hence the controlling step is likely to be charge transfer (activation)

#### **2.4.1.2 Pitting and Crevice Corrosion**

Pitting and crevice corrosion differ from general corrosion only in that the cathodic and anodic reactions are separated. The essential initiator of both is a small stagnant volume of solution in localized contact with the reacting metal. Pitting and crevice corrosion differ from each other only formally in that crevice corrosion occurs in tight crevices and other shielded areas of metal surfaces which are exposed to

electrolytes, while pitting may occur anywhere on a metal surface but requires a pit initiation phase. Pitting attack is extremely localized and varies widely both in the pit number density over the metal surface and in the pit (or cavity) shape. Most often aspect ratios (pit depth/pit diameter) are high - implying deep, penetrating perforations.

The most universally accepted model of pitting (and crevice) corrosion treats the propagating pit as an occluded anode [22]. Since the occluded cell volume is considered stagnant, the dissolved oxygen which is consumed by the cathodic reduction reaction can only be replaced by the process of diffusion. If the rate of diffusion into the cell falls below the rate of consumption of oxygen within the cell, this imbalance in the redox reactions results in a concentration of dissolved metal cations in the pit. The excess positive charge provides an electric potential gradient which is countered by increased migration of anions, often chloride ions, into the pit. Typically the metal salts (e.g. chlorides, sulfates) then hydrolyze, resulting in more acidic pit conditions. The reaction is autocatalytic if the electric potential driving force is greater than the oxygen concentration gradient caused by depletion. Separation of the anodic and cathodic processes is maintained and cathodic protection of the unshielded metal surfaces continues at the sacrifice of accelerated, localized penetration in the pit.



Pitting occurs in a wide variety of metals and alloys, however it is widely recognized [64] that the most severe pitting attack is associated with strongly passivating metals which exhibit very low general corrosion rates. Pits are more likely to develop in a metallurgically-inhomogeneous metal [56] owing to the different rates of attack upon compositionally-different areas of the surface.

Pit initiation commences when a local breakdown of a protective film occurs. This may result from a local surface imperfection such as an impurity, an emerging dislocation, or a surface scratch which alters, sometimes only momentarily, the rate of metal dissolution. The progression may proceed as described above, once this local anodic area has been established. In pitting corrosion, then, it is often instructive to group metal-environment systems into those in which pit initiation is the overall rate-determining step, and those in which the rate is determined by the rate of pit progression, or growth.

Gupta [27] concludes that in addition to general corrosion, 1040 steel (a low carbon steel similar to A216), depending on pH and sulfide level, will undergo pitting corrosion. He indicates that the most severe attack in neutral environments occurs at sulfide concentrations from 150 to 300 mg/l. These tests were performed at room temperature.

Jelinek and Neufeld [31] indicate that mild steels corroding in de-

aerated neutral bicarbonate-bearing sodium chloride solutions exhibit reduced pitting corrosion rates as a function of temperature up to 90°C, and thereafter, the temperature effect is reversed. Explanations presented in the work implicate an Fe-Cl reaction product in destabilizing the passive film.

Experimental observations in more repository-relevant environments, however, generally indicate much lower vulnerability to pitting corrosion. Canadillas, et. al. [6] have observed shallow, coalesced pits on a fine-grained, structural steel in a high magnesium brine denoted Q-brine. The pits were found to occupy much of the metal surface, and the pit depth was found to approach twice the the penetration due to general corrosion.

These results are consistent with the findings of Westerman [26], also in simulated repository brines, containing high concentrations of magnesium. Westerman observes an initial phase of distinct pitting-like attack, for which the rate eventually slows below that of the general corrosion penetration rate. It has been argued, that in the magnesium-rich brines, the initial pit-like attack is due to the more rapid oxidation of the alpha-ferrite grains [26]

Marsh [35] has postulated a pit progression rate which varies with time raised to the power of 0.49. This was developed for thick carbon

steel containers, but in typical (synthetic) argillaceous groundwaters as opposed to salt brines.

## **2.4.2 Microscopic Mechanisms**

### **2.4.2.1 Stress Corrosion Cracking**

In general, it is thought that the combination of three elements are necessary to induce stress corrosion cracking (SCC): tensile stress, alloy and environment. In fact, it is more general and instructive to speak of environmentally-assisted cracking, of which stress corrosion cracking is a subset.

Observations of stress corrosion cracking for ferritic alloys are found to occur in a tensile stress field of greater than 965 MPa [51], except in extremely potent chemical environments. There are far fewer observances of SCC in low strength steels than in high strength steels.

Relevant reported SCC agents for carbon steels include:

- Nitrates
- Hydroxides
- Carbonates
- Chlorides

Virtually all observations of SCC in low carbon steels are associated with some type of active-passive transition behavior and SCC agents act to shift the potential at the advancing crack tip into the cracking

regime. Beavers, et. al. [2] points out that a close relationship between the polarization (active-passive) behavior and the cracking susceptibility supports the slip dissolution/film rupture model of SCC.

Nitrates are found to be the most potent SCC agents in carbon steel systems. Parkins [44] indicates that not much is known regarding minimum concentrations for attack. Threshold stresses have been measured and tabulated by Parkins, however, and at least 178 MPa is required for the onset of SCC in boiling 1N sodium, potassium, lithium and calcium carbonate solutions. Ammonium nitrate can cause SCC at 92.5 MPa, at 1N concentrations. This may be attributable to the more acidic cation, which results in lower pH.

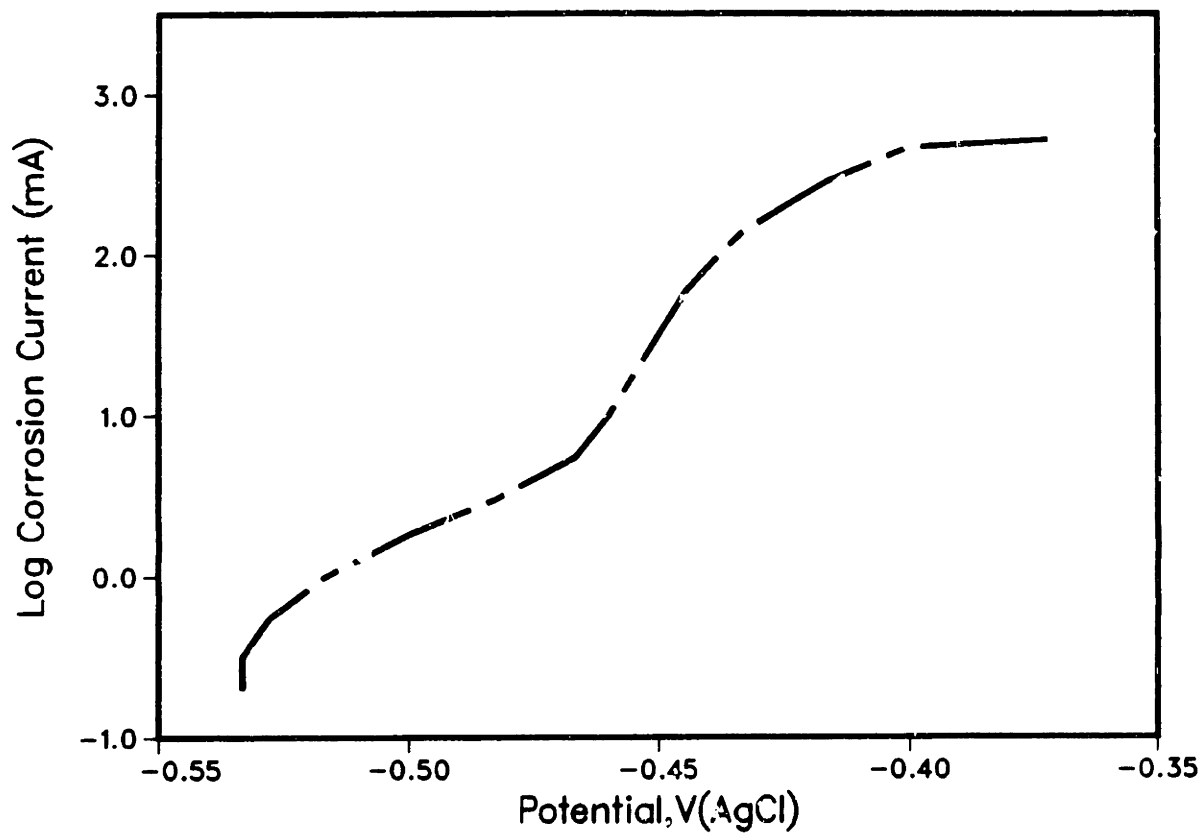
The classic "caustic embrittlement" of locomotive boilers is perhaps the first incidence of SCC of carbon steels. Failure analyses of these boiler components revealed brittle fracture in the region of cold working due to riveting [22], and significant sodium hydroxide deposits, indicating a participating role in the crack propagation. Sodium hydroxide was used as a general corrosion inhibitor in the primary. Temperature and concentration thresholds have been compiled by Beavers, et. al. [2] which indicate at 90°C 24% NaOH is required for SCC, while at boiling (atmospheric pressures) SCC has been observed at 5% concentrations.

Carbonate systems behave similarly to hydroxide systems and occur over a more limited potential range than nitrate systems. Sutcliffe, et. al. [53] has observed the initial evidence of cracking in 22°C, 1N sodium bicarbonate solutions, and below this temperature found no evidence. Parkins [44] has observed a threshold concentration of 0.25N in boiling solutions. All of the above systems were within the pH range of 8 to 10.

It is interesting to present the preliminary work of Pool [26] in Figure 2-8. This anodic polarization trace indicates there is little if any sign of an active passive transition (compare to Figure 2-6). There is a slight indication of a reduction in corrosion current near 1 mA, but this is not sufficient to suspect a transition, or to imply susceptibility.

Strauss and Bloom [52] investigated environmentally- induced cracking in low carbon steels by an array of various ferric oxide slurries at high (316°C) temperature. Individual mild steel capsules were prepared by crimping and welding short lengths of tubing. They report that while concentrated slurries of FeOOH alone did not produce cracking, the susceptibility was markedly changed after the addition of small (mixing with 0.0001M FeCl<sub>2</sub>) amounts of ferric chloride, and cracking was observed in as little as 3 hours at temperature. The attack was transgranular, as opposed to all citations mentioned above, and the

Figure 2-8: Anodic Polarization Behavior of A216 Steel in Magnesium Solutions



attack was observed to be preferentially in the plastically-deformed region near the weld or in the martensite-penetrated weld region.

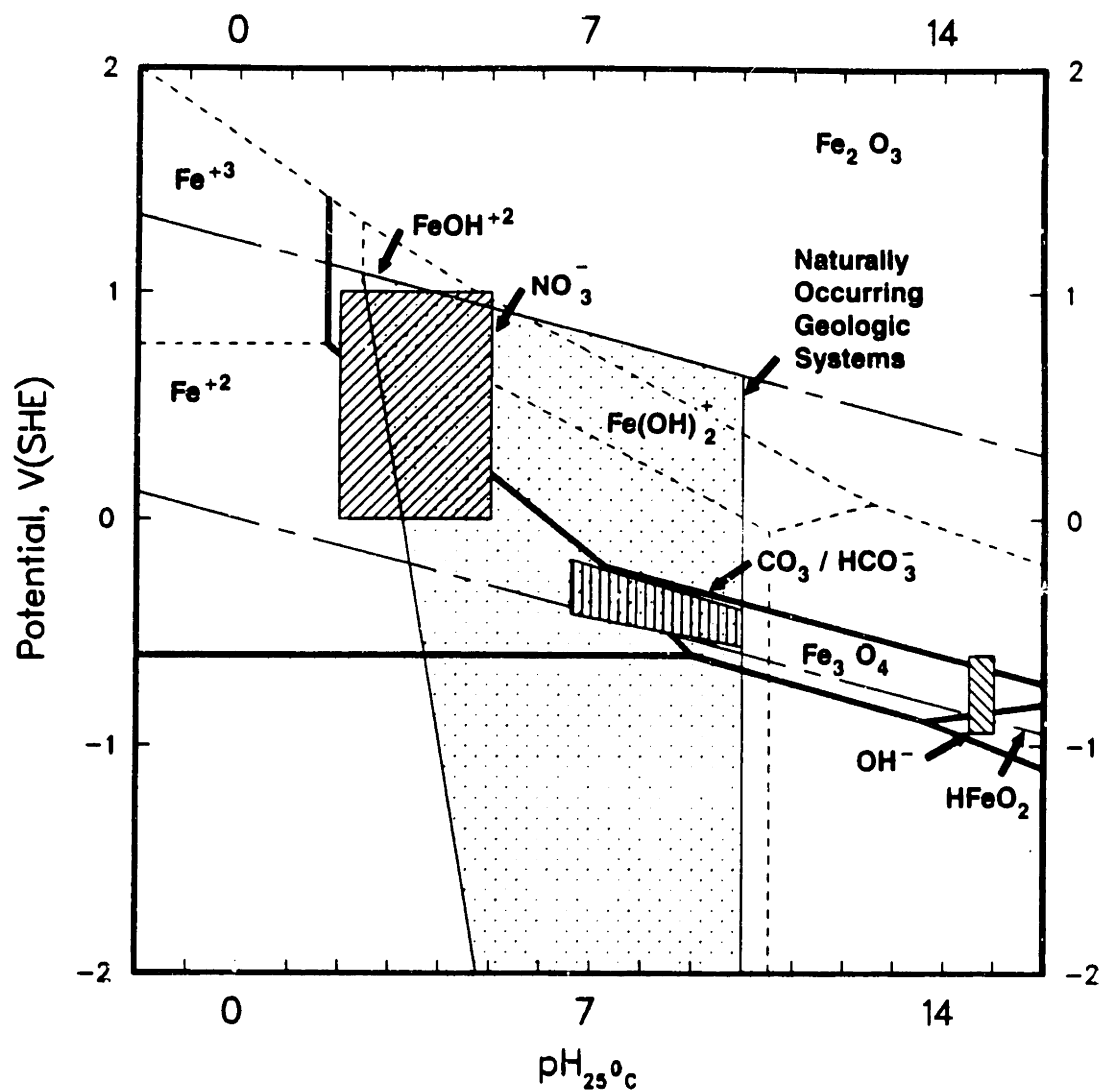
Finally, Ford [23] has assembled a potential-pH (pourbaix) diagram for iron which marks the susceptible regions for nitrate, carbonate/bicarbonate and hydroxide assisted SCC in low carbon steel. This work is presented in Figure 2-9 along with plausible ranges for chloride agent SCC and the region of natural (geologic) system Eh-pH space after Garrels [24].

#### **2.4.2.2 Hydrogen Embrittlement**

Hydrogen embrittlement mechanisms have been studied preferentially for the alloyed and high strength steels owing to their much higher susceptibility. High temperature moist environments, corrosion reactions and electrolysis are the major sources of atomic hydrogen. There is some evidence that much of the environmentally activated cracking in ferritic steels is due to the interaction of hydrogen and the advancing crack tip [22]. The majority of models developed thus far have concentrated on slip interference by dissolved hydrogen.

Blundy, et. al. [3] states, for mild steel hydrogen absorption has little embrittlement effect which is substantiated by the vast number of mild steel structures which are cathodically protected in seawater. Cathodic protection of these metals results in favorable environments for charging them with substantial amounts of hydrogen generated by the

Figure 2-9: Potential-pH Diagram for Iron Including Cracking Regimes (After Ford [20])





cathodic hydrogen evolution reaction. The low uptake of hydrogen in these steels is probably due to the low diffusivity of hydrogen in the ferrite grains, which is the major constituent of low strength mild steels.

The greatest concern for embrittlement will be the martensite ingrown weld material, the extent of which, and hence the susceptibility to this type of failure mechanism, must be determined after the benefits of annealing and alloy composition modifications can be assessed.

## 2.5 SUMMARY

In summary, the previous chapter has outlined the variables of interest in the degradation of waste package containers. The environment has been described and quantified, where possible. Thermal loading requirements have been reduced in the designs reviewed, Peak container-salt interface temperatures of 220°C have been revised by design to 136°C. The early thermal pulse is seen as the most severe in promoting corrosion - greater than 100°C for approximately 100 years. Estimates of fluid (water) availability are unrefined approximations at this time, lacking adequate phenomenological understanding of the basic mechanisms of transport for the most significant sources. Predictions of 8.5 to 850 liters per borehole accumulation in 1000 years have been referenced and indicate this uncertainty. Stress conditions are more tractable and have been calculated based on observed constitutive

relationships for similar bedded halite structures to that found at the Palo Duro site. However, discontinuity stresses, due to welding operations could represent the most vulnerable region of the container. This must be determined at some later time when prototype packages can be tested and the behavior of the process weldments can be quantitatively evaluated. The radiation environment has been shown to be sufficiently attenuated by the thick-walled container so as to be considered insignificant in primary effect.

Many investigations of corrosion related degradation mechanisms have been compiled from the literature. Microscopic threshold failure modes have been shown to be of less concern, by lack of observation, in the bulk metal than the mechanisms of general corrosion, pitting and crevice attack. Regions of vulnerability have been identified for container SCC, indicating brine compositions may contain sufficient SCC agents, however the stress and temperature thresholds lie above those expected in the package environment.

Stress corrosion cracking and hydrogen embrittlement, however, must be addressed in the weld zones. Until further fundamental investigations are performed for the weld type and environment of interest this potential "weak link" in the container will not be considered in the analysis of failure prediction herein.

General corrosion is adopted as the only degradation mechanism for the balance of this work, as it is the only mechanism with significant accompanying data.

x

### 3. DEVELOPMENT OF A METHODOLOGY TO SPECIFY UNCERTAINTY-OPTIMIZED EXPERIMENT DESIGNS

#### 3.1 TESTING REQUIREMENTS

It is evident that for nuclear waste container penetration, predictions over such a long design life will be accompanied by significant uncertainty. Testing requirements for a predefined, acceptable uncertainty at a one thousand year extrapolation from data (measurements) taken over hundredths to tenths (at best) of this interval will be undoubtedly great. Practical testing constraints will necessitate some prior strategy if a useful experimental program is to be undertaken. Models of failure are often adopted for this purpose, as is the case wherein lifetime distribution assumptions are made. This avenue is explored in the following section.

In the case where testing of a very reliable component under expected conditions cannot be undertaken due to the long design life, a specific type of testing under more severe environmental conditions is sometimes undertaken. This approach is called accelerated life testing. *Accelerated life testing* (sometimes called predictive testing) will be defined by distinguishing it from *accelerated testing*.

The goal of accelerated testing is to deduce the dominant failure mode for a device by subjecting that device to an environment of increased severity compared with that in-service. Accelerated life testing

differs from accelerated testing in that goal is to measure some reliability parameter of a device at intensified stress levels and from this data predict the performance at normal or expected use conditions. Implicit in the accelerated life testing approach is the requirement that the dominant physical mechanism of failure does not change from the in-service environment to the intensified environment, and the physics of failure must be understood so as to de-rate the intensified environment data correctly. When successful, accelerated life testing is one way to enhance the predictability validation of a process model.

### **3.1.1 Previous Work**

In the following paragraphs, previous work which is relevant to planning experiments for reliability demonstration (that is, the experiment design *and* the amount of data to be gathered) of nuclear waste containers is reviewed. In the context of the long design life goal of 1000 years, these methods are shown to provide insight but fail to establish the detailed methodology to plan an experimental program focused on such long extrapolations. The need for the present work is thus motivated and defined.

#### **3.1.1.1 Lifetime Distribution Approaches and Accelerated Life Testing**

One can, in principle, rationalize some particular lifetime distribution for the waste container in the specified repository conditions as an approach to the container failure prediction problem. Using such an assumed model of failure, it is possible, with some very

strong assumptions, to obtain a quantitative measure of the testing requirements which would support reliability predictions with some given probability. This procedure is generally referred to as "testing reliability hypotheses".

Thomas [54], in his creative application of standard reliability hypothesis testing to waste container failure, determines the number of required "container tests" which would be required to accept an hypothesis that the probability of the container lasting some given design life goal is either large, substantiating the high reliability case, or very small, substantiating the low reliability case.

Thomas's approach treats all tests alike, regardless of the control conditions, hence these container tests may be accelerated life tests, or tests at repository-like conditions. Thomas's approach generally indicates the magnitude of testing requirements for such long-time extrapolations and implicitly reveals some of the pitfalls of distributional approaches and accelerated testing. The basic developments are presented here in brief.

Taking Thomas's approach, the framework for the determination is to formulate the test hypotheses:

$H_0$                     The reliability of the container at L years is less than  $R_0$ , where  $R_0$  is small, 0.10.

$H_1$                     The reliability of the container at L years is greater than  $R_1$ , where  $R_1$  is large, 0.95.

If the failure distribution is presumed to be Weibull\* , the reliability for the waste container at fixed time t is given by:

$$R(t) = \exp(-(t/b)^c) \qquad (3.1)$$

with the definitions

$R(t) \equiv$  Reliability function at time t

$t \equiv$  Time

$b \equiv$  Characteristic life

$c \equiv$  Weibull shape parameter

The above hypotheses may be restated, mathematically, with the inequalities:

$$H_0 ; \quad R(L) \leq P_0 \qquad (3.2)$$

---

\*Mann, et. al. [34] indicate that the Weibull distribution has been used to model corrosion-driven failure. However, most derivations of the distribution suggest the failure mechanisms appropriately modeled by the Weibull distribution are those in which the degradation process is active at a number of preexisting flaws, and the time to failure is controlled by the combination of the most rapid degradation at the severest of these flaws. This suggests that the types of corrosion processes most appropriately modeled by a Weibull failure distribution are either localized or microscopic.

$$H_1; \quad R(L) \geq P_1 \quad (3.3)$$

The reliability for a container on test (the reliabilities above were for a container in service), for a test duration D, may be expressed as

$$R_{\text{Test}}(D) = \exp(-(fD/b)^c) \quad (3.4)$$

with the definitions

$R_{\text{Test}}(D) \equiv$  Reliability of a container on test

$D \equiv$  Reliability function at time (duration) D

$f \equiv$  Acceleration factor\*

$b \equiv$  Characteristic life

$c \equiv$  Weibull shape parameter

where Thomas [54] has provided for accelerated container life tests, mathematically, through the acceleration factor, f. This factor transforms the test duration, D (at the accelerated test conditions) to the "equivalent" in-service time (at repository conditions). A value of f greater than unity indicates that the test has been accelerated.

The above transformation in time was a simple scale change, whereas

---

\*Ratio of effective in-service time to actual time-on-test.



the transformation in reliability is not. The resulting relationship in reliability may be obtained by substituting the characteristic life parameter,  $b$ , from equation (3.1) into the container-on-test reliability expression, equation (3.4). Hence,

$$R_{\text{Test}}(t) = (R(t))^q \quad (3.5)$$

where

$$q = (fDIL)^c \quad (3.6)$$

The reliabilities corresponding to the hypotheses may readily be evaluated.

$$R_{\text{Test},0}(t) = (P_0)^q \quad (3.7)$$

$$R_{\text{Test},1}(t) = (P_1)^q \quad (3.8)$$

Thomas [54] shows that the probability of making a Type I error\* that is, accepting  $H_1$  when  $H_0$  is true, is equal to the product of all the success probabilities, where the success probability for a container is given by  $R_{\text{Test},0}$  in the case of the Type I error. Thus, the computed Type I error probability for  $n$  container tests is

---

\*See, for instance, Chapter 6 in Mann, et. al. [34] for further reading on the theory of testing reliability hypotheses.

$$\alpha = R_{\text{Test},0}^n \quad (3.9)$$

and similarly for Type II errors

$$\beta = 1 - R_{\text{Test},1}^n \quad (3.10)$$

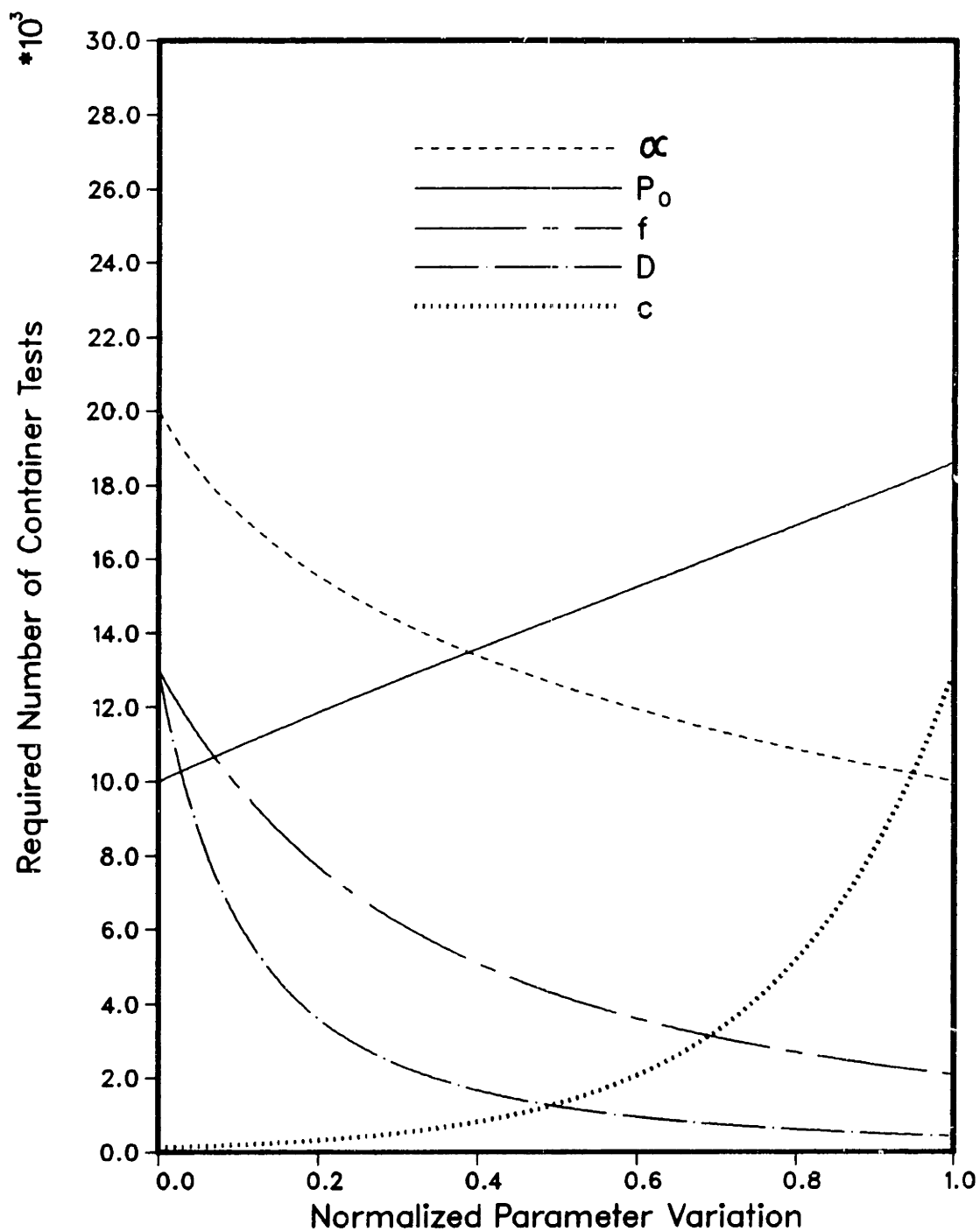
In a straightforward extension of the above, Thomas [54] assigns arbitrary maximum bounds on the probabilities of committing the Type I and Type II errors,  $\alpha$  and  $\beta$ , of  $\alpha^*$  and  $\beta^*$ , respectively, and develops the upper and lower bounding inequalities for specifying  $n$ , the number of tests which must be performed,

$$\frac{\ln(\alpha^*)}{\ln(R_{\text{Test},0})} \leq n \leq \frac{\ln(1 - \beta^*)}{\ln(R_{\text{Test},1})} \quad (3.11)$$

Indeed, if a solution exists for the above inequality, it is customary to select the minimum integer value greater than the lower bound. More complex approaches must be employed when no solution exists, and will not be discussed in this thesis.

Figure 3-1, present the results of the above under various assumed values for the parameters and acceptable probability assignments. As can be seen from the response to parameter variations exhibited, the most severe response is found in the variations of the shape parameter,

Figure 3-1: Test Requirements for Waste Containers  
 Based on a Weibull Failure Model  
 (after Thomas [52])



which was varied from one (Exponential Probability Density Function), and two (Rayleigh PDF). As it approaches the value three (off scale), the number of tests approaches two million. The reduction in tests provided by both  $f$  and  $D$  are prescribing more measurements at longer effective intervals. Hence, increases in  $f$  can be very misleading, as this presumes an exact knowledge of the relationship between the severely overstressed response in the component and the expected service environment behavior, which is seldom achieved. In fact, the most noteworthy "reliable" acceleration factor in engineering applications is observed in routine fatigue measurements, where predictable reductions in component life of 1/15 may be obtained. However, this statement must be qualified, as (1) analogous data at in-service conditions often exists for comparative evaluation, and (2) these estimates of times to failure already have large tolerances (uncertainties) built into the design. A confident acceleration factor of 10 is perhaps optimistic for the waste container.

The short life probability and the probability of making a Type I error, which is sometimes called the producers risk, are seen to have roughly the same effect for the ranges investigated. This has implications regarding the interpretation of applicable containment regulations. It must be cautioned that the approach is only valid for a single mode of failure.

### 3.1.2 Summary

The above sections indicate that there is quite a lack in the presently available techniques to develop effective test designs for the inherently long-lived component. This is probably due to the pervasive opinion that "Interpolation is generally regarded to be inherently 'safer' than extrapolation". There is a need to overcome these deficiencies in the context of the type of prediction problems encountered in the construction of such facilities and engineered components as in the nuclear waste repository described in Chapter 2. The methodology proposed and developed in this thesis provides one means for explicitly treating such long-lived components with a straightforward, albeit nonconventional approach to experiment design. The formal derivations follow in this chapter, while a practical test application is presented in Chapter 4.

### 3.2 MAXIMUM LIKELIHOOD APPROACH TO UNCERTAINTY ESTIMATION

For the design problem at hand, we are faced with the following:

1. Collection of all data relevant to waste container degradation by general corrosion.
2. Constructing a model which describes this process for the time interval over which the data were obtained.
3. Evaluating the uncertainty of model predictions extrapolated beyond the interval observations.

---

\*Christensen [8] p. 437.

4. Developing an experiment design methodology to generate data which is expected to reduce model prediction uncertainty most effectively.

The first task, data collection, is discussed in the following chapter, which addresses the application of uncertainty-optimized experiment design to the nuclear waste container life prediction problem. This chapter describes the general foundations of the methodology which was developed to accomplish the second, third and fourth tasks.

### 3.2.1 The Definition of Failure

One of the classic issues debated in reliability analysis is exactly how to define "failure" for the component under study. This is rather straightforward in the case of the instantaneous failure of a component while under demand. It is not as straightforward in the case in which the component undergoes steady degradation with an associated gradual decline in performance. Often, minimum performance specifications are prescribed and the component is said to have failed when a performance parameter falls below the threshold acceptable value. For the waste container, failure might be defined as container leakage and lifetime the time interval accumulated just prior to the onset of this leakage.

However, for the purpose of this investigation a definition of failure will *not* be postulated. Rather than adopting a single, design-specific definition of container failure (e.g. 4.0 cm of penetration by general

corrosion), methods will be developed considering the cumulative degradation incurred by the component through some specified design life goal. Justifications for making no definition of failure are:

- Any definition of failure under the single mechanism of general corrosion would be design specific, and as such a new definition of failure would be required for each container design iteration (e.g. 4.0 cm of penetration in a 10.0 cm thick container wall may constitute failure while a new cumulative failure penetration would have to be specified for a 12.0 cm container wall thickness).
- The bulk of container degradation and life test data is expected to be derived from material degradation tests, and little is expected to be generated by partial and/or full scale container (component) testing.
- Applicable regulations which normally provide a structure for developing component design requirements are not quantitatively specific and, as such are subject to interpretation.

An advantage of specifying the degradation rate as the dependent variable in the model is that it allows for incorporation of the projected in-service temporal behavior of the independent variables as functional expressions in the degradation rate law, or as discrete constant values over selected time intervals of interest.

### 3.2.2 Model Development as a Problem in Parameter Estimation

For generality, the degradation rate law (henceforth: rate law) must be able to assume any general functional form. This complicates the task of parameter estimation, as many simplified methods exist for linear models which are inappropriate for nonlinear models. Practically, for high reliability systems and components such as the waste container, knowledge of the physical process of degradation is not precisely known, and the functional form of the selected rate law may be incorrect. The presumption that the rate law chosen *is* correct, when not, may lead to an increase in the 'model, or structural uncertainty' component of the total uncertainty in predicted degradation. In this case a variety of functional forms may be compared by evaluation with the measured data. Furthermore, confidence in the selection of a functional form for the rate law may be heightened, *a priori*, by underpinning the form to that exhibited by similar physical processes.

The working hypothesis for the developments below will be to assume that the postulated model *is* of the correct functional form. This reduces the task of constructing a model suitable for the task of lifetime prediction to a problem of (nonlinear) parameter estimation.

The postulated model of the degradation rate,  $y$ , is a function of the independent variables (or, in the language of the experimentalist, the control variables),  $x_k$ , and the unknown parameters,  $b_j$ .



$$y = f(x_1, x_2, x_3, \dots, x_k; b_1, b_2, b_3, \dots, b_p) + \epsilon \quad (3.12)$$

The notation of capitals to indicate vectors is adopted, hence:

$$X = (x_1, x_2, x_3, \dots, x_k) \quad (3.13)$$

$$B = (b_1, b_2, b_3, \dots, b_p) \quad (3.14)$$

Thus the degradation rate may be more succinctly expressed as:

$$y = f(X; B) + \epsilon \quad (3.15)$$

The collection of available, relevant data will be referred to as the *model building database* and is represented as N observations of y and X, the n<sup>th</sup> of which is:

$$y_n, X_{1,n}, X_{2,n}, X_{3,n}, \dots, X_{k,n} \quad (3.16)$$

or just

$$y_n, X_n \quad (3.17)$$

We will assume that the expected value for the error (vector) is zero and that the errors for individual observations are independent hence, the expected value for y is:



The Libraries  
Massachusetts Institute of Technology  
Cambridge, Massachusetts 02139

Institute Archives and Special Collections  
Room 14N-118  
(617) 253-6888

This is the most complete text of the  
thesis available. The following page(s)  
were not included in the copy of the  
thesis deposited in the Institute Archives  
by the author:

pg. 89

$$E(y_n) = \tilde{y}(X_n; B) \quad (3.18)$$

where the tilda over the y is notation for the estimated value. A reference table of notation is provided in Table 3-1.

Making the assumption of normality, that is, the actual observed data exhibit a random, gaussian error about the expected value for y, the likelihood of observing all the measured data is given by the likelihood function

$$L(\sigma_n, B) = \prod_{n=1}^N (2\pi\sigma_n)^{-N/2} \exp \frac{-(y_n - \tilde{y}_n(B))^2}{2\sigma_n^2} \quad (3.19)$$

In the most ideal of situations an individual estimate of the gaussian standard deviation of each measurement in the model building database will be known. In practicality, it is often necessary to presume all the measurements possess a common standard deviation. This disadvantageous assumption may be improved upon pragmatically by employing other estimates of error. Examples of those commonly available even in relatively poor data situations are the calculated (expected) value for the dependent variable and the measured value. Often weighting of some common error value by the reciprocal of one or the other of these may result in an improved fit.

Maximizing the (above) likelihood relative to the parameter set, B, is mathematically equivalent to maximizing the natural logarithm of the likelihood with respect to the parameter set, B, and results in a more manageable system of equations,

$$L(\sigma_n, B) = \ln N(\sigma_n, B) \quad (3.20)$$

$$L(\sigma_n, B) = C + \sum_{n=1}^N \exp \frac{-(y_n - \tilde{y}_n(B))^2}{2\sigma_n^2} \quad (3.21)$$

As we are interested in obtaining the maximum of the above log likelihood function, we may arbitrarily assign the constant C to zero without loss of generality.

The system of equations derived by setting the parameter partial derivatives of the log likelihood function to zero is called the system of normal equations. There are P equations in P unknowns:

$$\frac{\partial L(B)}{\partial b_j} = \sum_{n=1}^N \frac{(y_n - \tilde{y}_n(B))}{\sigma_n^2} \frac{\partial \tilde{y}_n(B)}{\partial b_j}, \quad j=1, P \quad (3.22)$$

If we allow the B' to represent the maximum likelihood solution set of the B parameters,

$$\frac{\partial L(B')}{\partial b_j} = 0 = \sum_{n=1}^N \frac{(y_n - \tilde{y}_n(B'))}{\sigma_n^2} \frac{\partial \tilde{y}_n(B')}{\partial b_j} \quad (3.23)$$

Note also that the error sum of squares, SS(B), which is given by

$$SS(B) = \sum_{n=1}^N \frac{(y_n - \tilde{y}_n(B'))^2}{\sigma_n^2} \quad (3.24)$$

will assume its minimum value when the likelihood is maximum (compare equation (3.21)).

For the normal equations, an approach which leads to iterative solution may be obtained by assuming local linearity in the dependent variable - parameter space. This requires that the initial estimate of the B parameters be close to the solution B' values. Under these restrictions, we may expand a newly-defined function,  $z_j(B)$ ,

$$z_j(B) \equiv - \sum_{n=1}^N \frac{(y_n - \tilde{y}_n(B))}{\sigma_n^2} \frac{\partial \tilde{y}_n(B)}{\partial b_j} \quad (3.25)$$

as a Taylor series about the solution set B', hence:

$$z_j(B') \approx z_j(B) + \sum_{m=1}^P \frac{\partial z_j(B)}{\partial b_m} (b_m - b'_m) \quad (3.26)$$

At this point in the solution it is useful to improve upon the notation.

Define:

$$\Delta z_j \equiv Col(z_j(B') - z_j(B)) \quad (3.27)$$

$$P_{j,m} \equiv \begin{bmatrix} \frac{\partial z_1(B)}{\partial b_1} & \frac{\partial z_1(B)}{\partial b_2} & \dots & \frac{\partial z_1(B)}{\partial b_m} & \dots & \frac{\partial z_1(B)}{\partial b_p} \\ \frac{\partial z_2(B)}{\partial b_1} & \frac{\partial z_2(B)}{\partial b_2} & \dots & \frac{\partial z_2(B)}{\partial b_m} & \dots & \frac{\partial z_2(B)}{\partial b_p} \\ \frac{\partial z_j(B)}{\partial b_1} & \frac{\partial z_j(B)}{\partial b_2} & \dots & \frac{\partial z_j(B)}{\partial b_m} & \dots & \frac{\partial z_j(B)}{\partial b_p} \\ \frac{\partial z_p(B)}{\partial b_1} & \frac{\partial z_p(B)}{\partial b_2} & \dots & \frac{\partial z_p(B)}{\partial b_m} & \dots & \frac{\partial z_p(B)}{\partial b_p} \end{bmatrix} \quad (3.28)$$

$$\Delta B_m \equiv \text{Col}(b_m - b_m') \quad (3.29)$$

We may rewrite equation (3.24) as

$$\Delta Z_j = P_{j,m} \Delta B_m \quad (3.30)$$

Thus, the correction vector may be expressed as:

$$\Delta B_m = P_{j,m}^{-1} \Delta Z_j \quad (3.31)$$

The expanded form for a general element of the  $P^{-1}$  matrix is

$$P_{j,m}^{-1} = \left[ \begin{array}{ccc} N & \frac{\partial y_n(B)}{\partial b_m} & \frac{\partial y_n(B)}{\partial b_j} \\ \sum_{n=1}^N \frac{1}{\sigma_n^2} & & - \frac{\partial^2 y_n(B)}{\partial b_m \partial b_j} (y_n - y_n(B)) \end{array} \right]^{-1} \quad (3.32)$$

With an obvious extension in notation an iterative solution may be obtained simply by allowing for successive corrections on the B parameter set. Thus:

$$B_{i+1} = B_i + \Delta B_i \quad (3.33)$$

until some preset convergence criterion is met. Actually, convergence may be specified for the error sum of squares, on the parameters or preset for each parameter individually.

This local linearization technique has some drawbacks. The most notable is the relatively slow convergence. This is especially true of parameter spaces which possess broad, shallow minima. Various schemes have been suggested to combat the slow approach to convergence. In the cases of the broad, shallow minima, Box\* recommends reducing the calculated correction vector if the error sum of squares has been reduced in the iteration, and increasing the correction vector when the error sum of squares has been increased.

As can be noted from the above procedure, the parameter partial derivatives play a key role in arriving at the parameter solution set.

---

\*For further reading on empirical methods to combat the above and other drawbacks of these problems related to convergence, see Draper and Smith [15].

If these derivatives must be evaluated numerically (as some functional forms mandate), much machine time will be dedicated to this chore alone in a problem of substantial size and with large amounts of data. It is a benefit, from the numerical aspects of the procedure alone, to provide analytical derivatives along with the rate law functional form when possible.

With the formalism for model construction in place, it is now possible to analyze the resultant propagation of error which accompanies prediction in time, or "forecasting" with the model.

### 3.2.3 Extrapolation and Error Propagation

By way of review, what has been done in the above section is to apply the principle of maximum likelihood to a generalized rate law,  $y$ , assuming that the existing set of observations for the rate law, (the *Model Building Database*), is a subset of a population which obeys a gaussian error distribution. The principle of maximum likelihood postulates that the likelihood function, which is defined as the grand product of all these individual distributions at each observation, when maximized by the proper choice of parameters, yields statistics for which the observed state of affairs is most probable.

If the data is very noisy, exhibits much error, the likelihood function will be shallow and possibly possess many local minima, but if the data exhibit a central tendency about the expected value of the rate



law, the likelihood function will possess a sharp peak. Fisher [16] was responsible for calling the curvature of the likelihood function near the maximum the "information value" of the data\*.

The matrix given in Equation 3.25 is often called the Fisher Information matrix. When estimates of the B parameter set are obtained by general maximum likelihood techniques as was done above, this matrix is the asymptotic covariance matrix for B'. It can be easily shown that the diagonal elements of this matrix are the individual parameter variances. These mathematical relationships and some approximations are presented as follows.

For any function  $h$  which depends upon the random variables  $b_1, b_2, \dots, b_p$ ,

$$h = f(b_1, b_2, \dots, b_p) \quad (3.34)$$

we may express the variance, by definition, as:

$$\text{Var}(h) = E ((h - E(h))^2) \quad (3.35)$$

We will denote  $E(h)$  as  $\tilde{h}$  as was done previously. Maintaining

---

\*This definition of information has led to much confusion with a completely different definition of information arising in the communication engineering discipline ( $n \cdot \ln(n)$ ) which is more widely familiar. In fact, Christensen [8] advocates the alternative term "evidence" for this curvature about the maximum in lieu of "information"

consistency with the development of maximum likelihood estimates above, we will assume the expected value of the arbitrary function  $h$  is approximated well by (is equal to) the function  $h$ , evaluated at the maximum likelihood  $b'_j$  values.

Once again drawing on Taylor's formula to expand the function of interest, we may approximate the argument of the variance defined above, which we now denote  $g(B)$ , explicitly noting the functional dependence on the  $b_j$ , denoted by the vector  $B$ ,

$$g(B) \equiv (h - \tilde{h}(B'))^2 \quad (3.36)$$

Hence

$$g(B) = g(B') + \sum_{i=1}^P (b_i - b'_i) \frac{\partial g(B')}{\partial b_i} + \sum_{i=1}^P \sum_{j=1}^P (b_i - b'_i) (b_j - b'_j) \frac{\partial^2 g(B')}{\partial b_i \partial b_j} \quad (3.37)$$

With the relevant partial derivatives

$$\frac{\partial g(B')}{\partial b_i} = 2(h - \tilde{h}(B')) \frac{\partial h}{\partial b_i} \quad (3.38)$$

$$\frac{\partial^2 g(B')}{\partial b_i \partial b_j} = 2 \frac{\partial h}{\partial b_i} \frac{\partial h}{\partial b_j} + \frac{\partial^2 h}{\partial b_i \partial b_j} \quad (3.39)$$

This yields an approximate variance of

$$\begin{aligned}
\text{Var}(h) &= E((h - \tilde{h}(B'))^2) + 2 \sum_{i=1}^P (b_i - b'_i) (h - \tilde{h}(B)) \frac{\partial h}{\partial b_i} + \\
&\sum_{j=1}^P \sum_{i=1}^P (b_j - b'_j) (b_i - b'_i) \frac{\partial h}{\partial b_i} \frac{\partial h}{\partial b_j} + \\
&\frac{\partial^2 h}{\partial b_i \partial b_j} (h - \tilde{h}(B')) \tag{3.40}
\end{aligned}$$

With the parameter errors  $(b_i - b'_i)$  replaced with  $\sigma_{bi}$  the variance becomes

$$\begin{aligned}
\text{Var}(h) &= E((h - \tilde{h}(B'))^2) + 2 \sum_{i=1}^P \sigma_{bi} (h - \tilde{h}(B)) \frac{\partial h}{\partial b_i} + \\
&\sum_{j=1}^P \sum_{i=1}^P \sigma_{bj} \sigma_{bi} \frac{\partial h}{\partial b_i} \frac{\partial h}{\partial b_j} + \frac{\partial^2 h}{\partial b_i \partial b_j} (h - \tilde{h}(B')) \tag{3.41}
\end{aligned}$$

Maintaining the original assumptions on  $h$  all the  $h - \tilde{h}(B')$  terms vanish, yielding

$$\text{Var}(h) = \sum_{j=1}^P \sum_{i=1}^P \sigma_{bj} \sigma_{bi} \frac{\partial h}{\partial b_i} \frac{\partial h}{\partial b_j} \tag{3.42}$$

Comparing equation (3.42) with (3.32), we note the parameter second partial derivative term missing from the general variance expression, but maintained in the specific case. When the MLE solution to the parameter set is employed, however, this term vanishes. The resultant

$P$  matrix, the inverse of which we will call the "Error Matrix". This matrix is symmetric. The diagonal elements are the individual parameter uncertainties  $\sigma_{b_j}^2$  and the off-diagonal elements are the covariance terms  $\sigma_{b_i b_j}^2$ .

This leads to the standard relationship for evaluating the variance in our arbitrary function  $h$  as follows. If we define the row vector  $S$  as the  $P$  first partial derivatives of  $h$  with respect to  $b_j$ , the following well known relationship applies:

$$\sigma_h^2 = S P_{j,m}^{-1} S^T \quad (3.43)$$

Note the individual observation standard deviations,  $\sigma_n^2$ , may be (and will often have to be) assumed equivalent (homogeneous variance) and will just become a constant scalar multiplier. The appearance of the second partial term in equation (3.21) arises from the solution technique for the MLEs which was used and the particular assumption of a gaussian error distribution. In fact, this term is ultimately dropped from the numerical algorithm for error propagation as it is found to hinder convergence, and, within the accuracy of the data employed in the application to waste container degradation, is unnecessary.

For an extremely high reliability component, we are concerned with obtaining an estimate of the time-integrated degradation and the

associated uncertainty at some target design life goal. Furthermore, it is assumed that we possess some knowledge of the in service environment. Specifically, we must have a projection of the time dependent behavior of the independent variables in the rate law model.

We will define the target design life goal as  $t_d$  and the integrated degradation to the component as the accumulated damage,  $D$ . Hence, evaluated with the maximum likelihood parameter solution set:

$$D(B') \equiv \int_0^{t_d} y(X(t); B') dt \quad (3.44)$$

The accumulated damage becomes the relevant function for which we must evaluate the uncertainty. The relevant parameter partial derivative is given by:

$$\frac{\partial D(B')}{\partial b'_j} = \int_0^{t_d} \frac{\partial y(X(t); B')}{\partial b'_j} dt \quad (3.45)$$

The uncertainty in the accumulated damage at extrapolated design life  $t_d$  is given by:

$$\sigma_D = \sum_{j=1}^P \sum_{m=1}^P \frac{\partial D(B')}{\partial b'_j} \frac{\partial D(B')}{\partial b'_m} P_{j,m}^{-1} \quad (3.46)$$

Hence a  $2\sigma$  equitailed confidence interval for  $D$  is:

$$(D - 2\sigma_D, D + 2\sigma_D) \quad (3.47)$$

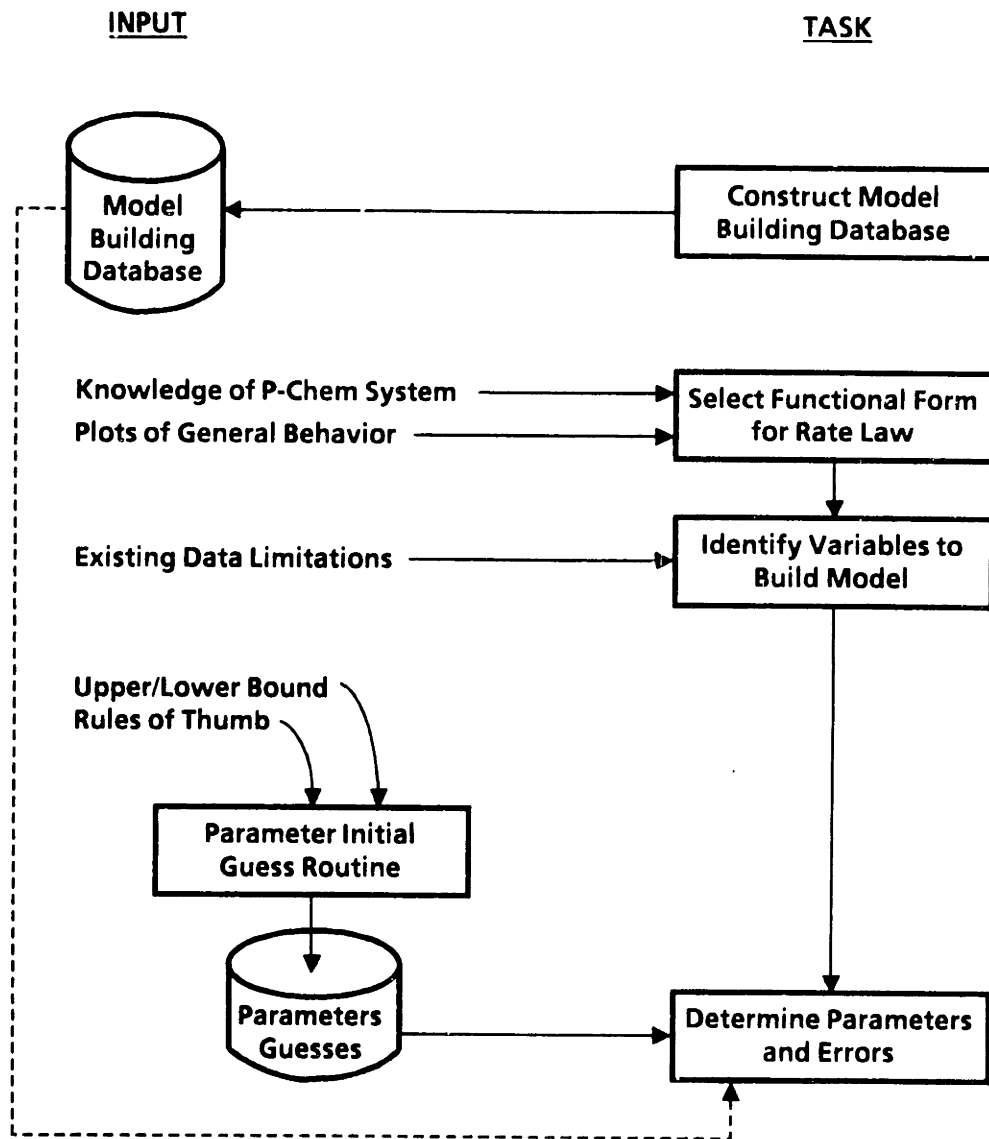
### 3.3 EXPERIMENT DESIGN: APPROACH

With both model development and uncertainty prediction techniques theoretically established in the previous sections, the overall logic for the design of uncertainty-optimized experiments can now be presented.

Figure 3-2 presents a simplified logic diagram outlining the steps in model development, including the pragmatic concerns under the column labeled "Input". As has been mentioned before (task 1 of section 3.2) the *model building database* must be constructed from all data relevant to the degradation process. This database must specifically include the degradation rate behavior at explicit times and corresponding control variable information. The model building database is the singly most important input required, hence a rigorous evaluation of the *relevance* of the data to the expected in-service environment must be performed. At this point, however, no data should be ruled out for reasons other than relevancy. The database should be pruned of "bad" data points only after its individual measure of error may be compared to estimates of deviation for the total population of data.

A rate law functional form(s) must be specified. As has been mentioned numerous times, this step requires sound underpinning to

Figure 3-2: Logic Diagram for Model Development



theoretical expectation. Knowledge of the physical-chemical system must be brought to bear on this identification. In recent studies of the reliability of various nuclear power plant systems and components, the idea of component "aging" while in service has enjoyed much interest. Carfagna and Gibson [7] have reviewed equipment aging theory and technology. They present a variety of general rate law functional forms for component aging, and discuss the applicability of these to the aging (degradation) of materials and devices in service in the nuclear industry. Based on this review, two general rate laws (Arrhenius and Eyring) are presented in Table 3-2.

It is not surprising that successful application of such first-principle models are usually achieved for rather simple, thermally-controlled degradation processes which are frequently chemical in nature. These formulations represent the endpoint of simplicity in degradation theories, and their unmodified use is likely to be the exception, not the rule. Most often, the rate law will be application-specific and the device and degradation phenomena will dictate the type and sophistication of the model employed.

After specifying the rate law functional form, the next task is to determine the important independent variables from which the model will be constructed. Often, in standard statistical analyses (e.g. regression analyses) these tasks are reversed. The formalism here



**Table 3-2:** The Arrhenius and Eyring Rate Law Models

---

---

THE ARRHENIUS MODEL

The Arrhenius model is usually applied to thermal aging in the form

$$R = B(t)e^{\phi/kT}$$

where:

R = Reaction rate

B(t) = Prefactor (usually a function of time)

$\phi$  = activation energy (eV)

k = Boltzmann's constant ( $0.8617 \times 10^{-4}$  eV/K)

T = absolute temperature (K)

THE EYRING MODEL

The Eyring model provides a thermodynamically more correct formulation and may include additional (nonthermal) stress terms.

$$R = aT^w \exp \frac{b}{kT} \exp \left[ \left( c + \frac{d}{kT} \right) f(S) \right]$$

where:

R = Reaction rate in the presence of applied stress

k = Boltzmann's constant

T = absolute temperature

a, b, c, d and w = experimentally determined constants  
independent of time, temperature,  
and stress

f(S) = a function of the applied stress

S = the applied stress

---

---

requires that the overall physical mechanism be understood first and the functional form of the rate law be accepted as correctly representing the physical process.

The independent variables are to be functionally incorporated into the rate law through modifying the value of some "characteristic dimension" of the system. This means, for example, that the solution chemistry, measured for instance as pH, might be incorporated into an Arrhenius rate law by altering the activation energy term. The activation energy term is thereby viewed as a "characteristic dimension" of the process model.

The importance of making a prudent initial guess for the parameter solution set cannot be overemphasized, especially in light of the local linearity assumption made in developing the algorithm for solving for the parameter correction vector. Utility computer programs may easily be written to facilitate exploration of the parameter space interactively. This is also the stage to incorporate engineering/scientific judgement in the overall model development scheme. This may take the form of constraint on parameter ranges to within bounding estimates of the rate behavior.

Still referring to the logic diagram Figure 3-2, the final calculations can be made and the model parameter solution set

determined, based on the theoretical approach presented in section 3.2. The fitting algorithm which solves the normal equations for the parameter solution set will be discussed in more detail below.

### 3.4 EXPERIMENT DESIGN: SIMULATION AND EVALUATION

Many mathematical/statistical techniques exist for the design of optimal experiments. The numerous techniques used in optimality theory for the design of experiments differ primarily in the distributional assumptions and the specific optimality criteria.

Harper [28] surveyed various classical methods of designing fixed, preplanned optimal experiments. In his thesis, Harper [28] proposes the use of algorithms which adapt the classical approaches of optimality theory to sequential experiment design. That is, design techniques which allow modification (or updating) of the fixed design after some fraction of the data has been obtained. This work was developed in the context of the "shelf life" problem and involved a short-lived perishable product as compared to a high reliability engineered component. Also, the above work was developed only for interest in binary acceptance data presumed to obey a logistic model.

The work presented herein is also an adaptive approach to experiment design but is unique in that there is never any "fixed" experiment design, generated *a priori*, upon which to iterate. Rather, the state of knowledge is assessed, by model construction from the model building

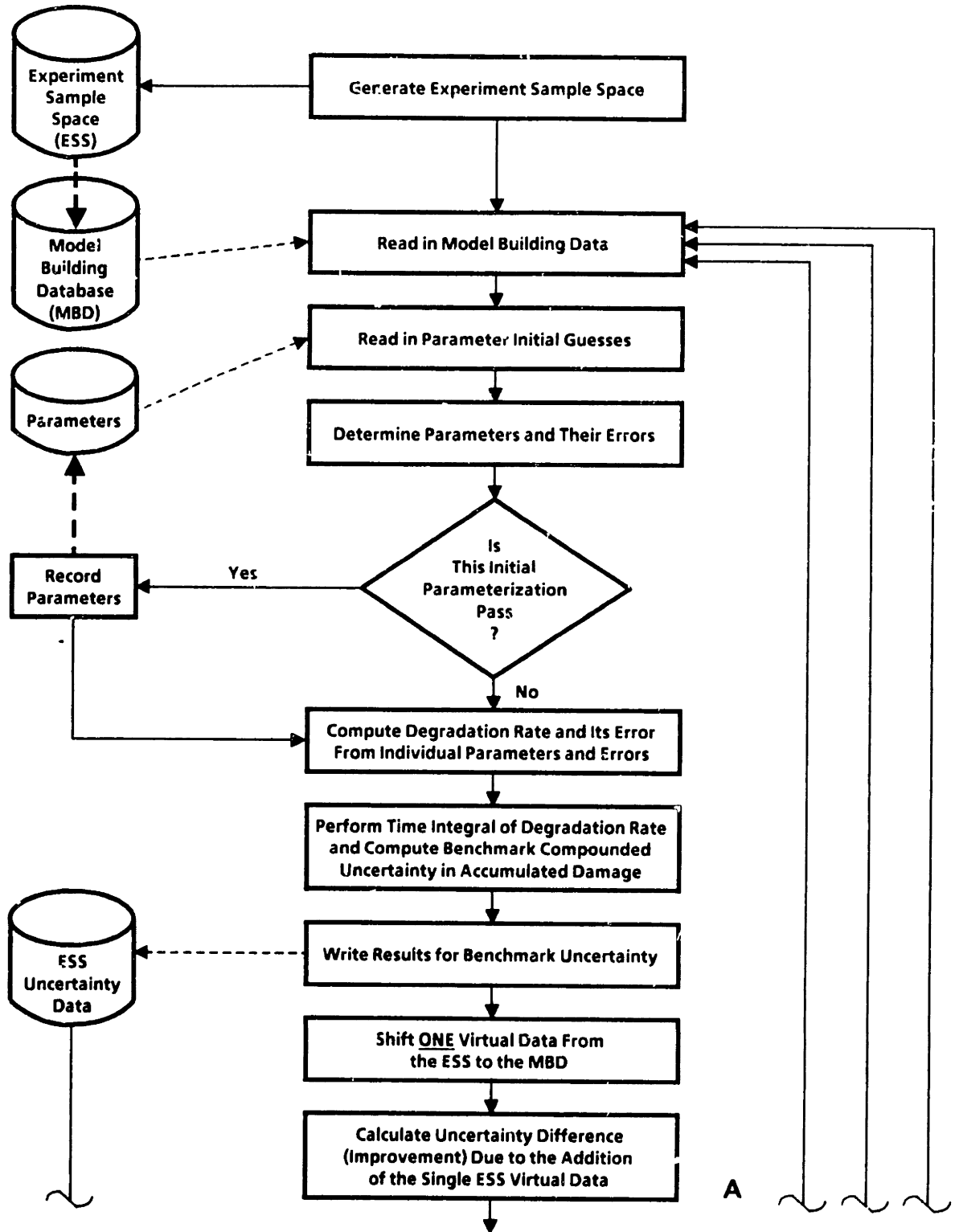
database, and a large collection of potential experiments are individually evaluated for their contribution to uncertainty reduction at the design life goal.

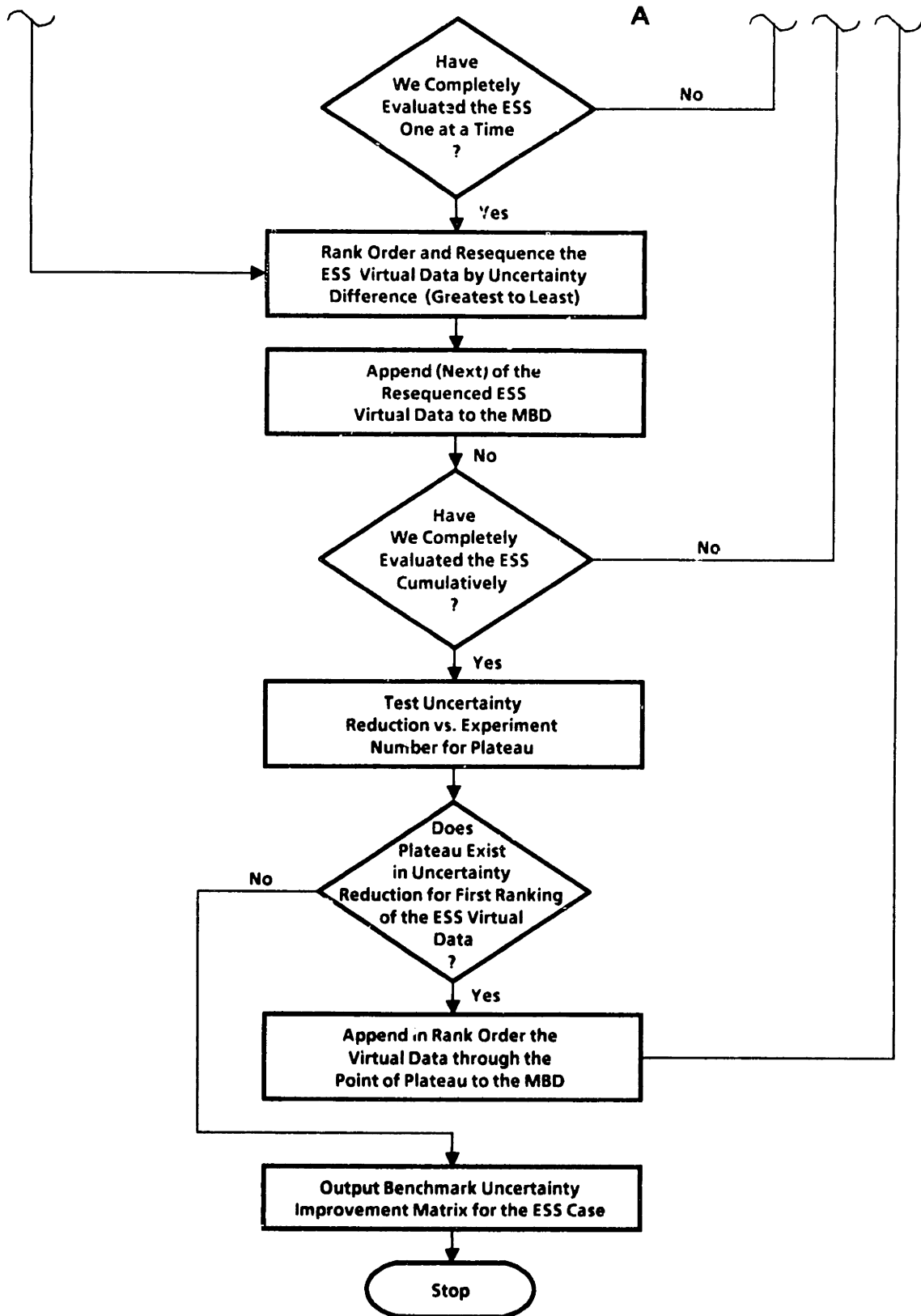
Figure 3-3 is a flowchart of the UNODEX computer program for the UNcertainty-Optimized Design of EXperiments. A source listing of the program written for this work, appears in Appendix C along with users documentation. The following sections describe the logic of the overall program and make numerous references to Figure 3-3.

#### **3.4.1 Construction of the Experiment Sample Space**

The first step in the design of uncertainty-optimized experiments is to construct the Experiment Sample Space (ESS). The ESS is a large set of candidate experiments established by restricting each of the Independent Variables (IVs) to a range such that the same mechanisms that are operating in the in-service environment will prevail. This is accomplished by reading (from a file) the preset bounds on each of the independent variables (IVs) and generating a specified number of discrete levels that the IV may assume between and including the bounding values. This is done for each of the IVs, thereby generating all combinations of IV levels. The Dependent Variable (DV) - degradation rate - is evaluated directly from the rate law using the maximum likelihood parameter estimates for each of the combinations generated and included in the ESS. These data in the ESS will be

Figure 3-3: Flowchart for Uncertainty Optimized Experiment Design





referred to as 'virtual' data as they are simulated by the fitted rate law. An error must be introduced and assigned to each of the virtual data points in the ESS so as to yield meaningful uncertainty reduction estimates.

Note that the set of experiments which are generated for the ESS need not be limited to the range of expected in-service conditions if no evidence exists which indicates that exceeding that range leads to significant departure from the expected governing physical and chemical processes. Thus this methodology directly addresses the role and feasibility of accelerated life testing.

Once the ESS is generated and saved, the maximum likelihood parameter estimation algorithm is activated (just as was done to determine the parameters). This algorithm is called FITSALL and solves the  $P$  normal equations for the incremental correction to the parameter initial guesses, equations (3.20). This algorithm is dynamically dimensioned and can solve multivariable, multiparameter nonlinear functional forms provided in the function  $Y0$  (the rate law). The convergence criteria are specified as a Cauchy convergence, that is the incremental change in an iteration, on the error sum of squares or on the parameters themselves. There are various other input controls which are fully documented in the appendix.

Upon determining the parameters and their errors on the initial model building pass, as was described in section 3.3 and in Figure 3-2, the parameter solution set is recorded in a file to be input as later guesses. The degradation rate law is fully specified by the function and the parameter solution set.

On the initial pass, the accumulated damage and associated uncertainty is estimated at the design life goal by the theoretical technique in 3.2.2. These serve as the reference values of damage and uncertainty for pointwise uncertainty reduction computations. They are also saved as a benchmark, or reference values for later comparison. The initial pass is complete at this point.

### **3.5 EXPERIMENT DESIGN: OPTIMIZATION**

The second phase of UNODEX begins by "shifting" the first data point representing a candidate experiment to be entered from the ESS into the Model Building Database (MBD). In this sense data (both IV and DV) representing the first potential experiment are incorporated into the actual MBD as though actually measured. We will refer to this as simulation of an experiment and the data will be termed virtual data. Then with the MBD plus one virtual data point, the maximum likelihood parameter estimation algorithm is activated to determine updated parameters, reflecting the addition of this additional virtual data point.



The starting guesses for the parameters are the solution set which was saved in the first pass. Hence, convergence is usually rapid due to the small contribution of a single data point. The procedure is repeated for each of the virtual data in the ESS. At the end of this pointwise uncertainty estimation, the ESS is sorted and rewritten in the order of greatest to least reduction in estimated uncertainty reduction. Hence, the variable which is ranked is

$$\Delta U = \sigma_D - \sigma'_D \quad (3.48)$$

In the above expression,  $\sigma_D$  is the uncertainty in penetration using the MBD only, and  $\sigma'_D$  is the uncertainty in penetration using the MBD + the *one* virtual data being evaluated. The final phase of the experiment design optimization is the evaluation of the uncertainty behavior at the design goal for the entire, resorted ESS. Experiments are added (without replacement) one-at-a-time from the ESS in the order determined to yield greatest to least improvement and the uncertainty reduction is calculated after each addition. This means that the final computation determines the improvement in projected uncertainty for the addition (simulation) of the first virtual experiment, then the first and second, then the first, second and third, *etc.*; until the entire ESS has been accumulated. The result of this calculation is a reduction-in-uncertainty profile dependent upon the amount of experimentation.

This type of information can allow the experimental planner to obtain an estimate of the testing requirements for a predetermined, acceptable uncertainty in accumulated damage at the design goal. The converse is also true in that an estimate of the uncertainty may be obtained for a given practical limit on experimentation.

It must be emphasized here that the above type of information must serve as a guide to experimental planning and not an absolute measure of the required number of tests, as

- The matrix employed to solve for the maximum likelihood parameter estimates was the asymptotic (infinite population) covariance matrix
- Local linearization may not be an adequate assumption, especially for poor initial parameter guesses
- Estimates of error for the virtual data may be superior to (less than) that actually obtained by measurement

### 3.6 SUMMARY

The previous chapter has laid the theoretical groundwork for the design of uncertainty-optimized experiments. The method is iterative and adaptive and provides a quantitative measure of an experiment's information value under the constraints and requirements of the application and in-service environment for the component under evaluation. It is a comparative method in that the asymptotic covariance matrix is used to determine the extrapolated uncertainty.

Hence, it determines the best calculable bound to the uncertainty and not an absolute measure.

The methodology has been presented in the most general sense, for any component-environment system experiencing gradual degradation in time. In the next chapter, the specifics of the particular application problem of interest, nuclear waste container life predictive testing, are introduced.

## 4. UNCERTAINTY-OPTIMIZED PREDICTIVE TESTING FOR A NUCLEAR WASTE CONTAINER

This chapter presents the application of the uncertainty-optimized experiment design technique to waste container penetration by general corrosion. Evaluation and assembly of the relevant data into a model building database is described, as well as the experimental methods used to obtain these data. Model development is presented, along with justification for the model's applicability and level of detail. The key task of assigning uncertainty to the virtual (or simulated) data in the experiment sample space is also discussed. Finally, a quantitative evaluation of the reduction of waste container penetration uncertainty at 300 and 1000 years is performed, yielding insight into the type and order of experiments which should be performed to reduce uncertainty most effectively.

### 4.1 THE EXPERIMENTAL DATA

Overwhelmingly, the body of experimental data describing the general corrosion rate of a low carbon steel in brine with compositions within the range identified in bedded halite formations has been directly commissioned by geologic nuclear waste isolation activities.

Data obtained by reviewing the technical literature have been found to be deficient in reporting the precision in principle independent variables, such as is the case pertaining to corrosion of chemical

process equipment wherein only a range of chemical conditions may be known and reported. The balance of the literature-obtained data are found to differ substantially from expected repository conditions in one or more of the independent variables.

This section serves as a review of the accessible data generated by nuclear waste disposal programs, describing the tests employed, the experimental conditions and relevance to this work.

#### **4.1.1 Immersion General Corrosion Tests**

In response to a need for standard methods to generate reliable and reproducible data measuring properties of materials used for permanent nuclear waste isolation, the US Department of Energy established the Materials Characterization Center (MCC) at Pacific Northwest Laboratory. The MCC draws upon related standard test methods such as those established by the American Society for Testing Materials (ASTM), among others. The MCC also develops new procedures and approves modifications to standard procedures where the special concerns of nuclear waste isolation require unique treatment.

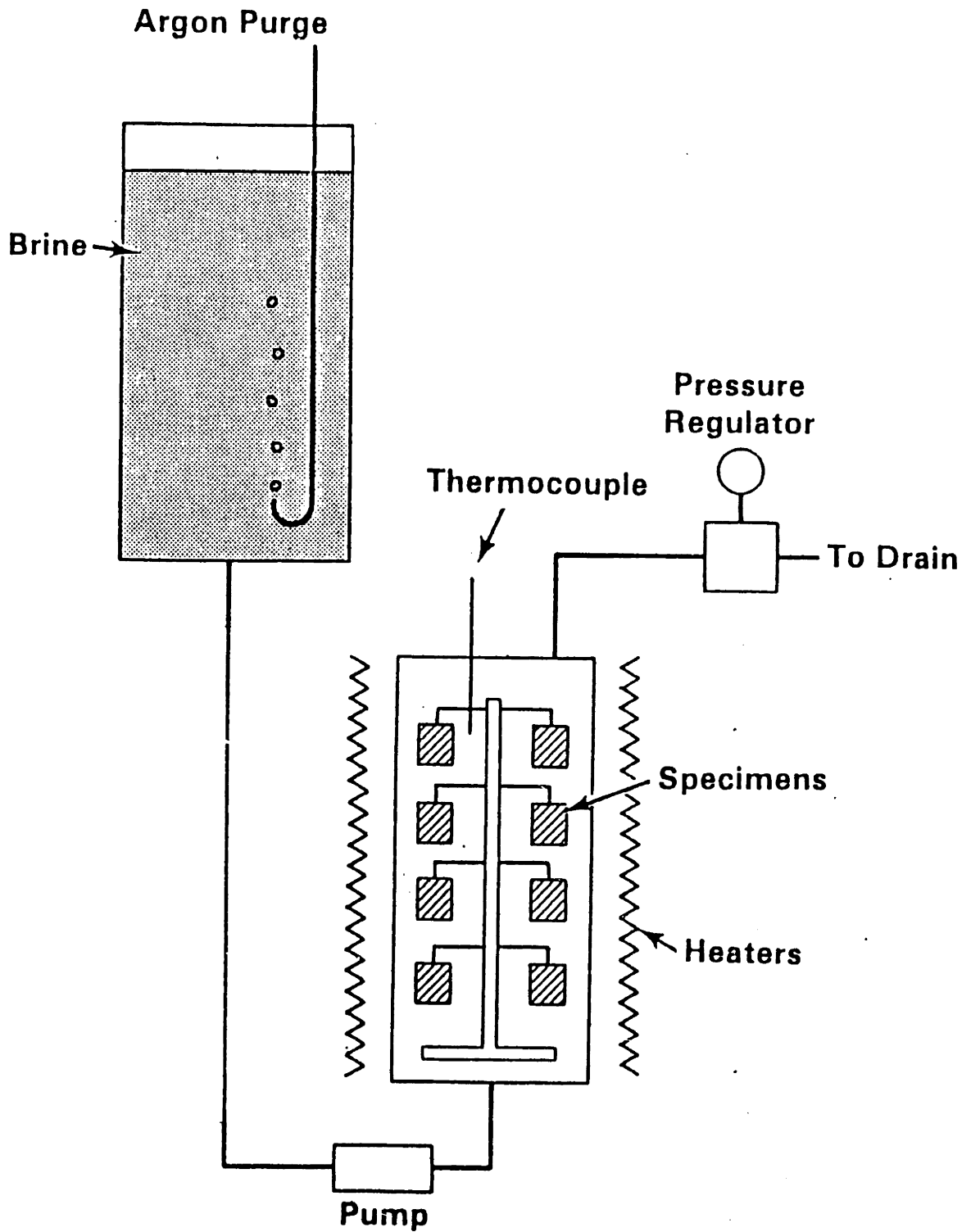
Two test methods have been developed by the MCC for evaluating both general and localized corrosion behavior of laboratory-scale specimens of waste container structural barrier materials exposed to flowing and static simulated groundwaters [36]. These tests are numbered MCC102s and MCC101s, respectively.

The autoclave system is illustrated in Figure 4-1. As indicated in the figure, corrosion specimens reside within a heated autoclave during the test. The specimens are well separated and the total surface area of specimen surface, hence, the number and size of the specimens, is determined by the autoclave volume. Brine, which is maintained anoxic by an argon purge system, is pumped through the autoclave, entering at the bottom of the vessel and exiting at the top head. Pressure and temperature are instrumented through the head.

The tests differ only in that the static immersion test allows for no solution (electrolyte) to enter or leave the autoclave during the test. The intent of the static test is to represent conditions where corrosion products are not removed from the corroding surface due to any flow mechanism. The flowing test specifies a solution refresh flow rate of roughly one vessel volume per day. The imposition of flow intends to control the electrolyte chemistry so as to be constant and to provide for the removal of corrosion products which are weakly adherent. The flowrate is not intended to simulate expected repository conditions.

The only variables which are controlled are the temperature of the autoclave and contents, and the flowrate of the solution. Both are maintained constant for the duration of the test. The other variables which could potentially affect the corrosion rate, notably the amount of dissolved oxygen and solution pH, are measured prior to the test but not

Figure 4-1: Schematic Diagram of the Immersion General Corrosion Test System



controlled. A large sealed reservoir of solution is maintained at relatively anoxic conditions by an argon purge system. The test methods specify the composition of reference electrolyte solutions which are derived from analyzed brines obtained from boreholes in the vicinity of the candidate Deaf Smith County, Texas salt repository site.

There are some slight deviations from the actual composition of the analyzed brines and those used in corrosion experiments. Permian Basin Brine 2, which was used for most of the immersion general corrosion tests, is essentially the same composition as Permian Basin Brine 1, (PBB1 in Chapter 2) with the calcium carbonate reduced by nearly 30 percent to avoid plugging of the refresh lines at the cooler points in the loop. Calcium carbonate has not been associated with a specific effect on general corrosion, hence this modification is not expected to alter the corrosion mechanisms. The balance of the test procedure is largely standard to aqueous autoclave general corrosion testing\*.

Both static and flowing test methods advise investigation of various oxygen concentrations appropriate to expected barrier-repository conditions over the life of the barrier. The methods specify the ratio of test vessel capacity to total surface area of the specimen array.

---

\*See, for example NACE TM-01-71, Autoclave Corrosion Testing of Metals in High-Temperature Water



The corrosion data derived from such tests are entirely gravimetric in nature. Weight loss measurements are obtained after removal of corrosion products and from this direct measurement, the uniform penetration (weight loss averaged over the reacting surface) and average uniform penetration rate (uniform penetration divided by test duration) may be determined.

Microscopy and corrosion product analysis are also routinely performed at test termination.

#### **4.1.2 Excess Salt Tests**

The excess salt tests are, at the time of this writing, not documented to the level of detail of the above MCC immersion tests. Both excess salt tests were developed to evaluate the general corrosion behavior of laboratory-scale specimens of barrier materials in the presence of repository-like solid halite. The intent was to evaluate this corrosion behavior in an environment which more closely simulated the expected conditions at the waste container boundary, in which no appreciable flow conditions exist and where the corrosion product material remains in contact with the active metal, whether adherent or not, due to the presence of solid phase salt adjacent to the corroding metal. There are two basic methods of performing this type of test, in welded closed test canisters, or in an autoclave.

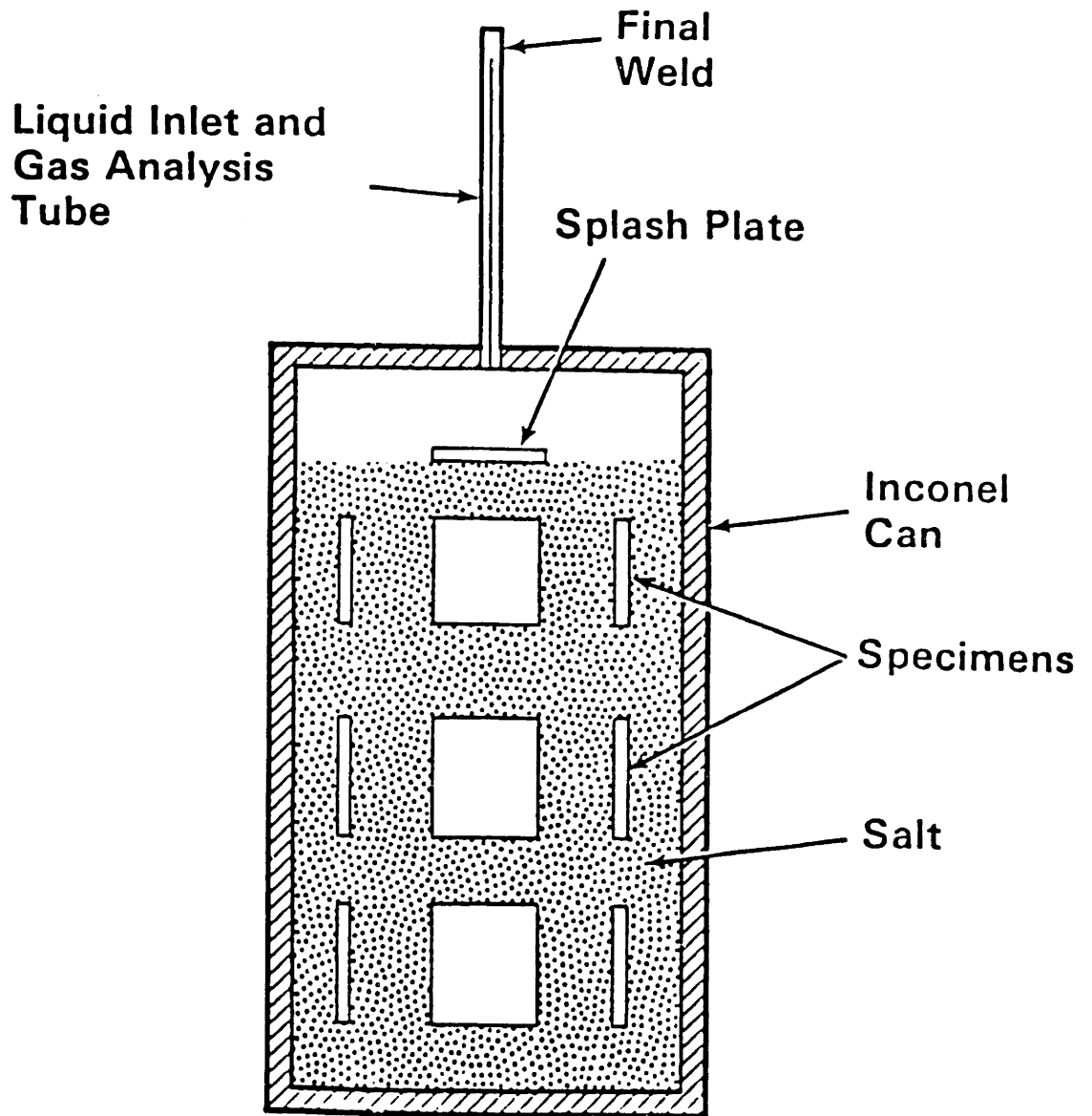
#### 4.1.2.1 Static Excess Salt Tests

General descriptive information is available for the static excess salt tests [61] accompanying the reporting of results from such tests. The test containers are newly fabricated of Inconel 600 or other suitably corrosion-resistant material and disposed of at the conclusion of the test. The Static Excess Salt Test is represented schematically in Figure 4-2.

These containers are loaded with predried solid salt and corrosion specimens as shown in the figure. The specified moisture is arrived at by fluid addition (by either brine or water) to the dry salt-specimen array through a liquid inlet tube which penetrates the top of the cylinder. The final closure weld is performed immediately following this fluid addition under inert conditions.

The experiment is run for a fixed time-at-temperature and is, other than the temperature, uncontrolled for the duration of the test. The strength of this type of test is that it can more closely simulate the expected conditions of a waste container exposed to a predominantly anoxic, static brine environment. The weakness of this type of test is that the test may not be controlled as readily as those performed in an autoclave and has not been instrumented so as to measure control variables other than temperature.

Figure 4-2: Schematic Diagram of the Static Excess Salt Test System



This type of test is a lower cost test than the immersion tests, because there is no requirement for the use of an autoclave. Instrumenting the test is precluded by design (sealed disposable test containers) and any penetrations into the test vessel would pose a safety hazard.

The brine solution pH is measured before (at the time of preparation) and after the test termination. Dissolved oxygen content of the solution added to the salt-specimen array is known only at the time of brine preparation, however, it should be noted that the brines are maintained in anoxic conditions from the time of preparation until use.

The static excess salt test yields standard gravimetrically-derived average uniform penetration rate data and standard corrosion product information.

#### **4.1.2.2 Autoclave Static Excess Salt Tests**

This type of test was also developed at Pacific Northwest Laboratories to measure the corrosion of fully-saturated salt environments. The test is essentially the same as the Static Excess Salt Tests with the additional feature of allowing specimens to be removed and the test resumed with minimal disturbance to the balance of the corrosion specimens. The Autoclave Excess Salt Test is illustrated Schematically in Figure 4-3. This system is not pumped like the immersion tests. Small, titanium, cuplike vessels are used to hold the corrosion

specimens, packed in dried, solid phase salt much like the static excess salt tests. These specimen holders are supported by an insulated test stand within the autoclave. The autoclave is filled with brine and maintained at pressure and temperature for the entire test.

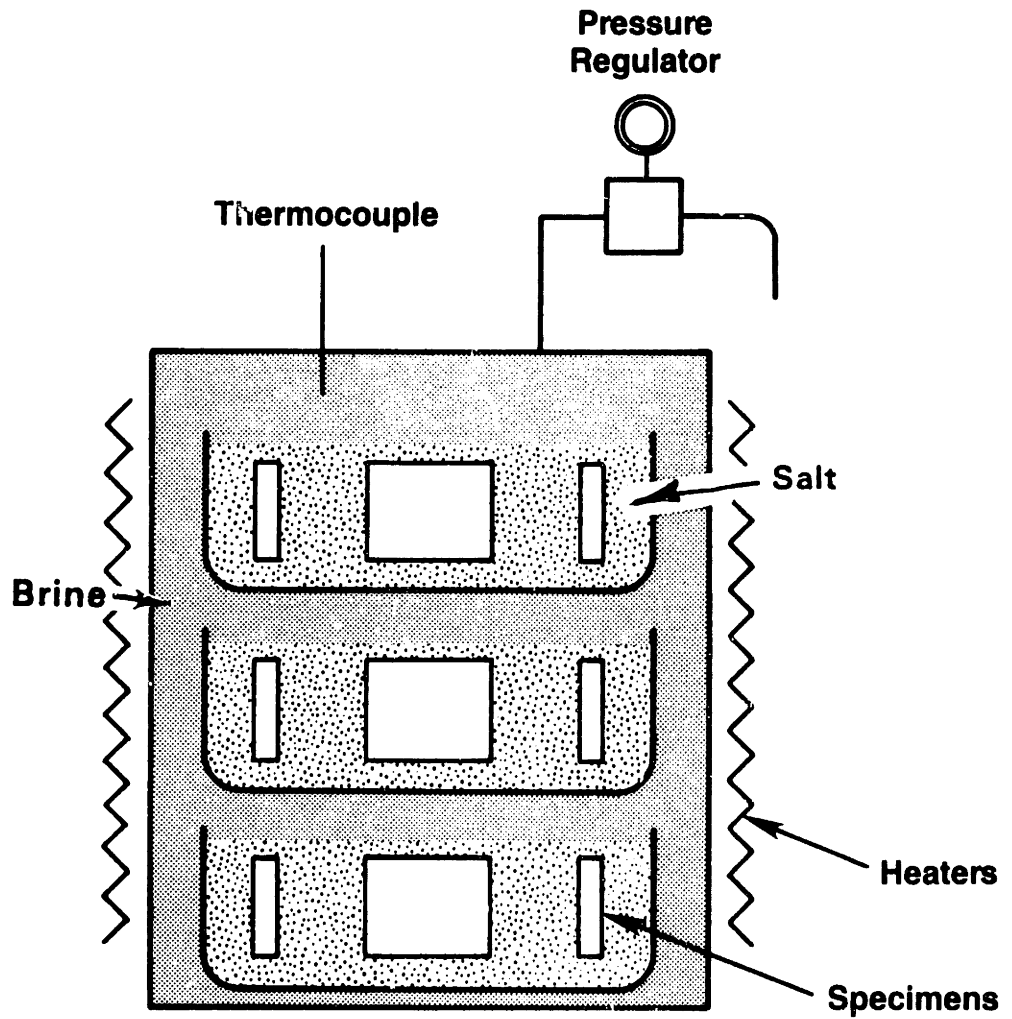
#### **4.1.3 Assembly of the Database**

With the intended purpose of developing a multivariable model of waste container alloy corrosion in the relevant environment by maximum likelihood parameter estimation, data generated via the experimental methods described above were assembled into a large database. These data were grouped together although they were obtained by different test methods. This grouping was necessary in order to obtain a sample possessing a significant range in each of the independent variables common to the measurements. The independent variables common to all tests and deemed potentially the most significant to the corrosion system under study (see model development section below) are:

- Temperature
- Dissolved Oxygen Concentration
- Magnesium Concentration
- Total Fraction of Water in the Test
- Time

The selected dependent variable is the average uniform penetration rate (henceforth called the corrosion rate).

**Figure 4-3:** Schematic Diagram of the Autoclave Excess Salt Test System



Some explanation follows regarding the above independent variables. Temperature was always held constant and reported for every measured corrosion rate. With the exception of only one series immersion general corrosion tests, the dissolved oxygen was controlled to - or was presumed to be - near the limits of control, as all brines were prepared or maintained under an argon purge system. This limit of control for brine at anoxic conditions for the experimental programs described above has been reported to be 0.05 ppm.

In all cases, the magnesium concentration was calculated from brine compositions particular to the test, and the ratio of brine to salt mass. Mass-average magnesium concentrations were calculated for all excess salt tests, and the brine solution magnesium concentration was used for the immersion tests.

The following three tables, 4-1, 4-2 and 4-3, display the conditions for which data were included in the corrosion database, later to be used to generate maximum likelihood estimates of the multivariable model parameters. The computer data file is included in an appendix to this thesis.

**Table 4-1: Test Conditions Summary for Data  
Generated by Immersion General Corrosion Tests**

Temperature (C)	Oxygen (ppm)	Magnesium w/f	Water w/o	Time (hrs)	Number (reps)
90	0.05	0.0465	76	745-4424	(6)
150	1.50	0.0001	76	736-5384	(13)
150	0.05	0.0001	76	336-5635	(30)
150	0.05	0.0468	76	144-4924	(12)
150	0.05	0.0009	76	677- 773	(4)



**Table 4-2: Test Conditions Summary for Data  
Generated by Static Excess Salt Corrosion Tests**

Temperature (C)	Oxygen (ppm)	Magnesium w/f	Water w/o	Time (hrs)	Number (reps)
90	0.05	0.0001	5	2155-2198	(3)
90	0.05	0.0001	20	2155	(3)
90	0.05	0.0034	5	2155	(3)
90	0.05	0.0134	5	2203	(6)
150	0.05	0.0001	5	2155	(3)
150	0.05	0.0001	20	2155-2198	(9)
150	0.05	0.0004	20	759	(4)
150	0.05	0.0034	5	2155	(3)
150	0.05	0.0042	5	2178	(6)
150	0.05	0.0081	10	2178	(6)
150	0.05	0.0134	20	2179	(3)
150	0.05	0.0170	20	767-2178	(12)
150	0.05	0.0220	25	2178-7031	(12)
150	0.05	0.0270	30	1659-2178	(12)
200	0.05	0.0001	5	2155	(3)
200	0.05	0.0034	5	2155	(5)

**Table 4-3: Test Conditions Summary for Data  
Generated by Autoclave Excess Salt Corrosion Tests**

Temperature (C)	Oxygen (ppm)	Magnesium w/f	Water w/o	Time (hrs)	Number (reps)
150	0.05	0.0468	76	762-2181	(4)
150	0.05	0.0353	53	672-2124	(8)

## 4.2 DEVELOPMENT OF A MULTIVARIABLE MODEL FOR GENERAL CORROSION

To date, there have been no published attempts to describe the fate of waste container alloys by uniform dissolution (or any other mechanism of slow degradation) in repository-relevant environments. This is largely due to the complexity of the geochemistry of brines expected at the repository horizon, and the uncertainty in the amount and mechanism of transport of these brines to the container surface. More mechanistic models will undoubtedly become available as onsite in-situ testing proceeds. Some simple correlations have been developed based on small samples of laboratory experiments, often called screening or scoping tests. These tests are usually performed to evaluate various alloys comparatively, rather than for the purpose of investigating the mechanisms underlying corrosion in the system.

What is required for an analysis of waste container degradation - and more importantly - its associated uncertainty, is a multivariable model of the general corrosion rate. The model should include the most significant variables understood to affect this rate. Also, projected time dependent behavior for all of these significant variables must be estimated, which will allow the computation of time- and environment-integrated penetration.

This section describes the model which has been developed as a first attempt at modeling the most significant of the variables - in

combination - shown to effect the general corrosion rate of the A216 low carbon steel in repository-relevant environments.

#### **4.2.1 Determination of the Principle Variables**

##### **4.2.1.1 Temperature**

Temperature at the waste container - salt brine interface will increase slightly to a maximum at approximately five years. The temperature will be ever-decreasing after that time (See Figure 2-4).

The system considered, a low carbon steel in neutral pH aqueous environment has been shown to exhibit ever decreasing but continuous corrosion behavior. This indicates that the overall corrosion product formed at the surface of the metal never provides a solution-impermeable passive film. The film which forms at these conditions acts to retard solution access to the active corroding surface.

Fluid transport through this film may be accomplished either by repeated formation-and-rupture with a gradual accumulation of non-adherent corrosion products surrounding the actively forming layer, or by the continuous formation of corrosion products (such as amakinite) which are permeable to aqueous solutions.

These types of chemical processes, which involve solution diffusion through a thickening corrosion product barrier and multiple reaction steps, may be thought of as having an apparent overall activation energy associated with the charge transfer step.

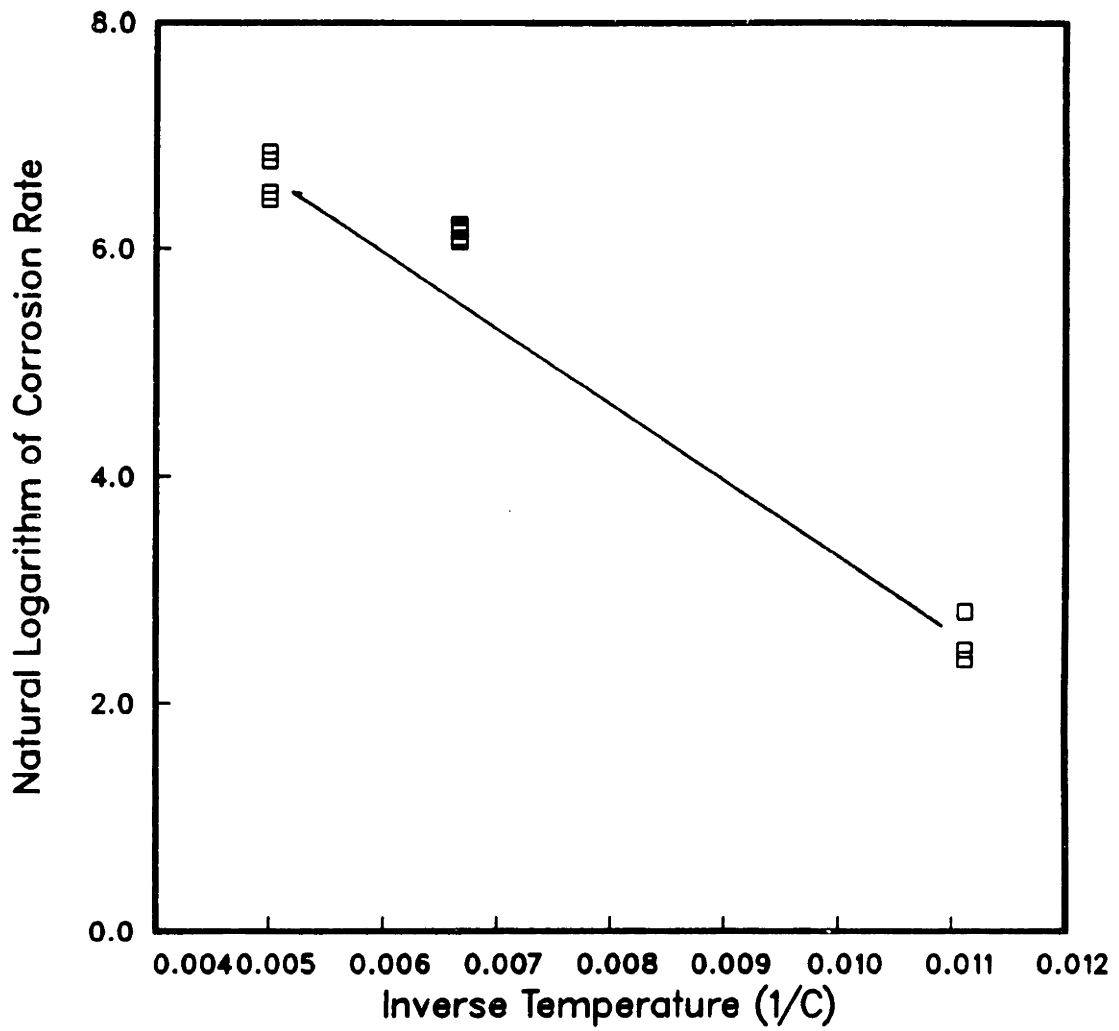
The sparse, compatible data at differing temperatures is presented in Figure 4-3 below. This plot presents the natural logarithm of the corrosion rate of the A216 alloy as a function of inverse test temperature in Figure 4-3. This type of plot is often called an Arrhenius plot; and the linear slope obtained from the curve is an estimate of the (constant) activation energy. Linearity implies a constant activation energy for a single physical degradation mechanism. Regarding the data at 150°C, these measurements are actually generated by an environment of higher magnesium concentration, 0.0042 as opposed to 0.0034. It will be discussed below that increased magnesium concentrations are shown to increase the corrosion rates nonlinearly. Accounting for the greater corrosion rate for the 150°C data might provide even more confidence in the linearity of the Arrhenius plot. The other test conditions were: anoxic (approximately 0.05 ppm), 5 weight percent water and a test duration approximately 2200 hours.

Based upon the line drawn in Figure 4-3, which, from the discussion above indicating the reasons for the higher corrosion rate at 0.0067, is essentially fitted to the endpoint data, the resulting activation energy is 13.32 kcal/mole.

The temperature at which the chemical reaction takes place will also determine what thermodynamically-stable corrosion products will form, the solubilities of chemical components in the brine, and potentially the arrival rate of thermomigrating brine.

Figure 4-4: Temperature Dependence of the Corrosion Rate

Arrhenius Plot of General Corrosion Rate  
for Select Static Excess Salt Tests



#### **4.2.1.2 Dissolved Oxygen**

Compatible data for immersion general corrosion tests conducted at anoxic (approximately 0.05 ppm) and oxic (approximately 1.50 ppm) conditions are presented in Figure 4-4. The vertical bars through the data represent actual measurement spread (bounded by the maximum and minimum observed rates) and the plotted points are the mean of the measurements.

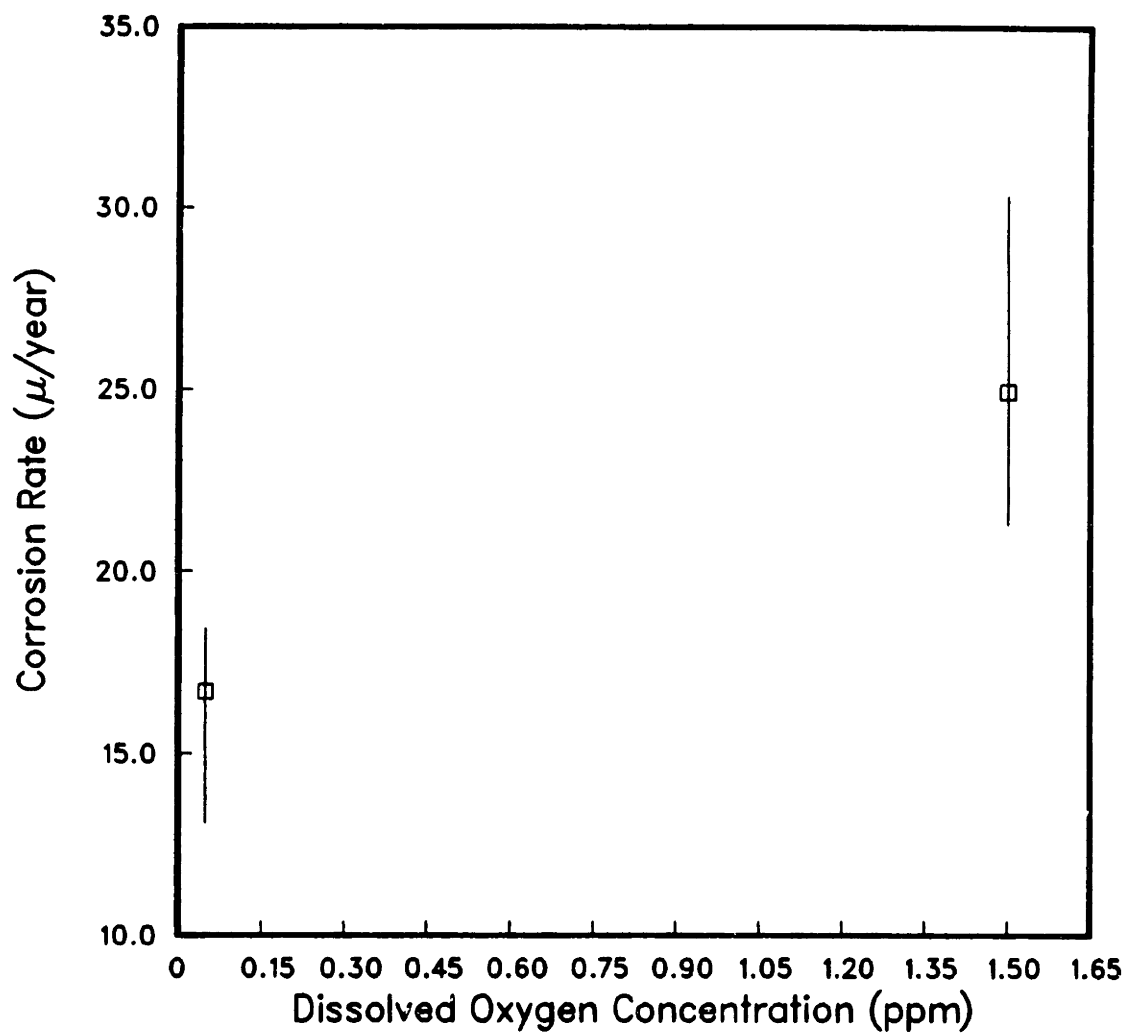
Clearly the oxygen-rich environment provides for more rapid dissolution of the metal. The increased oxygen level raises the system Eh (oxidation potential). It has been shown in Figure 2-8 the polarization behavior of A216 steel in magnesium-rich brines indicates the increase of corrosion rate (current) with Eh.

#### **4.2.1.3 Magnesium Concentration**

The results of polarization resistance measurements for A216 steel in electrolytes varying in magnesium ion concentration are excerpted from Golis [26] and presented in Figure 4-6. Data which are displayed as corrosion rate are actually inferred from measurements of resistance at the corroding metal surface. With a known electric potential, and the measured resistance, the corrosion current may be calculated. It has been noted previously (Chapter 2) that low carbon steels in highly concentrated magnesium brines exhibit greater corrosion rates, hence the importance of this variable in repository-relevant environments will not

Figure 4-5: Dissolved Oxygen Dependence of the Corrosion Rate

### Dependence of Corrosion Rate on Dissolved Oxygen Concentration





be further justified here. These electrochemically determined results appear to indicate a nonlinear, monotonic increase in general corrosion rates with magnesium concentration and further confirm the absence of any passivation behavior.

#### **4.2.1.4 Total Fraction of Water in the Test**

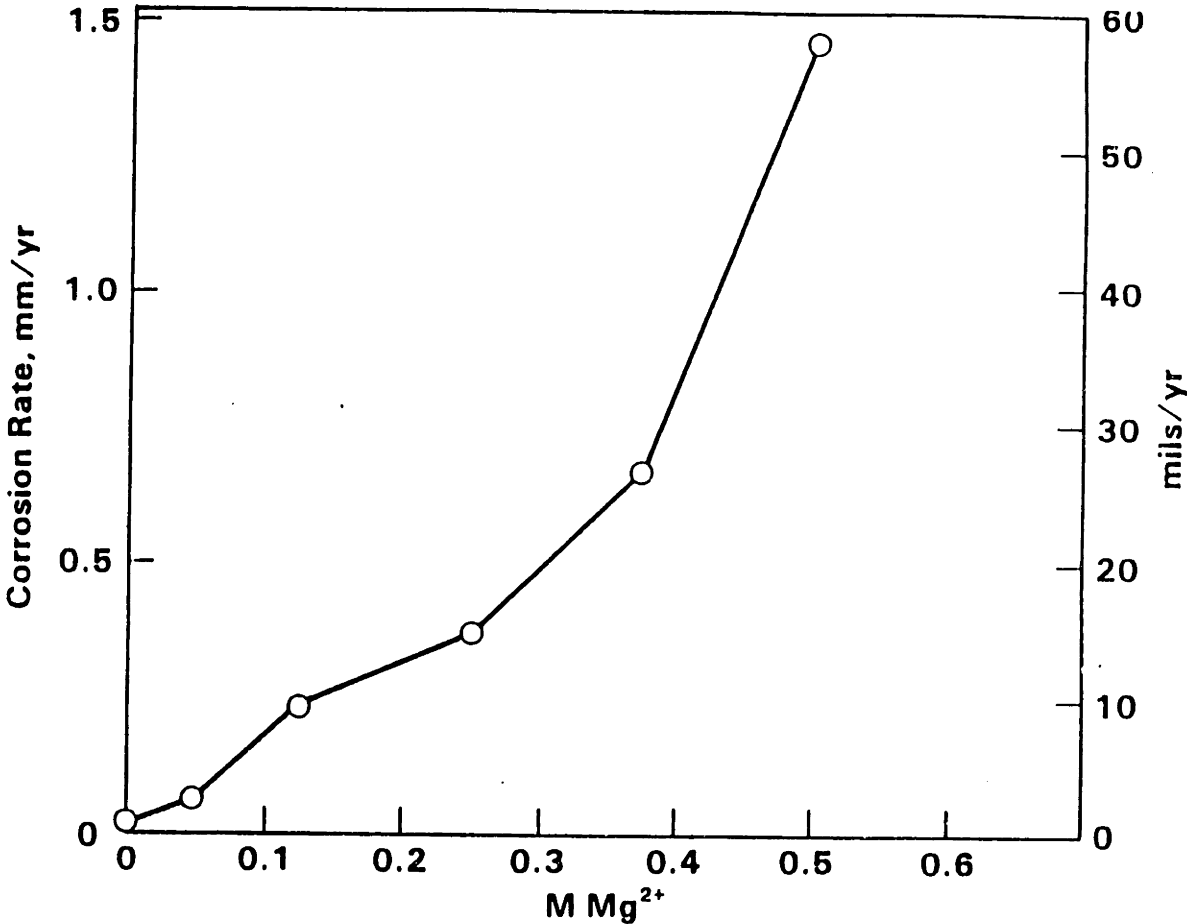
The variable referred to as 'total fraction of water in the test' attempts to represent the condition of dryness of the interfacial corroding environment. As has been discussed in Chapter 2, the bedded halite and mudstone host rock at the repository horizon are quite plastic and are suspected of flowing so as to contact the waste container surface in a relatively short time, (order of 1 year). The average moisture content of the halite and mudstone is approximately 1.64 weight percent. Based on this consideration it is assumed that the interfacial corroding environment may be represented by a time-dependent boundary condition of solid/liquid phase salt/brine throughout its life in service.

Data have been obtained for general corrosion in conditions from 5 weight percent water and the balance solid salt in a static excess salt test to all brine immersion tests which are 76 weight percent water, the balance being dissolved solids, predominantly sodium chloride.

The results of Westerman, et. al. taken from Golis [26] are presented for consistent static excess salt measurements conducted at 150°C, in

Figure 4-6: Corrosion Rate Dependence on Magnesium Concentration from [26]

Dependence of Corrosion Rate on Magnesium Ion Concentration



PBB1 salt/PBB3 brine in Figure 4-6. The tests were conducted for three months. The general trend in these results indicate an increasing corrosion rate with greater water fractions.

#### 4.2.1.5 Time

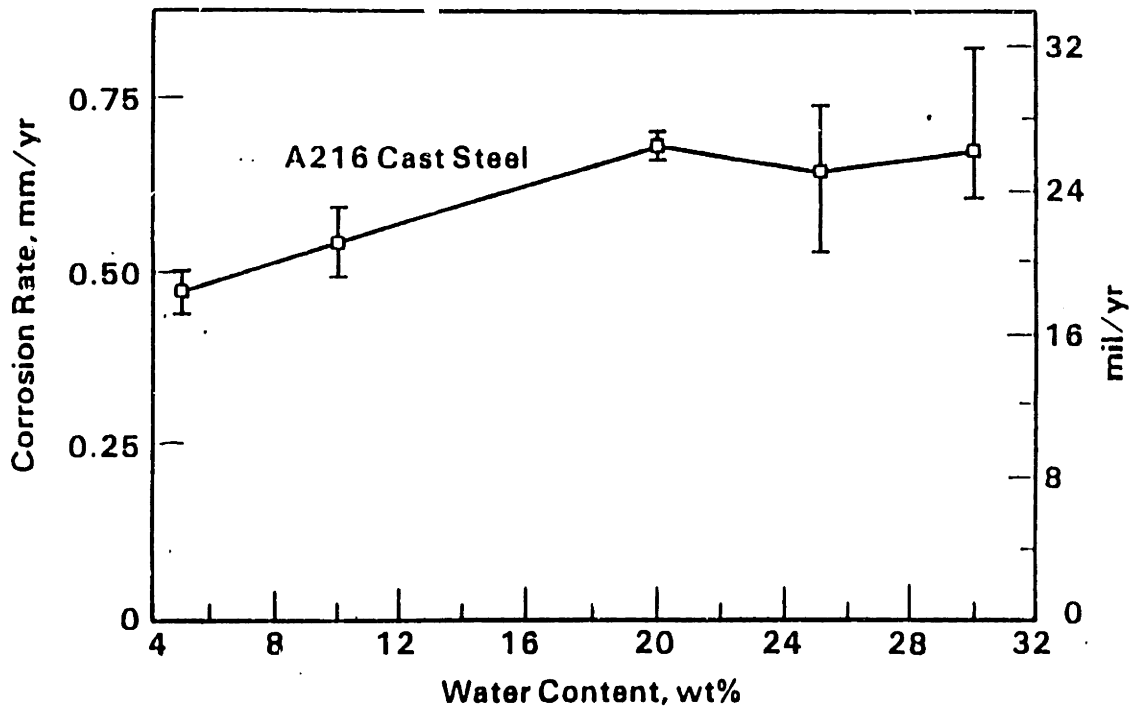
Finally, time is of course one of the principle variables affecting the general corrosion rate. Gross oxidation behavior of metals is most often investigated by measuring and empirically correlating the rate of oxidation (via weight loss measurements) with time. Rate constants are obtained in this way. Wagner [22] showed theoretically that a pure metal would obey a parabolic oxidation rate law, given that the oxidation rate was controlled by ionic diffusion through a continuously thickening oxide layer. This corrosion rate,  $y$ , is given by:

$$y = k t^{-1/2} \quad (4.1)$$

The parameter  $k$  is called the parabolic rate constant.

It should be pointed out that this behavior is derived for an ideal metal experiencing dissolution by a single oxidizer. Deviations of actual measurements to exhibit parabolic corrosion rate behavior often only indicate the presence of morphological inhomogenities [22] at the reacting metal surface and the developing oxide film. Time raised to other fractional powers are often correlated with empirical measurements to correct for this non-ideal behavior.

Figure 4-7: Water Content Dependence of the Corrosion Rate  
from [26]



Peters and Kuhn [46] have developed a correlation for a limited number of high-magnesium brine static excess salt tests. Their model assumes that the corrosion penetration was proportional to the magnesium ion concentration at the reacting metal surface. The resulting general functional form for the penetration rate,  $y$ , is

$$y = (A + B t)^{-1/2} \quad (4.2)$$

where  $A$  and  $B$  are fitted parameters. The time dependent penetration resulting from this model (from Golis [26]) is depicted in Figure 4-8.

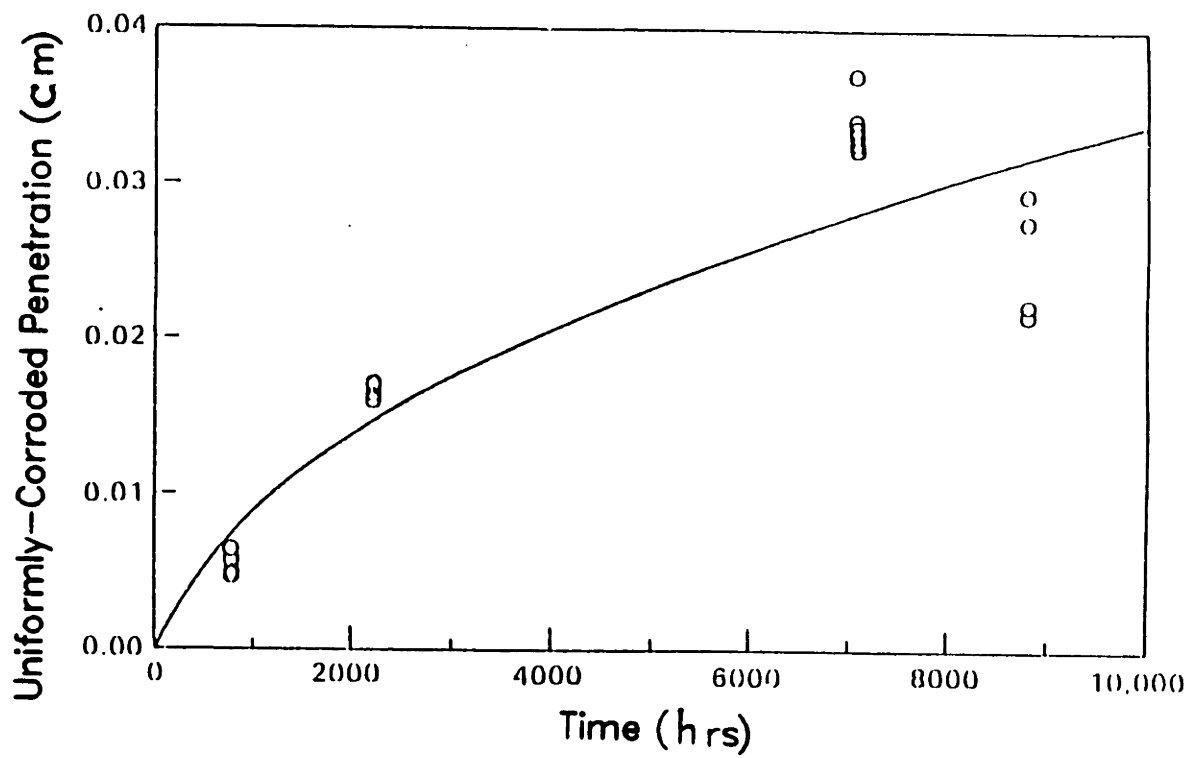
#### 4.2.2 Comparison of Models Considered

It may be concluded from the above information that the corrosion rate of A216 steel in repository like environments will corrode at a rate which:

- Increases with increasing dissolved oxygen concentration, magnesium concentration and total fraction of water at the reacting surface.
- Is controlled by less-than-linear kinetics, hence the gross time dependent behavior will depend on some reciprocal fractional power of time.
- Exhibits an apparent Arrhenius activation energy for the overall reaction process, hence may be cast in an overall Arrhenius formulation.

Table 4-4 presents the functional forms of the alternative models which were evaluated with the data set. A brief explanation of each model is included in the table. Also tabulated for the alternative

Figure 4-8: Uniform Penetration Time Dependence  
from [26]



models is the (unbiased) sum of the squared errors. This measure serves as a simple comparative criterion for goodness of fit which characterizes each of the equations. The models which include a polynomial time term exponentiated by a parameter diverged with even small changes made to this exponent parameter. Fixing the parameter at a constant value of 1/2 improved the convergence and fit considerably, as in model number 3 of the table. In the fitting of model 3, the maximum likelihood estimates determined did not result in any lower error sum of squares than the initial guess values. The fourth model, a steady state case, represented an attempt to investigate the need to include an explicit time-dependent term. This steady state functional form was abandoned, also due to lack of convergence. The fifth model, a modified Eyring Model, was chosen as the best among the alternatives. In this model the activation energy, parameter  $b_6$ , is reduced by a magnitude which is a linear function of the other three corrosion-accelerating variables; dissolved oxygen, magnesium concentration and total water fraction. This model has associated with it the lowest error sum-of-squares deviation which is achievable by any of the listed forms. The kinetic prefactor is also somewhat modified from Wagner's theoretical parabolic rate behavior, but can be forced to behave similarly depending upon the values of  $b_1$  and  $b_2$ .

**Table 4-4: Corrosion Rate Models Considered**

Model	Sum of Squares
$\frac{b_1}{(b_2+t)^{b_3}} \exp b_4 x[O] + b_5 x[Mg] + b_6 x[H_2O] \exp \frac{-b_7}{T}$	1.597*10 <sup>7</sup>
$\frac{b_1}{(b_2+t)^b} b_4 x[O] + b_5 x[Mg] + b_6 x[H_2O] \exp \frac{-b_7}{T}$	1.248*10 <sup>7</sup>
$\frac{b_1}{(b_2+t)^{1/2}} b_4 x[O] + b_5 x[Mg] + b_6 x[H_2O] \exp \frac{-b_7}{T}$	2.324*10 <sup>7</sup>
$b_1 b_4 x[O] + b_5 x[Mg] + b_6 x[H_2O] \exp \frac{-b_7}{T}$	1.059*10 <sup>7</sup>
$\frac{b_1}{(b_2+\sqrt{t})^b} \exp b_4 x[O] + b_5 x[Mg] + b_6 x[H_2O] \exp \frac{-b_7}{T}$	8.732*10 <sup>6</sup>

Where:

- t = Time (hours)
- [O] = Dissolved Oxygen
- [Mg] = Magnesium Concentration
- [H<sub>2</sub>O] = Water Fraction
- T = Temperature (°C)



### 4.2.3 Results of the Model

In order to predict the general corrosion penetration and uncertainty with the above model, the expected in-service environment must be specified for a time period extending to the desired design life of interest. This specification may take the form of known time varying values for the independent variables included in the model.

#### 4.2.3.1 Specification of the In-Service Environment

Results were obtained from the TEMP\* code for the temperature profile at the waste container surface as a function of time. The reference package design parameters of Table 2-1 were used in these calculations for a horizontally emplaced waste package. The other five variables, for lack of better assumptions, were held constant over the 1,000-year time projection. Table 4-5 lists the timesteps and the assumed value of the variable (held constant) in that timestep. These values will become the reference case for the time dependent environmental boundary conditions at the corroding metal surface. These conditions will be used as arguments to the corrosion rate law and to determine the time-integrated penetration. A limited number of variations in this assumption will be analyzed below.

Repeated fits of the data with various initial starting guesses indicated that the parameter for the constant activation energy,  $b_6$ ,

---

\*Wurm, *et. al.*, see reference [65]

**Table 4-5: Assumed In-Service Environmental Independent Variables**

Temperature (°C)	Dissolved Oxygen (ppm)	Magnesium Concentration (w/f)	Water Fraction (w/f)	Time (years)
134.6	0.05	0.05	0.05	1.0
134.9	0.05	0.05	0.05	2.0
134.4	0.05	0.05	0.05	5.0
130.7	0.05	0.05	0.05	10.0
124.5	0.05	0.05	0.05	20.0
106.7	0.05	0.05	0.05	50.0
89.4	0.05	0.05	0.05	100.0
75.3	0.05	0.05	0.05	200.0
72.0	0.05	0.05	0.05	300.0
66.1	0.05	0.05	0.05	500.0
59.9	0.05	0.05	0.05	1000.0

generally converged near the same constant value for minimum sum of square error. It was decided, based on the nearly always constant value obtained, 5793 ( $^{\circ}\text{C}$ ), to fix this parameter as a constant term at that value. This is physically consistent with the assumption that the apparent activation energy of the overall corrosion mechanism remains constant all but the variables oxygen, magnesium and water fraction which are explicitly included. This leads to a constant activation energy of 11.51 kcal/mole, which compares well to the estimated value of 13.32 kcal/mole arrived at from the simple Arrhenius plot, Figure 4-3.

In a similar way, the parameters for dissolved oxygen and water fraction were found to only weakly influence the overall fitting process. They were assigned the constant values which were obtained on the converged fit yielding the sum of square error value tabulated. All of the maximum likelihood estimate parameter values are presented in Table 4-6. These values were determined by the maximum likelihood estimation technique of Section 3.2.2, Equations (3.22), (3.31) and (3.33), codified in the FITSALL algorithm (a subroutine of the UNODEX Program in appendix). Relevant computational constraints on the problem are also presented in the table.

A scheme for weighting the ESS virtual data which is also used to weight the MBD is discussed in Section 4.3.1.1 below and will not be presented here. However, the following penetration and uncertainty results have been calculated employing this weighting scheme.

**Table 4-6: Maximum Likelihood Parameter Estimates  
for the Corrosion Rate Model**

TERMINATION CONDITION	NEGLIGIBLE CHANGE IN SUM OF SQUARES
NUMBER OF ITERATIONS	4
$B_1$	1.2782757E+11
$B_2$	7.8842731E+02
$B_3$	1.6418113E+04
ERROR SUM OF SQUARES	8.75412E+06
VARIANCE	4.89057E+04
SAMPLE STANDARD DEVIATION	2.21146E+02
AVERAGE DEVIATION	6.17274E+00
AVERAGE RELATIVE DEVIATION	-3.73631E+00

The multivariable model of general corrosion displayed as Table 4-4, number 5 becomes:

$$y = \frac{1.29 \times 10^{11}}{774.5 + \sqrt{t}} \exp 0.088[O] + 1.39 \times 10^{-8} [H_2O] + 1.62 \times 10^4 [Mg] - \frac{5793}{T}$$

using the fitted parameters of Table 4-6 where  $y$  is the penetration rate in  $\mu/\text{year}$ ,  $t$  is in hours and  $T$  in  $^{\circ}\text{C}$ .

We make the following explicit approximations and assumptions allowing the numerical evaluation of environment-dependent penetration and uncertainty:

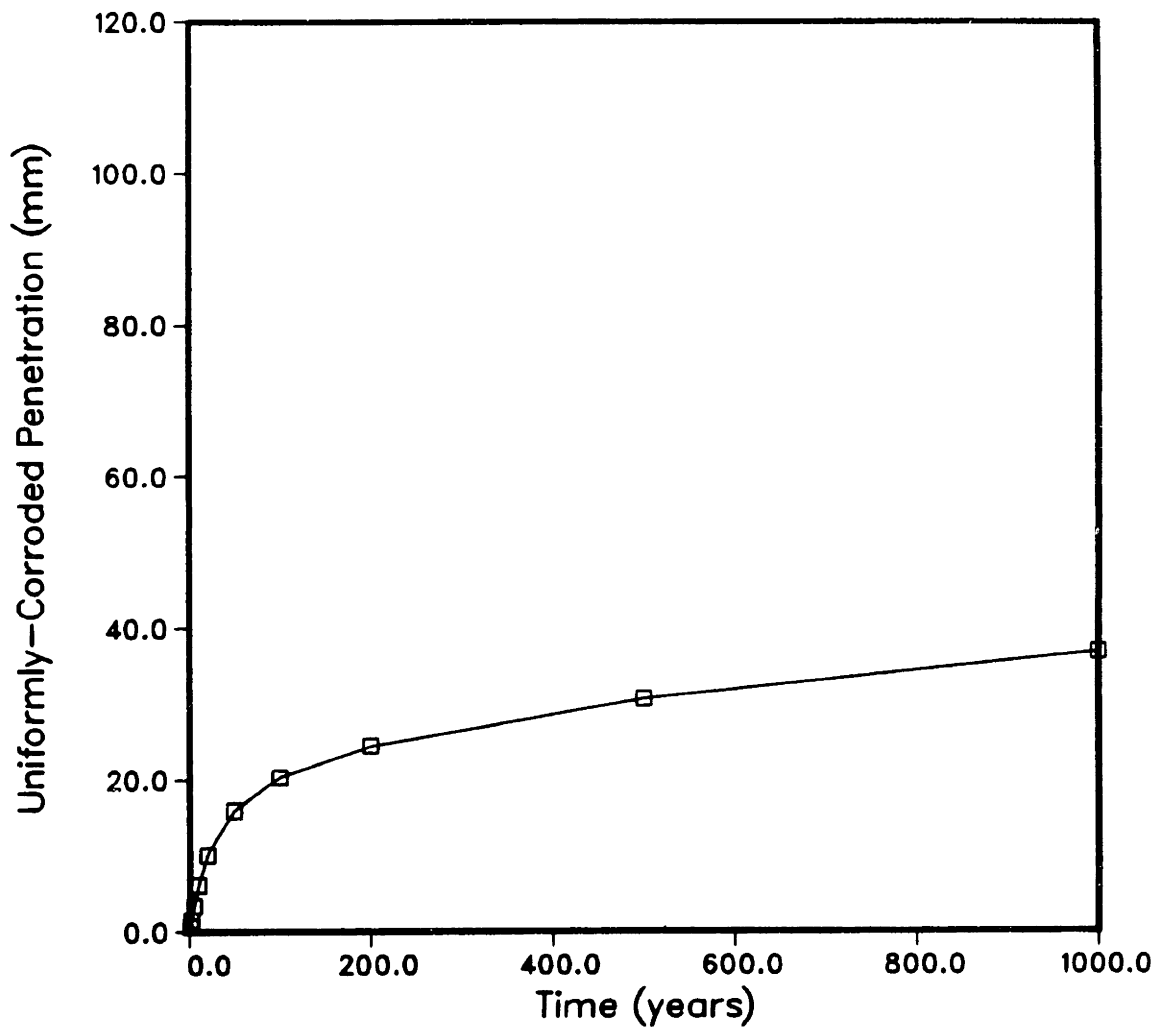
- The fitted constants (parameters) of the corrosion rate model and their uncertainty in a given time interval are independent from the other time intervals (Note the corrosion rate *is* time-dependent).
- All the influential environmental independent variables are represented in the rate law model.
- The functional form of the rate model is correct.
- The environmental independent variables may be approximated by constant values within each given time interval.
- The mechanism which produced the measured values in the Model Building Database, which was used to generate the MLE parameters, prevails over the independent variable space defined by the specified in-service environment.

#### 4.2.3.2 Analysis of Waste Container Penetration and Uncertainty

Given the multivariable model of general corrosion, the specified in-service environment and the assumptions above, the resultant penetration in time behavior is fully determined and presented in Figure 4-9.

**Figure 4-9: General Corrosion Container Penetration**  
Reference in-service boundary conditions: Temperature  
profile as given in Table 4-5, O:0.05 ppm,  
Mg:0.05 w/o, W:0.05 w/f

### Uniform Penetration Extrapolated to 1000 Years



This exhibited behavior possesses the salient feature of an ever declining corrosion rate, hence the time-integrated penetration slowly approaches an asymptotic value. If the 10,000 year value is selected for the asymptote\* this computed asymptotic value is 5.80 cm, hence the penetration only doubles the 1000 year value in the subsequent 9000 years.

Based on a total penetrated thickness of the container after the 1000 year interval of 2.93 cm, a corrosion allowance concept is quite acceptable. However, the more significant design parameter when considering very long term containment is the uncertainty in the above penetration. Based on the propagation of the random errors, described by Equations (3.43) - (3.46), the uncertainty in 2.93 cm at 1000 years is 2.11 cm, or 72% of the total. This uncertainty is assessed on the random error about the measured data and does not incorporate any uncertainty due to environmental boundary condition variations (*e.g.* arrival rate of brine) spatially nonuniform attack or other fundamental nonuniformities in general corrosion process (*e.g.* lack of homogeneity in the container itself). The reference penetration and  $2\sigma$  confidence interval are presented as Figure 4-10. The computed lower confidence bound was constrained by an assumed irreversibility condition. The

---

\*Most of the federal regulations and design constraints on the engineered barrier system end after this interval.

penetration along this bounding limit was never allowed to decrease, as metal deposition is not expected to be a viable mechanism for thickening of the container wall. This bound was fixed at its maximum value in time, once obtained, of 2.27 mm, at 10 years.

The reference conditions assumed for the cases illustrated in the above Figures 4-9 and 4-10 were calculated based upon relatively 'conservative' in-service environmental boundary conditions. Specifically the physical statements of these assumptions are

- There is infinite reserve of high-magnesium brine available via some means of transport to the container boundary.
- The rate of this brine availability is never the limiting step in the overall process of metal dissolution.
- The dissolved oxygen concentration in the brine is always anoxic (0.05 ppm)
- The container-salt interface is always characterized by 5 weight percent water (by brine) and 95 weight percent solid phase salt.

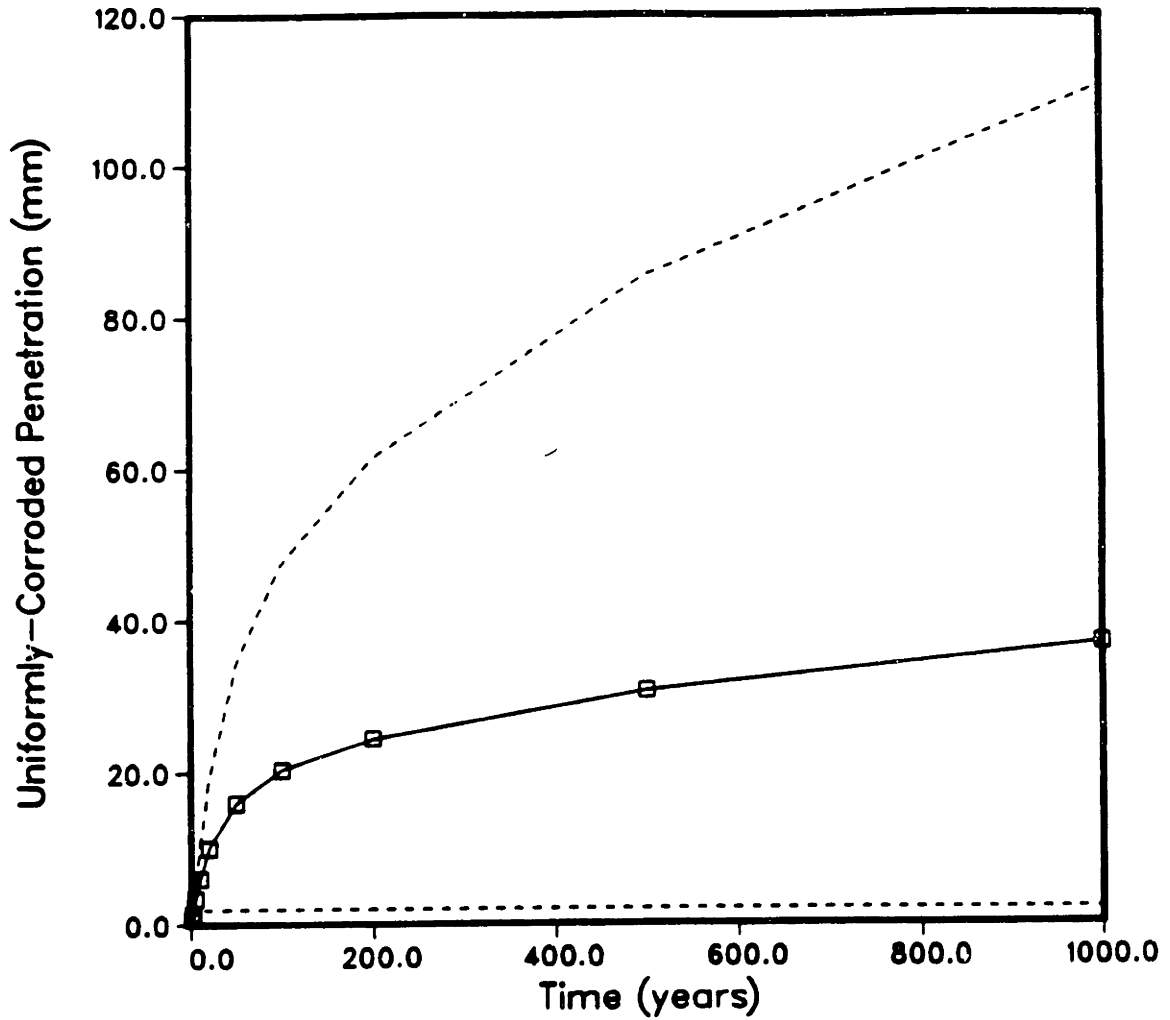
Due to the lack of knowledge regarding the above assumed environment, some limiting cases varying the assumed in-service environmental boundary conditions are commonly made and sensitivity of the results to these changes are determined.

The source of highly concentrated magnesium brine in halite formations such as in the Palo Duro Basin are the intracrystalline brine inclusions discussed in Section 2.3.2. These fluid inclusions are proposed to



**Figure 4-10:** General Corrosion Container Penetration and Uncertainty  
Reference in-service boundary conditions: Temperature  
profile as given in Table 4-5, O:0.05 ppm,  
Mg:0.05 w/o, W:0.05 w/f

### Uniform Penetration and 2 Sigma Confidence Bounds



migrate to the container surface due to thermal gradient-driven transport. The intercrystalline brine and brines resulting from water intrusion (by some unspecified mechanism) and subsequent dissolution of host rock salt are quite low in magnesium concentration, however. Hence it is useful to postulate that the relevant chemistry is that of a low magnesium brine which reflects both the water intrusion scenario and the mixing of intra- and intercrystalline brines before reaching the container interface.

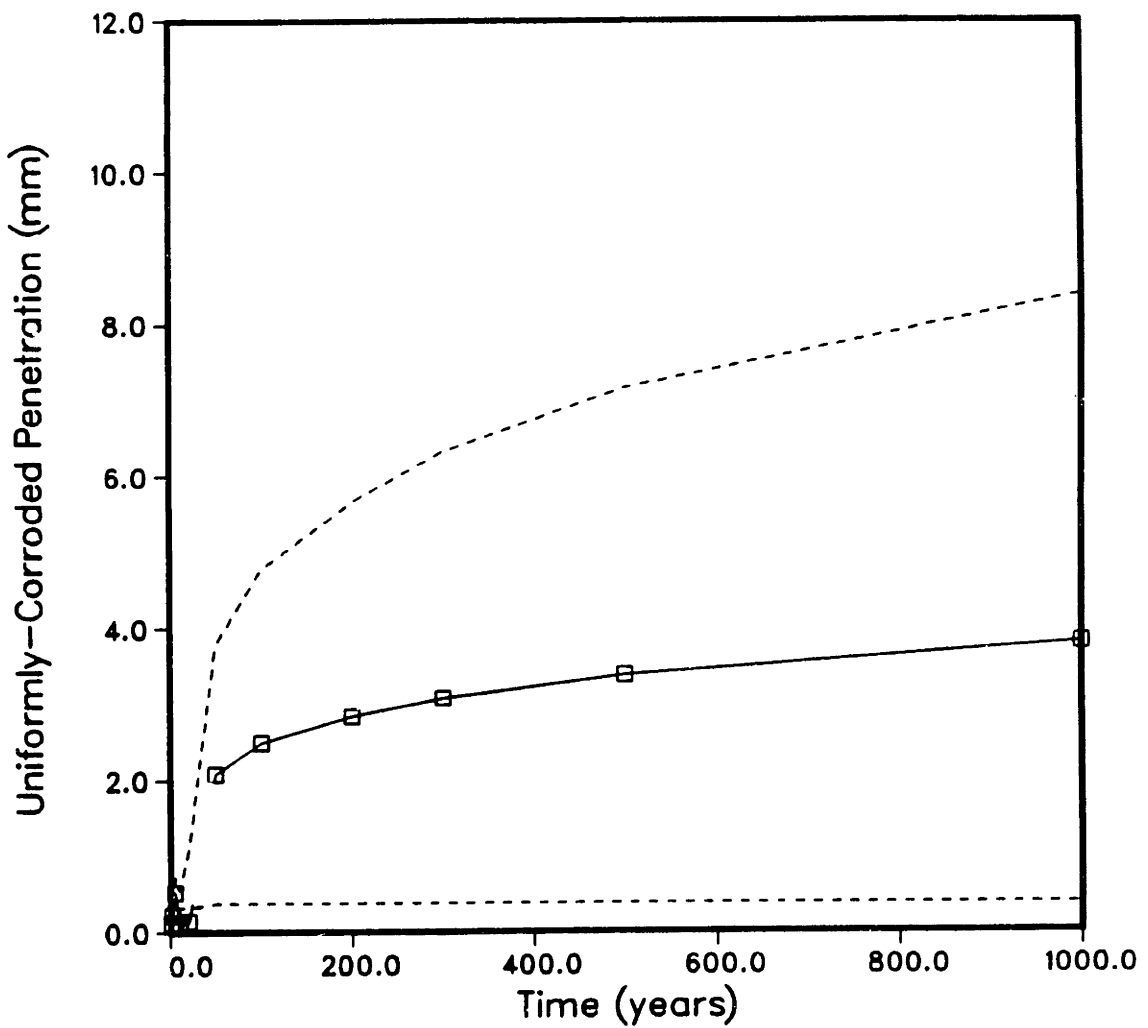
With all environmental conditions held the same as for the reference case except the magnesium concentration, which was fixed at 0.005 ppm, the results of Figure 4-11 are obtained.

The sensitivity of the corrosion rate to magnesium concentration is obvious from the results presented in Figure 4-11. Based on the low magnesium case, the total penetration after 1000 years is 3.81 mm with a standard error of 2.29 mm. The  $2\sigma$  confidence interval would yield a worst anticipated penetration of 8.39 mm.

In order to assess the scenario of limited brine availability, which may be justified on the bases of the theory of the existence of a thermal gradient 'cutoff' value for thermomigrating brine inclusions, the corrosion rate of the above model was fixed arbitrarily small after 200 years to 1 micron/year. The cutoff time was derived from the brine

Figure 4-11: General Corrosion Penetration and Uncertainty for Low Magnesium Brine Reference in-service boundary conditions: Temperature profile as given in Table 4-5, O:0.05 ppm, Mg:0.05 w/o, W:0.005 w/f

### Uniform Penetration and 2 Sigma Confidence Bounds



accumulation calculations published in the Final Environmental Assessment for the Deaf Smith County Texas site, USDOE [55]. Results of the Deaf Smith Environmental Assessment indicate, with a thermal gradient cutoff of  $0.125\text{ }^{\circ}\text{C}/\text{cm}$ , that the total volume of accumulated brine per package essentially reaches its asymptotic value of  $0.83\text{ m}^3$  at 200 years. The computations are based on the Jenks Equation (2.1).

The results of the corrosion rate cutoff at 200 years are presented in Figure 4-12 below. As can be observed in the figure, the uncertainty after the cutoff increases only slightly as changes in variance coefficients (Equation (3.43)) only alter the uncertainty in an infinitesimal rate, leading to a very small time-integrated change in accumulated penetration.

One final case in varying the in-service environmental conditions is necessary, that of the temperature profile. This is important to computations of container penetration for the reference commercial high level waste loading, which has a greater power output in the early years due to the higher loading of  $9.5\text{ kW}/\text{package}$  (compare Table 2-1). The temperatures employed for this waste container loading were obtained from results published in the Final Environmental Assessment for the Deaf Smith County Texas site, USDOE [55] and are tabulated in Table 4-7. As is demonstrated in Figure 4-13, according to the model of general corrosion developed above, higher temperatures result in much more rapid

Figure 4-12: General Corrosion Penetration and Uncertainty  
 Incorporating Brine Availability Cutoff at 200 Years  
 Reference in-service boundary conditions:  
 Temperature profile as given in Table 4-5,  
 O:0.05 ppm, Mg:0.05 w/o, W:0.05 w/f up to 200 years

### Uniform Penetration and 2 Sigma Confidence Bounds

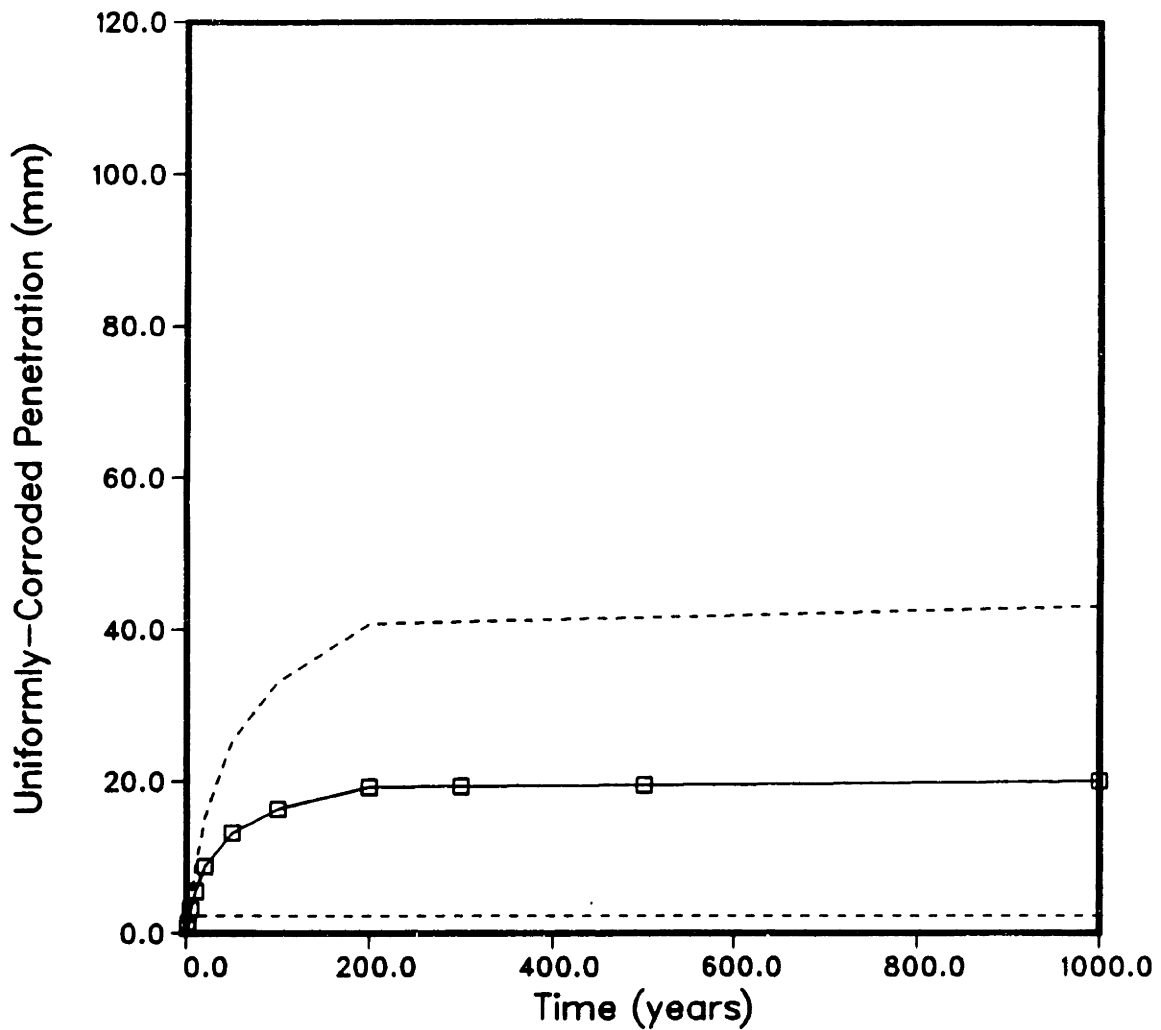


**Table 4-7: Container Boundary Temperatures for the Commercial High Level Waste Loading, 9.5 kW**

Time (years)	Temperature (°C)
1.0	212.0
2.0	220.0
5.0	227.0
10.0	225.0
20.0	205.0
50.0	152.0
100.0	114.0
200.0	94.0
300.0	84.0
500.0	74.0
1000.0	58.0

penetration early on. Near 300 years an asymptotic value of approximately 12.0 mm is achieved. The uncertainty bounds (upper) behave similarly, diverging little after this time interval.

#### **4.3 DESIGN OF EXPERIMENTS FOR OPTIMAL UNCERTAINTY REDUCTION**

The following section discusses the main results of the thesis, basing the presentation on the application to nuclear waste container penetration by general corrosion. The multivariable model developed above will be used solely to explore the topic of uncertainty-optimized experiment design.

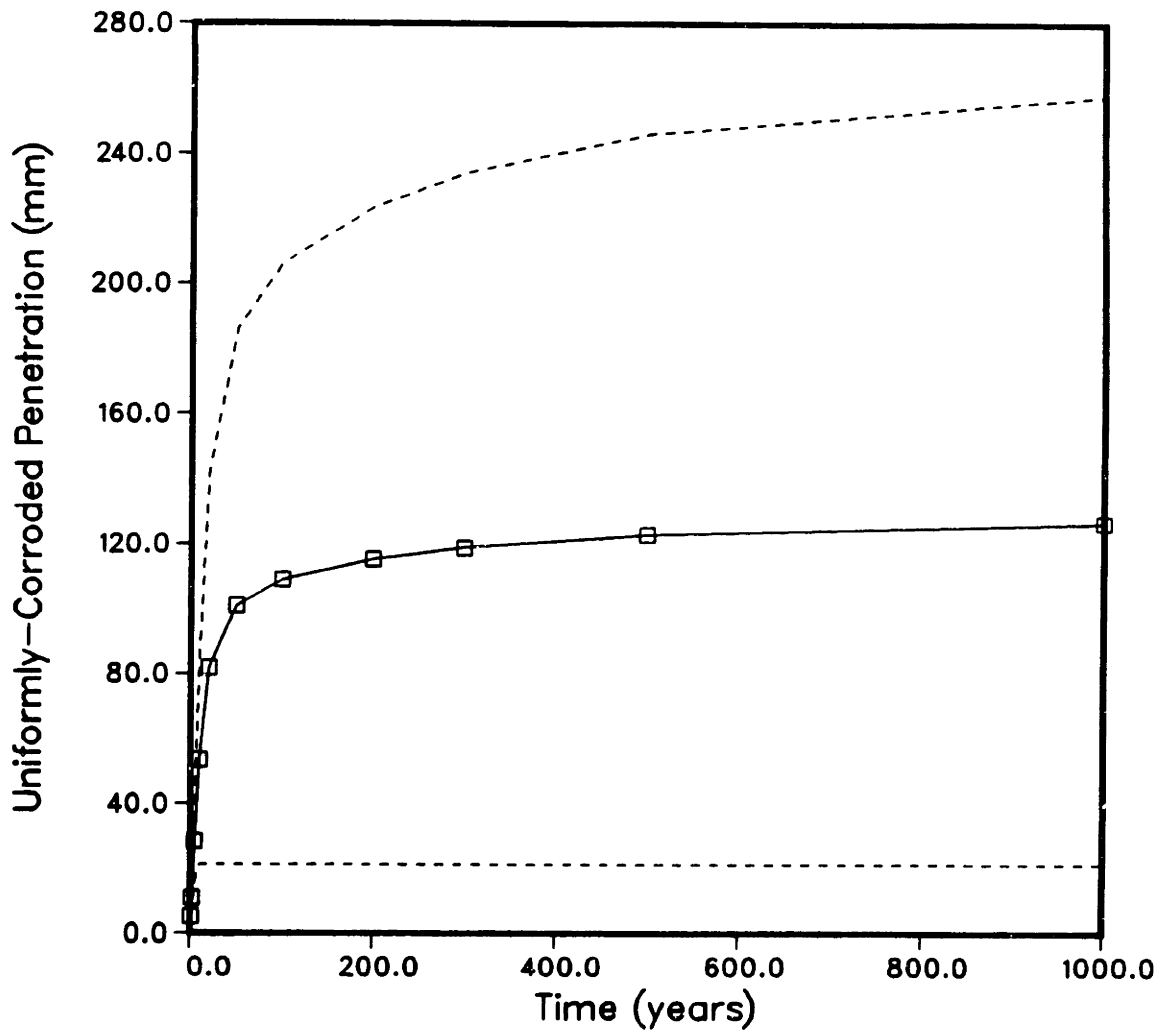
##### **4.3.1 Assignment of Uncertainty to the Virtual Data**

The methodology developed in Chapter 3 entails evaluation of a finite sample of potential experiments by generating values for the 'virtual' independent variable associated with a given prescribed potential experiment from the ESS. Thus, a key assumption associated with the methodology is that virtual data (values of the corrosion rate) may be estimated from the model itself. Using the values generated by the model itself, with no error, would drive the uncertainty to zero by including enough virtual data in the MBD. It is absolutely imperative, for the virtual data concept to possess quantitative credibility, to include a consistent measure of error with each of the virtual data in the ESS.

With this in mind, the next two sections discuss the development of a self-consistent model of virtual data error.

Figure 4-13: General Corrosion Penetration and Uncertainty  
 for Commercial High Level Waste Temperature Profile  
 Reference in-service boundary conditions:  
 Temperature profile as given in Table 4-7,  
 O:0.05 ppr., Mg:0.05 w/o, W:0.05 w/f

Uniform Penetration and 2 Sigma Confidence Bounds





#### 4.3.1.1 Discussion of the Components of Uncertainty in Predictive Modeling

Vesely and Rasmuson [60] differentiate between two types of uncertainty associated with probabilistic modeling, which are true for predictive modeling in general. They are:

- Uncertainty due to physical variability
- Uncertainty due to lack of knowledge

The first type of uncertainty, as pointed out in their work, is due to actual random behavior in a particular quantity of interest. It is this uncertainty which causes repeated measurements of a specific quantity to yield different values.

The second type of uncertainty, that due to lack of knowledge, results from incompleteness or imprecision in the model itself. Rish [49] identifies this same source of uncertainty, the uncertainty in the formulation of the model itself, as structural uncertainty. The salient feature which distinguishes the two types of uncertainty in predictive modeling is the impact of knowledge on the magnitudes. It is possible to greatly reduce the structural uncertainty with additional knowledge about the physical process, for example, the inclusion of an additional, competing reaction path in a corrosion process model.

Structural uncertainty is far more difficult to assess quantitatively

than physical variability. As has been mentioned previously, the working hypothesis necessary to develop the methods and techniques of this thesis was to assume *The model of general corrosion developed in this thesis is structurally correct, and that it includes all the significant independent variables affecting the corrosion process*, hence this eliminates the 'lack of knowledge' component of the total uncertainty. Based upon the current body of knowledge and data, this model has accounted for observed behavior.

#### 4.3.1.2 An Empirically-Consistent Model of Virtual Data Error

An ideal model of virtual data error would be based, in principle, upon a large sample of data generated at enough combinations of the independent variables so as to characterize the error throughout the variable space represented in the ESS to be evaluated. This is an idealization, however, as it will most often be the case that the ESS will be populated by many experiments which are combinations of the independent variables for which no measured values are available, and which have no quantitative measure of error associated with them. This is the case, for example, when accelerated life testing is being investigated by the UNODEX methodology.

Measurement precision (*e.g.* minimum measurable weight change for a corrosion specimen) may serve as a check on the lower bound of the error, but offers little information to facilitate making an estimate of the physical variability.

One approach taken was to characterize subsets of the MBD for which essentially replicate data existed (with the exception of slight differences in test duration) by fitting the data to various probability distribution functions. Six subsets of the MBD with the greatest sample sizes (from 6 to 15 replicate measurements) were consistently fit to 108 distributions with a software package developed by Christensen [10].

This software tool fits the data to each of 108 data distributions (Christensen [9]), generates descriptive statistics and computes measures of error in central tendency, minima and maxima, width, dispersion, asymmetry and peakedness. These measures of error, which are specific to each distribution, are then weighted and summed into a total measure of error for the fit. Individual weighting factors are adjusted for each candidate distribution so that, as an example, random data generated by a normal distribution produces the least total error for the fitted normal distribution.

Results of this approach indicated, for the data subsets considered, a consistently higher overall ranking given to the more truncated, rectangular distributions (*e.g.* Rectangular, Subbotin, Horseshoe, etc.). The normal distribution consistently appeared in the lower half of the 108 distributions ranked. The exercise provided confirmation that the sparseness of data resulted in too few observations to generate a reliable estimate of the mean and possessed a greater-than-anticipated standard deviation.

The approach taken to remedy the small sample size problem was to formulate a model of the absolute deviation (absolute value of the observed value - calculated value) by linear regression with the MBD. In this way, an empirically-consistent model of error may be generated - based upon actual data - which is functionally dependent upon the independent variable set (for the test conditions).

This same model of error was used to generate estimates of the error in measured values of the MBD, and these errors were, in turn, used as weighting factors for the fit. In this way, an iterative sequence determining the maximum likelihood estimates of the corrosion model and, in turn, the coefficients of the linear regression model of error was performed. The model of error, corrosion rate model and set of parameters and coefficients resulting from the above iteration to convergence (to 1% changes or less) is presented in Table 4-8.

As noted in Section 4.1.1. the average uniform penetration rate is being used as an approximation to the instantaneous corrosion rate. The form of the error model explicitly included the time-dependent contribution so as to follow the kinetic behavior, that is, to vary as the inverse square root of time. This is because it is expected that the error in the mass of metal loss by dissolution will not diverge so rapidly as to become an increasing function of time. Since the error in the penetration is less than linearly increasing with time, but the

instantaneous corrosion rate is approximated by dividing by time, the error in the corrosion rate is expected to decrease in time.

#### 4.3.2 Specification of the Experiment Sample Space

The technique of discretizing the population of all conceivable potential experiments into what has been termed the Experiment Sample Space will be reviewed below.

The UNODEX methodology of evaluating potential experiments for their value in reducing the uncertainty in the prediction of waste container penetration by general corrosion makes the following assumptions:

- The operable mechanism of general corrosion in the repository environment is preserved for all the test conditions established in the ESS. This is often stated as a constraint upon any type of accelerated life test.
- The model of general corrosion formulated above in Table 4-4 is structurally correct, and adequately describes the physical process for the entire independent variable space defined by the ESS, the MBD and the expected in-service conditions.

The following paragraphs present the logic for specification of the ESS virtual data ranges are specified.

Regarding the temperature range, the maximum limit was specified at the temperature of 220°C was selected, based upon early thermal calculations for CHLW, referenced in Section 2.3.1. This maximum container-salt interface temperature has been calculated more recently and is documented in Table 4-7 above, indicating the maximum value of

**Table 4-8: Convergence Steps in Obtaining the Empirically-Consistent Model of Virtual Data Error**

Iteration=	1	2	3	4	5	6
$a_1$	1.26714	1.27492	1.27381	1.27400	1.27398	1.27402
$a_2$	-21.3949	-15.8527	-15.3725	-14.9748	-14.8374	-14.7625
$a_3$	692.679	671.829	623.132	606.015	598.121	595.031
$a_4$	-0.21545	-0.15086	-0.14904	-0.14557	-0.14454	-0.14388
$b_1$	1.289+11	7.978+10	7.986+10	8.042+10	8.045+10	8.067+10
$b_2$	774.458	464.925	463.774	466.528	466.406	467.604
$b_3$	16243.59	16178.22	16139.07	16122.15	16115.05	16111.85

$$E = a_1 T + a_2 [O] + a_3 [Mg] + a_4 [H_2O] + \frac{a_5}{\sqrt{t}}$$

$$y = \frac{b_1}{b_2 + \sqrt{t}} \times \exp c_1 [O] + c_2 [H_2O] + b_3 [Mg] - \frac{c_4}{T}$$

227°C at 5 years. There is no published literature regarding any dominant mechanism different than that exhibited in the MBD measurements at these temperatures (150°C - 220°C).

The minimum temperature was selected to reflect ambient temperatures at the repository horizon, approximately 60°C.

Dissolved oxygen concentrations are expected to become anoxic (0.05 ppm) shortly after permanent closure. However it is conceivable that a waste container may be subject to contact with aerated brine for the entire operating period, as the degree to which brine will be aerated depends upon the rate of creep closure of the salt upon the container and the sealing capability of the salt against oxygen diffusion.

The maximum dissolved oxygen concentration was assumed to be 2.0 ppm for the ESS, in the interest of obtaining overstress test information on this variable.

Magnesium concentration limits were set at 0.001 and 0.06, reflecting concentration values of PBB3 (0.059) for the maximum value, and representing the dissolution scenario, in which 98.4 weight percent of the total brine derives from dissolution of the bedded halite and the remaining 1.6 weight percent from the included high-magnesium brine for the minimum value ( $0.984 \times 0.0001 + 0.016 \times 0.059 = 0.001$ ).

Total water fraction is specified at the limiting values of 5.0 weight percent (lowest test value) and 80.0 weight percent, corresponding to all brine (20.0 percent are dissolved solids) at the wetted surface.

Table 4-9 summarizes the above specifications for the ESS.

With the model of general corrosion, the experiment sample space and the in-service environment specified, it is now possible to generate uncertainty-optimized experiment designs.

#### **4.3.3 Notation and Review of UNODEX**

In all the experiment designs which follow, a shorthand notation will be adopted which uniquely identifies each potential experiment in the ESS under evaluation. Each experiment in the ESS has associated with it a unique 5-digit number composed of a 'level number' in each position 1 through 5 (left to right). The positions directly correspond to (1) Temperature, (2) Dissolved Oxygen Concentration (3) Magnesium Concentration, (4) Total Water Fraction and (5) Time, or duration of the test. The level numbers are assigned, starting from one (corresponding to the lowest value of the independent variable) and ranging to the number of discrete levels which that particular independent variable may assume. Hence for an ESS with limits on the independent variables as indicated in Table 4-9, and three (3) equispaced levels per independent variable, the virtual data number 11132 would correspond to a potential experiment conducted at the lowest level for temperature, 60°C, the



**Table 4-9: Limiting Values for the Experiment Sample Space**

Independent Variable	Minimum	Maximum
Temperature (°C)	60	220
Dissolved Oxygen (ppm)	0.05	2.0
Magnesium Concentration (w/f)	0.0001	0.06
Total Water Fraction (w/f)	0.05	0.80
Test Duration (hours)	750	20,000

lowest level for dissolved oxygen concentration of 0.05 ppm, the lowest level for magnesium concentration, that being 0.001 w/f, and to the highest level for water fraction 80 w/o, and the mid-level for time;  $(20,000 + 750)/2 = 10,375$  hours.

In the interest of exploring general effects and reducing complexity of data presentation, for the most part the ESS's investigated will be limited to 2 levels per variable. Hence only the extrema will be considered. This results in  $2^5 = 32$  virtual data representing potential experiments.

By way of quick review, the UNODEX methodology will be highlighted in this paragraph. Recall that the elements of the methodology are: a model building database (MBD), a virtual data experiment sample space (ESS), a multivariable model of general corrosion, a model of error due to physical variability as dependent upon the same dependent variable set used in the corrosion model, and an estimate of the time-dependent behavior of the independent variables for the in-service environment. UNODEX assembles the above elements so that the following sequence of computations may be performed:

1. The corrosion model is fitted with maximum likelihood estimates of the unknown model parameters and errors, based solely upon the MBD.
2. The uncertainty at the desired design life (300 or 1000 years) is calculated and referenced as the benchmark penetration and uncertainty.

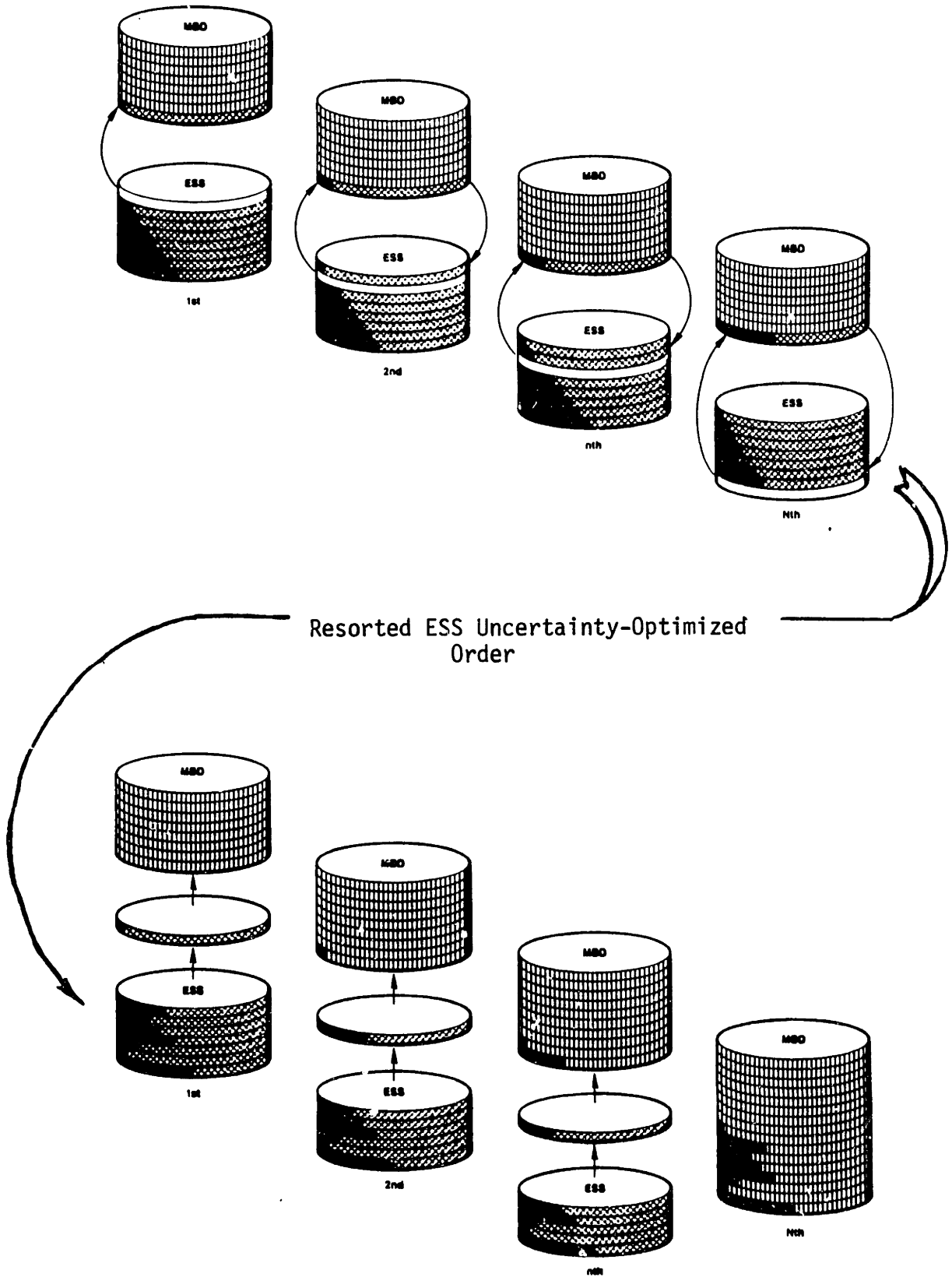
3. Virtual data from the ESS are sequentially evaluated, by shifting one virtual data point into the MBD, calculating the improvement in uncertainty based upon new parameter estimates (and errors), and shifting the virtual data point back out of the MBD again. This continues until each virtual data point in the ESS has an uncertainty reduction associated with it.
4. The virtual data are then cumulatively added to the MBD, in rank order, and the total reduction based on the cumulative addition is calculated at each step (*i.e.* the uncertainty reduction based on the addition of the first of the virtual data points, the first and second, the first, second and third, etc.).
5. After the ESS is evaluated cumulatively, based on the first ranking, the profile of the above uncertainty vs. number of experiments added is evaluated for the presence of a plateau, followed by a sharp discontinuity (section 4.3.5 discusses this phenomena in greater detail) and when this is found, all virtual data up to the point of the plateau are shifted into the MBD, the remaining virtual data are reevaluated sequentially as in 3. above.
6. This generates the total uncertainty reduction vs. number of experiments added, in Uncertainty-Optimized (UO) order.

The same information is displayed in Figure 3-3. Figure 4-14 illustrates the sequential swapping and cumulative addition of the virtual data into and from the MBD.

#### **4.3.4 Validation of the Methodology**

As a first exercise to apply the UNODEX methodology, and to gain the most readily achievable confidence (validation) in the predicted results, the straightforward application is made to evaluating an ESS which is limited to the same independent variable space as the MBD

Figure 4-14: Illustration of the Data Handling Steps in the UNODEX Methodology



itself. This application allows a pseudo-benchmarking of the results by determining the improvement in uncertainty due to the addition of more of the same type of data which was used to parameterize the model itself. It is intuitive that there should be no great improvement in the uncertainty at 300 years (chosen as the arbitrary design life for investigation) even with the total addition of essentially replicate data to the MBD. The reasons for improvement by this addition are due to the increased number of data and the less severe error in the virtual data as compared to the few outliers in the model building data which contribute significantly to the error.

The results of this evaluation do indeed confirm the expected results, as Figure 4-15 indicates. This figure displays the uncertainty at 300 years as a function of the added experiment number. Experiments are added in the uncertainty-optimized order, as defined above. The reference ESS values for the low levels (Table 4-9) were used, but the high levels for all the variables were held to the mean values for the MBD. These are: temperature 144°C, DO 0.0154 ppm, Mg 0.014 w/f, water fraction 41.8 w/o and test duration 2376 hours.

Total reduction in uncertainty for the addition of the 32 virtual experiments amounts to less than 1 mm. The uncertainty-optimized order of the experiments is presented as Table 4-10.

**Table 4-10: Uncertainty-Optimized Design for the Validation Exercise**

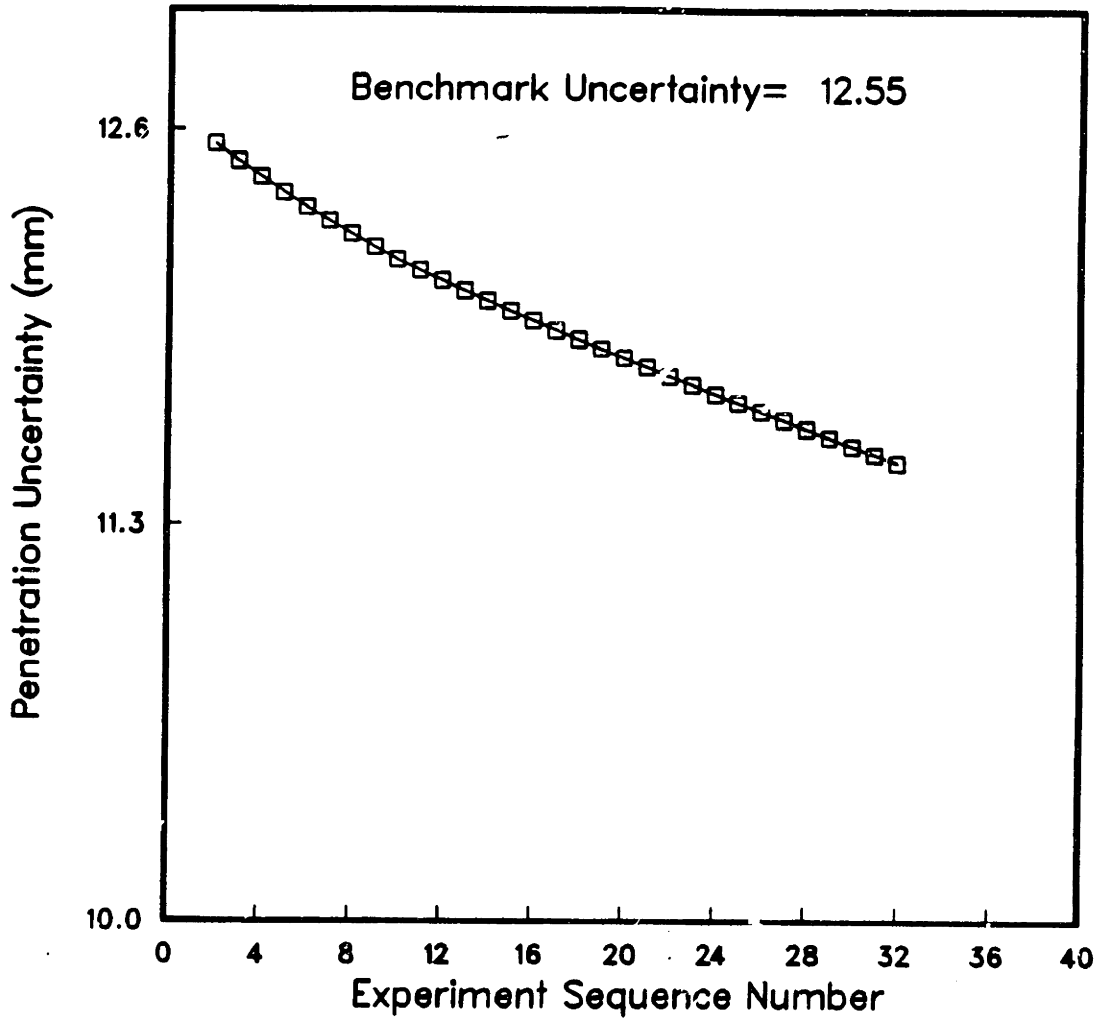
No.	$\Delta\sigma_D$ ( $\mu\text{m}$ )	$\sigma'_D$ ( $\mu\text{m}$ )
22221	5.649609E+01	1.249616E+04
21221	8.605237E-03	1.244463E+04
22211	1.583965E+02	1.239426E+04
21211	2.080244E+02	1.234463E+04
22121	2.528760E+02	1.229978E+04
21121	2.966465E+02	1.225601E+04
22111	3.403223E+02	1.221233E+04
21111	3.825566E+02	1.217010E+04
22222	4.168857E+02	1.213577E+04
21212	4.498223E+02	1.210283E+04
21222	4.833291E+02	1.206932E+04
22212	5.156807E+02	1.203697E+04
12221	5.475293E+02	1.200512E+04
11221	5.795283E+02	1.197313E+04
11121	6.104717E+02	1.194218E+04
11111	6.411768E+02	1.191148E+04
22112	6.715615E+02	1.188109E+04
11122	7.017432E+02	1.185091E+04
12212	7.321064E+02	1.182055E+04
12222	7.617949E+02	1.179086E+04
12211	7.913740E+02	1.176128E+04
21112	8.207051E+02	1.173195E+04
12121	8.494199E+02	1.170323E+04
12111	8.783096E+02	1.167434E+04
11211	9.065811E+02	1.164607E+04
11212	9.350127E+02	1.161764E+04
12112	9.632686E+02	1.158938E+04
11112	9.908730E+02	1.156178E+04
12122	1.018683E+03	1.153397E+04
11222	1.045891E+03	1.150676E+04
21122	1.073510E+03	1.147914E+04

$\Delta\sigma_D$  = Uncertainty Reduction ( $D = 300\text{years}$ )

$\sigma'_D$  = New Error ( $D = 300\text{years}$ )

Figure 4-15: Uncertainty Reduction for the Validation Exercise ESS

Improvement in Predicted  
Waste Container Penetration Uncertainty  
Penetration at 300 years = 21.24 mm  
Evaluation of ESS 231



#### 4.3.5 The Resequencing Frequency

One of the most interesting aspects of the UNODEX methodology has already been alluded to in the above descriptions of the computation sequence. Addition of all the virtual ESS data in the initially-sorted uncertainty-optimized order results in a pronounced discontinuous behavior in the plot of uncertainty vs. sequence number. One computation of such behavior is presented as Figure 4-16. The ESS specified for this application was the same as we have been calling the reference case (Table 4-9), except the number of levels per independent variable was chosen as 3 in order to better illustrate the behavior in 243 points.

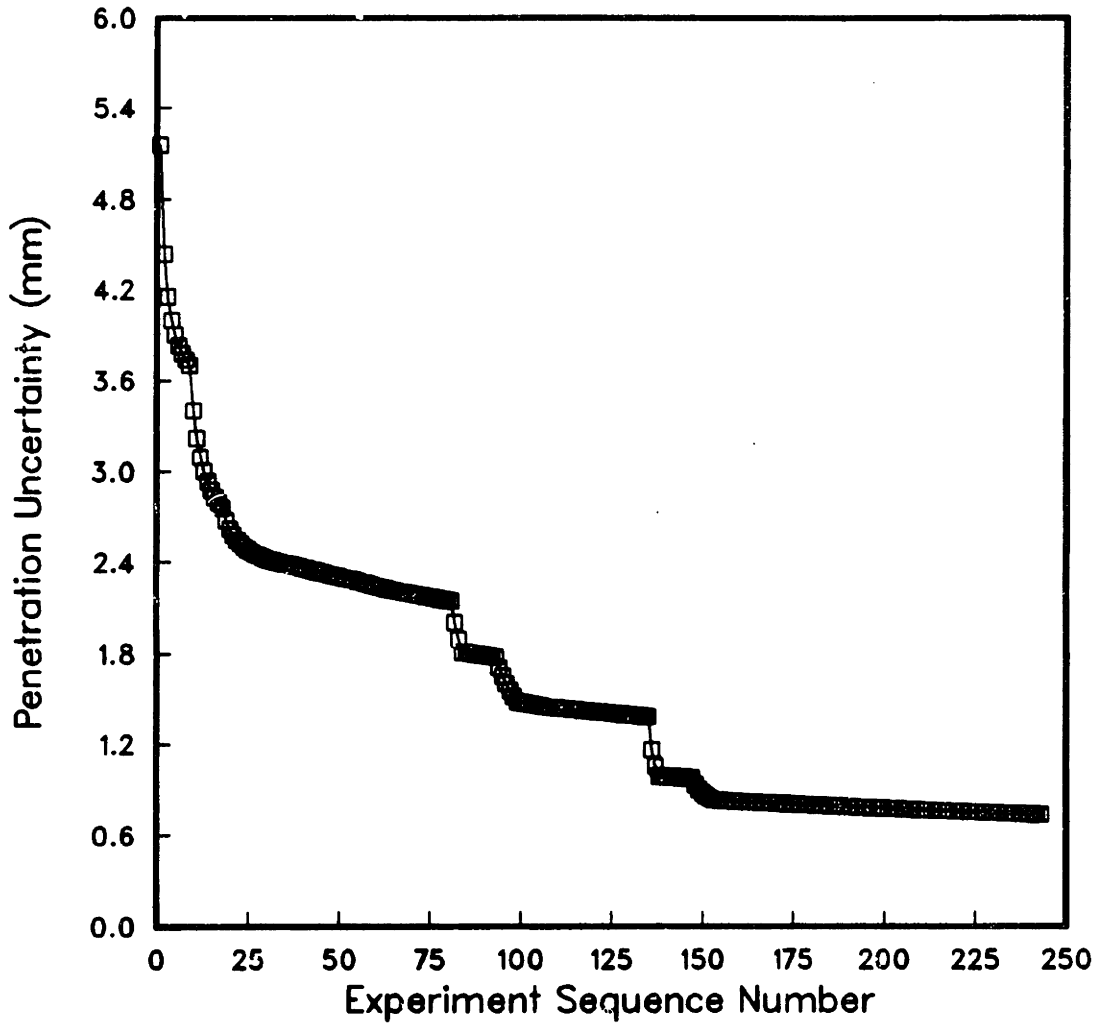
Figure 4-16 serves only to illustrate the discontinuities which may occur if resequencing is not employed. It does not represent quantitatively correct penetration and uncertainty, as no error weighting scheme was used to generate the results in this figure. For comparative purposes, Figure 4-17 presents results generated by resequencing the virtual ESS data after the 1<sup>st</sup>, 2<sup>nd</sup>, 10<sup>th</sup> and 125<sup>th</sup> experiment, based upon an algorithm in UNODEX which resequences the remaining virtual data upon detection of a plateau ('knee' in the curve).

This test algorithm steps through the incremental uncertainty difference vs. experiment number data, comparing the slope at a given



Figure 4-16: Uncertainty Reduction for the Case of no Resequencing

Improvement in Predicted  
Waste Container Penetration Uncertainty  
Penetration at 300 years = 27.85 mm  
Evaluation of ESS 110



point to the average of the three previous slopes. When the quotient of the new slope and the three-point-average falls below a predetermined criterion, (input parameter, in this case 0.20) the virtual data in ranked positions greater than the test value are all resequenced, by sequential evaluation.

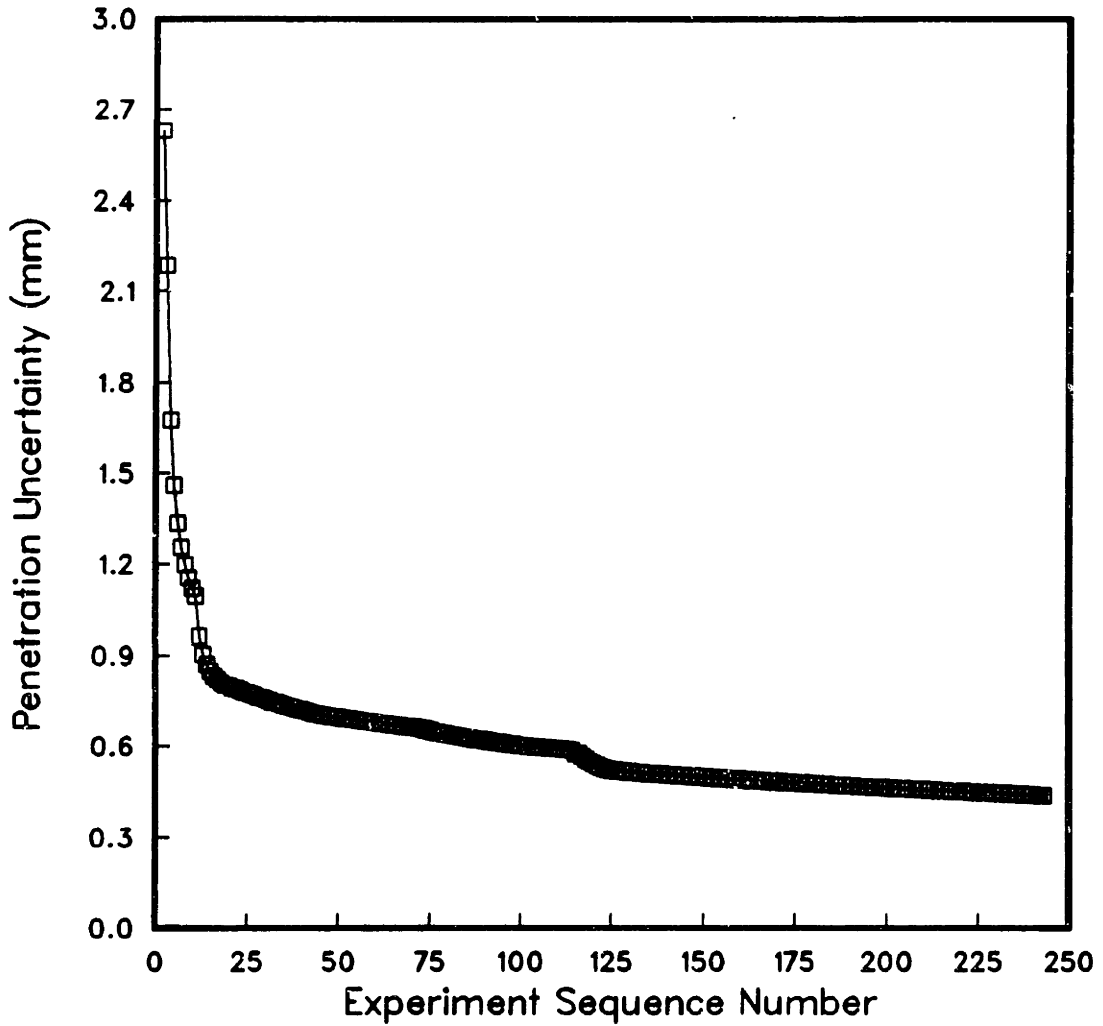
#### **4.3.6 Accelerated Life Testing and the First Point Uncertainty Reduction**

One of the primary conclusions of this thesis will be discussed in this section, that of the 'first point uncertainty reduction'. This section addresses itself to quantitatively evaluating accelerated life testing. The linkages established between model, data, virtual data and error provide the means to address accelerated life testing in a single variable at overstress conditions and for multiple variables at overstress test conditions.

Results of the reference ESS (for 2 levels per variable) are presented as Figure 4-18. The most striking feature of this evaluation is the magnitude of the uncertainty reduction associated solely with the addition of the first virtual data point. The penetration and uncertainty at 300 years based only on the MBD, the 'Benchmark Uncertainty', are 22.29 mm and 13.84 mm, (standard deviation) respectively. Table 4-11 accompanies the figure. It can be noted from the table that the first virtual data point, ranked the greatest for uncertainty reduction, is at all high levels of the independent

Figure 4-17: Uncertainty Reduction with Resequencing  
at Points 1, 2, 10, 125

Improvement in Predicted  
Waste Container Penetration Uncertainty  
Penetration at 300 years = 21.24 mm  
Evaluation of ESS 218



variables, namely point 22222. Uncertainty is reduced from 13.84 mm to 2.98 mm, or 78%. This counterintuitive result deserves some further explanation. The reference ESS conditions specify this point at a test duration of 20,000 hours, roughly an order of magnitude times the mean MBD test duration of 2376 hours. As well, all other variables, when at the maximum value represent a temperature, DO level and magnesium concentration which is unrepresented in the MBD.

It should be noted that the model contains data with test durations ranging from 300 to 7,000 hours, with a mean test duration of 2376 hours, hence the simulated test at 20,000 hours is a very long term test which becomes more important to extrapolations than the bulk of the MBD which is clustered at relatively short times.

Also, the test is an accelerated life test in all variables relative to in-service conditions, and with the functional relationship among the independent variables available via the corrosion rate model, the overstress conditions in the non-time independent variables in effect act to simulate a longer term test.

This large reduction in uncertainty may be explained in terms of the uniqueness of the test and hence the associated information gain due to this uniqueness. The first data point introduced is at an entirely new coordinate in the independent variable space. The information gain in

Figure 4-18: Results of Uncertainty Reduction for the Reference ESS

Improvement in Predicted Waste Container Penetration Uncertainty  
Penetration at 300 year = **22.29** mm  
Evaluation of ESS 201

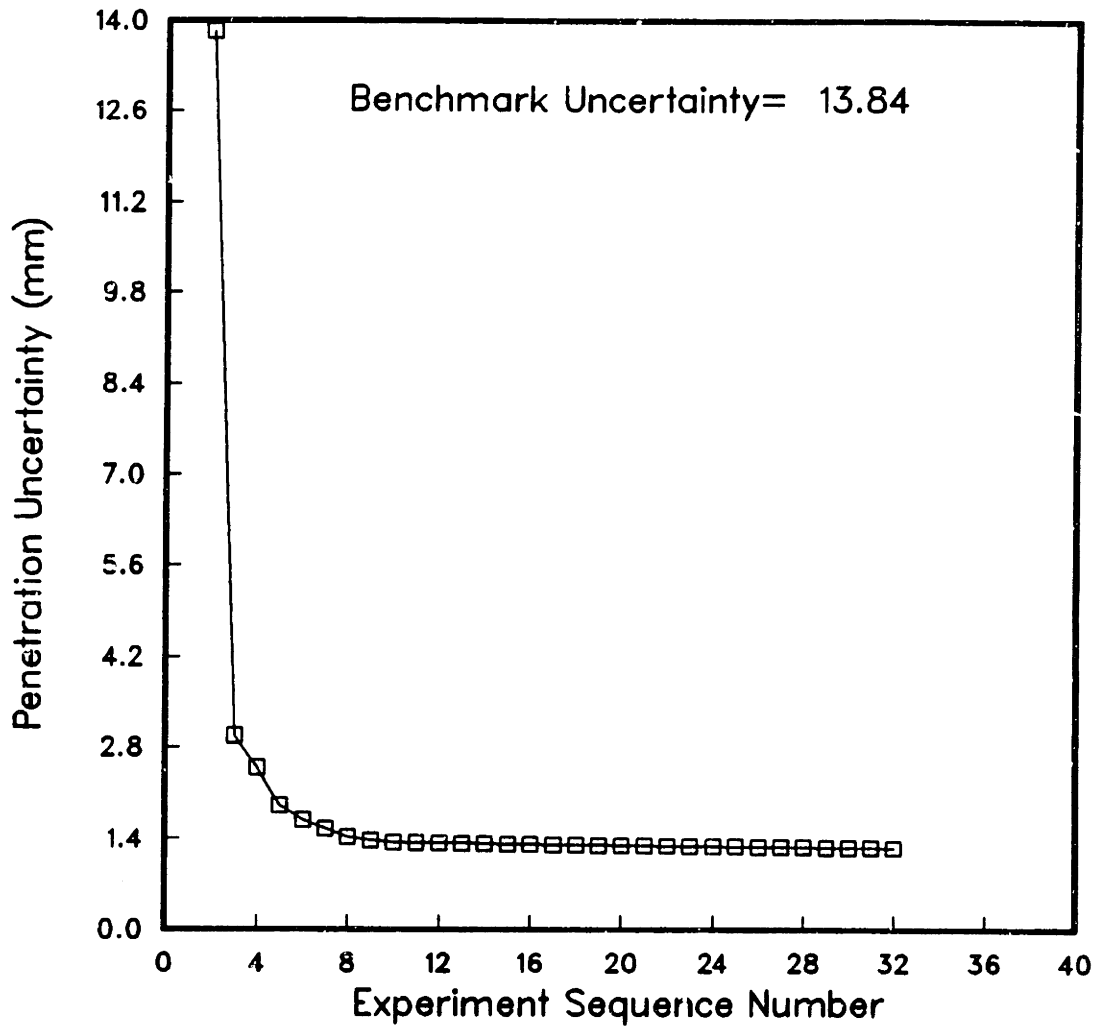


**Table 4-11:** Tabulation of Uncertainty Reduction for the Reference ESS

No.	$\Delta\sigma_D$ ( $\mu\text{m}$ )	$\sigma'_D$ ( $\mu\text{m}$ )
NONE		1.383987E+04
22222	1.086304E+01	2.976828E+03
22221	4.913547E+02	2.485474E+03
22212	5.699739E+02	1.915500E+03
21222	7.998251E+02	1.685649E+03
21212	9.323374E+02	1.553136E+03
22211	1.057440E+03	1.428034E+03
21221	1.110567E+03	1.374907E+03
21211	1.141975E+03	1.343499E+03
22122	6.111450E+00	1.337388E+03
22112	1.151111E+01	1.331988E+03
21122	1.662024E+01	1.326879E+03
21112	2.121997E+01	1.322279E+03
22121	2.778760E+01	1.315711E+03
22111	3.349988E+01	1.309999E+03
21121	3.864783E+01	1.304851E+03
21111	4.343325E+01	1.300066E+03
12222	4.696619E+01	1.296533E+03
12212	5.042419E+01	1.293075E+03
11222	5.372473E+01	1.289774E+03
11212	5.705945E+01	1.286440E+03
11121	6.028552E+01	1.283214E+03
12111	6.347546E+01	1.280024E+03
12121	6.665405E+01	1.276845E+03
11122	6.979736E+01	1.273702E+03
11111	7.292334E+01	1.270576E+03
11112	7.603174E+01	1.267467E+03
12221	7.912524E+01	1.264374E+03
12112	8.225342E+01	1.261246E+03
12211	8.529626E+01	1.258203E+03
11211	8.823401E+01	1.255265E+03
11221	9.132251E+01	1.252177E+03

$\Delta\sigma_D$  = Uncertainty Reduction ( $D = 300\text{years}$ )

$\sigma'_D$  = New Error ( $D = 300\text{years}$ )

the addition of a replicate data point doubles the local information, raising it from 1 to 2, while the gain in information in adding a unique data point raises the local information from 0 to 1. The absolute increase is the same, but the relative increase is essentially infinite. Based upon this interpretation, subsequent additions of data with similar independent variable values yield far less uncertainty reduction.

An exercise may be performed which generates the reduction in uncertainty due to this unique, first point as a function of the maximum test duration. Figure 4-19 presents the fractional reduction of the benchmark uncertainty due to this 'first point addition' presented functionally against maximum test time. The upper line on the curve is for 1000 year design life and the lower line is for 300 years. The results exhibited by this curve are far reaching. If a commitment is to be made to use accelerated life testing, the results presented here serve to quantify the benefit of longer test times, and provide numerical input to optimization analyses, such as the cost of uncertainty reduction.

The same type of results are tabulated for temperature in Figure 4-20. Results indicate that, for a fixed maximum test duration of 20,000 hours, the fractional uncertainty reduction due to 'first point' addition is nearly linear with maximum temperature.

Figure 4-19: First Point Uncertainty Reduction vs. Test Duration

Significance of the Maximum Test Duration  
for the Greatest  
Uncertainty-Reducing Test in the ESS

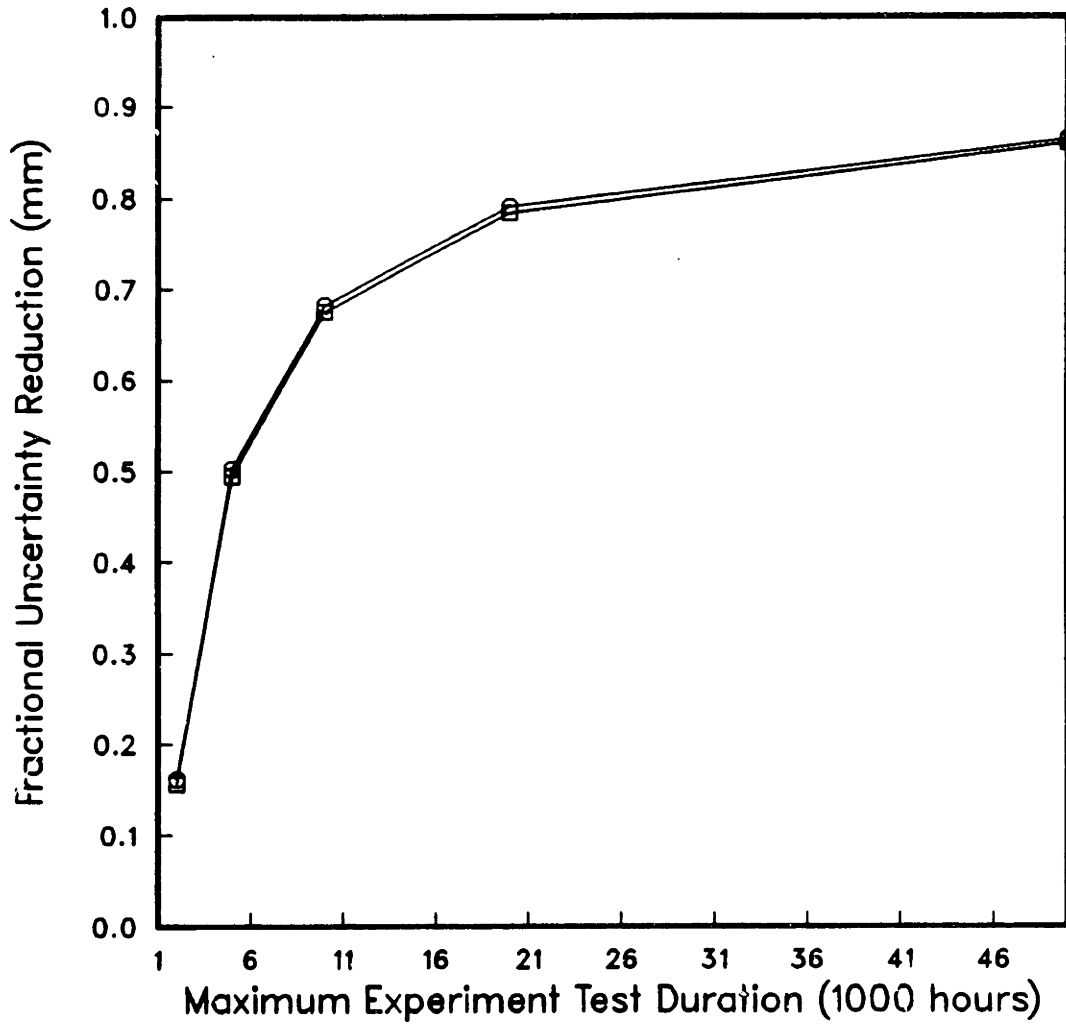
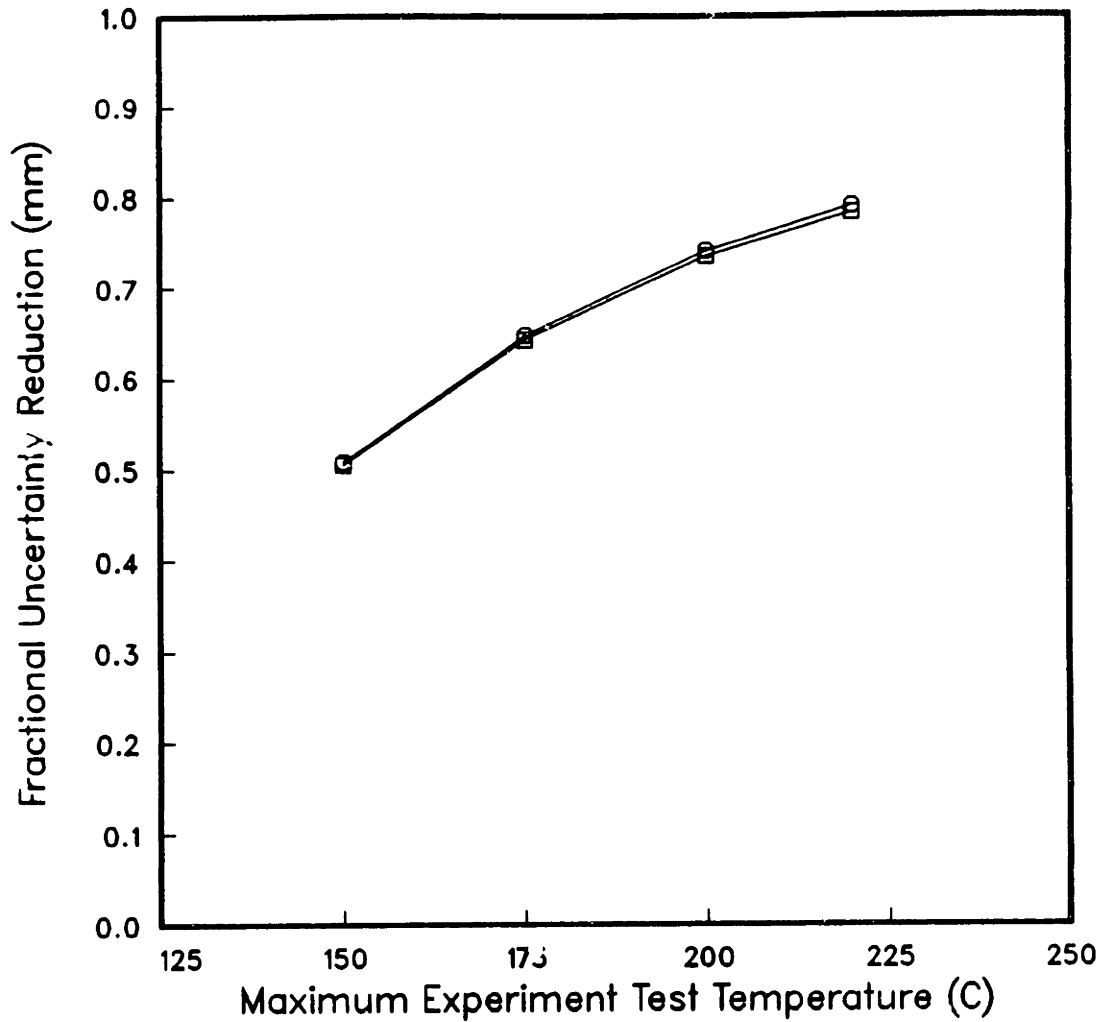




Figure 4-20: Uncertainty Reduction Dependence on Test Temperature for Multivariable-Accelerated Experiments

Significance of the Maximum Test Temperature for the Greatest Uncertainty-Reducing Test in the ESS

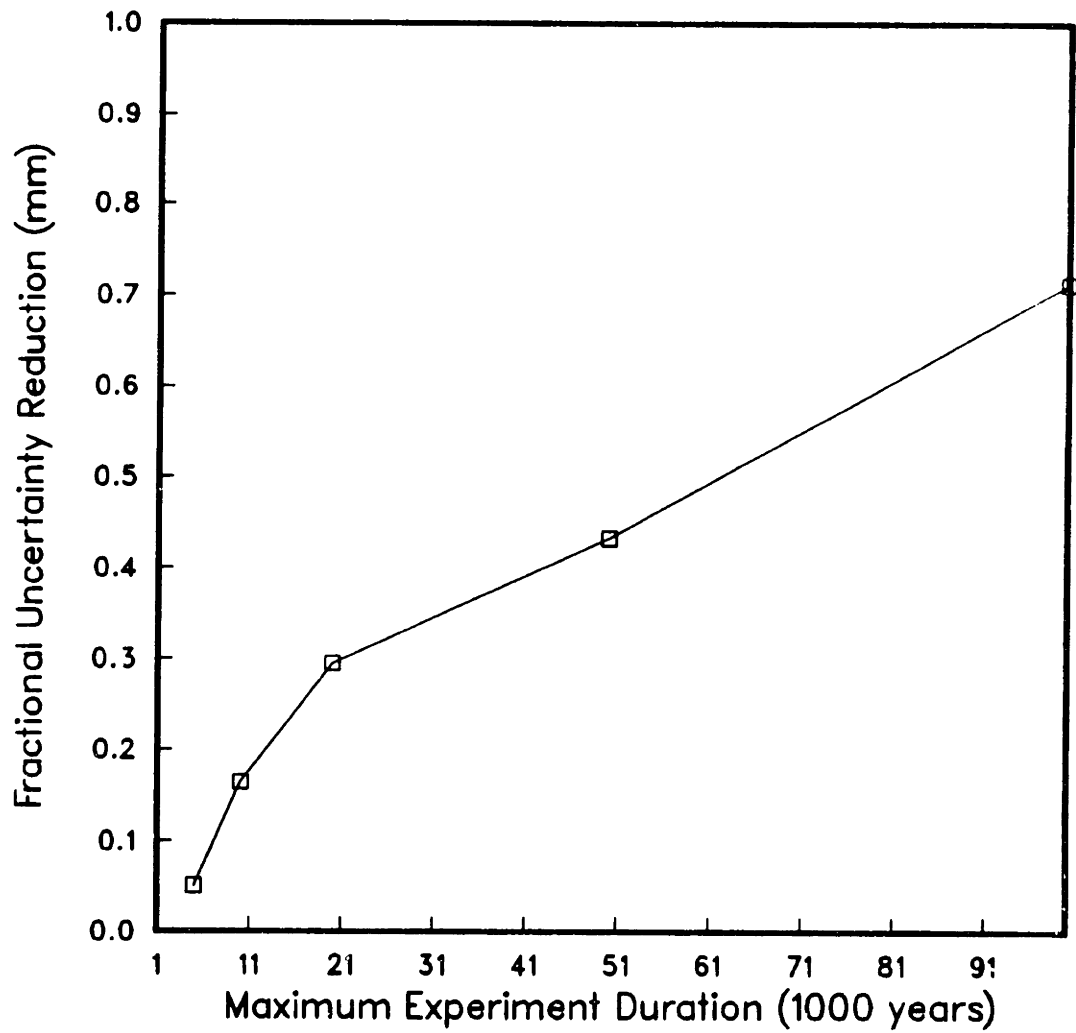


If there is some error in the structural form of the multivariable corrosion model, then the variable interactions may not be quantified correctly, and accelerated life testing in more than one overstress variable would not be appropriate. However, since the model describes the MBD adequately, it is possible to analyze the same type of behavior as above, while holding the maximum value for all but the overstress variable at the MBD mean values. This univariate accelerated life testing first point uncertainty reduction is displayed in Figure 4-21. As can be seen by comparing Figure 4-21 with Figure 4-19, single variable (thermal) accelerated life testing will require 100,000 hours of testing to generate approximately the same 'first point' uncertainty reduction as will accelerated life testing in all the independent variables for 10,000 hours. This order of magnitude difference in test duration clearly indicates the impact of successful accelerated life test data on total data requirements and the imperative need for a valid, detailed corrosion process model.

#### **4.3.7 Overall Trend in Uncertainty-Optimized Designs**

Finally, as a complimentary analysis to the above 'first point' uncertainty results the uncertainty-optimized experiment designs will be analyzed for general trends in the reference ESS and exercises are performed to determine the limits of these general trends in the following section.

Figure 4-21: Uncertainty Reduction Dependence on Test Duration for Thermally-Accelerated Experiments



#### 4.3.7.1 Reference ESS

The uncertainty-optimized design for the reference ESS is presented as Table 4-12, following. Virtual data ESS numbers appear in the final, optimized order, after resequencing at the 1<sup>st</sup>, 2<sup>nd</sup> and 8<sup>th</sup> virtual data point addition. The second column of the table presents the uncertainty at 300 years based upon the addition of all the virtual ESS data, cumulatively, up to the ESS number in the first column. The final columns list the calculated value for the corrosion rate, and the associated virtual data error.

As can be seen in the table the uncertainty-optimized design is constructed so that all of the high temperature data points rank greater than that obtained at lower temperatures which strongly indicates the overall importance of the test temperature in controlling uncertainty. The corrosion rate falls off monotonically and the error increases monotonically with decreasing uncertainty reduction for contiguous groups of data sharing a common test duration. In general then, for a fixed test time, low error, high corrosion rate experiments consistently rank the most favorable and low corrosion rate, high error experiments the least favorable.

Consistency in the trend is greatly diminished after the transition into the low temperature tests. The low temperature tests populate the very flat portion on the uncertainty-experiment curve. Differences in

**Table 4-12: The Uncertainty-Optimized Experiment Design for the Reference ESS**

No.	$\Delta\sigma_D$ ( $\mu\text{m}$ )	$\sigma'_D$ ( $\mu\text{m}$ )	$y$ ( $\mu\text{m}/\text{yr}$ )	$E$ ( $\mu\text{m}/\text{yr}$ )
22222	10863.04	2976.828	7420.586	276.1801
22221	491.3547	2485.474	9129.373	281.2977
22212	569.9739	1915.500	7420.525	286.9709
21222	799.8251	1685.649	7420.519	304.9669
21212	932.3374	1553.136	7419.980	315.7578
22211	1057.440	1428.034	9129.582	292.0886
21221	1110.567	1374.907	9129.812	310.0846
21211	1141.975	1343.499	9129.573	320.8755
22122	6.111450	1337.388	1079.122	241.0732
22112	11.51111	1331.988	1079.122	251.8641
21122	16.62024	1326.879	1079.121	269.8601
21112	21.21997	1322.279	1079.121	280.6509
22121	27.78760	1315.711	1327.774	246.1909
22111	33.49988	1309.999	1327.774	256.9818
21121	38.64783	1304.851	1327.772	274.9778
21111	43.43323	1300.066	1327.772	285.7686
12222	46.96619	1296.533	67.24272	72.33686
12212	50.42419	1293.075	67.23022	83.12771
11222	53.72473	1289.774	67.23260	101.1237
11212	57.05945	1286.440	67.23255	111.9146
11121	60.28552	1283.214	4.763974	71.13458
12111	63.47546	1280.024	4.763733	53.13856
12121	66.65405	1276.845	4.763735	42.34771
11122	59.97936	1273.702	3.871200	66.01690
11111	72.92334	1270.576	4.763800	81.92543
11112	76.03174	1267.467	3.871825	76.80775
12221	79.12524	1264.374	82.72289	77.45454
12112	82.25342	1261.246	3.871831	48.02088
12211	85.29626	1258.203	82.72179	88.24539
11211	88.23401	1255.265	82.71934	117.0323
11221	91.32251	1252.177	82.74504	106.2414

$\Delta\sigma_D$  = Uncertainty Reduction ( $D = 300\text{years}$ )

$\sigma'_D$  = New Error ( $D = 300\text{years}$ )

virtual data in this region of the ESS are very small, and the various experiments essentially contribute an equivalent uncertainty reduction.

The most interesting feature of the the uncertainty-optimized design is that the general trend is found to exhibit an oscillatory behavior in ranking long- and short-term data. As can be seen in the table, (see also the discussion in Section 4.3.6. above) the optimal experiment to perform first is the most unique experiment, the one which is the furthest from MBD in independent variable space. This point will be at the highest of the overstress conditions, and will yield the greatest corrosion rate and penetration. Due to the structure of the empirical error model (Table 4-8), this virtual data point also has a relatively small predicted error.

The addition of subsequent virtual data would appear to involve a simple rank ordering of those remaining points which would, each in turn, yield the greatest corrosion rate with the least error. This, however, is not the case. The complication arises when one considers that the addition of the first virtual data point to the MBD (it now becomes the same as a measured experimental observation) determines a new IV space. The next greatest uncertainty-reducing experiment will be the most unique, measured against the MBD plus the newly added virtual data.

Because the required extrapolation is in time\* to the desired design life, the optimal order of addition of virtual data will be driven by obtaining the greatest confidence in the time dependence of the corrosion rate. This is what leads to the oscillatory trend in ranking long- and short- term data.

Table 4-13 displays the first 16 (high temperature) virtual data from the uncertainty-optimized design of Table 4-12 above. This tabulation uses the independent variable names instead of the shorthand notation and is structured to expose the repeating trend. From this table (or Table 4-12) it can be seen that the calculated corrosion rate decreases from its value at all high IV levels, by reducing to the low level, the following independent variables:

$$W > O > (W+O) > Mg > (W+Mg) > (O+Mg) > (W+O+Mg)$$

in the indicated order.

The table indicates the first virtual data point is at all high levels. The first oscillation occurs when the second data point is added and all variables are held high, except time. The subsequent optimal additions are long time tests which reduce the corrosion rate by the smallest amount in each step, reducing water, dissolved oxygen, and

---

\*Note that *time* is the only variable which exceeds the range established by the ESS in the in-service environment.

both water and dissolved oxygen in sequence. The same sequence of three is repeated at short times, and then the magnesium level is reduced and the W, O, W+O sequence is repeated for long and short times.

This trend behavior is exhibited for ESS's about the reference case for a maximum test time of approximately 50,000 hours and a minimum of from 5,000 to 10,000 hours. The longer test times cause the corrosion rate to decrease such that high levels for the other variables act effectively to accelerate the degradation more than the actual test time and hence the uncertainty-optimized order of the reference case is not preserved exactly. As the maximum test time becomes too short, of the order of the mean for the MBD, long term tests become noncontributing.

#### **4.4 SUMMARY**

Summarizing, the main results of the thesis were presented in this chapter, the application of the uncertainty-optimized experiment design to waste container penetration.

In the process of accomplishing this goal, the body of experimental data relevant to the brine-steel corrosion system to be encountered in the repository was evaluated. It was found that only nuclear waste program specific-data would provide satisfactory detailed information. The data from various types of tests were reviewed and consolidated into a single database from which to generate maximum likelihood estimates of corrosion model parameters.



**Table 4-13: Oscillatory Nature of the Overall Trend in Uncertainty-Optimized Designs**

UO Number	Long Term Tests	Short Term Tests
1	- All Independent Variables at High Levels -	
2		t
3	W	
4	O	
5	W + O	
6		W + t
7		O + t
8		W + O + t
9	Mg	
10	W + Mg	
11	O + Mg	
12	W + O + Mg	
13		Mg + t
14		W + Mg + t
15		O + Mg + t
16		W + O + Mg + t

Various investigations of compatible subsets of the above and other relevant data were performed to determine the principle variables which should compose a multivariable model of general corrosion. Based upon separate effects behavior and fundamental principles of similar chemically-driven degradation processes, several test models were constructed. Based solely upon the performance of the alternative models when fitted to the database, the superior model was selected. The sensitivity of this model to various nonlinear regression controls, such as convergence criteria, weighting factors and starting guesses, was assessed, and the model found to be satisfactory, even when two of the five parameters were fixed as constants.

Assumptions regarding the expected time dependence of the in-service environment were made, and resulting time- and environment-integrated penetration and uncertainty were calculated for the assumed reference case and several known potential perturbations from the reference case.

Finally, the impact of performing a wide array of potential experiments was assessed for impact on uncertainty reduction at 300 and 1000 year design lives. The concept and techniques of simulating 'virtual' data are developed and the methodology is effectively validated by comparing the uncertainty reduction for the 'virtual' data against the actual measured data in the database. Accelerated testing in one (temperature) and multiple control variables was quantitatively

evaluated. Two primary techniques which evaluate potential experiments are developed and results presented; 'first point' uncertainty reduction and overall trend in uncertainty-optimized designs.

The primary results of this application are:

- Optimization of the experiment design requires multiple passes at resequencing the virtual ESS data.
- The uncertainty-optimized experiment design always exhibits a large reduction in uncertainty associated with the most unique (as compared to the model building database) overstress experiment. In this sense, accelerated life testing is identified as viable.
- Quantitative evaluations of the uncertainty reduction associated with multivariable accelerated life testing indicate a strong nonlinear uncertainty reduction with total test duration.
- Overall trend behavior for uncertainty-optimized designs indicate a strong tendency to oscillate between repeated sequences of long- and short-term tests. This is driven by the necessity of establishing the corrosion rate vs. time behavior at the test time extrema, thus enabling the most confident extrapolation.

The entire application necessarily makes the working hypothesis that: *The model of general corrosion developed in this thesis is structurally correct, and that it includes all the significant independent variables affecting the corrosion process.* In fact, knowledge of the waste container corrosion process is not complete at all, and dealing with that uncertainty will necessitate, in addition to further fundamental research, the implementation of the UNODEX methodology with many different corrosion rate models.

## 5. SUMMARY, CONCLUSIONS AND RECOMMENDATIONS FOR FUTURE STUDY

### 5.1 INTRODUCTION

The history of developments within the nuclear fuel cycle, particularly the more recent policy decisions regarding antiproliferation have effectively locked the light water reactor into a most inefficient operating mode, the 'once-through' fuel cycle. One significant consequence of this type of wasteful nuclear energy economy is the problem of disposal of rapidly accumulating spent fuel.

The passage of the Nuclear Waste Policy Act of 1982 [57], has, with some urgency, charged the US Department of Energy with the responsibility of administering the nation's effort for ultimate disposal of High-Level Nuclear Waste in mined geologic repositories.

Federal regulators have been motivated particularly by the large inventory (70,000 MT) of radioactive material intended for disposal in this potential repository, and the long term radiological threat that such an inventory could potentially pose to the human environment for many generations, to develop regulations applicable over thousands of years. Specific federal regulations have been written, one of which focuses on providing an early containment of radionuclides within engineered waste containers for from a minimum of 300 to 1000 year time periods. The logic behind this time particular time period is that it roughly corresponds with the time interval during which radioactivity and

heat generation are dominated by the decay of fission products (most notably Cs<sup>137</sup> and Sr<sup>90</sup>). Most physical and chemical changes to waste package components which can potentially affect mechanical stability and isolation are at their highest during the first 1000 years.

Since no permanent high-level nuclear waste repository has ever been built or operated, and in light of the above mentioned long design lives, assessment of performance will require extrapolation beyond existing technical experience. Regulators have recognized that the unique difficulties associated with credible validation of performance predictions over 1000 year container design lives demand a unique experimental treatment. Specifically, federal regulations call for the use of accelerated tests; "Demonstration of compliance ...will involve the use of data from accelerated tests and predictive models...".\*

## 5.2 PURPOSE OF THE WORK

The stated purpose of this work has been to quantify the impact that additional experimental data may provide on the uncertainty in nuclear waste container penetration predictions, before these experiments have actually been performed. By developing a methodology to accomplish this task, the techniques to design an experimental test matrix ranking (from a pre-specified collection of potential experiments) the candidate tests under evaluation from greatest to least uncertainty reduction at the

---

\*Code of Federal Regulations, Title 10, Part 60 [59]

desired design life. These experiment designs are termed uncertainty-optimized (UO).

The methodology developed for this purpose couples a mechanistic multivariable model of the corrosion process, a model building database (MBD) consisting of laboratory-measured data relevant to corrosion performance of A216 steel in simulated repository brines, a model of error (uncertainty) propagation, predictions of waste container-repository in-service conditions and a collection of 'virtual' (or simulated) experiment data representing the potential experiments under evaluation for their impact on uncertainty reduction. The virtual data constitute the experiment sample space (ESS).

The above methodology required accomplishing the following major objectives in this thesis:

- Compile and characterize the repository environment as it impacts waste container degradation by corrosion
- Identification of the principle waste container corrosion mechanism and the environmental variables which affect this mechanism in repository-relevant conditions
- Assemble a database of measurements generated by the corrosion mechanism which are suitable to construct a model
- Develop a parametric model of waste container corrosion, and an algorithm to estimate the parameters based upon model building data
- Specify the expected time-dependent waste container in-service environment

- Develop an algorithm to propagate uncertainties in the time- and environment-integrated penetration
- Develop an automatic means of virtual data handling so that the virtual data is evaluated for penetration uncertainty reduction and added to the model building data in uncertainty-optimized order

### 5.3 ASSESSMENT OF THE MODEL

Arguments are made in Chapter 2 which justify the assumed model of failure (general corrosion) for a waste container in service. The results of high-magnesium brine static excess salt tests indicate magnesium is incorporated in the corrosion product oxide, and that this oxide is non-protective as active metal dissolution proceeds throughout the test.

The simple structure, low strength, and absolute lack of observation of microscopic (threshold) failure mechanisms for the A216 alloy provide justification for ruling out these mechanisms as a category. Caution is urged, however, in making this type of assumption for the container at the location of head-to-container joining. Weldments may lead to significantly altered microstructure and possibly large localized residual stresses. This thesis has analyzed the general corrosion attack of the A216 alloy and made the assumption that the container behaves as the alloy, ignoring design-specific features which might possibly constitute a 'weak link' to failure. This is because no detailed design information relative to final container head closure was

available at the time. The weak link potentially provided by the effects of welding are deferred to future research.

The very simple model of general corrosion for steel in magnesium-bearing brines explains all gross trends identified in the experimental data. This model has been developed largely drawing upon the consistent validity of the Arrhenius (and, more generally, the Eyring) functional form to explain chemical reaction-driven processes. The database itself has been compiled from a variety of specialized test programs. As such, unidentified, uncontrolled variables may differ from test type to test type. It is expected the fit of the model would improve greatly if a consistent database were available. At present, however, it is concluded that the corrosion rate model developed for the purpose of this thesis is entirely consistent with the available data. Largely in agreement with Peters and Kuhn [46], the kinetic behavior was found to be very nearly parabolic.

#### **5.4 ASSESSMENT OF THE EXPERIMENT DESIGN METHODOLOGY**

After extensive searching of the published literature, it was concluded that great deficiencies exist related to the explicit mathematical treatment of extrapolation. This is especially true of applied situations which involving large (factor of 10 to 100) extrapolations beyond the interval over which experimental observations have been made.



The theoretical development of a methodology to specify uncertainty-optimized experiment designs is presented in Chapter 3. Uncertainty-optimized is defined at the beginning of this thesis to mean that the product experimental design, if performed, is expected to generate data which will yield the greatest reduction in uncertainty at some desired extrapolated time value such as the design life of a waste container.

The methodology to generate uncertainty-optimized experiment designs has been developed in the form of a Fortran computer program called UNODEX (UNcertainty-Optimized DEsign of eXperiments), included as Appendix A. The UNODEX computational procedure is as follows:

1. The specified corrosion model (in general nonlinear, multivariable, and multiparameter) is fitted with maximum likelihood estimates of the unknown model parameters and errors, based solely upon the MBD.
2. The uncertainty (standard deviation) at the desired design life (300 or 1000 years) is calculated and referenced as the benchmark penetration and uncertainty.
3. Virtual data point from the ESS are sequentially evaluated, by shifting one virtual data point into the MBD, calculating the improvement in uncertainty based upon new parameter estimates (and errors), and shifting the virtual data point back out of the MBD again. This continues until each virtual data point in the ESS has an uncertainty reduction associated with it.
4. The virtual data are then cumulatively added to the MBD, in rank order, and the total reduction based on the cumulative addition is calculated at each step (*i.e.* the uncertainty reduction based on the addition of the first of the virtual data point, the first and second, the first, second and third, etc.).

5. After the ESS is evaluated cumulatively, based on the first ranking, the profile of the above uncertainty vs. number of experiments added is evaluated for the presence of a plateau, followed by a sharp discontinuity (section 4.3.5 discusses this phenomena in greater detail) and when this is found, all virtual data up to the point of the plateau are shifted into the MBD, the remaining virtual data are reevaluated sequentially as in item 3. above.

This generates the total uncertainty reduction vs. number of experiments added, in Uncertainty-Optimized (UO) order. The underlying assumptions of the UNODEX methodology and their limitations are discussed below.

First and foremost, the working hypothesis made in this work is that *The model of general corrosion developed in this thesis is structurally correct, and that it includes all the significant independent variables affecting the corrosion process.* This effectively eliminates any uncertainty due to lack of knowledge of the physical process and allows the explicit quantitative evaluation of the uncertainty (or random behavior) in the physical process itself. In fact, knowledge of the waste container corrosion process is not complete at all, and dealing with that uncertainty will necessitate, in addition to further research, the implementation of the UNODEX methodology with many different corrosion rate models.

The parameter estimates, which are determined by a maximum likelihood approach are based upon the asymptotic covariance matrix as determined

in Equation (3.43). This results from the numerically-necessary assumption of local linearity about initial guess values for the parameters. Use of the true parameter covariance matrix would prove to be mathematically intractable and frustrate convergence.

The assumption of local linearity in the parameter space is expected to prove valid, provided sufficient exploration of the parameter space is done before selecting initial guesses. This was the case for all models compared in this thesis.

The assumption was made that penetration and uncertainty in a given time interval was independent from all other time intervals. The author can think of no evidence to the contrary at the present level of corrosion model detail.

It is also assumed that the corrosion rate (dependent variable) for the virtual data under evaluation can be estimated by the model itself. This leads to simulated corrosion rate values for the ESS virtual data which lie exactly on the fitted model-predicted curve. There is no inconsistency in this procedure, as: 1) these precise values are weighted by an empirically-consistent error, and 2) only the uncertainty due to physical variability is being addressed in the thesis.

The determination of the virtual data error is a key element in the validity of the results of this work. As outlined in Section 4.3.1.2, a

simple linear regression model was formulated incorporating each of the independent variables in the corrosion rate model. As the MLE parameter estimates depend upon the weighting of the data, this same error model was used to weight the actual model building data. This approach permitted iteration between the corrosion model and the error model to determine the coefficients and parameters which were empirically-consistent.

In point of fact, the actual data included some significant outliers, which will not be the case with virtual data. In this sense the virtual data error model does not provide the worst possible error measure for the potential experiment, but it also does not provide the least. There is a smoothing effect in this determination of error, which effectively assigns the error expected for many repeated measurements.

## 5.5 ASSESSMENT OF THE RESULTS

Strong assumptions about the expected in-service environment are made in Section 4.3.2.1. These follow the so-called conservative approach to assessing the corrosion performance employed extensively, for example, in the Environmental Assessment for the potential Deaf Smith County Texas site\*. These assumptions are:

- There is infinite reserve of high-magnesium brine available via some means of transport to the container boundary.

---

\*Reference [55]

- The rate of this brine availability is never the limiting step in the overall process of metal dissolution.
- The dissolved oxygen concentration in the brine is always anoxic (0.05 ppm)
- The container-salt interface is always characterized by 5 weight percent water (by brine) and 95 weight percent solid phase salt.

Based solely on the model building data, penetration and uncertainty are calculated. Results indicate 2.93 cm of uniformly penetrated container thickness at 1000 years with an uncertainty,  $\sigma$  of 2.11 cm, or 72%. Employing a standard  $2\sigma$  confidence interval, the maximum penetration at 1000 years becomes 7.15 cm (2.81 inches).

Variations of the environmental conditions revealed a strong sensitivity to temperature, as when the commercial high level waste temperature profile was employed (9.5 kW vs. 6.6kW). Penetration and uncertainty at 1000 years became approximately 12 cm and 13 cm, respectively.

Two major techniques in interpreting the resultant uncertainty-optimized designs were implemented in the thesis: i) the 'first point' uncertainty reduction and ii) the periodic trend.

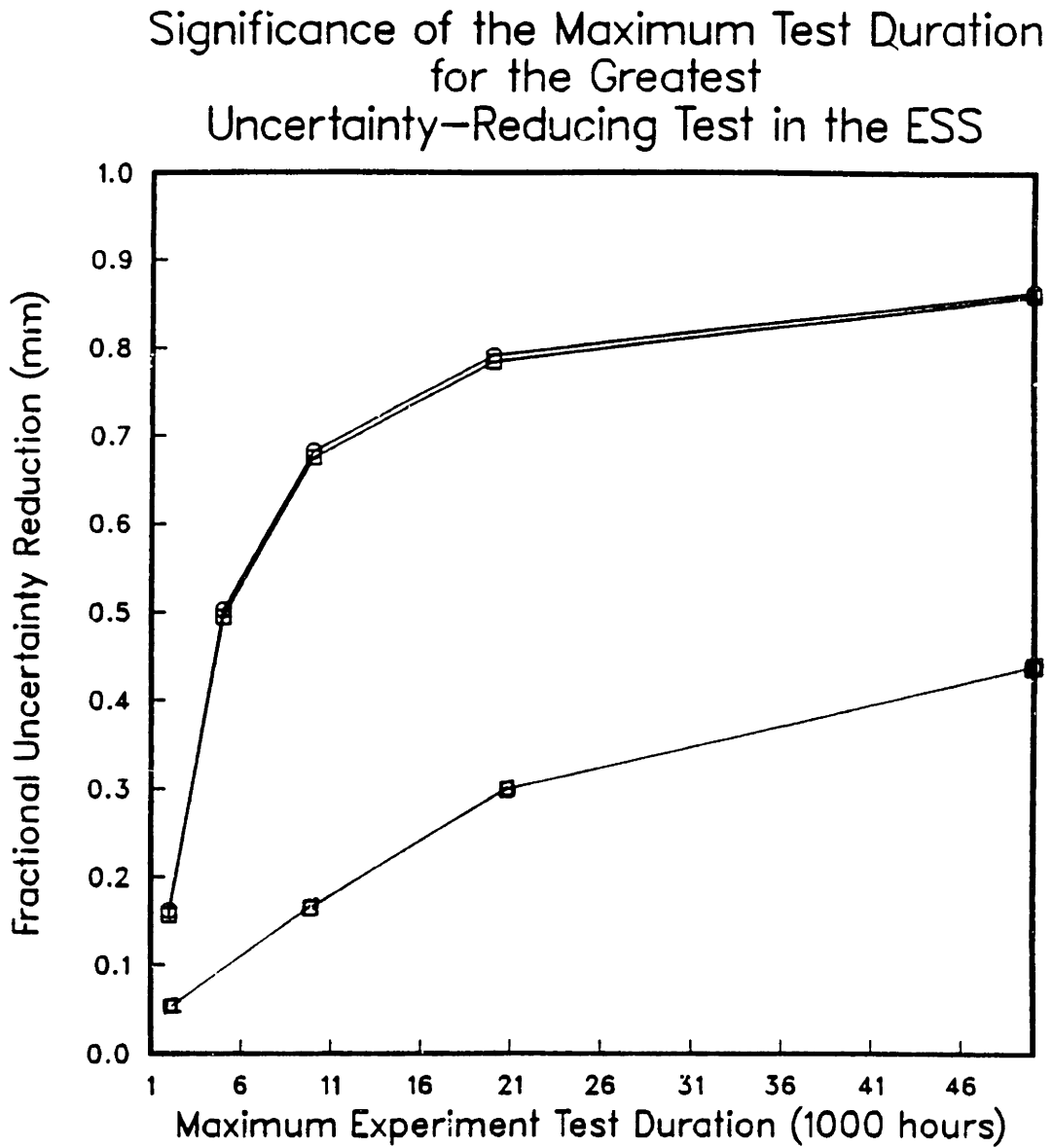
The first technique tabulates the reduction in uncertainty due to the addition of the first virtual data point to the MBD (Selected as that with maximum uncertainty reduction). Findings indicate:

1. The large uncertainty reduction associated only with this first point is due to its uniqueness relative to the model building data, as highly overstressed test conditions often provide.
2. The first point is nearly always associated with the test with all independent variables at their maximum values, that is, the most severe multivariable accelerated life test.
3. The magnitude is strongly nonlinear for varying test durations, implying, for a set of given problem constraints, significant diminishing returns exist for longer test times.
4. The magnitude is essentially linearly dependent on test temperatures, with all the other variables at their high levels.
5. When all variables are held at essentially in-service values, and time is varied, the fractional uncertainty reduction is essentially one order of magnitude lower than in the case of multivariable (all variables overstressed) accelerated life testing.

These important results are repeated here as Table 5-1.

When analyzed, it was found that the overall trend behavior for the uncertainty-optimized designs indicate a strong tendency to oscillate between repeated sequences of long- and short-term tests. This is driven by the necessity of establishing the corrosion rate vs. time behavior at the test extrema, thus enabling the most confident extrapolation.

Figure 5-1: Response of First Point Uncertainty Reduction



## 5.6 CONCLUSIONS

Concluding, in the context of this project - designing experiments to best meet the goal of quantitatively assessing the uncertainty of extrapolations of 1000 years - there is a very important role for both highly accelerated life testing and standard experiments conducted at essentially in-service conditions.

The later is imperative to develop the detailed corrosion process model. The former methodology is imperative, once the best model is available, to design and plan an appropriate experimental program which will provide the most effective reduction in uncertainty at the waste container design life.

The contribution and role of this new methodology, then, may be viewed as an intermediate step between lab and field data taking due to the direct incorporation of the in-service environment in the experiment design.

## 5.7 RECOMMENDATIONS FOR FUTURE STUDY

In order of importance, the following recommendations for future study are made.

1. A totally different problem should be analyzed, one possessing data on in-service failures, laboratory-measured short term data and a detailed, well-established process model. By this means a confirmatory exercise may be performed, providing a true test of the methodology.
2. Cost, Risk and other general functions should be developed and incorporated into the optimization variable as an option.



3. Much more diverse data should be obtained for A216 steel corrosion rate in brines to provide a better model building database.

## REFERENCES

- [1] Anthony, T. R. and H. E. Cline.  
Thermal Migration of Liquid Droplets Through Solids.  
*Journal of Applied Physics* 442:3380, 1971.
- [2] Beavers, J. A., N. G. Thompson and R. N. Parkins.  
Stress-Corrosion Cracking of Low Strength Carbon Steels in  
Candidate High Level Repository Environments: Environmental  
Effects.  
*Nuclear and Chemical Waste Management* 5:279, 1985.
- [3] Blundy, R. F., R. Royce, P. Poole and L. L. Shreir.  
Effect of pressure and Stress on Permeation of Hydrogen Through  
Steel.  
*NACE. Volume 5. Stress Corrosion Cracking and Hydrogen Embrittlement  
of Iron Base Alloys.*  
National Association of Corrosion Engineers, Houston, TX, 1973,  
pages 636.
- [4] Bonnel, A., F. Dabosi, M. Daprat, M. Keddani and B. Tribollet.  
Corrosion Inhibition Study of a Carbon Steel in Neutral Chloride  
Solutions by Impedance Techniques.  
*Journal of the Electrochemical Society* 130(4):753, April, 1983.
- [5] Bradshaw, R. L. and W. C. McClain, Eds.  
*Project Salt Vault: A Demonstration of the Disposal of High-Activity  
Solidified Wastes in Underground Salt Mines.*  
Technical Report ORNL-4555, Oak Ridge National Laboratory, April,  
1971.
- [6] Canadillas, F., E. Smailos and R. Koester.  
Corrosion Studies on the Suitability of Mild Steel for the Design  
of Canisters for the Disposal of High Level Waste Products.  
October, 1981.
- [7] Carfagno, S. P. and R. J. Gibson.  
*A Review of Equipment Aging Theory and Technology.*  
Technical Report EPRI-NP-1558, Electric Power Research Institute,  
September, 1980.  
Final Report.

- [8] Christensen, R. A.  
*Entropy Minimax Sourcebook. Volume 5: Multivariate Statistical Modeling.*  
Entropy Limited, Lincoln, MA, 1983.
- [9] Christensen, R. A.  
*Entropy Minimax Sourcebook. Volume VIII: Data Distributions.*  
Entropy Limited, Lincoln, MA, 1984.
- [10] Christensen, R. A.  
*Entropy Minimax Sourcebook: Statistical Distributions Software Sourcebook.*  
Entropy Limited, Lincoln, MA, 1987, in Press.
- [11] Claiborne, H. C., L. D. Rickertsen and R. F. Graham.  
*Expected Environments in High-Level Nuclear Waste and Spent Fuel Repositories in Salt.*  
Technical Report ORNL/TM-7201, Oak Ridge National Laboratory,  
August, 1980.
- [12] Clark, D. (editor).  
*Proceedings of Salt Repository Projects' Workshop on Brine Migration - DRAFT.*  
To Be Published, Berkeley, CA, 1986.  
held at the University of California, Berkeley.
- [13] Cunanne, J. C.  
Personal Communication Regarding Waste Package Near-Field  
Conditions: A Compilation of Available Information at Battelle  
Memorial Institute, Office of Nuclear Waste Isolation in  
December, 1984.
- [14] Dabosi, F., C. Deslouis, M. Daprat and M. Keddam.  
Corrosion Inhibition Study of a Carbon Steel in Neutral Chloride  
Solutions by Impedance Techniques.  
*Journal of the Electrochemical Society* 130(4):761, April, 1983.
- [15] Draper, N. and H. Smith.  
*Applied Regression Analysis, Second Edition.*  
John Wiley and Sons, Inc., 1981.
- [16] Fisher, R. A.  
*Statistical Methods for Research Workers.*  
Macmillan Publishing Company, 1970.

- [17] Fisher, R. S.  
*Host Rock Geochemistry of the Palo Duro Basin, Texas.*  
Technical Report OF-WTWI-1984-11, Texas Bureau of Economic  
Geology, 1984.  
Prepared for U. S. Department of Energy.
- [18] Fisher, R.S.  
*Amount and Nature of Occluded Water in Bedded Salt, Palo Duro Basin,  
Texas.*  
Technical Report TBEG Circular - in Press, Texas Bureau of  
Economic Geology, 1985.
- [19] Fleisher, M.  
*Glossary of Mineral Species 1980.*  
Minerological Record, Tucson, AZ, 1980.
- [20] Fluor Technology, Inc.  
*Site Characterization Plan Conceptual Design Report WORKING DRAFT.*  
Technical Report ???, Fluor Technology, Inc., Irvine, CA, April,  
1986.  
To Be Published.
- [21] Foley, C. L., J. Kruger and C. J. Bechtoldt.  
Electron Diffraction Studies of Active, Passive and Transpassive  
Oxide Films Formed on Iron.  
*Journal of the Electrochemical Society* 114(10):994, October, 1967.
- [22] Fontana, Mars G. and Norbert D. Greene.  
*Corrosion Engineering.*  
McGraw Hill Book Co., Inc., 1978.  
Second Edition.
- [23] Parkins, R. N. (editor).  
*Corrosion Processes.*  
Applied Science Publishers, 1982.
- [24] Garrels, Robert M. and Charles L. Christ.  
*Solutions, Minerals and Equilibria.*  
Harper and Row Publishers, Inc., 1965.

- [25] Ghantous, N. Y.  
*Preliminary Repository Thermal/Thermomechanical Analyses of the Site Characterization Plan-Conceptual Design at the Deaf Smith Site with Horizontal Package Emplacement DRAFT.*  
Technical Report BMI/ONWI-???, Battelle Memorial Institute, Office of Nuclear Waste Isolation, August, 1986.  
To Be Published.
- [26] Golis, M.  
Presentation Material from the Salt Repository Project - Nuclear Regulatory Commission Meeting on January 22-24, 1986, held at Battelle Memorial Institute, Columbus, OH.
- [27] Gupta, D. V. S.  
Corrosion Behavior of 1040 Carbon Steel I. Effect of pH and Sulfide Ion Concentrations in Aqueous Neutral and Alkaline Solutions at Room Temperature.  
*Corrosion* 37(11):611, November, 1981.
- [28] Harper, W. V.  
*Consideration of Optimal Design for Binary Response Experiments.*  
PhD thesis, The Ohio State University, 1984.
- [29] Hovorka, S. D., B. A. Luneau and S. Thomas.  
*Stratigraphy of Bedded Halite in the Permian San Andreas Formation Units 4 and 5, Palo Duro Basin, Texas - DRAFT.*  
Technical Report OF-WTWI-1985-9, Texas Bureau of Economic Geology, Austin, TX, 1985.
- [30] Isherwood, D.  
*Geoscience Data Base Handbook for Modelling a Nuclear Waste Repository.*  
Technical Report NUREG/CR-0912, Lawrence Livermore Laboratory, Livermore, CA, January, 1981.
- [31] Jelinek, J. and P. Neufeld.  
Temperature Effect on Pitting Corrosion of Mild Steel in De-aerated Sodium Bicarbonate-Chloride Solutions.  
*Corrosion Science* 20:489, 1980.
- [32] Jenks, G. H. and H. C. Claiborne.  
*Brine Migration in Salt and its Implications in Geologic Disposal of Nuclear Waste.*  
Technical Report ORNL-5815, Oak Ridge National Laboratory, Oak Ridge, TN, 1981.

- [33] Loken, H. C., G. D. Callahan, D. K. Svalstad and R. A. Wagner.  
*Thermomechanical Analysis of Conceptual Repository Designs of the  
Paradox and Permian Basins.*  
Technical Report RSI-204, Re/Spec, 1984.
- [34] Mann, N. R., R. E. Schafer and N. D. Singpurwalla.  
*Methods for Statistical Analysis of Reliability and Life Data.*  
John Wiley and Sons, Inc., 1974.
- [35] Marsh, G. P.  
Carbon Steel Canisters for the Containment of Nuclear Waste.  
In *Transactions of the American Nuclear Society*, pages 292. AERE  
Harwell, 198?
- [36] Materials Characterization Center.  
*Test Methods Submitted for Nuclear Waste Materials Handbook.*  
Technical Report PNL-3990, Battelle Pacific Northwest Laboratory,  
1986.
- [37] Maxwell, D. E., B. W. Dial and W. Yeung.  
*A Simple Computational Model to Estimate the Horizontal Stress  
Differences on the Canister Overpack.*  
Technical Report SATR-84-4, Science Applications, Incorporated,  
August, 1984.
- [38] McCauley, V. S. and G. E. Raines.  
*Expected Brine Movement at Potential Nuclear Waste Repository Salt  
Sites.*  
Technical Report BMI/ONWI-???, Office of Nuclear Waste Isolation,  
Battelle Memorial Institute, 1985.  
To Be Published.
- [39] McEvily, Jr., A. J.  
On the Role of Defects in Crack Initiation in Welded Structures.  
*Significance of Defects in Welded Structures.*  
University of Tokyo Press, Tokyo, Japan, 1974.
- [40] E. G. McNulty.  
*Expected Near Field Thermal Performance for Nuclear Waste Repositories  
at Potential Salt Sites.*  
Technical Report BMI/ONWI-???, Office of Nuclear Waste Isolation,  
Battelle Memorial Institute, 1985.  
To Be Published.

- [41] Means, J.  
Memorandum: J. Means to T. Steinborn, on Maximum and Realistic Brine Estimates of the Lower San Andreas Unit 4, Deaf Smith and Swisher County Sites, Palo Duro Brine, Texas, on October 1, 1985.
- [42] National Research Council of the National Academy of Sciences.  
*The disposal of Radioactive Waste on Land.*  
Technical Report 519, National Academy of Sciences, Washington, DC, 1957.  
Report of the Committee on Waste Disposal, Division of Earth Sciences.
- [43] Olander, D. R.  
*A Study of Thermal-Gradient-Induced Migration of Brine Inclusions in Salt: Final Report.*  
Technical Report BMI/ONWI-538, Office of Nuclear Waste Isolation, Battelle Memorial Institute, August, 1984.
- [44] Parkins, R. N.  
Environmental Aspects of Stress-Corrosion Cracking in Low-Strength Ferritic Steels.  
*Stress-Corrosion Cracking and Hydrogen Embrittlement of Iron-Base Alloys.*  
National Association of Corrosion Engineers, Houston, 1977, pages 601.
- [45] Park, J. R. and D. D. McDonald.  
Impedence Studies of the Growth of Porous Magnetite Films on Carbon Steel in High Temperature Aqueous Systems.  
*Corrosion Science* 23(4):295, 1983.
- [46] Peters, R. D. and W. L. Kuhn.  
*Model for Corrosion of Metal Barrier Materials in High- and Low-Magnesium Brines.*  
Technical Report PNL-???, Pacific Northwest Laboratory, 1985.  
To Be Published.
- [47] Pisigan, Jr., R. A. and J. E. Singley.  
Evaluation of Water Corrosivity Using the Langlier Index and Relative Corrosion Rate Models.  
*Materials Performance* 24(4):26, April, 1985.

- [48] Reference Repository Conditions Interface Working Group.  
*Results of Repository Conditions Study for Commercial and Defense High-Level Nuclear Waste and Spent Fuel in Salt.*  
Technical Report ONWI-483, Office of Nuclear Waste Isolation,  
Columbus, OH, 1983.
- [49] Rish, W. R.  
*Characterizing Uncertainty in Estimating Impacts from Energy Systems:  
Two Case Studies.*  
PhD thesis, Carnegie-Mellon University, 1982.
- [50] Soo, P., Editor.  
*Review of the DOE Waste Package Program Subtask 1.1 - National Waste  
Package Program April 1982 - September 1982.*  
Technical Report NUREG/CR-2482, Vol. 3, Brookhaven National  
Laboratory, Upton, NY, 1982.  
Prepared for U. S. Nuclear Regulatory Commission.
- [51] Staehle, R. W., J. Hochtman, R. D. McCreight, J. E. Slater  
(editor).  
*NACE. Volume 5: Stress Corrosion Cracking and Hydrogen  
Embrittlement of Iron Base Alloys.*  
National Association of Corrosion Engineers, Houston, TX, 1973.
- [52] Strauss, M. B. and M. C. Bloom.  
Cracking of Low Carbon Steel by Ferric Chloride Solutions.  
*Corrosion* 16:109, 1960.
- [53] Sutcliffe, J. M., R. R. Fessler, W. K. Boyd and R. N. Parkins.  
Stress-Corrosion Cracking of Carbon Steel in Carbonate Solutions .  
*Corrosion* 28:313, 1972.
- [54] Thomas, R. E.  
*A Feasibility Study Using Hypothesis Testing to Demonstrate Containment  
of Radionuclides Within Waste Packages.*  
Technical Report BMI/ONWI-599, Battelle Memorial Institute, Office  
of Nuclear Waste Isolation, April, 1986.
- [55] U. S. Department of Energy.  
*Nuclear Waste Policy Act Environmental Assessment Deaf Smith County  
Site, Texas.*  
Technical Report DOE/RW-0069, U. S. Department of Energy, May,  
1986.



- [56] Uhlig, Herbert H.  
*Corrosion and Corrosion Control.*  
John Wiley and Sons, Inc., 1963.
- [57] United States Congress.  
Nuclear Waste Policy Act of 1982.  
Public Law 97.425, 42 USC 10101-10226.
- [58] U. S. Department of Energy.  
General Guidelines for the Recommendation of Sites for the Nuclear  
Waste Repositories; Final Siting Guidelines.  
in Code of Federal Regulations, Title 10, Part 960.
- [59] U. S. Nuclear Regulatory Commission.  
Disposal of High-Level Radioactive Wastes in Geologic  
Repositories.  
in Code of Federal Regulations, Title 10, Part 60.
- [60] Vesely, W. E and D. M. Rasmusen.  
Uncertainties in Nuclear Probabilistic Risk Analyses.  
*Risk Analysis* 4(4):313-322, 1984.
- [61] Westerman, R. E., J. H. Haberman, S. G. Pitman, B. A. Pulsipher  
and L. A. Sigalla.  
*Corrosion and Environmental-Mechanical Characterization of Iron-Base  
Nuclear Waste Package Structural Barrier Materials.*  
Technical Report PNL-5426, Pacific Northwest Laboratories,  
September, 1985.  
Annual Report--FY 1984.
- [62] Westinghouse Electric Corporation.  
*Engineered Waste Package Conceptual Design: Defense High Level Waste  
(Form 1), Commercial High Level Waste (Form 1), and Spent Fuel  
(Form 2) Disposal in Salt.*  
Technical Report ONWI-438, Office of Nuclear Waste Isolation,  
Battelle Memorial Institute, Pittsburgh, PA, April, 1983.
- [63] Westinghouse Electric Corporation.  
*Waste Package Reference Conceptual Designs for a Repository in Salt.*  
Technical Report BMI/ONWI-517, Battelle Memorial Institute,  
February, 1986.
- [64] Wilde, B. E.  
Classnotes: MetalEn 735, Advanced Corrosion, Ohio State  
University, 1985.

- [65] Wurm, K. J., S. G. Bloom and W. G. Atterbury.  
*TEMP: A Finite-Line Heat Transfer Code for Geologic Repositories for  
Nuclear Waste - DRAFT.*  
Technical Report ONWI-???, Office of Nuclear Waste Isolation,  
March, 1985.  
To Be Published.

## **A. List of Acronyms**

ASTM	American Society for Testing Materials
CHLW	Commercial High-Level Waste
CSF	Consolidated Spent Fuel
DHLW	Defense High-Level Waste
EA	Environmental Assessment
ESS	Experiment Sample Space
HLW	High-Level Waste
ISF	Intact Spent Fuel
MBD	Model Building Database
MCC	Materials Characterization Center
MLE	Maximum Likelihood Estimates
NACE	National Association of Corrosion Engineers
NRC	Nuclear Regulatory Commission
ORNL	Oak Ridge National Laboratory
PBB	Permian Basin Brine
PDF	Probability Distribution Function
PWR	Pressurized Water Reactor
RRC-IWG	Reference Repository Conditions Interface Working Group
SS	Stainless Steel

UNODEX	UNcertainty-Optimized Design of eXperiments
UO	Uncertainty-Optimized
USDOE	United States Department of Energy

## **B. Dataset Used for the Analysis of Waste Container General Corrosion**

## B.1 Description of the Data

The following file lists the general corrosion data used as the basis of the work. Some of the data has yet to be published. Most of the data has been published in the references authored by Westerman, et. al.

The "M" field indicates the material type, 1 corresponds to A216 Steel. The "E" field indicates an environment code, however it is completely specified in the other fields. CR is the dependent variable used throughout the work, corrosion rate. WI and WF are initial and final weights. Area is self-explanatory. T, in °C, O2 in ppm, MG in weight fraction, H2O in weight percent, and TT expressed in hours are the five independent variables, Temperature, dissolved oxygen, magnesium concentration, water fraction and test total time. TD is the down time for the test where applicable.

## **B.2 File Listing**

182	M	E	CR	WI	WF	AREA	T	O2	MG	H2O	TD	TT	MBCOR
P530X1X	2X20.62X14.1605	X14.1266	X4.0782X150X0.05X0.0001X76X	41X	696X	AGC							
P531X1X	2X11.11X14.1771	X14.0294	X4.0743X150X0.05X0.0001X76X	114X	5635X	AGC							
P532X1X	2X12.65X14.1359	X13.9676	X4.0811X150X0.05X0.0001X76X	114X	5635X	AGC							
P533X1X	2X10.36X14.1369	X13.9989	X4.0850X150X0.05X0.0001X76X	114X	5635X	AGC							
P534X1X	2X12.15X14.1560	X13.9944	X4.0811X150X0.05X0.0001X76X	114X	5635X	AGC							
P535X1X	2X13.32X14.2159	X14.0383	X4.0908X150X0.05X0.0001X76X	114X	5635X	AGC							
P536X1X	2X15.25X14.1525	X14.0479	X4.0908X150X0.05X0.0001X76X	66X	2897X	AGC							
P537X1X	2X16.81X14.2059	X13.9946	X4.0811X150X0.05X0.0001X76X	428X	5321X	AGC							
P538X1X	2X16.23X14.2217	X14.0178	X4.0840X150X0.05X0.0001X76X	428X	5321X	AGC							
P539X1X	2X16.71X14.1792	X13.9891	X4.0850X150X0.05X0.0001X76X	428X	5321X	AGC							
P540X1X	2X18.94X14.1427	X14.1116	X4.0732X150X0.05X0.0001X76X	41X	696X	AGC							
P541X1X	2X18.45X14.2126	X13.9308	X4.0908X150X0.05X0.0001X76X	428X	5321X	AGC							
P542X1X	2X13.09X14.2099	X14.0452	X4.0840X150X0.05X0.0001X76X	428X	5321X	AGC							
P543X1X	2X13.02X13.9079	X13.8190	X4.0732X150X0.05X0.0001X76X	68X	2897X	AGC							
P544X1X	2X18.88X14.1028	X13.8657	X4.0801X150X0.05X0.0001X76X	428X	5321X	AGC							
P545X1X	2X26.53X14.1928	X13.8553	X4.0850X150X1.50X0.0001X76X	782X	5384X	OGC							
P546X1X	2X21.74X14.1911	X13.9147	X4.0821X150X1.50X0.0001X76X	81X	5384X	OGC							
P547X1X	2X27.60X13.9014	X13.7125	X4.0675X150X1.50X0.0001X76X	38X	2908X	OGC							
P548X1X	2X28.18X14.0968	X13.0477	X4.0811X150X1.50X0.0001X76X	0X	736X	OGC							
P549X1X	2X26.55X14.1001	X13.7826	X4.0811X150X1.50X0.0001X76X	81X	5384X	OGC							
P550X1X	2X30.34X14.1494	X13.7644	X4.0743X150X1.50X0.0001X76X	81X	5384X	OGC							
P551X1X	2X24.11X14.2305	X13.9240	X4.0801X150X1.50X0.0001X76X	81X	5384X	OGC							
P552X1X	2X14.94X14.2179	X14.1155	X4.0714X150X1.50X0.0001X76X	36X	2908X	OGC							
P553X1X	2X21.29X14.0262	X13.7562	X4.0714X150X1.50X0.0001X76X	81X	5384X	OGC							
P554X1X	2X26.31X14.1614	X14.1157	X4.0674X150X1.50X0.0001X76X	0X	736X	OGC							
P555X1X	2X23.43X14.2017	X13.9046	X4.0703X150X1.50X0.0001X76X	81X	5384X	OGC							
P556X1X	2X21.79X14.1989	X13.9224	X4.0742X150X1.50X0.0001X76X	81X	5384X	OGC							
P557X1X	2X28.69X14.0682	X13.7042	X4.0732X150X1.50X0.0001X76X	81X	5384X	OGC							
P515X1X	2X29.41X14.19270X14.1394	X4.1025X150X0.05X0.0001X76X	0X	768X	IC1								
P516X1X	2X16.31X14.16140X14.0771	X4.1025X150X0.05X0.0001X76X	510X	2180X	IC1								
P517X1X	2X14.36X14.05040X13.9149	X4.1094X150X0.05X0.0001X76X	726X	3974X	IC1								
P519X1X	2X15.44X14.15400X13.9675	X4.0957X150X0.05X0.0001X76X	1405X	5099X	IC1								
P520X1X	2X11.60X14.16550X14.0582	X4.1025X150X0.05X0.0001X76X	726X	3974X	IC1								
P521X1X	2X12.53X14.13100X13.9794	X4.1025X150X0.05X0.0001X76X	1405X	5099X	IC1								
P522X1X	2X10.23X14.13280X14.0364	X4.1025X150X0.05X0.0001X76X	726X	3974X	IC1								
P523X1X	2X12.68X14.13450X13.9814	X4.0996X150X0.05X0.0001X79X	1405X	5099X	IC1								
P529X1X	2X13.67X14.18370X14.1588	X4.1162X150X0.05X0.0001X76X	0X	768X	IC1								
P650X1X13X483.7X1.8408	X1.3373	X0.8263X150X0.05X0.0042X	5X	0X	2178X	XS2A							
P652X1X13X429.3X1.8566	X1.4141	X0.8186X150X0.05X0.0042X	5X	0X	2178X	XS2A							
P653X1X13X488.1X1.8463	X1.3422	X0.8198X150X0.05X0.0042X	5X	0X	2178X	XS2A							
P665X1X13X499.0X1.8459	X1.3323	X0.8173X150X0.05X0.0042X	5X	0X	2178X	XS2A							
P670X1X13X469.8X1.8493	X1.3614	X0.8250X150X0.05X0.0042X	5X	0X	2178X	XS2A							
P674X1X13X442.2X1.8539	X1.3952	X0.8237X150X0.05X0.0042X	5X	0X	2178X	XS2A							
P639X1X13X496.9X1.8626	X1.3472	X0.8237X150X0.05X0.0081X	10X	0X	2178X	XS2B							
P646X1X13X565.6X1.8357	X1.2472	X0.8261X150X0.05X0.0081X	10X	0X	2178X	XS2B							
P656X1X13X537.7X1.8634	X1.3047	X0.8250X150X0.05X0.0081X	10X	0X	2178X	XS2B							
P660X1X13X584.2X1.8634	X1.2503	X0.8263X150X0.05X0.0081X	10X	0X	2178X	XS2B							
P673X1X13X482.8X1.8427	X1.3411	X0.8250X150X0.05X0.0081X	10X	0X	2178X	XS2B							
P687X1X13X534.0X1.8419	X1.2853	X0.8275X150X0.05X0.0081X	10X	0X	2178X	XS2B							
P635X1X13X687.3X1.8378	X1.1237	X0.8250X150X0.05X0.0170X	20X	0X	2178X	XS2C							
P644X1X13X646.3X1.8620	X1.1883	X0.8275X150X0.05X0.0170X	20X	0X	2178X	XS2C							
P662X1X13X656.3X1.8590	X1.1781	X0.8237X150X0.05X0.0170X	20X	0X	2178X	XS2C							
P666X1X13X669.4X1.8065	X1.1176	X0.8172X150X0.05X0.0170X	20X	0X	2178X	XS2C							
P667X1X13X660.5X1.8517	X1.1632	X0.8276X150X0.05X0.0170X	20X	0X	2178X	XS2C							
P672X1X13X691.3X1.8493	X1.1355	X0.8198X150X0.05X0.0170X	20X	0X	2178X	XS2C							
P642X1X13X664.6X1.8205	X1.1375	X0.8160X150X0.05X0.0220X	25X	0X	2178X	XS2D							
P645X1X13X739.2X1.8477	X1.0735	X0.8316X150X0.05X0.0220X	25X	0X	2176X	XS2D							



P851X1X13X815.1X1.8850	X1.2208	XO.8314X150X0.05X0.0220X25X	OX.2178X.XS2D
P859X1X13X519.5X1.8508	X1.3128	XO.8224X150X0.05X0.0220X25X	OX.2178X.XS2D
P869X1X13X826.7X1.8218	X1.1757	XO.8186X150X0.05X0.0220X25X	OX.2173X.XS2D
P886X1X13X822.2X1.8450	X1.1965	XO.8275X150X0.05X0.0220X25X	OX.2178X.XS2D
P843X1X13X821.4X1.8563	X1.2085	XO.8284X150X0.05X0.0270X30X	OX.2178X.XS2E
P858X1X13X747.4X1.8460	X1.0694	XO.8250X150X0.05X0.0270X30X	OX.2178X.XS2E
P861X1X13X596.3X1.8466	X1.2289	XO.8224X150X0.05X0.0270X30X	OX.2178X.XS2E
P868X1X13X583.9X1.8372	X1.2244	XO.8263X150X0.05X0.0270X30X	OX.2178X.XS2E
P879X1X13X615.8X1.8585	X1.2186	XO.8250X150X0.05X0.0270X30X	OX.2178X.XS2E
P885X1X13X806.5X1.8405	X1.0064	XO.8211X150X0.05X0.0270X30X	OX.2178X.XS2E
P837X1X13X415.9X1.8429	XO.4582	XO.8186X150X0.05X0.0170X20X	OX.7031X.XS3EE
P841X1X13X407.9X1.8510	XO.4826	XO.8250X150X0.05X0.0170X20X	OX.7031X.XS3EE
P854X1X13X420.8X1.8374	XO.4257	XO.8250X150X0.05X0.0170X20X	OX.7031X.XS3EE
P855X1X13X463.7X1.8325	XO.2838	XO.8213X150X0.05X0.0170X20X	OX.7031X.XS3EE
P871X1X13X405.2X1.8584	XO.5033	XO.8224X150X0.05X0.0170X20X	OX.7031X.XS3EE
P878X1X13X426.3X1.8359	XO.4102	XO.8724X150X0.05X0.0170X20X	OX.7031X.XS3EE
P838X1X13X777.0X1.8424	X1.2318	XO.8187X150X0.05X0.0270X30X	OX.1859X.XS3F
P847X1X13X793.3X1.8320	X1.2029	XO.8263X150X0.05X0.0270X30X	OX.1859X.XS3F
P840X1X13X899.6X1.8376	X1.2844	XO.8238X150X0.05X0.0270X30X	OX.1859X.XS3F
P876X1X13X625.6X1.8211	X1.1346	XO.8104X150X0.05X0.0270X30X	OX.1859X.XS3F
P888X1X13X556.0X1.8453	X1.4064	XO.8224X150X0.05X0.0270X30X	OX.1859X.XS3F
P890X1X13X892.2X1.8410	X1.2955	XO.8211X150X0.05X0.0270X30X	OX.1859X.XS3F
P836X1X13X541.6X1.8414	X1.8437	XO.8224X150X0.05X0.0170X20X	OX.787X.XS3G
P840X1X13X688.3X1.8275	X1.5854	XO.8162X150X0.05X0.0170X20X	OX.787X.XS3G
P863X1X13X588.2X1.8473	X1.6399	XO.8224X150X0.05X0.0170X20X	OX.787X.XS3G
P864X1X13X721.6X1.8558	X1.5904	XO.8288X150X0.05X0.0170X20X	OX.787X.XS3G
P880X1X13X654.0X1.8615	X1.6232	XO.8211X150X0.05X0.0170X20X	OX.787X.XS3G
P882X1X13X537.8X1.5017	X1.3088	XO.8081X150X0.05X0.0170X20X	OX.787X.XS3G
P849X1X13X821.2X1.8414	X1.5430	XO.8187X150X0.05X0.0270X30X	OX.787X.XS3H
P875X1X13X653.6X1.8330	X1.5932	XO.8284X150X0.05X0.0270X30X	OX.787X.XS3H
P877X1X13X528.2X1.8574	X1.6643	XO.8237X150X0.05X0.0270X30X	OX.787X.XS3H
P883X1X13X807.9X1.8268	X1.5319	XO.8224X150X0.05X0.0270X30X	OX.787X.XS3H
P864X1X13X594.2X1.8340	X1.6174	XO.8213X150X0.05X0.0270X30X	OX.787X.XS3H
P889X1X13X588.1X1.8681	X1.4546	XO.8179X150X0.05X0.0270X30X	OX.787X.XS3H
Q433X1X11X12.07X2.7870	X2.7823	XO.8888X150X0.05X0.0004X20X	OX.759X.XS4E
Q489X1X11X12.58X2.7380	X2.7311	XO.8882X150X0.05X0.0004X20X	OX.759X.XS4E
Q493X1X11X10.80X2.7411	X2.7369	XO.8855X150X0.05X0.0004X20X	OX.759X.XS4E
Q505X1X11X8.355X2.7458	X2.7425	XO.8855X150X0.05X0.0004X20X	OX.759X.XS4E
Q369X1X13X727.6X2.7446	X2.4599	XO.8908X150X0.05X0.0170X20X	OX.780X.XS4H
Q526X1X13X553.8X2.7407	X2.5243	XO.8895X150X0.05X0.0170X20X	OX.780X.XS4H
Q598X1X13X491.1X2.7538	X2.5630	XO.8842X150X0.05X0.0170X20X	OX.780X.XS4H
Q609X1X13X536.3X2.7606	X2.5510	XO.8895X150X0.05X0.0170X20X	OX.780X.XS4H
Q387X1X13X811.6X.2.63185X.2.32345X0.8805X150X0.05X0.0468X76X			72X.782X.GC1
Q389X1X13X846.0X.2.64330X.2.32030X0.8846X150X0.05X0.0468X76X			72X.782X.GC1
Q390X1X13X797.8X.2.66310X.1.78995X0.8859X150X0.05X0.0468X76X			80X.2181X.GC1
Q391X1X13X757.8X.2.63850X.1.80785X0.8872X150X0.05X0.0468X76X			80X.2181X.GC1
Q363X1X.3X1157.X.2.62000X.2.20190X0.8827X150X0.05X0.0469X76X			48X.723X.GC2
Q364X1X.3X1133.X.2.63420X.2.22470X0.8827X150X0.05X0.0469X76X			48X.723X.GC2
Q385X1X.3X1048.X.2.62500X.1.29830X0.8813X150X0.05X0.0469X76X			54X.2540X.GC2
Q388X1X.3X1042.X.2.62155X.1.29355X0.8855X150X0.05X0.0469X76X			54X.2540X.GC2
Q370X1X.3X937.3X.2.62945X.0.61755X0.8827X150X0.05X0.0469X76X			170X.4294X.GC2
Q371X1X.3X947.9X.2.62095X.0.57990X0.8853X150X0.05X0.0469X76X			170X.4294X.GC2
Q398X1X.3X45.25X.2.63255X.2.61555X0.8703X.90X0.05X0.0465X76X			OX.745X.GC3
Q399X1X.3X68.24X.2.62435X.2.59875X0.8890X.90X0.05X0.0465X76X			OX.745X.GC3
Q396X1X.3X57.29X.2.64980X.2.58710X0.8731X.90X0.05X0.0465X76X			20X.2163X.GC3
Q397X1X.3X39.06X.2.64340X.2.80105X0.8650X.90X0.05X0.0465X76X			20X.2163X.GC3
Q394X1X.3X58.26X.2.64225X.2.51515X0.8743X.90X0.05X0.0465X76X			42X.4424X.GC3
Q395X1X.3X58.39X.2.64765X.2.52220X0.8678X.90X0.05X0.0465X76X			42X.4424X.GC3

Q405X1X53X679.7X	2.62345X	2.37720X0.8683X150X0.05X0.0353X53X	OX	720X	GC4
Q406X1X53X695.5X	2.64805X	2.39415X0.8750X150X0.05X0.0353X53X	OX	720X	GC4
Q403X1X53X942.1X	2.65480X	1.64790X0.8683X150X0.05X0.0353X53X	65X	2124X	GC4
Q404X1X53X916.5X	2.62900X	1.65095X0.8670X150X0.05X0.0353X53X	65X	2124X	GC4
Q497X1X53X28.02X	2.63045X	2.62105X0.8618X 90X0.05X0.0327X53X	75X	672X	GC5
Q499X1X53X33.73X	2.64255X	2.63120X0.8640X 90X0.05X0.0327X53X	75X	672X	GC5
Q495X1X53X29.55X	2.63180X	2.60000X0.8710X 90X0.05X0.0327X53X	76X	2119X	GC5
Q496X1X53X28.08X	2.60070X	2.57320X0.8588X 90X0.05X0.0327X53X	76X	2119X	GC5
Q517X1X33X164.8X	2.59740X	2.54150X0.8644X150X0.05X0.0009X76X	OX	677X	GC8
Q519X1X33X152.1X	2.64105X	2.58930X0.8670X150X0.05X0.0009X76X	OX	677X	GC8
Q513X1X34X421.2X	2.61455X	2.45125X0.8655X150X0.05X0.0102X76X	OX	773X	GC7
Q514X1X34X414.5X	2.63370X	2.47300X0.8655X150X0.05X0.0102X76X	OX	773X	GC7
Q512X1X39X793.3X	2.64730X	2.58960X0.8717X150X0.05X0.0468X76X	OX	144X	GC8
Q490X1X39X588.0X	2.62730X	2.53030X0.8627X150X0.05X0.0468X76X	OX	330X	GC8
Q520X1X35X224.4X	2.62435X	2.53995X0.8644X150X0.05X0.0049X76X	OX	751X	GC9
Q522X1X35X245.9X	2.62150X	2.52830X0.8710X150X0.05X0.0049X76X	OX	751X	GC9
Q509X1X39X564.9X	2.64065X	2.54555X0.8672X150X0.05X0.0468X76X	OX	335X	GC10
Q503X1X38X1457.X	2.62750X	2.38270X0.8657X150X0.05X0.0468X76X	OX	335X	GC12
Q533X1X39X540.9X	2.64925X	2.55810X0.8629X150X0.05X0.0468X76X	OX	337X	GC13X
Q539X1X38X1926.X	2.59835X	2.27570X0.8577X150X0.05X0.0468X76X	OX	336X	
Q535X1X18X13.00X	2.66155X	2.65940X0.8620X150X0.05X0.0001X76X	OX	336X	
T502X1X19X59.79X	2.62095X	2.61105X0.8633X150X0.05X0.0001X76X	OX	336X	
Q536X1X18X11.17X	2.65200X	2.65015X0.8635X150X0.05X0.0001X76X	OX	336X	
T515X1X18X56.94X	2.59780X	2.58820X0.8607X150X0.05X0.0001X76X	OX	336X	
Q537X1X 1X28.78X	2.62880X	2.62405X0.8605X150X0.05X0.0001X76X	OX	336X	
T517X1X 1X61.40X	2.59840X	2.58825X0.8618X150X0.05X0.0001X76X	OX	336X	
Q384X1X11X07.32X	2.75195X	2.74385X0.8693X150X0.05X0.0001X20X	OX	2193X	ES1
Q385X1X11X10.16X	2.74080X	2.72950X0.8735X150X0.05X0.0001X20X	OX	2198X	ES1
Q386X1X11X10.31X	2.72070X	2.70930X0.8682X150X0.05X0.0001X20X	OX	2198X	ES1
Q410X1X53X53.50X	2.72305X	2.66330X0.8748X 90X0.05X0.0134X20X	OX	2203X	ES2
Q411X1X53X55.46X	2.75865X	2.69635X0.8799X 90X0.05X0.0134X20X	OX	2203X	ES2
Q426X1X53X67.68X	2.73415X	2.65790X0.8826X 90X0.05X0.0134X20X	OX	2203X	ES2
R967X1X53X43.44X	4.64340X	4.58950X0.9718X 90X0.05X0.0134X20X	OX	2203X	ES2
R972X1X53X45.46X	4.65940X	4.60325X0.9676X 90X0.05X0.0134X20X	OX	2203X	ES2
R979X1X53X28.82X	4.65910X	4.62345X0.9690X 90X0.05X0.0134X20X	OX	2203X	ES2
Q414X1X53X489.1X	2.70570X	2.15885X0.8655X150X0.05X0.0134X20X	OX	2179X	ES6
Q418X1X53X559.8X	2.73045X	2.11135X0.8782X150X0.05X0.0134X20X	OX	2179X	ES6
Q422X1X53X388.3X	2.72710X	2.29680X0.8777X150X0.05X0.0134X20X	OX	2179X	ES6
Q431X1X51X24.75X	2.72865X	2.70110X0.8817X150X0.05X0.0001X20X	OX	2179X	ES8
Q432X1X51X20.76X	2.74635X	2.72345X0.8737X150X0.05X0.0001X20X	OX	2179X	ES8
Q436X1X51X04.43X	2.71110X	2.70820X0.8764X150X0.05X0.0001X20X	OX	2179X	ES8
Q452X1X51X17.69X	2.77315X	2.75365X0.8826X150X0.05X0.0001X20X	OX	2155X	ES8A
Q461X1X51X25.16X	2.72560X	2.69790X0.8815X150X0.05X0.0001X20X	OX	2155X	ES8A
Q489X1X51X18.86X	2.75285X	2.73240X0.8682X150X0.05X0.0001X20X	OX	2155X	ES8A
Q434X1X51X07.83X	2.69855X	2.68805X0.8695X 90X0.05X0.0001X20X	OX	2155X	ES10
Q435X1X51X08.78X	2.71990X	2.71040X0.8689X 90XC.05X0.0001X20X	OX	2155X	ES10
Q438X1X51X08.37X	2.73365X	2.72455X0.8709X 90X0.05X0.0001X20X	OX	2155X	ES10
Q455X1X51X06.33X	2.66780X	2.66070X0.8735X150X0.05X0.0001X05X	OX	2155X	ES14
Q480X1X51X06.67X	2.73850X	2.73125X0.8709X150X0.05X0.0001X05X	OX	2155X	ES14
Q467X1X51X08.15X	2.75780X	2.74895X0.8695X150X0.05X0.0001X05X	OX	2155X	ES14
Q444X1X51X03.09X	2.74255X	2.73220X0.8695X 90X0.05X0.0001X05X	OX	2155X	ES16
Q456X1X51X03.08X	2.72125X	2.71790X0.8711X 90X0.05X0.0001X05X	OX	2155X	ES16
Q463X1X51X02.90X	2.72730X	2.72415X0.8695X 90X0.05X0.0001X05X	OX	2155X	ES16
Q450X1X51X107.8X	2.72950X	2.61205X0.8722X200X0.05X0.0001X05X	OX	2155X	ES18
Q451X1X51X89.43X	2.73365X	2.63625X0.8722X200X0.05X0.0001X05X	OX	2155X	ES18
Q453X1X51X80.83X	2.74190X	2.65360X0.8748X200X0.05X0.0001X05X	OX	2155X	ES18
Q472X1X53X422.0X	2.75265X	2.27415X0.8669X150X0.05X0.0034X05X	OX	2155X	ES20
Q473X1X53X335.0X	2.72065X	2.35635X0.8708X150X0.05X0.0034X05X	OX	2155X	ES20

Q476X1X53X320.3X	2.70940X	2.36165X0.	8695X150X0.	05X0.	0034X05X	OX	2155X	ES20
Q481X1X53X11.83X	2.74450X	2.73160X0.	8735X 90X0.	05X0.	0034X05X	OX	2155X	ES22
Q484X1X53X16.51X	2.74000X	2.72215X0.	8656X 90X0.	05X0.	0034X05X	OX	2155X	ES22
Q485X1X53X10.90X	2.72155X	2.70975X0.	8671X 90X0.	05X0.	0034X05X	OX	2155X	ES22
Q483X1X53X881.7X	2.72540X	1.77500X0.	8631X200X0.	05X0.	0034X05X	OX	2155X	ES24
Q486X1X53X883.2X	2.74365X	1.78895X0.	8656X200X0.	05X0.	0034X05X	OX	2155X	ES24
Q438X1X53X950.0X	2.71975X	1.89580X0.	8631X200X0.	05X0.	0034X05X	OX	2155X	ES24
Q690X1X53X625.9X	2.75550X	2.05810X0.	8922X200X0.	05X0.	0034X05X	OX	2155X	ES24
T 53X1X53X668.6X	2.70315X	1.98160X0.	8642X200X0.	05X0.	0034X05X	OX	2155X	ES24

## C. THE UNODEX SYSTEM COMPUTER PROGRAM

## C.1 Users Documentation

### C.1.1 Input to UNODEX

Input to UNODEX consists of the following:

VARIABLE	DESCRIPTION
----------	-------------

---

---

Card 1: Format(I4)

IESSNO	Problem Identifier Number
--------	---------------------------

---

Card 2: Format(I4)

NTLNS	Number of Title Lines Following
-------	---------------------------------

---

Card(s) 3: Format(NTLNS\*A60)

TITLE(1)	Title Cards
----------	-------------

TITLE(NTLNS)

---

Card 4: Format(I4)

NIV	Number of Independent Variables
-----	---------------------------------

---

Card(s) 5: Format(NIV(A12,2F10.5,I5))

NAME(1),XH(1),XL(1),NLEV(1)

Name of IV, high level, low level and number of levels the IV is to assume in the generation of the experiment sample space.

NAME(NIV),XH(NIV),XL(NIVH),NLEV(NIV)

---

Card 6: Format(19I4,4E10.1)

- CNTROL(1)        Number (of total number) of parameters to be fitted
- CNTROL(2)        Total number parameters
- CNTROL(3)        Number of data points
- CNTROL(4)        Dimensions of the A-array and 1st dimension of the B-array, must be at least the largest value of CNTROL(2)
- CNTROL(5)        Total number variables (1 dependent + any number of independent)
- CNTROL(6)        Limit on number of iterations
- CNTROL(7)        Print control  
= 0: no intermediate output wanted  
= +1: Print input data  
= +2: Print sum of squares and parameter values  
= +4: Print normal equations  
= +8: Print restrained change mechanism  
=+16: Print point-by-point comparison
- CNTROL(8)        Index identifying the weighting function for the sum of squares  
= 1: 1.0  
= 2: 1/OBS  
= 3: 1/CALC  
= 4: OBS  
= 5: CALC  
= 6:  $1/Z(C5,N)$ ,  $Z(C5,N) = \text{ERROR IN OBS VAL OF Y}$

= 7:  $Z(C5,N)$   
 = 8:  $1/MX(O,C)$  = Inverse of the maximum of the observed  
 and the calculated values

CNTROL(9)      Convergence criteria control

CNTROL(10)     Parameter variation constraint for restrained change  
 mechanism  
 = 0: Unconstrained parameter changes  
 > 0: Limit on percentage change of parameter expressed  
 in units in tens of percent

CNTROL(11)     Control for overriding the restrained change mechanism  
 =1: Overriding permitted, unconstrained changes in the  
 parameters are permitted  
 =0: No overriding

CNTROL(12)     Control for overriding sum of square reduction test  
 =Number of overrides permitted per iteration

CNTROL(13)     Parameter change option

CNTROL(14)     NOT USED

CNTROL(15)     Derivative specification control  
 = 1: Analytic derivative provided in a user-defined  
 function called DYDB.FOR  
 = 0: No Derivative function provided, calculate  
 derivatives numerically

CNTROL(16)     Total number of problems to be solved

CNTROL(17)     Number of sets of guesses

CNTROL(18)     Number of different dependent variable expressions  
 prepared in Y0.FOR

CNTROL(19)     Y Index identifying which (of multiple) expression(s)  
 for Y0 to use

SCONVG          Cauchy convergence on error sum of squares

PCONVG            Cauchy convergence on parameters  
BCONVG            Cauchy convergence on individual parameter  
ADEL              Convergence on detection of plateau in uncertainty  
                  reduction vs experiment number.

---

Card 7: Format(2I4)

NTIMES            Number of timesteps for error propagation routine  
IDLIFE            The timestep at which the uncertainty is minimized

---

Card(s) 8: Format(NIV\*(NTIMES\*E10.5))

XINSERV(I,J),I=1,NIV, J=1,NTIMES  
                  Values for the in-service environmental boundary  
                  conditions.

---

Card 9: Format(2I5,CNTROL(1)\*E11.4)

IB,IC,BTRIAL(I),I=1,CNTROL(1)  
                  Total number of parameters, number to be fitted this  
                  trial and trial values (initial guesses) for the  
                  parameters

---

---





## C.2 Program Source Listing

```

PROGRAM UNODEX
C *****UNODEX
C *
C *
C * The UNODEX Program September 1986 UNODEX
C *
C * UNCertainty Optimized Design of EXperiments UNODEX
C *
C *
C * By A. J. Wolford UNODEX
C * Department of Nuclear Engineering UNODEX
C * Massachusetts Institute of Technology UNODEX
C * Developed in partial fulfillment of his ScD UNODEX
C * at, and with thanks to UNODEX
C * The Battelle Memorial Institute UNODEX
C * Columbus, Ohio UNODEX
C *
C * and UNODEX
C *
C * R. A. Christensen UNODEX
C * R. F. Eilbert UNODEX
C * Entropy, Ltd. UNODEX
C * Lincoln, Massachusetts UNODEX
C *
C *
C * Original version FITSALL algorithm credits: UNODEX
C *
C * by R. A. Christensen, T. A. Reichert, and others UNODEX
C * Physics and Chemistry Depts. UNODEX
C * University of California, Berkeley UNODEX
C * 1968-1969 UNODEX
C *
C *****UNODEX
C *****UNODEX
C * EXAMPLE: UNODEX
C *****UNODEX
C
C Y(N) = ( B(1) + B(2)*X(1,N) ) * EXP( -B(3)/X(2,N) ) UNODEX
C
C B(J) = J-TH PARAMETER TO BE FITTED UNODEX
C X(I,N) = OBSERVED VALUE OF I-TH INDEP VARIABLE FOR N-TH DATA PT UNODEX
C Y(N) = OBSERVED VALUE OF DEPENDENT VARIABLE FOR N-TH DATA POINT UNODEX
C
C (FITSALL IS ABLE TO LOOP OVER DIFFERENT FUNCT. FORMS FOR Y(N)) UNODEX
C
C *****UNODEX
C * INPUT READ ON LOGICAL UNIT 12: UNODEX
C *****UNODEX
C.. ALL CNTROL(1,24) ARE VIA COMMON/CNTROL UNODEX
C
C
C
C CNTROL(1)=NB (NUMBER OF B'S): NUMBER (OF TOTAL NUMBER) OF UNODEX
C PARAMETERS TO BE FITTED UNODEX
C
C CNTROL(2)=M3: TOTAL # PARAMETERS UNODEX
C
C CNTROL(3)=-INT3: NUMBER DATA POINTS UNODEX

```

C	BDIM=CNTR(4)=DIMS OF A-ARRAY & 1ST DIM OF B-ARRAY,	UNODEX
C	MUST BE AT LEAST THE LARGEST VALUE OF CNTR(2)	UNODEX
C		UNODEX
C	CNTR(5)=NVAR: TOTAL NUMBER VARIABLES	UNODEX
C	(1 DEPENDENT + ANY NUMBER OF INDEPENDENT)	UNODEX
C		UNODEX
C	CNTR(6)=LIMIT: LIMIT ON # ITERATIONS	UNODEX
C		UNODEX
C	CNTR(7): PRINT CONTROL	UNODEX
C	= 0: NO INTERMEDIATE OUTPUT WANTED	UNODEX
C	= +1: PRINT INPUT DATA	UNODEX
C	= +2: PRINT SUMSQ & PARM VALS	UNODEX
C	= +4: PRINT NORMAL EQUATIONS	UNODEX
C	= +8: PRINT RESTRAINED CHANGE MECHANISM	UNODEX
C	=+16: PRINT POINT-BY-POINT COMPARISON	UNODEX
C		UNODEX
C	CNTR(8)=LL: INDEX IDENTIFYING WEIGHTING FCN FOR SSQ	UNODEX
C	= 1: 1.0	UNODEX
C	= 2: 1/OBS	UNODEX
C	= 3: 1/CALC	UNODEX
C	= 4: OBS	UNODEX
C	= 5: CALC	UNODEX
C	= 6: 1/Z(C5,N), Z(C5,N) = ERROR IN OBS VAL OF Y	UNODEX
C	= 7: Z(C5,N)	UNODEX
C	= 8: 1/MX(0,C) [...INVERSE OF MAX OF OBS & CALC VALS]	UNODEX
C		UNODEX
C	CNTR(9)=CONVERGENCE CRITERIA CONTROL	UNODEX
C	= 1:	UNODEX
C	= 2:	UNODEX
C	TO BTEST -- IT SWITCHES FROM PCONVG TO BCONVG]	UNODEX
C		UNODEX
C	CNTR(10)=KNTR10: RESTRAINED CHANGE MECHANISM: PARAMETER	UNODEX
C	VARIATION CONSTRAINT IN TENS OF PERCENT	UNODEX
C	= 0: UNCONSTRAINED PARAMETER CHANGES	UNODEX
C	> 0: LIMIT ON PERCENTAGE CHANGE OF PARAMETERS	UNODEX
C	[EXPRESSED IN UNITS OF TENS OF PERCENT]	UNODEX
C		UNODEX
C	CNTR(11)=CONTROL FOR OVERRIDING RESTRAINED CHANGE MECHANISM	UNODEX
C	=1: OVERRIDING PERMITTED	UNODEX
C	(UNCONSTRAINED CHANGES ALLOWED WHEN OVERRIDDEN)	UNODEX
C	=0: NO OVERRIDING	UNODEX
C		UNODEX
C	CNTR(12)=CONTROL FOR OVERRIDING SSQ REDUCTION TEST	UNODEX
C	=NUMBER OF OVERRIDES PERMITTED	UNODEX
C	(NEGATIVE VALUE ACTIVATES WRONG WAY MECHANISM)	UNODEX
C		UNODEX
C	CNTR(13)= ?? (PARAMETER CHANGE OPTION ?)	UNODEX
C		UNODEX
C	CNTR(14)=[NOT USED]	UNODEX
C		UNODEX
C	CNTR(15)=DERIVATIVE CONTROL	UNODEX
C	= 1: ANALYTIC DERIVATIVE PROVIDED IN A FN NAMED DYDB	UNODEX
C	= 0: NOT PROVIDED, NUMERICAL DERIVS WILL BE COMPUTED	UNODEX
C		UNODEX
C	CNTR(16)=TOTAL NUMBER OF PROBLEMS TO BE SOLVED	UNODEX
C		UNODEX
C	CNTR(17)=NSETS=NUMBER OF SETS OF GUESSES	UNODEX
C		UNODEX

```

C      CNTRL(18)=NUMBER OF DIFFERENT DV EXPRESSIONS PREPARED IN YO UNODEX
C
C      CNTRL(19)=Y INDEX (TO LET YCOMP.FR & DERIV.FR KNOW WHICH UNODEX
C      EXPRESSION TO USE OF Y) (MUST NOT EXCEED CNTRL(18)) UNODEX
C
C      CNTRL(20)=NN: NUMBER OF ITERATIONS USED UNODEX
C
C      CNTRL(21)=IHOLD: TERMINATION CODE UNODEX
C      =0: OPTION REDUNDANCY, EXPRESSION CHG INDICATED UNODEX
C      =1: CAUCHY CONVERGENCE OF PARAMETERS UNODEX
C      =2: CAUCHY CONVERGENCE OF SUM OF SQUARES UNODEX
C      =3: HIT LIMIT ON # ITERATIONS UNODEX
C      =4: EQNS SINGULAR UNODEX
C      =5: NO SSQ REDUCTION - GUESS AGAIN UNODEX
C
C      CNTRL(22)=INITIAL ENTRY FLAG UNODEX
C      =1: INITIAL ENTRY TO GAUSS.FR; IN YCOMP.FR, UNODEX
C      SET Z( , ) = OBSERVED VALUES UNODEX
C      =0: SUBSEQUENT ENTRY; IN YCOMP.FR COMPUTE VALUE OF Y UNODEX
C
C      CNTRL(23)=II: SEQUENCE # OF PROBLEM BEING PROCESSED UNODEX
C      [MAX IS CNTRL(18)] UNODEX
C
C      CNTRL(24)=K: SEQUENCE # OF GUESS SET BEING PROCESSED UNODEX
C
C      CNTRL(25)= [NOT USED] UNODEX
C
C      IB=TOTAL # PARAMETERS THIS TRIAL UNODEX
C
C      IC=# PARAMETERS TO BE FITTED THIS TRIAL UNODEX
C
C      BTRIAL(1,...,IB)=INITIAL GUESS OF PARAMETER VALUES UNODEX
C
C *****UNODEX
C *      DEFINITIONS AND COMMENTS *UNODEX
C *****UNODEX
C
C      NDIM=2ND DIMENSION OF Z( , ), MUST BE AT LEAST NPTS UNODEX
C      NPTS=IABS(CNTRL(3))=# DATA POINTS UNODEX
C      (NEGATIVE VALUE INDICATES INITIAL ENTRY FOR UNODEX
C      PRELIMINARY CALLS TO YCOMP.FR AND GAUSS.FR) UNODEX
C
C      MDIM=1ST DIMENSION OF Z( , ) UNODEX
C      MDIM UNODEX
C      =VARS....[USUALLY] UNODEX
C      =VARS+1...[IF CNTRL(8)=6 OR 7, TO GIVE ROOM FOR ERR UNODEX
C
C      IBCHN UNODEX
C
C      L=TRIAL SEQUENCE # UNODEX
C
C      NLAB=NUMBER OF LAB DATA POINTS UNODEX
C
C      NPARAM=DIMENSION OF PARAM( , ), UNODEX
C      (...MUST BE AT LEAST THE LARGEST VALUE OF CNTRL(2)) UNODEX
C
C      NVIR=NUMBER OF VIRTUAL DATA POINTS UNODEX
C

```

```

C *****UNODEX
C *          LOGICAL UNITS/CHANNEL USEAGE          *UNODEX
C *****UNODEX
C          UNODEX
C          UNODEX
C.....CHANNEL USAGE:          UNODEX
C          UNODEX
C          UNODEX
C          CHANNEL 1:  MODEL BUILDING DATA (MBCOR.DAT)          UNODEX
C          UNODEX
C          CHANNEL 2:  EXPLANATORY OUTPUT (USER.OUT)          UNODEX
C          UNODEX
C          CHANNEL 3:  VIRTUAL (HYPOTHETICAL EXPERIMENT) INDEPENDENT          UNODEX
C                   VARIABLE DATA, GENERATED BY GENVIRT.FOR          UNODEX
C                   (VIRCOR.DAT)          UNODEX
C          UNODEX
C          CHANNEL 4:  B-PARAMETER INIOTIAL 'GUESS' VALUES (BTRIAL.DAT)          UNODEX
C          UNODEX
C          CHANNEL 8:  ECHELON UNCERTAINTY EVALUATION (DELTAS.DAT)          UNODEX
C          UNODEX
C          CHANNEL 12: PROBLEM INPUT CONTROL DECK (JOB.DAT)          UNODEX
C          UNODEX
C          UNODEX
C*****UNODEX
C*****UNODEX
C          PARAMETER NDT5=1250          UNODEX
C          PARAMETER NVMAX=1250          UNODEX
C          COMMON X(8,NDT5),Y(1,NDT5),E(1,NDT5) !;MAKE CONSIST WITH YCOMP          UNODEX
C          DIMENSION PARAM(10),AC(100)          UNODEX
C          DIMENSION XH(10), XL(10), NLEV(10)          UNODEX
C          DIMENSION TEMP(NVMAX)          UNODEX
C          INTEGER LT(NVMAX), UT(NVMAX)          UNODEX
C          INTEGER CNTROL          UNODEX
C          INTEGER NTLNS,NIV,NTIMES          UNODEX
C          CHARACTER*80 TITLE          UNODEX
C          CHARACTER*12 NAME(10)          UNODEX
C          CHARACTER*8 TOD          UNODEX
C          CHARACTER*9 MDY          UNODEX
C          COMMON/IESS/IESSNO          UNODEX
C          COMMON/TITLE/TITLE(5)          UNODEX
C          COMMON/CNTROL/CNTROL(25)          UNODEX
C          COMMON/CONVG/SCONVG,PCONVG,BCONVG          UNODEX
C          COMMON/XINSERV/XINSERV(5,11), SIGREF(11)          UNODEX
C          COMMON/LABEL/LLAB(2)          UNODEX
C          COMMON/XV/XVIR(5,NVMAX), IVIR(NVMAX), LVIR(2,NVMAX),          UNODEX
C          +          DS(NVMAX), DDS(NVMAX), YVIR(NVMAX)          UNODEX
C          UNODEX
C.. OPEN LOGICAL UNITS          UNODEX
C          UNODEX
C.. CHANNEL 1 >> MBCOR.DAT: LAB DATA (INPUT RAW DATA)          UNODEX
C          OPEN (UNIT=1,FILE='MBCOR.DAT',STATUS='OLD')          UNODEX
C          CALL FOPEN(1,'MBCOR1.DT')          UNODEX
C          UNODEX
C.. CHANNEL 2 >> USER.OUT: EXPLANATORY OUTPUT          UNODEX
C          OPEN (UNIT=2,FILE='USER.OUT',STATUS='NEW',          UNODEX
C          +          CARRIAGECONTROL='LIST')          UNODEX
C          UNODEX
C.. CHANNEL 3 >> VIRCOR.DAT: VIRTUAL (HYPOTHETICAL EXPERIMENT) IV DATA          UNODEX

```

```

      OPEN (UNIT=3,FILE='VIRCOR.DAT',STATUS='NEW',
+       CARRIAGECONTROL='LIST') UNODEX
      UNODEX
      UNODEX
C.. CHANNEL 4 >> BTRIAL.DAT: B PARAMETER TRIAL GUESSES UNODEX
      OPEN (UNIT=4,FILE='BTRIAL.DAT',STATUS='NEW', UNODEX
+       CARRIAGECONTROL='LIST') UNODEX
      UNODEX
C.. CHANNEL 6 >> CONSOLE.OUT: NORMAL SYS$OUT OUTPUT UNODEX
C      OPEN (UNIT=6,FILE='CONSOLE.OUT',STATUS='NEW', UNODEX
      UNODEX
      UNODEX
C.. CHANNEL 8 >> DS.DAT: UNCERTAINTY IMPROVEMENT DATA UNODEX
      OPEN (UNIT=8,FILE='DS.DAT',STATUS='NEW',CARRIAGECONTROL='LIST') UNODEX
C      + CARRIAGECONTROL='LIST') UNODEX
      UNODEX
C.. CHANNEL 9 >> FOUT.DAT: ERROR MATRIX UNODEX
      OPEN (UNIT=9,FILE='FOUT',STATUS='NEW',CARRIAGECONTROL='LIST') UNODEX
      UNODEX
C.. CHANNEL 12 >> JOB.DAT: PROBLEM INPUT CONTROL DECK UNODEX
C      OPEN (UNIT=12,FILE='JOB.DAT',STATUS='OLD', UNODEX
C      + CARRIAGECONTROL='LIST') UNODEX
      UNODEX
C***** UNODEX
C*          BEGIN INITIALIZATION *UNODEX
C***** UNODEX
C.. READ IN PROBLEM TITLE FROM PRIMARY JOB CONTROL FILE UNODEX
      UNODEX
C.. IESSNO=EXPERIMENT SAMPLE SPACE NUMBER, OR MAY BE USED UNODEX
C   IN GENERAL AS A PROBLEM IDENTIFIER NUMBER UNODEX
      UNODEX
      READ(12,81)IESSNO UNODEX
      WRITE(6,81)IESSNO UNODEX
      UNODEX
C.. NTLINES=NUMBER OF DESCRIPTIVE PROBLEM TITLE LINES FOLLOWING UNODEX
C   MAXIMUM IS 5 UNODEX
      UNODEX
      READ(12,81)NTLNS UNODEX
81  FORMAT(I4) UNODEX
      WRITE(6,81)NTLNS UNODEX
      READ(12,83) (TITLE(IT),IT=1,NTLNS) UNODEX
83  FORMAT(A80) UNODEX
      WRITE(6,83) (TITLE(IT),IT=1,NTLNS) UNODEX
      UNODEX
      CALL DATE(MDY) UNODEX
      CALL TIME(TOD) UNODEX
      WRITE(2,101)TITLE(1),MDY,TOD UNODEX
101 FORMAT(10X,' UNODEX V1.0: ',15X,A80,4X,A9,' ',A8) UNODEX
      WRITE(2,85) (TITLE(ITITL),ITITL=2,NTLNS) UNODEX
85  FORMAT(4(44X,A80,/)///) UNODEX
      WRITE(2,80) IESSNO UNODEX
80  FORMAT(50X,'EVALUATION OF ESS ',I5) UNODEX
      WRITE(2,30) UNODEX
30  FORMAT(///,'*****',/,
+      '* BEGIN INPUT PROBLEM AND JOB CONTROL DATA *',/,
+      '*****',///) UNODEX
      UNODEX
C.. READ IN GENVIRT SETUP DATA FROM PRIMARY JOB CONTROL FILE UNODEX
      UNODEX
      READ(12,81)NIV UNODEX

```

	WRITE(8,81)NIV	UNODEX
	READ(12,984) (NAME(KG),XH(KG),XL(KG),NLEV(KG),KG=1,NIV)	UNODEX
	WRITE(8,840) (NAME(KG),XH(KG),XL(KG),NLEV(KG),KG=1,NIV)	UNODEX
984	FORMAT(A12,2F10.5,I5)	UNODEX
840	FORMAT(A12,2E12.5,I5)	UNODEX
	C.. READ IN CONTROL VARIABLES FROM PRIMARY JOB CONTROL FILE	UNODEX
	READ(12,1) (CNTROL(I),I=1,19),SCONVG,PCONVG,BCONVG,ADEL	UNODEX
	WRITE(8,1) (CNTROL(I),I=1,19),SCONVG,PCONVG,BCONVG,ADEL	UNODEX
1	FORMAT(19I4,4E10.1)	UNODEX
	NPARAM=CNTROL(2)	UNODEX
	NVARS=CNTROL(5)	UNODEX
	IF (NIV.NE.(NVARS-1)) WRITE(8,*)'INPUT DATA ERROR, CHECK NIV'	UNODEX
	NIV=NVARS-1	UNODEX
	IF(CNTROL(18).LE.0)CNTROL(18)=1	UNODEX
	C.. READ IN PROJECTIONS OF EXPECTED IN-SERVICE ENVIRONMENT	UNODEX
	C FOR ALL INDEPENDENT VARIABLES	UNODEX
	READ(12,77) NTIMES, IDLIFE	UNODEX
	WRITE(8,77) NTIMES, IDLIFE	UNODEX
77	FORMAT(2I4)	UNODEX
	DO 51 ISV=1,NIV	UNODEX
	READ(12,850) (XINSERV(ISV,JSV),JSV=1,NTIMES)	UNODEX
	WRITE(8,850) (XINSERV(ISV,JSV),JSV=1,NTIMES)	UNODEX
850	FORMAT(13E10.5)	UNODEX
51	CONTINUE	UNODEX
	C.. GENERATE VIRTUAL IV DATA	UNODEX
	CALL GENVRT(NAME,NIV,XH,XL,NLEV,NVIR)	UNODEX
	WRITE(8,*)'NVIR=',NVIR	UNODEX
D	WRITE(8,990)	UNODEX
990	FORMAT(/,1X,'RETURNED FROM MODULE GENVRT')	UNODEX
	REWIND 3	UNODEX
	C.. READ LAB DATA (IV'S AND DV)	UNODEX
	CALL BWRITE(NLAB)	UNODEX
D	WRITE(8,991)	UNODEX
991	FORMAT(/,1X,'RETURNED FROM MODULE BWRITE')	UNODEX
	DO 5 I=1,NLAB	UNODEX
	IF(CNTROL(19).EQ.2) Y(1,I)=ALOG(Y(1,I))	UNODEX
	E(1,I)=ERE(X(1,I))	UNODEX
C	WRITE(8,*)' E(1,I)=' ,E(1,I)	UNODEX
5	CONTINUE	UNODEX
	C.. HAVE FITSALL.FOR READ ITS VERY FIRST GUESSES FROM CHANNEL #12	UNODEX
C	IBCHN=INPUT B (PARAMETERS) CHANNEL, THIS CHANNEL MUST BE SET	UNODEX
C	BEFORE LINE 2222	UNODEX
	IBCHN=12	UNODEX
	JTOT=0	UNODEX
	JADD=0	UNODEX





```

C   MODEL BUILDING DATA ONLY.  THESE REFERENCE VALUES ARE USED          UNODEX
C   TO MEASURE SUBSEQUENT IMPROVEMENT VIA ADDITIONAL DATA                UNODEX
                                     UNODEX
      CALL ERPROP(PARAM,NPARAM,AC,SUMC,NB,NIV,CNTR0L(19),
+      CNTR0L(3),IOUTER,IPHASE,NTIMES,IDLIFE)                             UNODEX
D   WRITE(6,981)                                                            UNODEX
981  FORMAT(/,1X,'RETURNED FROM ERPROP INITIALIZATION PASS')             UNODEX
                                     UNODEX
C*****UNODEX
C*      INITIALIZATION COMPLETE      BEGIN SEQUENTIAL EVALUATION          *UNODEX
C*****UNODEX
                                     UNODEX
C.. SET CALCULATION SEQUENCE FLAG (IPHASE) TO 2 INDICATING SEQUENTIAL    UNODEX
C   EVALUATION BEGINNING.  ASSIGN SCRATCH DEVICE LOGICAL UNIT NUMBER      UNODEX
C   UNODEX
      IPHASE=2                                                                UNODEX
      IVCHN=3                                                                  UNODEX
C.. LOOP OVER VIRTUAL DATA POINTS                                         UNODEX
C   READ(IVCHN,490)NVIR                                                      UNODEX
490  FORMAT(I4)                                                                UNODEX
301  DO 50 IOUTER=1,NVIR                                                       UNODEX
      WRITE(6,3)IOUTER                                                         UNODEX
      WRITE(2,3)IOUTER                                                         UNODEX
      3  FORMAT(/,1X,'PHASE 2 ** EVALUATING EXPERIMENT NUMBER: ',I5)        UNODEX
                                     UNODEX
C.. APPEND NEXT VIRTUAL DATA POINT TO END OF DATA MATRIX                UNODEX
      CALL ADVIRT(IOUTER,NLAB,X(1,INT3),Y(1,INT3),E(1,INT3),
+      PARAM,NPARAM,NIV)                                                      UNODEX
D   WRITE(6,993)                                                            UNODEX
993  FORMAT(/,1X,'RETURNED FROM MODULE ADVIRT')                             UNODEX
                                     UNODEX
      CALL FITSALL(INT3,PARAM,NPARAM,AC,SUMC,IBCHN,NTLNS)                   UNODEX
D   WRITE(6,994)                                                            UNODEX
994  FORMAT(/,1X,'RETURNED FROM MODULE FITSALL')                           UNODEX
                                     UNODEX
C.. COMPUTE ERROR PROPAGATION                                               UNODEX
      CALL ERPROP(PARAM,NPARAM,AC,SUMC,NB,NIV,CNTR0L(19),
+      CNTR0L(3),IOUTER,IPHASE,NTIMES,IDLIFE)                             UNODEX
D   WRITE(6,995)                                                            UNODEX
995  FORMAT(/,1X,'RETURNED FROM MODULE ERPROP')                             UNODEX
50   CONTINUE                                                                  UNODEX
                                     UNODEX
C.. SORT AND PRINT OUTPUT                                                  UNODEX
                                     UNODEX
      CALL RSORT(DS,IVIR,NVIR,UT,LT)                                          UNODEX
      DO 3029 I=1,NVIR                                                         UNODEX
      J=IVIR(I)                                                                UNODEX
      DSM=-DS(I)                                                                UNODEX
      WRITE(2,2020)IVIR(I),LVIR(1,J),LVIR(2,J),DSM,DDS(J)                   UNODEX
2020  FORMAT(1X,I5,'-',2I3,1P2E15.6)                                         UNODEX
3029  CONTINUE                                                                  UNODEX
                                     UNODEX
C*****UNODEX
C*      BEGINNING ECHELON EVALUATION                                         *UNODEX
C*****UNODEX
                                     UNODEX
      IPHASE=3                                                                UNODEX
                                     UNODEX

```





```

NLEV3=NLEV(3)
NLEV4=NLEV(4)
NLEV5=NLEV(5)
NLEV6=NLEV(6)
IF(NIV.LT.6)NLEV6=0
IF(NIV.LT.5)NLEV5=0
IF(NIV.LT.4)NLEV4=0
IF(NIV.LT.3)NLEV3=0
IF(NIV.LT.2)NLEV2=0

GOTO (1,2,3,4,5,6),NIV

8 I6=0
88 I6=I6+1
5 I5=0
55 I5=I5+1
4 I4=0
44 I4=I4+1
3 I3=0
33 I3=I3+1
2 I2=0
22 I2=I2+1
1 I1=0
11 I1=I1+1
I(6)=I6
I(5)=I5
I(4)=I4
I(3)=I3
I(2)=I2
I(1)=I1
DO 42 M=1,NIV
IM=I(M)
42 X(M,LIMIT)=X(M,IM)
WRITE(3,175)INOREC,(I(M),M=1,NIV),(X(M,LIMIT),M=1,NIV)
175 FORMAT(1X,'V',I4,'X',5I1,1P5E11.4)
WRITE(6,180)INOREC,(I(M),M=1,NIV)
180 FORMAT(1X,'V',I4,'X',5I1)
DO 832 M=1,NIV
XVIR(M,INOREC)=X(M,LIMIT)
832 CONTINUE
IVIR(INOREC)=INOREC
LVIR(1,INOREC)=I1*10+I2
LVIR(2,INOREC)=I3*100+I4*10+I5
INOREC=INOREC+1
IF(I1.LT.NLEV1)GOTO 11
IF(I2.LT.NLEV2)GOTO 22
IF(I3.LT.NLEV3)GOTO 33
IF(I4.LT.NLEV4)GOTO 44
IF(I5.LT.NLEV5)GOTO 55
IF(I6.LT.NLEV6)GOTO 88
NVIR=INOREC-1
RETURN
END
SUBROUTINE BWRITE(NLAB)
C *****
C * THE BWRITE ROUTINE READS THE MODEL BUILDING CORROSION DATA * BWRITE
C * FROM FILE MBCOR1.DAT ON CHANNEL 1 INTO COMMON ARRAYS X AND Y.* BWRITE
C * * BWRITE

```

```

C *      NLAB=      NUMBER OF LABORATORY-MEASURED MODEL BUILDING DATA * BWRITE
C *      NVIR=      NUMBER OF VIRTUAL IV DATA CONTAINED IN VIRCOR.DAT * BWRITE
C *      Y(1,M)     OBSERVED VALUE OF CORROSION RATE (THE ONLY DV) * BWRITE
C *                      FOR THE M-TH DATA * BWRITE
C *      X(I,M)     MEASURED VALUE OF THE I-TH I.V. FOR THE M-TH DATA * BWRITE
C *                      * BWRITE
C *      DURING DEVELOPMENT THE BWRITE ROUTINE READ THE MODEL BUILDING * BWRITE
C *      DATA AND WROTE IT TO A BINARY STORAGE FILE, HENCE THE SOME * BWRITE
C *      WHAT UNFITTING NAME - B(inary)WRITE.FOR * BWRITE
C *****
C      PARAMETER NDTs=1250 * BWRITE
C      COMMON X(8,NDTS),Y(1,NDTS),E(1,NDTS) * BWRITE
C      COMMON/BB/LAB(7,500) * BWRITE
D      WRITE(6,990) * BWRITE
990    FORMAT(/,1X,'ENTERED MODULE BWRITE') * BWRITE
      READ(1,490) NLAB * BWRITE
490    FORMAT(I4) * BWRITE
      DO 20 IBWRT1=1,NLAB * BWRITE
      READ(1,505) (LAB(K,IBWRT1),K=1,4),Y(1,IBWRT1),(X(J,IBWRT1),
+          J=1,4),X(6,IBWRT1),X(5,IBWRT1),(LAB(K,IBWRT1),K=5,7) * BWRITE
504    FORMAT(1X,2A2,1X,A1,1X,A2,1X,F8.3,1X,F4.0,1X,F5.2,1X,F7.5,
+ 1X,F3.0,1X,F5.0,1X,F6.0,2X,3A2) * BWRITE
20    CONTINUE * BWRITE
      CLOSE(UNIT=1) * BWRITE
      WRITE(6,991)NLAB * BWRITE
991    FORMAT(I4,' MODEL BUILDING DATA RECORDS READ') * BWRITE
505    FORMAT(2A2,1X,A1,1X,A2,1X,F5.2,2BX,F3.0,1X,F4.2,1X,F6.5,
+ 1X,F2.0,1X,F4.0,1X,F5.0,2X,3A2) * BWRITE
      RETURN * BWRITE
      END * BWRITE
      SUBROUTINE ADVIRT(IOUTER,NM1,X,Y,E,PARAM,NPARAM,NIV) * ADVIRT
C ***** * ADVIRT
C      THE ADVIRT ROUTINE EVALUATES THE DV FROM THE VIRTUAL IV DATA * ADVIRT
C      AND ADDS THE VIRTUAL DATA TO THE MODEL BUILDING DATABASE FILE * ADVIRT
C      MBCOR.DAT * ADVIRT
C * * ADVIRT
C      Y(1) = CORROSION RATE (DV) * ADVIRT
C * * ADVIRT
C      X(1)=TEMP * ADVIRT
C      X(2)=OX * ADVIRT
C      X(3)=MG * ADVIRT
C      X(4)=H2O * ADVIRT
C      X(5)=TOT TIME * ADVIRT
C ***** * ADVIRT
C      PARAMETER NVMAX=1250 * ADVIRT
C      DIMENSION X(1),Y(1),PARAM(1),E(1) * ADVIRT
C      COMMON/CORDAT/XX(8) * ADVIRT
C      COMMON/LABEL/LLAB(2) * ADVIRT
C      COMMON/XV/XVIR(5,NVMAX),IVIR(NVMAX),LVIR(2,NVMAX),
+  * ADVIRT
      DS(NVMAX),DDS(NVMAX),YVIR(NVMAX) * ADVIRT
D      WRITE(6,990) * ADVIRT
990    FORMAT(/,1X,'ENTERED MODULE ADVIRT') * ADVIRT
      JJ=IVIR(IOUTER) * ADVIRT
      DO 40 J=1,5 * ADVIRT

```







	DO 1000 II=1,III	FITSAL
C	WRITE(6,991)II	FITSAL
991	FORMAT(/,3X,'DO 1000: II=',I3)	FITSAL
	CNTR0L(23)=II	FITSAL
	IF(CNTR0L(18).LE.1)GOTO 35	FITSAL
C..	AT THIS POINT, STATEMENTS MAY BE ENTERED FOR INPUTTING INFORMATION	FITSAL
C	ABOUT II-TH PROBLEM SUCH AS CNTR0L(3), CNTR0L(5), CNTR0L(17),	FITSAL
C	CNTR0L(18), ETC.	FITSAL
C		FITSAL
C		FITSAL
C		FITSAL
C		FITSAL
	35 LAST=1	FITSAL
	IF(CNTR0L(17).LE.0)CNTR0L(17)=1	FITSAL
	IF(CNTR0L(18).LE.0)CNTR0L(18)=1	FITSAL
	BB=0.4*ALOG10(PCONVG)	FITSAL
	IF(BCONVG.LE.0.)BCONVG=10.**BB	FITSAL
	NSETS=CNTR0L(17)	FITSAL
C..	READ IN NSETS OF GUESSES	FITSAL
	DO 50 L=1,NSETS	FITSAL
C	WRITE(6,992)L	FITSAL
992	FORMAT(/,5X,'DO 50: L=',I3)	FITSAL
	READ(IBCHN,40)IB,IC,(BTRIAL(I),I=1,IB)	FITSAL
40	FORMAT(2I5,7E11.4,(/,8E11.4))	FITSAL
C	WRITE(2,44)L,IB,IC,(BTRIAL(I),I=1,IB)	FITSAL
C 44	FORMAT(3I5,1P7E15.5/(15X,7E15.5))	FITSAL
	I=0	FITSAL
	LASTP2=LAST+2	FITSAL
	NEXT=LASTP2+IB-1	FITSAL
	DO 45 K=LASTP2,NEXT	FITSAL
	I=I+1	FITSAL
45	CORE(K)=BTRIAL(I)	FITSAL
	CORE(LAST)=IB	FITSAL
	LASTP1=LAST+1	FITSAL
	CORE(LASTP1)=IC	FITSAL
50	LAST=NEXT+1	FITSAL
C...	SET UP MEMORY LOCATIONS IN CORE-ARRAY	FITSAL
	BDIM=CNTR0L(4)	FITSAL
	LOCZ=4*BDIM+LAST	FITSAL
	LOCA=LOCZ+MDIM*NDIM+1	FITSAL
	MINDIM=LOCA+BDIM*BDIM-1	FITSAL
	WRITE(6,333) MINDIM	FITSAL
	WRITE(2,333) MINDIM	FITSAL
333	FORMAT(/,1X'MINIMUM CORE DIMENSION ='I8)	FITSAL
	NEXT=1	FITSAL
C...	THE FOLLOWING ERRORH VALUE HAS BEEN CHANGED - 1.E60 TO 1.OE38	FITSAL
	ERRORH=1.OE38	FITSAL
C..	LOOP OVER NSETS SETS OF GUESSES	FITSAL



```

      GOTO 19
18  WRITE(2,9)
      9  FORMAT (/,1X,'THE FOLLOWING INFORMATION IS TO BE PRINTED OUT: '/FITSAL
+ ' INPUT DATA  SUMSQ AND PARAMETER VALUES  NORMAL EQ MATRICES', FITSAL
+ '  RESTRAINED CHANGE MECHANISM  POINT BY POINT COMPARISON') FITSAL
      C... IDENTIFY INTERMEDIATE PRINT OPTIONS SELECTED FITSAL
          DO 22 J=1,5 FITSAL
              L=1 FITSAL
              IF(BIN(CNTR0L(7),J).GT.0.)L=2 FITSAL
              NPRINT(J)=IPRINT(L) FITSAL
22  CONTINUE FITSAL
          WRITE(2,21)(NPRINT(J),J=1,5) FITSAL
21  FORMAT (5X,A3,18X,A3,21X,A3,25X,A3,28X,A3,/) FITSAL
      C.. SET AND DOCUMENT LL=WEIGHTING FCN INDEX FITSAL
19  LL=CNTR0L(8) FITSAL
      WRITE(2,12)CNTR0L(8),IFORM(LL) FITSAL
12  FORMAT(' CNTR0L(8) =',I3,' SO MINIMIZE LEAST SQUARES FITSAL
+      WEIGHTED BY (' ,A9,' )') FITSAL
      C... DOCUMENT RESTRAINED CHANGE MECHANISM FITSAL
          IF(CNTR0L(10).EQ.0)WRITE(2,15) FITSAL
15  FORMAT(' CNTR0L(10) = 0, SO UNCONSTRAINED PARAMETER CHANGES') FITSAL
      C.. NOTE: POSITIVE CNTR0L(10) IS IN UNITS OF TENS OF PERCENT FITSAL
          ICHANG=CNTR0L(10)*10 FITSAL
          IF(CNTR0L(10).NE.0)WRITE(2,14) ICHANG FITSAL
14  FORMAT(' CNTR0L(10) NONZERO, PARAMETERS CAN CHANGE BY AT MOST',FITSAL
+      I4,' PERCENT') FITSAL
      C.. DOCUMENT STARTING GUESSES FOR THIS PASS FITSAL
          WRITE(2,7) FITSAL
7  FORMAT(1X,'STARTING GUESSES FOR THE PARAMETERS B(J)') FITSAL
      LASPM3=LAST+M3-1 FITSAL
          WRITE (2,80) (JPC,JPC=1,M3) FITSAL
80  FORMAT(6X,' J :',6X,I2,8(11X,I2)) FITSAL
          WRITE(2,3)(CORE(I),I=LAST,LASPM3) FITSAL
3  FORMAT(6X,' B(J): '1P10E13.4) FITSAL
      C.. DOCUMENT ARRAY DIMENSIONS FITSAL
          WRITE(2,8)M,N,NDIM,BDIM FITSAL
8  FORMAT(/,1X,'NONLINEAR REGRESSION ARRAY DIMENSIONS ARE: ',/, FITSAL
+      6X,'ERROR MATRIX:  Z(' ,I2,' ,',I3,' )',/, FITSAL
+      6X,'PARAMETERS:  B(' ,I2,' )',/, FITSAL
          IF(BIN(CNTR0L(7),2).GT.0.)WRITE(2,70) FITSAL
70  FORMAT(///,'*****',/, FITSAL
+      '* BEGIN INTERMEDIATE NORMAL EQUATION MATRICES*',/, FITSAL
+      '*****',/))FITSAL
      C.. SET INITIAL ENTRY FLAG FOR YCOMP.FR AND GAUSS.FR FITSAL
          CNTR0L(22)=1 FITSAL

```

```

C.. CNTR0L(3) < 0 ON 1ST PASS OF ?                                FITSAL
C.. K=1 ON 1ST PASS OF DO 200 LOOP                                FITSAL
C.. FILL CORE( ) FROM LOCZ TO LOCZ+NDIM*MDIM-1 WITH OBSERVED DATA FITSAL
      IF(CNTR0L(3).LT.0.AND.K.EQ.1)Y=YCOMP(1,CORE(LAST),CORE(LOCZ),
      +      MDIM,NDIM,BDIM)                                       FITSAL
      IF(NPTS.NE.IABS(CNTR0L(3)))NPTS=IABS(CNTR0L(3))             FITSAL
      IF(BIN(CNTR0L(7),1).EQ.1.)CALL PRINDA(CNTR0L,CORE(LOCZ),MDIM,
      +      NDIM)                                                  FITSAL
C.. PERFORM FITTING TO MINIMIZE ERROR                             FITSAL
      CALL GAUSS(CORE(LOCB),CORE(LOCZ),MDIM,NDIM,BDIM,CORE(LOCA)) FITSAL
C.. COMPUTE ERRORS & UNCERTAINTIES, AND OUTPUT RESULTS           FITSAL
      CALL FINALE(CORE(LOCB),CORE(LOCZ),MDIM,NDIM,BDIM,CORE(LOCA),
      +      ERROR,SUMSQ)                                           FITSAL
      IF(CNTR0L(21).EQ.0)WRITE(6,107)                               FITSAL
      IF(CNTR0L(21).EQ.1)WRITE(6,102)PCONVG                       FITSAL
      IF(CNTR0L(21).EQ.2)WRITE(6,103)SCONVG                       FITSAL
      IF(CNTR0L(21).EQ.3)WRITE(6,104)                             FITSAL
      IF(CNTR0L(21).EQ.4)WRITE(6,105)                             FITSAL
      IF(CNTR0L(21).EQ.5)WRITE(6,106)                             FITSAL
      IF(CNTR0L(21).EQ.0)WRITE(2,107)                              FITSAL
      IF(CNTR0L(21).EQ.1)WRITE(2,102)PCONVG                       FITSAL
      IF(CNTR0L(21).EQ.2)WRITE(2,103)SCONVG                       FITSAL
      IF(CNTR0L(21).EQ.3)WRITE(2,104)                             FITSAL
      IF(CNTR0L(21).EQ.4)WRITE(2,105)                             FITSAL
      IF(CNTR0L(21).EQ.5)WRITE(2,106)                             FITSAL
102  FORMAT (//,1X,'CAUCHY CONVERGENCE OF PARAMETER ISS.'        FITSAL
      +      ' NO PARAMETER ESTIMATED TO NEED FRACTIONAL CHANGE   FITSAL
      +      EXCEEDING',1PE11.3)                                    FITSAL
103  FORMAT (//,1X,'CAUCHY CONVERGENCE OF SUM OF SQUARES.',      FITSAL
      +      ' FRACTIONAL REDUCTION IN MINIMUM SUMSQ IS LESS THAN', FITSAL
      +      1PE11.3)                                              FITSAL
104  FORMAT (//,1X,'TERMINATION DUE TO LIMIT ON NUMBER OF ',    FITSAL
      +      'ITERATIONS')                                         FITSAL
105  FORMAT (//,1X,'TERMINATION DUE TO SINGULARITY OF NORMAL EQS ') FITSAL
106  FORMAT (//,1X,'NO SUM OF SQUARES REDUCTION IN LEAST SQUARES INTERFITSAL
      +      ----GUESS AGAIN ')                                     FITSAL
107  FORMAT (//,1X,'OPTION REDUNDANCY - - - EXPRESSION CHANGE ', FITSAL
      +      'INDICATED')                                          FITSAL
C.. HAVE WE IMPROVED ?                                           FITSAL
      IF(ERROR.GE.ERRORH)GOTO 200                                  FITSAL
C.. NEW LOW IN ERROR, SO RESET HOLDING OF PARAMETER VALUES     FITSAL
      DO 150 I=1,M3                                               FITSAL
150   PARAM(I)=CORE(LOCB-1+I)                                       FITSAL
      DO 160 I=1,NB                                               FITSAL
      DO 180 J=1,NB                                               FITSAL
      IJ=J+NB*(I-1)                                               FITSAL
180   AC(IJ)=CORE(LOCA-1+J+BDIM*(I-1))                             FITSAL
      SUMC=SUMSQ                                                  FITSAL
C.. UPDATE LOWEST ERROR SO FAR                                    FITSAL
      ERRORH=ERROR                                                FITSAL
200   CONTINUE                                                    FITSAL

```

```

C.. OUTPUT BEST PARAMETER VALUES FOUND AND ASSOCIATED A-MATRIX
C >>>CHANEL CHANGE 5 TO 9!!
    WRITE(9,300)(PARAM(I),I=1,M3)
    WRITE(9,300)SUMC
300  FORMAT(1X,1P10E13.6)
    K1=1
    DO 500 I=1,NB
    K2=K1+BDIM-1

    WRITE(9,300)(AC(K),K=K1,K2)
    K1=K2+1
500  CONTINUE
1000 CONTINUE

    REWIND IBCHN
    CNTROL(8) =KNTR8
    CNTROL(10)=KNTR10
    CNTROL(11)=KNTR11
    CNTROL(12)=KNTR12
    CNTROL(19)=KNTR19

    RETURN
    END

    SUBROUTINE GAUSS(B,Z,MDIM,NDIM,BDIM,A)

C     SEEKS PARAMETER VALUES TO MINIMIZE:
C
C     SUM [ W*(YOBS-YCALC) ] **2
C
C     BY SOLVING
C
C     SUM [ W*DY/DB(1) * W*(YOBS-YCALC) ]
C     SUM [ W*DY/DB(2) * W*(YOBS-YCALC) ]
C     .
C     .
C     SUM [ W*DY/DB(JJ)*W*(YOBS-YCALC) ]
C
C     FIRST ORDER SOLUTION IS:
C
C     BNEW(K) = BOLD(K) + [ SUM [ W*DY/DB(K) * W*DYDB(J) ]**(-1) *
C                          SUM [ W*DY/DB(K) * W*(YOBS-YCALC) ]
C
C.. INPUT:
C     Z(1,I)=OBSERVED VALUE OF Y FOR I-TH DATA POINT
C     Z(MDIM,I)=ERROR IN OBSERVED VALUE OF Y FOR I-TH DATA POINT
C     MDIM=1ST DIMENSION OF Z( , )
C     NDIM=2ND DIMENSION OF Z( , )
C     BDIM=DIMENSIONS OF A-ARRAY AND 1ST DIMENSION OF B-ARRAY
C     CNTROL(1)= # OF PARAMETERS BEING FITTED (ABS VAL)
C     CNTROL(6)=LIMIT ON # OF ITERATIONS
C     CNTROL(7)=INTERMEDIATE OUTPUT PRINT FLAG
C     CNTROL(9)=CONVERGENCE CRITERIA CONTROL
C         =1:
C         =2:
C     (MAY BE TEMPORARILY SET AT 3 FOR PASSING TO BTEST.FR)
C     CNTROL(10)=PARAMETER VARIATION CONSTRAINT FLAG

```

```

C           = 0: UNCONSTRAINED PARAMETER CHANGES           GAUSS
C           > 0: LIMIT ON PERCENTAGE CHANGE OF PARAMETERS   GAUSS
C           (EXPRESSED IN UNITS OF TENS OF PERCENTS)       GAUSS
C   CNTROL(11)=CONTROL FOR OVERRIDING RESTRAINED CHANGE    GAUSS
C           MECHANISM (WHEN JUMP TO STATEMENTS # 34, 28 OR 38) GAUSS
C           = 1: OVERRIDING PERMITTED                       GAUSS
C           = 0: NO OVERRIDING                              GAUSS
C   CNTROL(12)=OVERRIDE LIMIT                               GAUSS
C           [NEGATIVE VALUE SPECIFIES WRONG WAY MECHANISM] GAUSS
C   CNTROL(13)= ?? (PARAMETER CHANGE OPTION ?)             GAUSS
C   CNTROL(22)=INITIAL ENTRY FLAG                           GAUSS
C           =1: 1ST ENTRY                                    GAUSS
C           =0: SUBSEQUENT ENTRY                             GAUSS
C   SCONVG=CAUCHY CONVERGENCE CRITERION FOR SUM OF SQUARES GAUSS
C   PCONVG=CAUCHY CONVERGENCE CRITERION FOR PARAMETERS    GAUSS
C   BCONVG=INCREASED VALUE OF PCONVG FOR SPECIAL CASES    GAUSS
C
C.. INTERMEDIATE:
C   A(K,J)=SUM OVER DATA POINTS OF PRODUCT OF DY/DP(K) AND DY/DP(J) GAUSS
C   B(J,1)=ESTIMATED VALUE OF J-TH PARAMETER               GAUSS
C   B(J,2)=OLD ESTIMATED VALUE OF J-TH PARAMETER           GAUSS
C   B(J,3)=SUM OVER DATA POINTS OF PRODUCT OF DEVIATION AND PARTIAL GAUSS
C           DERIVATIVE OF Y WITH RESPECT TO K-TH PARAMETER GAUSS
C   B(J,4)=WEIGHTED DERIVATIVE OF Y WITH RESPECT TO K-TH PARAMETER GAUSS
C
C.. OUTPUT:
C   B(J,1)=ESTIMATED VALUE OF J-TH PARAMETER               GAUSS
C   A(J,I)=COVARIANCE COEFFICIENT FOR J-TH AND I-TH PARAMETERS GAUSS
C   A(J,J)=VARIANCE COEFFICIENT FOR J-TH PARAMETER         GAUSS
C   CNTROL(1) MAY BE CHANGED ON CALL TO YCOMP.FR           GAUSS
C   CNTROL(10)=PARAMETER VARIATION CONSTRAINT FLAG         GAUSS
C           (MAY BE ALTERED BY THIS ROUTINE)                GAUSS
C   --1: DON'T CHANGE A- AND B-ARRAYS; CONTINUE ON NEGLIGIBLE GAUSS
C           CHANGE IN SUM OF SQUARES TILL FACLIM HIT        GAUSS
C   --2: DON'T CHANGE A- AND B-ARRAYS; WEIGHT SSQ BY NUMBER-JJ GAUSS
C           (IN SETUP.FR FROM FINALE.FR)                    GAUSS
C   --3: DON'T CHANGE A- AND B-ARRAYS                       GAUSS
C   CNTROL(11)=0: NO MORE OVERRIDING OF RESTRAINED CHG MCHM PERMTD GAUSS
C   CNTROL(12)=0: NO MORE OVERRIDING PERMITTED             GAUSS
C   CNTROL(20)=NUMBER OF ITERATIONS USED                   GAUSS
C   CNTROL(21)=TERMINATION CODE                             GAUSS
C   CNTROL(22)=INITIAL ENTRY FLAG (IS RESET TO 0 BY THIS ROUTINE) GAUSS
C
C           EXTERNAL BTEST                                  GAUSS
C           INTEGER CNTROL,BDIM                             GAUSS
C           COMMON/CNTROL/CNTROL(25)                        GAUSS
C           COMMON/CONVG/SCONVG,PCONVG,BCONVG              GAUSS
C           REAL A(BDIM,BDIM),B(BDIM,4),Z(MDIM,NDIM),S(24,6),P(24) GAUSS
C           LOGICAL L1,L2,L3,L4,L5                          GAUSS
C
C.. BINARY BITS FROM INTEGERS                               GAUSS
C   BIN(K,J) = 0. : J-TH BIT OF K IS 0                     GAUSS
C           = 1. : J-TH BIT OF K IS 1                       GAUSS
C           BIN(K,J)=0.5-0.5*(-1.)**(K/2**(J-1))           GAUSS
C
C.. SET CNTROL(22)=0 TO INDICATE COMPLETION OF INITIAL ENTRY GAUSS
C   WRITE(6,980)                                           GAUSS

```

```

990   FORMAT(/, 1X, 'ENTERED MODULE GAUSS')
      IF(CNTR0L(22).EQ.0)GOTO 5
      GAUSS
      GAUSS
      GAUSS
C.. SET DETERM=1. ON INITIAL ENTRY
      DETERM=1.
      GAUSS
      CNTR0L(22)=0
      GAUSS
2   FORMAT(/, 'CYCLE   SUM OF SQUARES   *****',
+ '***** B(J) PARAMETERS *****',/)
      GAUSS
      GAUSS
5   NN=0
      GAUSS
      NOR=0
      GAUSS
      NWW=0
      GAUSS
      NWFLAG=0
      GAUSS
      NVSTORE=0
      GAUSS
      PCHGSS=0.
      GAUSS
      GAUSS
C.. IS RESTRAINED CHANGE MECHANISM ACTIVATED ?
      IF(CNTR0L(10).LE.0)GOTO 7
      GAUSS
      GAUSS
      GAUSS
C.. INITIAL VALUE OF VARIATIONAL FACTOR
      FAC=0.1*FLOAT(CNTR0L(10))
      GAUSS
      GAUSS
      GAUSS
C.. LIMIT ON PARAMETER VARIATIONS
      FACLIM=CNTR0L(10)
      GAUSS
      GOTO 8
      GAUSS
7   FAC=1.0
      GAUSS
      FACLIM=FAC
      GAUSS
8   OLFAC=0.
      GAUSS
      JJ=IABS(CNTR0L(1))      ! # PARAMETERS BEING FITTED
      GAUSS
      LIMIT=CNTR0L(6)      ! LIMIT ON # OF ITERATIONS
      GAUSS
      L=CNTR0L(7)          ! INTERMEDIATE OUTPUT PRINT FLAG
      GAUSS
      L1=.FALSE.
      GAUSS
      L2=.FALSE.
      GAUSS
      L3=.FALSE.
      GAUSS
      L4=.FALSE.
      GAUSS
      L5=.FALSE.
      GAUSS
      IF(BIN(L,1).EQ.1.)L1=.TRUE.
      GAUSS
      IF(BIN(L,2).EQ.1.)L2=.TRUE.
      GAUSS
      IF(BIN(L,3).EQ.1.)L3=.TRUE.
      GAUSS
      IF(BIN(L,4).EQ.1.)L4=.TRUE.
      GAUSS
      IF(BIN(L,5).EQ.1.)L5=.TRUE.
      GAUSS
      CNTR0L(20)=NN          ! # OF ITERATIONS
      GAUSS
      GAUSS
C.. TERMINATION CODE IS CONTINUALLY UP-DATED BY THIS ROUTINE)
      CNTR0L(21)=89
      GAUSS
      GAUSS
      GAUSS
      GAUSS
      GAUSS
C.. MAKE 2-ND COPY OF INPUT GUESSES
      DO 3 J=1, JJ
      GAUSS
3   B(J,2)=B(J,1)
      GAUSS
C   WRITE(2,*)'B(J,2)= ',B(J,2)
      GAUSS
      SCALE=0.5
      GAUSS
      MARK10=CNTR0L(10)      ! PARAMETER VARIATION CONSTRAINT FLAG
      GAUSS
C   PRINT *, 'CNTR0L =', (CNTR0L(J), J=1, 19)
      GAUSS
      GAUSS
C.. COMPUTE PARTIAL DERIVATIVES AND COMPUTE A- & B-MATRICES
      GAUSS
10  CALL SETUP(B,Z,A,SUMSQ,MDIM,NDIM,BDIM)
      GAUSS
      GAUSS

```

C.. ARE THE EQUATIONS SINGULAR ?	GAUSS
IF(DETERM.NE.O.)GOTO 12	GAUSS
WRITE(2,13)	GAUSS
13  FORMAT(/,' THE FOLLOWING NORMAL EQUATIONS ARE SINGULAR')	GAUSS
CALL DMPMAT(CNTR0L,BDIM,A,B(1,3))	GAUSS
C.. TERMINATE BECAUSE EQUATIONS ARE SINGULAR	GAUSS
CNTR0L(21)=4	GAUSS
RETURN	GAUSS
C.. IF NOT CHANGING A- & B-ARRAYS AND PRINT WANTED OF RESTRAINED	GAUSS
C    CHANGE MECHANISM, GOTO 21	GAUSS
12  IF(CNTR0L(10).LE.-1.AND.L4)GOTO 21	GAUSS
IF(CNTR0L(10).LE.-1)GOTO 25	GAUSS
IF(L3)CALL DMPMAT(CNTR0L,BDIM,A,B(1,3))	GAUSS
C.. IF ON INITIAL ITERATION:	GAUSS
21  IF(NN.EQ.O)SQMIN=SUMSQ	GAUSS
C.. IF PRINT WANTED OF SUMSQ & PARM VALS	GAUSS
IF(L2)WRITE(2,2)	GAUSS
IF(L2)WRITE(2,14)NN,SUMSQ,(B(J,1),J=1,JJ)	GAUSS
14  FORMAT(1H0 I2,1P2E21.7,4E15.7/(E45.7,4E15.7))	GAUSS
C.. IF NOT CHANGING A- & B-ARRAYS, GO AND TEST CONVERGENCE	GAUSS
IF(CNTR0L(10).LE.-1)GOTO 25	GAUSS
C    IF(CNTR0L(20).LE.LIMIT)GOTO 20	GAUSS
CC.. TERMINATE BECAUSE HIT LIMIT ON NUMBER OF ITERATIONS	GAUSS
C    CNTR0L(21)=3	GAUSS
C    RETURN	GAUSS
C  20  CONTINUE	GAUSS
IF(JJ.NE.1)GOTO 16	GAUSS
B(1,3)=B(1,3)/A(1,1)	GAUSS
A(1,1)=1./A(1,1)	GAUSS
GOTO 160	GAUSS
C.. INVERT A-MATRIX & UP-DATE 3-RD COLUMN OF B-MATRIX	GAUSS
C.. NOTE: ONLY USING M=1 ROW OF B-ARRAY	GAUSS
16  CONTINUE	GAUSS
PPP=1.	GAUSS
DO 4444 I88=1,JJ	GAUSS
PPP=PPP*A(I88,I88)	GAUSS
4444  CONTINUE	GAUSS
WRITE(2,994)PPP	GAUSS
994  FORMAT(1X,'PPP=',1PE15.6)	GAUSS
CALL MATINV(A,JJ,B(1,3),1,DETERM,BDIM)	GAUSS
WRITE(2,995)DETERM	GAUSS
995  FORMAT(1X,'DETERM=',1PE15.6)	GAUSS
C    DO 5555 I88=1,BDIM	GAUSS
C    DO 5555 J88=1,BDIM	GAUSS
C5555  A(I88,J88)=SNGL(AAA(I88,J88))	GAUSS
160  CONTINUE	GAUSS
IF(CNTR0L(20).LE.LIMIT)GOTO 20	GAUSS
C.. TERMINATE BECAUSE HIT LIMIT ON NUMBER OF ITERATIONS	GAUSS
CNTR0L(21)=3	GAUSS
RETURN	GAUSS



C.. IF NOT PRINTING NORMAL EQNS, GOTO 17	GAUSS
20 IF(.NOT.L3)GOTO 17	GAUSS
C.. HOLD TERMINATION CODE	GAUSS
IHOLD=CNTR0L(21)	GAUSS
C.. TEMPORARILY SET TERMINATION CODE AT 70	GAUSS
C (IN CASE YCOMP.FR NEEDS TO KNOW SOURCE OF CALL)	GAUSS
C (NO NEED TO DO THIS IF NOT CALLING DMPMAT.FR)	GAUSS
CNTR0L(21)=70	GAUSS
CALL DMPMAT(CNTR0L,BDIM,A,B(1,3))	GAUSS
C.. RESTORE TERMINATION CODE	GAUSS
CNTR0L(21)=IHOLD	GAUSS
C.. UP-DATE ITERATION COUNTER	GAUSS
17 NN=NN+1	GAUSS
WRITE(6,998)NN	GAUSS
998 FORMAT(10X,'ITER # =',I3)	GAUSS
CNTR0L(20)=NN ! ITERATION COUNTER	GAUSS
RESCAL=0.5	GAUSS
IF(DETERM.EQ.0.)GOTO 10	GAUSS
C.. LOAD S(I,1-4 & 6)	GAUSS
DO 11 I=1,JJ	GAUSS
S(I,4)=-1.	GAUSS
IF(B(I,3).LT.0..AND.B(I,1).LT.0..OR.B(I,3).GT.0..AND.	GAUSS
+B(I,1).GT.0.)S(I,4)=1.	GAUSS
S(I,1)=B(I,1)	GAUSS
S(I,3)=B(I,3)	GAUSS
S(I,6)=S(I,4)	GAUSS
11 S(I,2)=(FAC-OLFAC)*S(I,1)*S(I,4)	GAUSS
C.. IF PRINTING NORMAL EQNS, ALSO PRINT S-MATRIX	GAUSS
IF(L3)WRITE(2,23)((S(J,I),I=1,4),J=1,JJ)	GAUSS
23 FORMAT (/, ' S PARAMETERS ',/(1P4E12.4))	GAUSS
C.. TEST FOR CONVERGENCE & UP-DATE PARM ESTIMATES IF CONVERGED	GAUSS
40 CALL BTEST(CNTR0L,B,BDIM)	GAUSS
C.. HAVE WE CONVERGED ?	GAUSS
IF(CNTR0L(21).NE.1)GOTO 45	GAUSS
36 IF((CNTR0L(10).EQ.-1).AND.(FAC.NE.FACLIM))GOTO 9	GAUSS
IF(CNTR0L(10).GE.0.AND.NVSTORE.NE.0)GOTO 2212	GAUSS
C.. TERMINATION, CAUCHY CONVERGENCE OF PARAMETERS	GAUSS
IF(CNTR0L(10).NE.-1)RETURN	GAUSS
CNTR0L(21)=5 !NO SSQ RED; ISSUE 'GUESS AGAIN' REQ. IF NOR	GAUSS
C.. ARE OVERRIDES PERMITTED ?	GAUSS
IF(CNTR0L(12).LE.0)GOTO 18	GAUSS
C.. UPDATE COUNT OF NUMBER OF OVERRIDES	GAUSS
NOR=NOR+1	GAUSS
WRITE(6,345)NOR	GAUSS
345 FORMAT(10X,'OVERRIDE(12): NOR=',I3)	GAUSS
IF(L2)WRITE(2,82)NOR,SQMIN	GAUSS

62	FORMAT (' NO CONVERGENCE IN SCALING INTERVAL. OVERRIDE ',	GAUSS
+	'MECHANISM NOW OPERABLE - OVERRIDE ',I3,	GAUSS
+	' SUM OF SQUARES MINIMUM IS',1PE14.6)	GAUSS
		GAUSS
C..	HAVE WE EXCEEDED PERMISSIBLE NUMBER OF OVERRIDES ?	GAUSS
	IF(NOR.GT.CNTR0L(12))GOTO 57	GAUSS
		GAUSS
C..	ARE WE ON FIRST OVERRIDE ?	GAUSS
	IF(NOR.NE.1)GOTO 38	GAUSS
		GAUSS
C..	ON FIRST OVERRIDE, SO LOAD S(J,5) & P(J) WITH CURRENT VARIANCE	GAUSS
C	COEFFICIENTS AND PARAMETER ESTIMATES	GAUSS
	DO 58 J=1,JJ	GAUSS
	S(J,5)=A(J,J)	GAUSS
58	P(J)=S(J,1)	GAUSS
	ICYC=CNTR0L(20)-1	GAUSS
	GOTO 38	GAUSS
		GAUSS
C..	EXCEEDED OVERRIDE LIMIT, SO WRAP-UP AND GET OUT	GAUSS
C..	UP-DATE VARIANCE COEFFICIENTS AND PARAMETER ESTIMATES	GAUSS
57	DO 59 J=1,JJ	GAUSS
	A(J,J)=S(J,5)	GAUSS
59	B(J,1)=P(J)	GAUSS
	NOR=NOR-1	GAUSS
	IF(L2)WRITE(2,80)NOR,ICYC	GAUSS
80	FORMAT(/,' AFTER 'I3' OVERRIDES REFERENCE ITERATION ',I4)	GAUSS
	RETURN	GAUSS
18	IF(CNTR0L(12).EQ.0)GOTO 2212	GAUSS
		GAUSS
C..	NEGATIVE CNTR0L(12) SPECIFIES WRONG WAY MECHANISM	GAUSS
	IF(L2)WRITE(2,29)SQMIN	GAUSS
29	FORMAT (' NO CONVERGENCE IN SCALING INTERVAL. WRONGWAY ',	GAUSS
+	'MECHANISM NOW OPERABLE SUM OF SQUARES MINIMUM IS ',	GAUSS
+	1PE14.6)	GAUSS
	IF(NWW.NE.0)GOTO 299	GAUSS
	DO 290 J=1,JJ	GAUSS
	S(J,5)=A(J,J)	GAUSS
290	P(J)=S(J,1)	GAUSS
	ICYC=CNTR0L(20)-1	GAUSS
299	SMAX=ABS(S(1,3)/S(1,1))	GAUSS
	DO 84 J=2,JJ	GAUSS
	IF(ABS(S(J,3)/S(J,1)).GT.SMAX)SMAX=ABS(S(J,3)/S(J,1))	GAUSS
84	CONTINUE	GAUSS
		GAUSS
C..	UP-DATE PARAMETER ESTIMATES	GAUSS
	DO 33 J=1,JJ	GAUSS
	SFRAC=ABS(S(J,3)/(SMAX*S(J,1)))	GAUSS
33	B(J,1)=S(J,1)-0.05*S(J,6)*S(J,1)*SFRAC	GAUSS
	CNTR0L(10)=-1	GAUSS
	IF(NWW.GE.IABS(CNTR0L(12)))GOTO 22	GAUSS
	NWW=NWW+1	GAUSS
	NWFLAG=1	GAUSS
	GOTO 10	GAUSS
		GAUSS
C..	UP-DATE VARIANCE COEFFICIENTS AND PARAMETER ESTIMATES	GAUSS
22	DO 220 J=1,JJ	GAUSS
	A(J,J)=S(J,5)	GAUSS
220	B(J,1)=P(J)	GAUSS

```

                IF(L2)WRITE(2,221)ICYC                                GAUSS
221  FORMAT (/,' WRONGWAY LIMIT EXCEEDED',                          GAUSS
      +          ' REFERENCE ITERATION',I4)                          GAUSS
2212 IF(CNTR0L(11).EQ.0.AND.CNTR0L(12).EQ.0)GOTO 15                ! 11  GAUSS
      IF(CNTR0L(11).EQ.0)RETURN                                      ! 11  GAUSS
      IF(CNTR0L(21).EQ.1.OR.CNTR0L(21).EQ.2)CNTR0L(21)=69        GAUSS
      IF(NVSTORE.NE.0.AND.SQMIN.GE.PCHGSS)GOTO 2219                GAUSS
      CN13=CNTR0L(13)                                             ! 13  GAUSS
      NUMBEE=JJ                                                    GAUSS
      DO 2214 J=1,JJ                                              GAUSS
C     CN13=CNTR0L(13)                                             ! 13  GAUSS
C     NUMBEE=JJ                                                    GAUSS
      S(J,5)=A(J,J)                                               GAUSS
      IF(CNTR0L(12).GE.0.OR.CNTR0L(21).EQ.69)P(J)=S(J,1)        GAUSS
2214 CONTINUE                                                    GAUSS
C.. WORDING OF FOLLOWING STATEMENT CHANGED *****                GAUSS
2219 IF(SQMIN.NE.PCHGSS)GOTO 223                                  GAUSS
      WRITE(2,226)                                                 GAUSS
226  FORMAT(/,' PARAMETER CHANGE OPTION UNAVAILABLE')            GAUSS
      WRITE(10,226)                                                GAUSS
      CNTR0L(21)=0                                                GAUSS
      NVSTORE=YCOMP(NDIM+1,B,Z,MDIM,NDIM,BDIM)                    GAUSS
C.. NOTE: CALL TO YCOMP WITH FIRST ARG= NDIM+1 CAN CHANGE CNTR0L(1) GAUSS
      IF(NVSTORE.NE.0)GOTO 2265                                    GAUSS
      CNTR0L(13)=CN13                                             ! 13  GAUSS
      CNTR0L(1)=NUMBEE                                            GAUSS
      JJ=NUMBEE                                                    GAUSS
      DO 2262 J=1,NUMBEE                                          GAUSS
C     CNTR0L(13)=CN13                                             ! 13  GAUSS
C     CNTR0L(1)=NUMBEE                                            GAUSS
C     JJ=NUMBEE                                                    GAUSS
      A(J,J)=S(J,5)                                               GAUSS
2262 B(J,1)=P(J)                                                 GAUSS
C.. TERMINATE BECAUSE OF OPTION REDUNDANCY                        GAUSS
      RETURN                                                       GAUSS
2265 NVSTORE=0                                                    GAUSS
      JJ=IABS(CNTR0L(1))                                          GAUSS
      CNTR0L(11)=0                                               ! 11  GAUSS
      CNTR0L(12)=0                                               GAUSS
      GOTO 28                                                       GAUSS
223  PCHGSS=SQMIN                                                GAUSS
      NVSTORE=YCOMP(NDIM+1,B,Z,MDIM,NDIM,BDIM)                    GAUSS
      NVAB=IABS(NVSTORE)                                          GAUSS
      NEWNV=IABS(CNTR0L(1))                                       GAUSS
      WRITE(2,225)NVAB,NEWNV                                       GAUSS
225  FORMAT(/,1X,'THE NUMBER OF LSTSQ PARAMETERS HAS BEEN ',      GAUSS
      +          'CHANGED FROM',I3,' TO',I3)                      GAUSS
      WRITE(8,225)NVAR,NEWNV                                       GAUSS
      NN=CNTR0L(20)                                               GAUSS
      JJ=IABS(CNTR0L(1))                                          GAUSS
      GOTO 28                                                       GAUSS
C.. UP-DATE PARAMETER ESTIMATES                                  GAUSS

```

15	DO 1 J=1, JJ	GAUSS
1	B(J, 1)=S(J, 1)	GAUSS
	RETURN	GAUSS
		GAUSS
45	IF((MARK10.EQ.0).OR.(CNTROL(10).EQ.-1))GOTO 46	GAUSS
		GAUSS
	DO 47 J=1, JJ	GAUSS
	IF(ABS(B(J, 3)).LE.ABS(FAC*S(J, 1)))GOTO 48	GAUSS
	B(J, 3)=S(J, 4)*FAC*S(J, 1)	GAUSS
	IF(ABS(B(J, 3)).EQ.ABS(S(J, 1)).AND.S(J, 4).EQ.-1.)	GAUSS
	+B(J, 3)=B(J, 3)+SIGN(SCONVG, S(J, 1)) ! ***** 1.OE-12 *****	GAUSS
	GOTO 47	GAUSS
48	S(J, 2)=B(J, 3)	GAUSS
	S(J, 4)=0.	GAUSS
47	CONTINUE	GAUSS
		GAUSS
C..	IS S(J, 4)=4 FOR ALL J ?	GAUSS
	DO 52 J=1, JJ	GAUSS
	IF(S(J, 4).NE.0.)GOTO 46	GAUSS
52	CONTINUE	GAUSS
		GAUSS
C..	IF S(J, 4)=0 FOR ALL J, THEN SET FAC=FACLIM	GAUSS
	FAC=FACLIM	GAUSS
		GAUSS
C..	UP-DATE PARAMETER ESTIMATES	GAUSS
46	DO 50 J=1, JJ	GAUSS
50	B(J, 1)=(B(J, 2)+B(J, 3))	GAUSS
	IF(CNTROL(10).NE.-1)CNTROL(10)=-3	GAUSS
	GOTO 10	GAUSS
		GAUSS
C..	TEST CAUCHY CONVERGENCE OF SUM OF SQUARES	GAUSS
C	WE HAVE CONVERGED WHEN NEW SUMSQ REDUCES OLD SQMIN BY A FRACTION	GAUSS
C	OF SCONVG OR LESS	GAUSS
25	TEST=ABS((SUMSQ-SQMIN)/SQMIN)	GAUSS
	IF(TEST.GT.SCONVG)GOTO 30	GAUSS
	CNTROL(21)=2	GAUSS
	IF((CNTROL(10).EQ.-1).AND.(FAC.NE.FACLIM))GOTO 9	GAUSS
	WRITE(2, 251)	GAUSS
251	FORMAT(/, ' NEGLIGIBLE CHANGE IN SUM OF SQUARES')	GAUSS
C..	TERMINATE BECAUSE OF NEGLIGIBLE CHANGE IN SUM OF SQUARES	GAUSS
	IF(NVSTORE.EQ.0)RETURN	GAUSS
		GAUSS
	GOTO 2212	GAUSS
		GAUSS
9	RESCAL=0.5	GAUSS
		GAUSS
C..	SET TERMINATION CODE TO 89	GAUSS
	CNTROL(21)=89	GAUSS
		GAUSS
C..	STORE OLD VALUE OF FAC	GAUSS
	OLFAC=FAC	GAUSS
		GAUSS
C..	INCREASE VARIATIONAL FACTOR (BUT NOT GREATER THAN FACLIM)	GAUSS
	FAC=2.*FAC	GAUSS
	IF(FAC.GT.FACLIM)FAC=FACLIM	GAUSS
	CNTROL(10)=MARK10	GAUSS
		GAUSS
C..	UP-DATE ITERATION COUNTER	GAUSS

	NN=NN+1	GAUSS
	PRINT *, 'ITER # =', NN	GAUSS
	DO 41 J=1, JJ	GAUSS
	B(J, 3)=S(J, 3)	GAUSS
41	S(J, 2)=(FAC-OLFAC)*S(J, 1)*S(J, 4)	GAUSS
	GOTO 45	GAUSS
		GAUSS
30	IF(SUMSQ.LT.SQMIN)GOTO 34	GAUSS
		GAUSS
C..	WORDING OF FOLLOWING STATEMENT CHANGED *****	GAUSS
	IF(NWFLAG.LE.O)GOTO 71	GAUSS
	NWFLAG=O	GAUSS
	GOTO 38	GAUSS
		GAUSS
71	CNTROL(10)=-1	GAUSS
	DIFFAC=FAC-OLFAC	GAUSS
	SCAFAC=RESCAL*DIFFAC	GAUSS
	RESCAL=SCALE*RESCAL	GAUSS
	IF((MARK10.NE.O).OR..NOT.L4)GOTO 24	GAUSS
		GAUSS
	DO 27 J=1, JJ	GAUSS
27	B(J, 3)=SCALE*B(J, 3)	GAUSS
		GAUSS
C..	TEST FOR CONVERGENCE & UP-DATE PARM ESTIMATES IF CONVERGED	GAUSS
	CALL BTEST(CNTROL, B, BDIM)	GAUSS
		GAUSS
C..	WORDING OF FOLLOWING STATEMENT CHANGED *****	GAUSS
C..	HAVE WE CONVERGED ?	GAUSS
	IF(CNTROL(21).NE.1)GOTO 39	GAUSS
	IF(L4)WRITE(2, 42)	GAUSS
42	FORMAT(/, ' PARTITION LESS THAN MESH LIMIT - - -	GAUSS
+	RECYCLE RESTRAINT MECHANISM')	GAUSS
	GOTO 38	GAUSS
39	IF(L4)WRITE(2, 28)SCAFAC, OLFAC	GAUSS
28	FORMAT(/, ' NO REDUCTION IN SUM OF SQUARES. RESCALE ',	GAUSS
+	'PARAMETERS ', //, ' RESTRAINED CHANGE MECHANISM SET ',	GAUSS
+	'AT (' , E11.4, '+', F7.4, ') TIMES THE PREDICTED LSTSQ',	GAUSS
+	' CORRECTION.')	GAUSS
	GOTO 46	GAUSS
		GAUSS
24	DO 31 J=1, JJ	GAUSS
	S(J, 2)=SCALE*S(J, 2)	GAUSS
	B(J, 3)=S(J, 2)	GAUSS
31	CONTINUE	GAUSS
		GAUSS
C..	HOLD CNTROL(9), WHICH SPECIFIES THE DEPENDENT VARIABLE	GAUSS
	INTER=CNTROL(9)	GAUSS
		GAUSS
C..	IF OLFAC=O, DON'T RELAX CONVERGENCE CRITERION	GAUSS
	IF(OLFAC.EQ.O.)GOTO 81	GAUSS
		GAUSS
C..	TEMPORARILY SET CNTROL(9) TO 3, THUS RELAXING CONVERGENCE CRITERION	GAUSS
C	& BY-PASSING PARM ESTIMATE UP-DATE	GAUSS
	CNTROL(9)=3	GAUSS
		GAUSS
C..	TEST FOR CONVERGENCE	GAUSS
81	CALL BTEST(CNTROL, B, BDIM)	GAUSS
		GAUSS

```

C.. RESTORE CNTROL(9)
      CNTROL(9)=INTER
      DO 37 J=1,JJ
      IF(ABS(S(J,3)).GT.FAC*S(J,1))B(J,3)=S(J,2)+OLFAC*S(J,1)*S(J,4)
37  CONTINUE

C.. WORDING OF FOLLOWING STATEMENT CHANGED *****
      IF(CNTROL(21).NE.1)GOTO 44
      IF(L4)WRITE(2,42)
      GOTO 38

44  IF(L4)WRITE(2,63)SCAFAC,OLFAC
63  FORMAT (/,' NO REDUCTION IN SUM OF SQUARES. RESCALE ',
+       'PARAMETERS ',//,' RESTRAINED CHANGE MECHANISM SET',
+       'AT (' ,E11.4,'+',F7.4,') TIMES THE VALUE OF THE ',
+       'ORIGINAL PARAMETER')
      GOTO 40
34  SQMIN=SUMSQ
      WRITE(2,987)SQMIN
987  FORMAT(1X,'NEW SQMIN=',1PE15.6)
      NOR=0
28  NW=0
      NWFLAG=0
38  IF(MARK10.GE.1)FAC=0.1*FLOAT(MARK10)
      NN=CNTRLO(20)
      OLFAC=0.

C.. UP-DATE 2ND COPY OF PARAMETER ESTIMATES
      DO 35 J=1,JJ
35  B(J,2)=B(J,1)

C.. WORDING OF FOLLOWING STATEMENT CHANGED *****
      IF(NVSTORE.NE.0.AND.CNTRLO(11).EQ.1)GOTO 231      ! 11
      CNTRLO(10)=MARK10
      GOTO 10

231  CNTRLO(10)=0
      GOTO 10

      END

      SUBROUTINE SETUP(B,Z,A,SUMSQ,MDIM,NDIM,BDIM)

C  CALLED BY GAUSS.FR & FINALE.FR
C.. INPUT:
C  CNTRLO(1) = TOTAL # PARAMETERS (ABS VAL)
C  CNTRLO(3) = # DATA POINTS (ABS VAL)
C  CNTRLO(8) = I.D. # FOR WEIGHTING FCN SELECTED
C  CNTRLO(10) = PARAMETER CHANGE CONSTRAINT CONTROL
C  = -3: DON'T CHANGE A- & B-ARRAYS
C  = -2: DON'T CHANGE A- & B-ARRAYS, WEIGHT SSQ BY NUMBER-JJ
C  = -1: DON'T CHANGE A- & B-ARRAYS
C  = 0: UNCONSTRAINED CHANGE PERMITTED
C  > 0: LIMIT ON PERCENTAGE CHANGE PERMITTED
C  Z(1,N)=OBSERVED VALUE OF Y FOR N-TH DATA POINT
C  Z(MDIM,N)=ERROR IN OBSERVED VALUE OF Y FOR N-TH DATA POINT
C  MDIM=1ST DIMENSION OF Z( , )
C  NDIM=2ND DIMENSION OF Z( , )

```

```

C          BDIM=DIMENSIONS OF A-ARRAY AND 1ST DIMENSION OF B-ARRAY          SETUP
C          SETUP
C.. OUTPUT:                                                                    SETUP
C          B(K,4)=WEIGHTED DERIVATIVE OF Y WITH RESPECT TO K-TH PARAMETER    SETUP
C          B(K,3)=SUM OVER DATA POINTS OF PRODUCT OF DEVIATION AND PARTIAL  SETUP
C          DERIVATIVE OF Y WITH RESPECT TO K-TH PARAMETER                    SETUP
C          A(K,J)=SUM OVER DATA POINTS OF PRODUCT OF DY/DB(K) AND DY/DB(J)  SETUP
C          SUMSQ=VARIANCE FOR THE FIT                                         SETUP
C          SETUP
C          INTEGER CNTROL, BDIM                                               SETUP
C          COMMON/CNTROL/CNTROL(25)                                           SETUP
C          REAL A(BDIM, BDIM), B(BDIM, 4), Z(MDIM, NDIM)                       SETUP
C          WRITE(2, *) 'CNTROL=', (CNTROL(I), I=1, 25)                         SETUP
C          WRITE(2, *) 'MDIM, NDIM, BDIM=', MDIM, NDIM, BDIM                  SETUP
C          SETUP
C          JJ=IABS(CNTROL(1))          ! # PARAMETERS BEING FITTED             SETUP
C          LL=CNTRL(8)          ! WEIGHTING FCN INDEX                          SETUP
C          WRITE(2, *) 'ENTERED SETUP, LL=', LL                               SETUP
C          WRITE(2, *)                                                     SETUP
C.. IF CNTROL(10) < 0, DON'T CHANGE A- AND B-ARRAYS                           SETUP
C          IF(CNTRL(10).LE.-1)GOTO 6                                          SETUP
C          DO 5 J=1, JJ                                                       SETUP
C          B(J,3)=0.                                                         SETUP
C          DO 5 K=1, JJ                                                       SETUP
C          5 A(J,K)=0.                                                         SETUP
C          6 NUMBER=IABS(CNTRL(3))          ! # DATA POINTS (ABS VAL)         SETUP
C.. INITIALIZE SSQ                                                            SETUP
C          SUMSQ=0.                                                           SETUP
C.. HOLD TERMINATION CODE                                                     SETUP
C          IHOLD=CNTRL(21)                                                    SETUP
C.. TEMPORARILY SET TERMINATION CODE TO 68 (IN CASE YCOMP.FR NEEDS TO        SETUP
C          IDENTIFY THE FIRST CALL FROM SETUP.FR)                             SETUP
C          CNTROL(21)=68                                                       SETUP
C          ZERO=1./FLOAT(NUMBER-JJ)                                           SETUP
C          IF(CNTRL(10).EQ.-2)ZERO=1.                                         SETUP
C          SETUP
C.. LOOP OVER DATA POINTS                                                    SETUP
C          DO 15 N=1, NUMBER                                                  SETUP
C          SETUP
C          WRITE(2, *) '**** N= ', N                                          SETUP
C          SETUP
C.. COMPUTE Y FOR N-TH DATA POINT, USING THE OBSERVED VALUES OF THE        SETUP
C          N VARS-1 INDEPENDENT VARIABLES                                    SETUP
C          AND THE INPUTTED VALUES OF THE CNTROL(2) PARAMETERS              SETUP
C          WRITE(2, *) 'N, MDIM, NDIM, BDIM=', N, MDIM, NDIM, BDIM          SETUP
C          WRITE(2, *) 'CALLING YCOMP, LL=', LL                               SETUP
C          SETUP
C          YC=YCOMP(N, B, Z, MDIM, NDIM, BDIM)                                SETUP
C          SETUP
C          WRITE(2, *) 'RETURNED FROM YCOMP, LL=', LL                         SETUP
C.. RESTORE TERMINATION CODE                                                  SETUP
C          CNTROL(21)=IHOLD                                                    SETUP
C          IF(NUMBER.NE.IABS(CNTRL(3)))GOTO 6          ; ??????????          SETUP
C.. NOTE OBSERVED VALUE OF Y FOR N-TH DATA POINT                            SETUP
C          ZN=Z(1, N)                                                         SETUP
C.. COMPUTE DEVIATION FOR N-TH DATA POINT                                    SETUP
C          DELY=ZN-YC                                                         SETUP

```

C	WRITE(2,*)'N,ZN, YC=',N,ZN, YC	SETUP
C..	BRANCH ACCORDING TO WEIGHTING FCN SELECTED	SETUP
	W=1.	SETUP
C	WRITE(2,*)'LL=',LL	SETUP
	GOTO (50,42,43,44,45,46,47,48),LL	SETUP
42	W=1./ZN	SETUP
	GOTO 50	SETUP
43	W=1./YC	SETUP
	GOTO 50	SETUP
44	W=ZN	SETUP
	GOTO 50	SETUP
45	W=YC	SETUP
	GOTO 50	SETUP
46	W=1./Z(MDIM,N)	SETUP
	GOTO 50	SETUP
47	W=Z(MDIM,N)	SETUP
	GOTO 50	SETUP
48	IF (ABS(ZN).GT.ABS(YC)) W=ZN	SETUP
	IF (ABS(YC).GE.ABS(ZN)) W=YC	SETUP
50	DELY=DELY*W	SETUP
C	WRITE(2,*)'W=',W	SETUP
C..	COMPUTE WEIGHTED SUM OF SQUARED DEVIATIONS	SETUP
C	[ALSO WEIGHTED BY NUMBER-JJ IF CNTRL(10)=3]	SETUP
	SUMSQ=SUMSQ+(DELY**2)/(FLOAT(NUMBER-JJ)*ZERO)	SETUP
C..	IF CNTRL(10)<0, DON'T CHANGE A- & B-ARRAYS	SETUP
	IF(CNTRL(10).LE.-1)GOTO 15	SETUP
C	; NOTE: NEED TO COMPLETE THE DO 15 LOOP	SETUP
	DO 10 K=1,JJ	SETUP
C	WRITE(2,*)'K=',K	SETUP
	B(K,4)=W*DERIV(K,N,B,Z,BDIM,MDIM,NDIM)	SETUP
	B(K,3)=B(K,3)+B(K,4)*DELY	SETUP
10	CONTINUE	SETUP
C..	UP-DATE ON-DIAGONAL AND UPPER-TRIANGLE TERMS OF A-MATRIX	SETUP
	DO 14 J=1,JJ	SETUP
	DO 14 K=J,JJ	SETUP
C	H=AMAX1(.001*ABS(B(K,1)),1.E-07)	SETUP
C	DYDJ1=B(J,4)	SETUP
C	BHOLD=B(K,1)	SETUP
C	B(K,1)=B(K,1)+H	SETUP
C	DYDJ2=W*DERIV(J,N,B,Z,BDIM,MDIM,NDIM)	SETUP
C	B(K,1)=BHOLD	SETUP
C	DY2DJK=(DYDJ2-DYDJ1)/H	SETUP
C		SETUP
C	TERM2=-DELY*DY2DJK	SETUP
C	TERM1=B(J,4)*B(K,4)	SETUP
C	WRITE(2,*)'N=',N	SETUP



```

C      WRITE(2,*)'J,K=',J,K                                SETUP
C      PRINT *,'TERM1,TERM2=',TERM1,TERM2                SETUP
C      PRINT *,'DELY,DY2DJK=',DELY,DY2DJK                SETUP
                                                    SETUP
      A(J,K)=A(J,K)+B(J,4)*B(K,4) ! - DELY*DY2DJK        SETUP
                                                    SETUP
14     CONTINUE                                           SETUP
15     CONTINUE                                           SETUP
                                                    SETUP
      DO 444 J=1,BDIM                                     SETUP
      DO 444 K=1,BDIM                                     SETUP
C      WRITE(2,*)'J,K=',J,K                                SETUP
C      WRITE(2,*)'A(J,K)= ',A(J,K)                        SETUP
C      WRITE(2,*)'B(J,4),B(K,4)=',B(J,4),B(K,4)          SETUP
444    CONTINUE                                           SETUP
      IF(CNTR0L(10).LE.-1)GOTO 99                        SETUP
C..  FILL-IN LOWER-TRIANGLE OF A-MATRIX WITH IMAGE OF UPPER-TRIANGLE
C      (A-MATRIX IS SYMMETRIC)
      DO 20 K=2,JJ
      L=K-1
      DO 20 J=1,L
20     A(K,J)=A(J,K)
                                                    SETUP
99     CONTINUE                                           SETUP
      RETURN
      END
      SUBROUTINE MATINV(A,N,B,M,DETERM,IDM)
C      MATRIX INVERSION ROUTINE
C      CALLED BY GAUSS.FR
C.....INPUT:
C      A(K,J) = SUM [ DY/DB(K) * DY/DB(J) ] ... ( FROM SETUP.FR )
C      N = ORDER OF A-MATRIX TO INVERT
C      B(K,1) = SUM [ DY/DB(K) * (Y0BS-YCALC) ] ..( = B(K,3) IN GAUSS)
C      M = NUMBER OF COLS OF B-MATRIX TO MULTIPLY BY INVERSE OF A-MTX
C      IDM = DIMS OF A- & B-MATRICES, MUST BE AT LEAST MAX OF N & M
C.....OUTPUT:
C      A( , ) = [A]**(-1) = INVERSE OF ORIGINAL A-MATRIX
C      DETERM = DETERMINANT OF A-MATRIX
C      B( , ) = [A]**(-1) * [B]
C.....
      DIMENSION A(IDM,IDM),B(IDM,IDM)
      DIMENSION IPIVOT(24),INDEX(24,2),PIVOT(24)
      COMMON/DUMMY/IROW,ICOLUM,AMX
      EQUIVALENCE (IROW,JROW),(ICOLUM,JCOLUM),(AMX,T,SWAP)
C.....
      DETERM=1.0
      DO 20 J=1,N
20     IPIVOT(J)=0
      DO 550 I=1,N
      AMX=0.0
      DO 105 J=1,N
      IF(IPIVOT(J)-1)80,105,80
C.....
80     DO 100 K=1,N

```

	IF(IPIVOT(K)-1)80,100,740	MATINV
80	IF(ABS(AMX)-ABS(A(J,K)))85,100,100	MATINV
85	IROW=J	MATINV
	ICOLUM=K	MATINV
	AMX=A(J,K)	MATINV
100	CONTINUE	MATINV
105	CONTINUE	MATINV
	IF(AMX)110,800,110	MATINV
110	IPIVOT(ICOLUM)=IPIVOT(ICOLUM)+1	MATINV
	IF(IROW-ICOLUM)140,260,140	MATINV
140	DETERM=-DETERM	MATINV
	DO 200 L=1,N	MATINV
	SWAP=A(IROW,L)	MATINV
	A(IROW,L)=A(ICOLUM,L)	MATINV
200	A(ICOLUM,L)=SWAP	MATINV
	IF(M)260,260,210	MATINV
210	DO 250 L=1,M	MATINV
	SWAP=B(IROW,L)	MATINV
	B(IROW,L)=B(ICOLUM,L)	MATINV
250	B(ICOLUM,L)=SWAP	MATINV
280	INDEX(I,1)=IROW	MATINV
	INDEX(I,2)=ICOLUM	MATINV
	PIVOT(I)=A(ICOLUM,ICOLUM)	MATINV
	DETERM=DETERM*PIVOT(I)	MATINV
	A(ICOLUM,ICOLUM)=1.0	MATINV
350	DO 350 L=1,N	MATINV
	A(ICOLUM,L)=A(ICOLUM,L)/PIVOT(I)	MATINV
	IF(M)380,380,360	MATINV
360	DO 370 L=1,M	MATINV
370	B(ICOLUM,L)=B(ICOLUM,L)/PIVOT(I)	MATINV
380	DO 550 L1=1,N	MATINV
	IF(L1-ICOLUM)400,550,400	MATINV
400	T=A(L1,ICOLUM)	MATINV
	A(L1,ICOLUM)=0.0	MATINV
450	DO 450 L=1,N	MATINV
	A(L1,L)=A(L1,L)-A(ICOLUM,L)*T	MATINV
	IF(M)550,550,480	MATINV
480	DO 500 L=1,M	MATINV
500	B(L1,L)=B(L1,L)-B(ICOLUM,L)*T	MATINV
550	CONTINUE	MATINV
	DO 710 I=1,N	MATINV
	L=N+1-I	MATINV
630	IF(INDEX(L,1)-INDEX(L,2))830,710,830	MATINV
	JROW=INDEX(L,1)	MATINV
	JCOLUM=INDEX(L,2)	MATINV
	DO 705 K=1,N	MATINV
	SWAP=A(K,JROW)	MATINV
	A(K,JROW)=A(K,JCOLUM)	MATINV
	A(K,JCOLUM)=SWAP	MATINV

705	CONTINUE	MATINV
710	CONTINUE	MATINV
740	RETURN	MATINV
800	DETERM=0.	MATINV
	RETURN	MATINV
	END	MATINV
	SUBROUTINE BTEST(CNTR0L,B,BDIM)	BTEST
C	CALLED BY GAUSS.FR	BTEST
C		BTEST
C..	INPUT:	BTEST
C	CNTR0L(1) = # PARAMETERS BEING FITTED (ABS VAL)	BTEST
C	CNTR0L(9) = CONVERGENCE CRITERION CONTROL	BTEST
C	= 1 OR 2: FCONVG=PCONVG, E.G. 1.E-5	BTEST
C	= 3:    FCONVG=BCONVG, E.G. 1.E-2	BTEST
C	B(J,2)=CURRENT ESTIMATE OF J-TH PARAMETER	BTEST
C	B(J,3)=INCREMENT TO NEW ESTIMATE OF J-TH PARAMETER	BTEST
C	BDIM=1ST DIMENSION OF B-ARRAY	BTEST
C		BTEST
C..	INTERMEDIATE:	BTEST
C	FCONVG=CONVERGENCE CRITERION	BTEST
C	(TEST MADE ON RELATIVE ABSOLUTE DEVIATION)	BTEST
C		BTEST
C..	OUTPUT:	BTEST
C	CNTR0L(21)=1: CAUCHY CONVERGENCE OF PARAMETERS	BTEST
C	OPTIONAL OUTPUT [IF CNTR0L(9).NE.3]	BTEST
C	B(J,1)=B(J,2)+B(J,3)	BTEST
		BTEST
	INTEGER CNTR0L(25),BDIM	BTEST
	REAL B(BDIM,4)	BTEST
	COMMON/CONVG/SCONVG,PCONVG,BCONVG	BTEST
		BTEST
	JJ=IABS(CNTR0L(1))    ! # PARAMETERS BEING FITTED	BTEST
	FCONVG=PCONVG	BTEST
	IF(CNTR0L(9).EQ.3)FCONVG=BCONVG	BTEST
		BTEST
C..	TEST CAUCHY CONVERGENCE OF PARAMETERS	BTEST
C	WE HAVE CONVERGED WHEN NO PARAMETER IS ESTIMATED TO NEED TO BE	BTEST
C	CHANGED BY MORE THAN A FRACTION FCONVG	BTEST
	DO 2 J=1,JJ	BTEST
	DENOM=ABS(B(J,2))	BTEST
	IF(DENOM.LT.1.0E-8)DENOM=1.0	BTEST
	TEST=ABS(B(J,3)/DENOM)	BTEST
C..	RETURN IMMEDIATELY [WITHOUT CHANGING CNTR0L(21) AND B(J,1)] IF NOT	BTEST
C	CONVERGED	BTEST
	IF(TEST.GT.FCONVG)RETURN	BTEST
2	CONTINUE	BTEST
		BTEST
	IF(CNTR0L(9).EQ.3)GO TO 8	BTEST
		BTEST
C..	IF PARAMETER CONVERGENCE CRITERIA SATISFIED, UP-DATE PARAMETER	BTEST
C	ESTIMATES	BTEST
	DO 3 J=1,JJ	BTEST
3	B(J,1)=(B(J,2)+B(J,3))	BTEST
		BTEST
C..	SET FLAG TO INDICATE CONVERGENCE	BTEST



```

C.. COMPUTE SUM OF SQUARED DEVIATIONS FOR THIS FIT
      SS=SUMSQ*FLOAT(NUMBER-JJ)
      FINALE
      FINALE
      FINALE
C.. COMPUTE STANDARD DEVIATION FOR THIS FIT
      SDFIT=SQRT(SUMSQ)
      FINALE
      WRITE(2,1)CNTROL(20),(B(J),J=1,JJ)
      FINALE
D      WRITE(6,1)CNTROL(20),(B(J),J=1,JJ)
      FINALE
      1  FORMAT(/,5X,'AFTER ',I3,' ITERATIONS',/,
      +      8X,'THE MINIMIZING VALUES OF THE PARAMETERS ARE:',/,
      +      (1X,1P5E15.7))
      FINALE
      WRITE(2,12)(SDPRM(I),I=1,JJ)
      FINALE
D      WRITE(6,12)(SDPRM(I),I=1,JJ)
      FINALE
      12  FORMAT(/,5X,'WITH THE FOLLOWING STD. DEVIATIONS:',/,
      +      (1X,1P5E15.7))
      FINALE
      WRITE(2,13)SS,SUMSQ,SDFIT
      FINALE
      13  FORMAT(//,' THE SUM OF SQUARES,VARIANCE AND SAMPLE STD. DEV',
      +      'IATION FOR THIS FIT ARE',1P3E16.5)
      FINALE
      FINALE
C.. STD DEV OF 1ST PARM
      FINALE
C.. IS PRINTING OF POINT-BY-POINT COMPARISONS WANTED ?
      IF(CNTROL(7).LT.16)GOTO 90
      FINALE
      FINALE
C.. PRINTING OF POINT-BY-POINT COMPARISON WANTED, SO DO IT
      FINALE
      WRITE(2,2)
      FINALE
      2  FORMAT(//,'*****',
      +      '*****',/)
      FINALE
      WRITE(2,3)
      FINALE
      3  FORMAT(//,'NUMBER LABEL Y OBSERVED',
      +      ' Y CALCULATED',
      +      ' OBS-CALC (OBS-CALC)/OBS ',/)
      FINALE
      90  DO 10 N=1,NUMBER
      FINALE
      FINALE
C.. COMPUTED VALUE OF Y FOR N-THE DATA POINT
      FINALE
      YC=YCOMP(N,B,Z,MDIM,NDIM,BDIM)
      FINALE
      FINALE
C.. DEVIATION (OBS-CALC)
      FINALE
      DELY=Z(1,N)-YC
      FINALE
      FINALE
C.. RELATIVE DEVIATION (RATIO TO OBSERVED VALUE)
      FINALE
      IF(Z(1,N).NE.O.)RATIO=DELY/Z(1,N)
      FINALE
      IF(Z(1,N).EQ.O.)RATIO=1.OE30
      FINALE
      FINALE
C.. ABSOLUTE RELATIVE DEVIATION
      FINALE
      ABSRAT=ABS(RATIO)
      FINALE
      AV=AV+DELY
      FINALE
      AV1=AV1+RATIO
      FINALE
      AV2=AV2+ABSRAT
      FINALE
      IF(CNTROL(7).GE.16)WRITE(2,5)N,LAB(5,N),LAB(6,N),LAB(7,N),
      +      LAB(1,N),LAB(2,N),Z(1,N),YC,DELY,RATIO
      FINALE
      5  FORMAT(I5,3X,5A2,1PE23.5,E17.5,2E19.5)
      FINALE
      ABSVAL=ABS(DELY)
      FINALE
      FINALE
C.. FIND LARGEST ABS DEV
      FINALE
      IF(YMAX.GT.ABSVAL)GOTO 7
      FINALE
      YMAX=ABSVAL
      FINALE
      YYMAX=DELY
      FINALE
      MARK=N
      FINALE
      FINALE

```

```

C.. FIND LARGEST ABS REL DEV
7   IF(ZMAX.GT.ABSRAT)GOTO 10
    ZMAX=ABSRAT
    ZZMAX=RATIO
    MARK1=N

10  CONTINUE
    D=NUMBER
    AV=AV/D
    AV1=AV1/D
    AV2=AV2/D
    RTMNSQ=SQRT(SUMSQ)
C   WRITE(6,11)AV,AV1,AV2,YYMAX,MARK,ZMAX,MARK1,RTMNSQ
    WRITE(2,11)AV,AV1,AV2,YYMAX,MARK,ZMAX,MARK1,RTMNSQ
11  FORMAT(//,
+     ' AVERAGE DEVIATION           ',1PE14.5,/,
+     ' AVERAGE REL DEV             ',E14.5,/,
+     ' AVE ABS REL DEV               ',E14.5,/,
+     ' MAXIMUM DEVIATION             ',E14.5,6X,
+     ' AT POINT ',I4,/,
+     ' MAXIMUM REL DEV               ',E14.5,6X,
+     ' AT POINT ',I4,/,
+     ' ROOT MEAN SQUARE DEVIATION   ',E14.5)

    RETURN
    END

SUBROUTINE PRINDA(CNTR0L,Z,MDIM,NDIM)

C   CALLED BY FITSALL.FR

    INTEGER CNTR0L(25)
    REAL Z(MDIM,NDIM)

    N=IABS(CNTR0L(3))
    NVAR=CNTR0L(5)
    MN=MINO(NVAR,10)

    WRITE(2,5)
5   FORMAT(' INPUT DATA',/, ' I      DV      IV # 1',
+         ' .....')
    DO 20 I=1,N
    WRITE(2,10)I,(Z(J,I),J=1,MN)
10  FORMAT(1X,I4,5X,1P10E11.3)
    IF(NVAR.GE.11)WRITE(2,15)(Z(J,I),J=11,NVAR)
15  FORMAT(10X,1P10E11.3)
20  CONTINUE

    RETURN
    END
SUBROUTINE DMPMAT(CNTR0L,BDIM,A,B)

C   CALLED BY GAUSS.FR

    INTEGER CNTR0L(25),BDIM
    DIMENSION A(BDIM,BDIM),B(BDIM)

```

```

WRITE(2,5)
5  FORMAT(// ' I B(I,3) A(I,1) A(I,2) ..... ')
      JJ=IABS(CNTR0L(1))
      MBD=MINO(JJ,10)
      DO 20 I=1, JJ
      WRITE(2,10) I, B(I), (A(I, J), J=1, MBD)
10  FORMAT(1H0, I4, 2X, 1PE10.3, 5X, 10E11.3)
      IF(JJ.GE.11) WRITE(2,15) (A(I, J), J=11, JJ)
15  FORMAT(22X, 1P10E11.3)
20  CONTINUE
      RETURN
      END
      FUNCTION YCOMP(N, B, Z, MDIM, NDIM, BDIM)
C.. INPUT:
C      N=DATA POINT INDEX
C      B(J)=VALUE OF J-TH PARAMETER
C      BDIM=DIMENSION OF B-ARRAY
C      MDIM=1ST DIMENSION OF Z-ARRAY
C      NDIM=2ND DIMENSION OF Z-ARRAY
C      CNTR0L(1)= # PARAMETERS BEING FITTED
C      CNTR0L(2)= TOTAL # PARAMETERS
C      CNTR0L(3)=#DATA POINTS (ABS VAL)
C      CNTR0L(5)=TOTAL NUMBER OF VARIABLES
C      CNTR0L(19)=Y INDEX
C      CNTR0L(21)=TERMINATION CODE
C      CNTR0L(22)=COMPUTATION CONTROL FOR YCOMP
C              = 0: YCOMP=COMPUTED VALUE OF Y FOR N-TH DATA POINT
C              > 0: Z( , ) = OBSERVED VALUES FOR N-TH DATA POINT
C
C      INPUT FROM BLANK COMMON:
C      X(K,I) = OBSERVED VALUE OF K-TH INDEPENDENT VARIABLE FOR I-TH
C
C      Y(L,I) = OBSERVED VALUE OF L-TH DEPENDENT VARIABLE FOR I-TH
C
C      E(L,I) = ERROR IN OBSERVED VALUE OF L-TH DEPENDENT VARIABLE
C
C.. OUTPUT:
C      YCOMP=COMPUTED VALUE OF Y
C      Z(1,I)=OBSERVED VALUE OF DEPENDENT VARIABLE Y FOR I-TH DATA PT
C      Z(2,I)=OBSERVED VALUE OF 1-ST INDEPENDENT VARIABLE FOR I-TH
C
C      Z(3,I)=OBSERVED VALUE OF 2-ND INDEPENDENT VARIABLE FOR I-TH
C
C      Z(4,I)=ERROR IN OBSERVED VALUE OF Y FOR I-TH DATA POINT
C      CNTR0L(1)=
C
C      PARAMETER NDT5=1250
C      INTEGER CNTR0L, BDIM
C      COMMON/CNTR0L/CNTR0L(25)

```

```

COMMON X(6,NDTS),Y(1,NDTS),E(1,NDTS)
DIMENSION B(BDIM),Z(MDIM,NDIM)

C.. SPECIAL CASES:
C   1-N: ORDINARY
C   NDIM+1: PARAMETER CHANGE OPTION FROM GAUSS.FR
C   67: FROM DERIV.FR
C   68: FROM SETUP.FR (1ST DATA POINT)
C   69: FROM GAUSS.FR (AFTER INCREASING FAC)
C   70: FROM GAUSS.FR (WHEN PRINTING NORMAL EQNS AFTER MATINV)

C       PRINT *, 'YCOMP: N,NDIM=',N,NDIM
       IF(N.NE.NDIM+1)GOTO 9
C       PRINT *, 'YCOMP(NDIM+1,'

C.. SPECIAL CASE [IF N=NDIM+1], ADJUST NUMBER OF PARAMETERS
       ISTORE=CNTR0L(1)      ! # PARAMETERS BEING FITTED

       IF(CNTR0L(21).EQ.0)GOTO 1111
C.. NOTE: WORDING OF FOLLOWING STATEMENT ALTERED *****
       IF(CNTR0L(1).NE.IABS(CNTR0L(2)))GOTO 1108
       CNTR0L(1)=IABS(CNTR0L(2))-1
       GOTO 1110
1108   CNTR0L(1)=IABS(CNTR0L(2))
1110   YCOMP=ISTORE
       RETURN

1111   CNTR0L(1)=IABS(CNTR0L(2))
       GOTO 1110

9      NVAR5=CNTR0L(5)
       NIV=NVAR5-1
       IF(CNTR0L(22).EQ.0)GOTO 20

C.. CNTR0L(22)=1, INDICATING INITIAL ENTRY, SO LOAD Z( , ) WITH
C       OBSERVED VALUES
       NPTS=IABS(CNTR0L(3))  ! # DATA POINTS

       IDV=CNTR0L(19)
       IDV=1
       DO 4 I=1,NPTS
         J=1
         Z(1,I)=Y(IDV,I)      ! OBSERVED DV
C.. IF MDIM GIVES ENOUGH ROOM, LOAD ERROR FOR I-TH DATA POINT
       IF(MDIM.GT.CNTR0L(5)) Z(MDIM,I)=E(IDV,I) ! ERR IN OBS DV
       DO 3 K=1,NIV
         J=J+1
         Z(J,I)=X(K,I)      ! OBSERVED K-TH IV
3      CONTINUE
4      CONTINUE

       RETURN

C.. CNTR0L(22)=0, INDICATING SUBSEQUENT ENTRY, SO COMPUTE VALUE OF Y
20   NB=IABS(CNTR0L(2))      ! TOTAL NUMBER OF PARAMETERS
C   TYPE *, 'NB=',NB
       YCOMP=YO(Z(2,N),NIV,B,NB,CNTR0L(19))
C   TYPE *, 'YCOMP=',YCOMP

```





```

RETURN
END

SUBROUTINE ERPROP(B,M3,A,SUM,NB,NIV,IDV,KNTRL3,
+
I OUTER,IPHASE,NTIMES,IDLIFE)

C INPUTS.....
C B=MAX LIKELIHOOD PARAMETER VALUES
C M3= TOTAL # OF PARAMETERS
C A=ERROR MATRIX FOR B
C NB=# OF PARAMETERS WHICH WERE FITTED
C XD=DESIGN VALUE FOR INDEPENDENT VARIABLES
C NIV=# OF INDEPENDENT VARIABLES
C IDV=FUNCT. FORM OPTION SWITCH
C -NEEDS TO BE UP TO DATE (CONSISTENT WITH NUMERICAL PARTIALS)!!

C OUTPUTS.....
C D=CORROSION DEPTH AT DESIGN-VALUE TIMES
C SIGD=UNCERTAINTY IN D

PARAMETER NVMAX=1250
PARAMETER (NSTPS = 13)
DIMENSION B(1),A(NB,NB),PYPB(12)
DIMENSION PENREF(NSTPS)
DIMENSION XD(10)
INTEGER CNTROL
COMMON/LABEL/LLAB(2)
COMMON/CNTROL/CNTROL(25)
COMMON/XINSERV/XINSERV(5,11),SIGREF(11)
COMMON/XV/XVIR(5,NVMAX),IVIR(NVMAX),LVIR(2,NVMAX),
+
DS(NVMAX),DDS(NVMAX),YVIR(NVMAX)

D WRITE(6,990)
990 FORMAT(/,1X,'ENTERED MODULE ERPROP')

WRITE(2,4)
4 FORMAT(/,' TIME DEPTH UNCERTAINTY',/,
+ ' YRS MICROMS MICROMS')

WNORM=SUM
TO=0.
D=0.

C JTERMC=0
C IF(CNTROL(21).EQ.5)JTERMC=1
SS=0.
DO 11 K=1,NB
11 PYPB(K)=0.
C.. LOOP THROUGH ALL THE TIME STEPS

DO 1 I=1,11

DO 61 MM=1,4
XD(MM)=XINSERV(MM,I)
61 CONTINUE

C.. DT=TIME INCREMENT IN YEARS
C.. XD(5)=TOTAL TIME IN HOURS

```





ISTART=LT(INDEX)	RSORT
IEND=UT(INDEX)	RSORT
GOTO 5	RSORT
END	RSORT
FUNCTION YO(X,NIV,B,NPARAM, IDV)	YO
	YO
DIMENSION X(1), B(1)	YO
	YO
C WRITE(2,*)'NPARAM= ',NPARAM	YO
C WRITE(2,*)'(X(I),I=1,5)= ',(X(I),I=1,5)	YO
C WRITE(2,*)'(B(I),I=1,4)= ',(B(I),I=1,4)	YO
	YO
C.. BRANCH ACCORDING TO NUMBER OF PARAMETERS BEING FITTED	YO
GOTO (1,2,3,4,5,6),NPARAM	YO
	YO
C.. FIT USING B(1) ONLY: OVERALL LEVEL	YO
1 P=B(1)/(1450.0+SQRT(X(5)))	YO
2 Q=(1.E-6*(X(2)*10000./32.+X(4)/4./18.)+16100.0*X(3)-5793.)/	YO
+ (X(1)+273.)	YO
IF(NPARAM.EQ.1) GOTO 100	YO
	YO
C.. ADD B(2): TIME	YO
GOTO 10	YO
	YO
C.. ADD B(3): MAGNESIUM	YO
3 Q=(1.E-6*(X(2)*10000./32.+X(4)/4./18.)+B(3)*X(3)-5793.)/	YO
+ (X(1)+273.)	YO
GOTO 10	YO
	YO
C.. ADD B(4): OXYGEN	YO
4 Q=(B(4)*(X(2)*10000./32.+X(4)/4./18.)+B(3)*X(3)-5793.)/	YO
+ (X(1)+273.)	YO
GOTO 10	YO
	YO
C.. ADD B(5): O2 & H2O SEPARATELY	YO
5 Q=(B(5)*X(2)+B(3)*X(3)+B(4)*X(4)-5793.)/(X(1)+273.)	YO
GOTO 10	YO
	YO
C.. ADD B(6): TEMPERATURE	YO
6 Q=(B(5)*X(2)+B(3)*X(3)+B(4)*X(4)-B(6))/(X(1)+273.)	YO
	YO
10 P=B(1)/(B(2)+SQRT(X(5)))	YO
	YO
100 IF(IDV.NE.2)YO=P*EXP(Q)	YO
IF(IDV.EQ.2)YG=ALOG(P)+Q	YO
	YO
C WRITE(2,*)'P,Q,YO= ',P,Q,YO	YO
	YO
RETURN	YO
END	YO
	YO
FUNCTION DYDB(X,NIV,B,NB,K, IDV)	DYDB
	DYDB
	DYDB
DIMENSION X(NIV),B(NB)	DYDB
	DYDB
EE=1.	DYDB
IF(IDV.NE.2)EE=YO(X,NIV,B,NB, IDV)	DYDB

	<b>GOTO(1,2,3,4,5,6),K</b>	<b>DYDB</b>
		<b>DYDB</b>
<b>1</b>	<b>DYDB=EE/B(1)</b>	<b>DYDB</b>
	<b>RETURN</b>	<b>DYDB</b>
		<b>DYDB</b>
<b>2</b>	<b>DYDB=-EE/(B(2)*SQRT(X(5)))</b>	<b>DYDB</b>
	<b>RETURN</b>	<b>DYDB</b>
		<b>DYDB</b>
<b>3</b>	<b>DYDB=EE*X(3)/(X(1)+273.)</b>	<b>DYDB</b>
	<b>RETURN</b>	<b>DYDB</b>
		<b>DYDB</b>
<b>4</b>	<b>IF(NB.EQ.4)DYDB=EE*(X(2)*10000./32.+X(4)/4./18.)/(X(1)+273.)</b>	<b>DYDB</b>
	<b>IF(NB.GE.5)DYDB=EE*X(4)/(X(1)+273.)</b>	<b>DYDB</b>
	<b>RETURN</b>	<b>DYDB</b>
		<b>DYDB</b>
<b>5</b>	<b>DYDB=EE*X(2)/(X(1)+273.)</b>	<b>DYDB</b>
	<b>RETURN</b>	<b>DYDB</b>
		<b>DYDB</b>
<b>6</b>	<b>DYDB=-EE/(X(1)+273.)</b>	<b>DYDB</b>
	<b>RETURN</b>	<b>DYDB</b>
		<b>DYDB</b>
	<b>END</b>	<b>DYDB</b>

### C.2.1 Annotated Sample Output from UNODEX

# C.2.1 Annotated Sample Output from UNODEX

UNODEX V1.C: WASTE CONTAINER PENETRATION UNCERTAINTY  
3x3 REF MATRIX, 360 YEAR  
20,000 HR MAX TIME  
19-JAN-87 23:34:48  
EVALUATION OF ESS 201

\*\*\*\*\*  
\* BEGIN INPUT PROBLEM AND JOB CONTROL DATA \*  
\*\*\*\*\*  
C. Edited echo of input data follows.  
C. JADD is the value of virtual data points which have been permanently shifted into the ESS.  
C. At this level in the program the value is zero and initial parameter fitting follows, along with  
C. pointwise sequential evaluation of the ESS virtual data.  
\*\*\*\*\*  
JADD = \*\*\*\*\*

\*\*\*\*\*  
MINIMUM CORE DIMENSION = 1312  
NONLINEAR REGRESSION CONTROLS ARE:  
1 2 3 4 5 6 7 8 9 10 11 12 13 14 15 16 17 18 19  
NUMBER OF PARAMETERS  
NUMBER OF DATA POINTS 182  
NUMBER OF VARIABLES 6  
LIMIT ON NUMBER OF ITERATIONS 10

CONVERGENCE CRITERIA: SCOMVG = 5.000E-07 PCOMVG = 1.000E-05 BCOMVG = 1.000E-02

THE FOLLOWING INFORMATION IS TO BE PRINTED OUT:  
C. All the print options are invoked on this run, an abbreviated sample follows.

INPUT DATA	SUMSQ	AND	PARAMETER	VALUES	NORMAL	Eq	MATRICES	RESTRAINED	CHANGE	MECHANISM	PCINT	BY	POINT	COMPARISON
YES	YES		YES		YES		YES		YES				YES	
CONTROL(8)	=	6	SO	MINIMIZE	LEAST	SQUARES								
CONTROL(10)	NONZERO,	PARAMETERS	S	CAN	CHANGE	BY	AT	MOST	40	PERCENT				
STARTING	GUESSES	FOR	THE	PARAMETERS	B(J)									
J:	1													
B(J):	2.3500E+11	1.4500E+03	1.8100E+04											
NONLINEAR	REGRESSION	ARRAY	DIMENSIONS	ARE:										
ERROR	MATRIX:	Z( 7,182)												
PARAMETERS:	B( 4)													

\*\*\*\*\*  
\* BEGIN INTERMEDIATE NORMAL EQUATION MATRICES \*  
\*\*\*\*\*  
C. Input data echo, one example follows, this option will be omitted subsequently, and replaced  
C. with "INPUT DATA"  
C.

INPUT DATA	I	DV	IV	#	1	.....	.....	.....	.....	.....	.....	.....	.....	.....	.....	.....	.....	.....	.....
1	2.082E+01	1.500E+02	5.000E-02	1.000E-04	7.600E+01	6.980E+02													
2	1.111E+01	1.500E+02	5.000E-02	1.000E-04	7.600E+01	5.635E+03													
3	1.285E+01	1.800E+02	5.000E-02	1.000E-04	7.800E+01	5.635E+03													





128	7.833E+02	1.500E+02	1.500E+02	5.000E-02	4.880E-02	7.600E+01	1.440E+02
129	5.880E+02	1.500E+02	1.500E+02	5.000E-02	4.880E-02	7.600E+01	3.300E+02
130	2.244E+02	1.500E+02	1.500E+02	5.000E-02	4.880E-02	7.600E+01	7.510E+02
131	2.459E+02	1.500E+02	1.500E+02	5.000E-02	4.880E-02	7.600E+01	7.510E+02
132	5.649E+02	1.500E+02	1.500E+02	5.000E-02	4.880E-02	7.600E+01	3.350E+02
133	1.457E+03	1.500E+02	1.500E+02	5.000E-02	4.880E-02	7.600E+01	3.350E+02
134	5.409E+02	1.500E+02	1.500E+02	5.000E-02	4.880E-02	7.600E+01	3.370E+02
135	1.928E+03	1.500E+02	1.500E+02	5.000E-02	4.880E-02	7.600E+01	3.380E+02
136	1.300E+01	1.500E+02	1.500E+02	5.000E-02	1.000E-04	7.600E+01	3.380E+02
137	5.979E+01	1.500E+02	1.500E+02	5.000E-02	1.000E-04	7.600E+01	3.380E+02
138	1.117E+01	1.500E+02	1.500E+02	5.000E-02	1.000E-04	7.600E+01	3.380E+02
139	5.694E+01	1.500E+02	1.500E+02	5.000E-02	1.000E-04	7.600E+01	3.380E+02
140	2.878E+01	1.500E+02	1.500E+02	5.000E-02	1.000E-04	7.600E+01	3.380E+02
141	6.140E+01	1.500E+02	1.500E+02	5.000E-02	1.000E-04	7.600E+01	3.380E+02
142	7.320E+00	1.500E+02	1.500E+02	5.000E-02	1.000E-04	2.000E+01	2.198E+03
143	1.018E+01	1.500E+02	1.500E+02	5.000E-02	1.000E-04	2.000E+01	2.198E+03
144	1.031E+01	1.500E+02	1.500E+02	5.000E-02	1.000E-04	2.000E+01	2.188E+03
145	5.350E+01	9.000E+01	5.000E+02	5.000E-02	1.340E-02	2.000E+01	2.203E+03
146	5.548E+01	9.000E+01	5.000E+02	5.000E-02	1.340E-02	2.000E+01	2.203E+03
147	6.768E+01	9.000E+01	5.000E+02	5.000E-02	1.340E-02	2.000E+01	2.203E+03
148	4.344E+01	9.000E+01	5.000E+02	5.000E-02	1.340E-02	2.000E+01	2.203E+03
149	4.848E+01	9.000E+01	5.000E+02	5.000E-02	1.340E-02	2.000E+01	2.203E+03
150	2.882E+01	9.000E+01	5.000E+02	5.000E-02	1.340E-02	2.000E+01	2.203E+03
151	4.891E+02	1.500E+02	1.500E+02	5.000E-02	1.340E-02	2.000E+01	2.179E+03
152	5.598E+02	1.500E+02	1.500E+02	5.000E-02	1.340E-02	2.000E+01	2.179E+03
153	3.883E+02	1.500E+02	1.500E+02	5.000E-02	1.340E-02	2.000E+01	2.179E+03
154	2.475E+02	1.500E+02	1.500E+02	5.000E-02	1.000E-04	2.000E+01	2.179E+03
155	2.078E+01	1.500E+02	1.500E+02	5.000E-02	1.000E-04	2.000E+01	2.179E+03
156	4.430E+00	1.500E+02	1.500E+02	5.000E-02	1.000E-04	2.000E+01	2.179E+03
157	1.769E+01	1.500E+02	1.500E+02	5.000E-02	1.000E-04	2.000E+01	2.155E+03
158	2.518E+01	1.500E+02	1.500E+02	5.000E-02	1.000E-04	2.000E+01	2.155E+03
159	1.888E+01	1.500E+02	1.500E+02	5.000E-02	1.000E-04	2.000E+01	2.155E+03
160	7.830E+00	9.000E+01	5.000E+02	5.000E-02	1.000E-04	2.000E+01	2.155E+03
161	8.780E+00	9.000E+01	5.000E+02	5.000E-02	1.000E-04	2.000E+01	2.155E+03
162	8.370E+00	9.000E+01	5.000E+02	5.000E-02	1.000E-04	2.000E+01	2.155E+03
163	6.330E+00	1.500E+02	1.500E+02	5.000E-02	1.000E-04	5.000E+00	2.155E+03
164	6.670E+00	1.500E+02	1.500E+02	5.000E-02	1.000E-04	5.000E+00	2.155E+03
165	6.150E+00	1.500E+02	1.500E+02	5.000E-02	1.000E-04	5.000E+00	2.155E+03
166	3.080E+00	9.000E+01	5.000E+02	5.000E-02	1.000E-04	5.000E+00	2.155E+03
167	3.080E+00	9.000E+01	5.000E+02	5.000E-02	1.000E-04	5.000E+00	2.155E+03
168	2.900E+00	9.000E+01	5.000E+02	5.000E-02	1.000E-04	5.000E+00	2.155E+03
169	1.078E+02	2.000E+02	5.000E+02	5.000E-02	1.000E-04	5.000E+00	2.155E+03
170	8.943E+01	2.000E+02	5.000E+02	5.000E-02	1.000E-04	5.000E+00	2.155E+03
171	8.083E+01	2.000E+02	5.000E+02	5.000E-02	1.000E-04	5.000E+00	2.155E+03
172	4.220E+02	1.500E+02	1.500E+02	5.000E-02	3.400E-03	5.000E+00	2.155E+03
173	3.330E+02	1.500E+02	1.500E+02	5.000E-02	3.400E-03	5.000E+00	2.155E+03
174	3.233E+02	1.500E+02	1.500E+02	5.000E-02	3.400E-03	5.000E+00	2.155E+03
175	1.183E+01	9.000E+01	5.000E+02	5.000E-02	3.400E-03	5.000E+00	2.155E+03
176	1.851E+01	9.000E+01	5.000E+02	5.000E-02	3.400E-03	5.000E+00	2.155E+03
177	1.080E+01	9.000E+01	5.000E+02	5.000E-02	3.400E-03	5.000E+00	2.155E+03
178	8.817E+02	2.000E+02	5.000E+02	5.000E-02	3.400E-03	5.000E+00	2.155E+03
179	8.832E+02	2.000E+02	5.000E+02	5.000E-02	3.400E-03	5.000E+00	2.155E+03
180	9.500E+02	2.000E+02	5.000E+02	5.000E-02	3.400E-03	5.000E+00	2.155E+03
181	6.259E+02	2.000E+02	5.000E+02	5.000E-02	3.400E-03	5.000E+00	2.155E+03
182	6.688E+02	2.000E+02	5.000E+02	5.000E-02	3.400E-03	5.000E+00	2.155E+03

C. Now the normal equations follow.  
C. See Source Listing for comments defining B(,) and A(,)  
I B(I,3) A(I,1) A(I,2) A(I,3) .....  
0 1 3.581E-11 1.461E-20 -2.308E-12 2.540E-13  
0 2 -5.815E-03 -2.308E-12 3.240E-04 -4.018E-05  
0 3 9.852E-04 2.540E-13 -4.018E-05 5.887E-06

66	6.158E+02	1.500E+02	5.000E-02	2.700E-02	3.000E+01	2.178E+03
67	8.085E+02	1.500E+02	5.000E-02	2.700E-02	3.000E+01	2.178E+03
68	4.158E+02	1.500E+02	5.000E-02	1.700E-02	2.000E+01	7.031E+03
69	4.078E+02	1.500E+02	5.000E-02	1.700E-02	2.000E+01	7.031E+03
70	4.208E+02	1.500E+02	5.000E-02	1.700E-02	2.000E+01	7.031E+03
71	4.837E+02	1.500E+02	5.000E-02	1.700E-02	2.000E+01	7.031E+03
72	4.052E+02	1.500E+02	5.000E-02	1.700E-02	2.000E+01	7.031E+03
73	4.283E+02	1.500E+02	5.000E-02	1.700E-02	2.000E+01	7.031E+03
74	7.770E+02	1.500E+02	5.000E-02	2.700E-02	3.000E+01	1.859E+03
75	7.833E+02	1.500E+02	5.000E-02	2.700E-02	3.000E+01	1.859E+03
76	6.988E+02	1.500E+02	5.000E-02	2.700E-02	3.000E+01	1.859E+03
77	6.296E+02	1.500E+02	5.000E-02	2.700E-02	3.000E+01	1.859E+03
78	5.560E+02	1.500E+02	5.000E-02	2.700E-02	3.000E+01	1.859E+03
79	8.922E+02	1.500E+02	5.000E-02	2.700E-02	3.000E+01	1.859E+03
80	5.418E+02	1.500E+02	5.000E-02	1.700E-02	2.000E+01	7.870E+02
81	8.883E+02	1.500E+02	5.000E-02	1.700E-02	2.000E+01	7.870E+02
82	8.882E+02	1.500E+02	5.000E-02	1.700E-02	2.000E+01	7.870E+02
83	7.218E+02	1.500E+02	5.000E-02	1.700E-02	2.000E+01	7.870E+02
84	6.540E+02	1.500E+02	5.000E-02	1.700E-02	2.000E+01	7.870E+02
85	5.378E+02	1.500E+02	5.000E-02	1.700E-02	2.000E+01	7.870E+02
86	8.212E+02	1.500E+02	5.000E-02	2.700E-02	3.000E+01	7.870E+02
87	6.938E+02	1.500E+02	5.000E-02	2.700E-02	3.000E+01	7.870E+02
88	5.282E+02	1.500E+02	5.000E-02	2.700E-02	3.000E+01	7.870E+02
89	8.078E+02	1.500E+02	5.000E-02	2.700E-02	3.000E+01	7.870E+02
90	5.842E+02	1.500E+02	5.000E-02	2.700E-02	3.000E+01	7.870E+02
91	5.881E+02	1.500E+02	5.000E-02	2.700E-02	3.000E+01	7.870E+02
92	1.207E+01	1.500E+02	5.000E-02	4.000E-04	2.000E+01	7.590E+02
93	1.298E+01	1.500E+02	5.000E-02	4.000E-04	2.000E+01	7.590E+02
94	1.080E+01	1.500E+02	5.000E-02	4.000E-04	2.000E+01	7.590E+02
95	8.355E+00	1.500E+02	5.000E-02	4.000E-04	2.000E+01	7.590E+02
96	7.278E+02	1.500E+02	5.000E-02	4.000E-04	2.000E+01	7.590E+02
97	5.538E+02	1.500E+02	5.000E-02	1.700E-02	2.000E+01	7.800E+02
98	4.911E+02	1.500E+02	5.000E-02	1.700E-02	2.000E+01	7.800E+02
99	5.383E+02	1.500E+02	5.000E-02	1.700E-02	2.000E+01	7.800E+02
100	8.118E+02	1.500E+02	5.000E-02	4.880E-02	7.800E+01	7.820E+02
101	8.480E+02	1.500E+02	5.000E-02	4.880E-02	7.800E+01	7.820E+02
102	7.878E+02	1.500E+02	5.000E-02	4.880E-02	7.800E+01	7.820E+02
103	7.578E+02	1.500E+02	5.000E-02	4.880E-02	7.800E+01	7.820E+02
104	1.157E+03	1.500E+02	5.000E-02	4.880E-02	7.800E+01	2.181E+03
105	1.133E+03	1.500E+02	5.000E-02	4.880E-02	7.800E+01	2.181E+03
106	1.048E+03	1.500E+02	5.000E-02	4.880E-02	7.800E+01	2.230E+02
107	1.043E+03	1.500E+02	5.000E-02	4.880E-02	7.800E+01	2.230E+02
108	8.373E+02	1.500E+02	5.000E-02	4.880E-02	7.800E+01	2.840E+03
109	9.478E+02	1.500E+02	5.000E-02	4.880E-02	7.800E+01	2.840E+03
110	4.525E+01	9.000E+01	5.000E-02	4.850E-02	7.800E+01	4.284E+03
111	6.824E+01	9.000E+01	5.000E-02	4.850E-02	7.800E+01	4.284E+03
112	5.725E+01	9.000E+01	5.000E-02	4.850E-02	7.800E+01	7.450E+02
113	3.908E+01	9.000E+01	5.000E-02	4.850E-02	7.800E+01	7.450E+02
114	8.628E+01	9.000E+01	5.000E-02	4.850E-02	7.800E+01	2.183E+03
115	5.638E+01	9.000E+01	5.000E-02	4.850E-02	7.800E+01	2.183E+03
116	6.787E+02	1.800E+02	5.000E-02	4.530E-02	5.300E+01	4.424E+03
117	6.855E+02	1.800E+02	5.000E-02	4.530E-02	5.300E+01	4.424E+03
118	9.421E+02	1.500E+02	5.000E-02	3.530E-02	5.300E+01	7.200E+02
119	9.185E+02	1.500E+02	5.000E-02	3.530E-02	5.300E+01	7.200E+02
120	2.802E+01	9.000E+01	5.000E-02	3.270E-02	5.300E+01	2.124E+03
121	3.373E+01	9.000E+01	5.000E-02	3.270E-02	5.300E+01	2.124E+03
122	2.955E+01	9.000E+01	5.000E-02	3.270E-02	5.300E+01	8.720E+02
123	2.608E+01	9.000E+01	5.000E-02	3.270E-02	5.300E+01	8.720E+02
124	1.648E+02	1.500E+02	5.000E-02	9.000E-04	7.800E+01	2.119E+03
125	1.521E+02	1.500E+02	5.000E-02	9.000E-04	7.800E+01	2.119E+03
126	4.212E+02	1.500E+02	5.000E-02	1.020E-02	7.800E+01	8.770E+02
127	4.145E+02	1.500E+02	5.000E-02	1.020E-02	7.800E+01	8.770E+02

```

CYCLE  SUM OF SQUARES  ***** B(J) PARAMETERS *****
0 0      2.0672446E+02      2.3500000E+11  1.4500000E+03  1.6100000E+04

      I  B(I,3)  A(I,1)  A(I,2)  .....
0 1  -8.714E+1;  6.347E+23  4.048E+15  2.411E+14
0 2  -3.833E+03  4.048E+15  2.582E+07  1.615E+08
0 3  2.272E+01  2.411E+14  1.615E+08  7.801E+08

5 PARAMETERS
2.3500E+11 -9.4000E+10 -5.7142E+11 -1.0000E+00
1.4500E+03 -5.8000E+02 -3.6332E+03 -1.0000E+00
1.6100E+04 6.4400E+03 2.2718E+01 1.0000E+00

CYCLE  SUM OF SQUARES  ***** B(J) PARAMETERS *****
0 1      2.0680780E+02      1.4100000E+11  8.7000000E+02  1.6122718E+04

NO REDUCTION IN SUM OF SQUARES. RESCALE PARAMETERS

RESTRAINED CHANGE MECHANISM SETAT ( 0.2000E+00+ 0.0000) TIMES THE VALUE OF THE ORIGINAL PARAMETER

CYCLE  SUM OF SQUARES  ***** B(J) PARAMETERS *****
0 1      2.0672847E+02      1.8800001E+11  1.1600000E+03  1.6111359E+04

NO REDUCTION IN SUM OF SQUARES. RESCALE PARAMETERS

RESTRAINED CHANGE MECHANISM SETAT ( 0.1000E+00+ 0.0000) TIMES THE VALUE OF THE ORIGINAL PARAMETER

CYCLE  SUM OF SQUARES  ***** B(J) PARAMETERS *****
0 1      2.0671628E+02      2.1150001E+11  1.3050000E+03  1.6105880E+04
NEW SQMIN= 2.067163E+02

      I  B(I,3)  A(I,1)  A(I,2)  .....
0 1  4.921E-11  1.784E-20  -2.824E-12  2.610E-13
0 2  -7.933E-03  -2.824E-12  4.446E-04  -4.434E-05
0 3  1.103E-03  2.610E-13  -4.434E-05  5.844E-08

CYCLE  SUM OF SQUARES  ***** B(J) PARAMETERS *****
0 1      2.0671828E+02      2.1150001E+11  1.3050000E+03  1.6105880E+04

      I  B(I,3)  A(I,1)  A(I,2)  .....
0 1  -4.368E+11  4.213E+23  2.396E+15  1.962E+14
0 2  -2.804E+03  2.693E+15  1.726E+07  1.328E+08
0 3  1.522E+01  1.962E+14  1.328E+08  7.950E+05

5 PARAMETERS
2.1150E+11 -8.4600E+10 -4.3677E+11 -1.0000E+00
1.3050E+03 -5.2200E+02 -2.8038E+03 -1.0000E+00
1.6106E+04 6.4423E+03 1.5218E+01 1.0000E+00

CYCLE  SUM OF SQUARES  ***** B(J) PARAMETERS *****

```

```

0 2      2.0707491E+02      1.2690000E+11      7.8300000E+02      1.8120897E+04
NO REDUCTION IN SUM OF SQUARES. RESCALE PARAMETERS
RESTRAINED CHANGE MECHANISM SETAT ( 0.2000E+00+ 0.0000) TIMES THE VALUE OF THE ORIGINAL PARAMETER
CYCLE  SUM OF SQUARES      ***** B(J) PARAMETERS *****
0 2      2.0677219E+02      1.6920001E+11      1.0440000E+03      1.6113288E+04
NO REDUCTION IN SUM OF SQUARES. RESCALE PARAMETERS
RESTRAINED CHANGE MECHANISM SETAT ( 0.1000E+03+ 0.0000) TIMES THE VALUE OF THE ORIGINAL PARAMETER
CYCLE  SUM OF SQUARES      ***** B(J) PARAMETERS *****
0 2      2.0672910E+02      1.9035000E+11      1.1745000E+03      1.8109484E+04
NO REDUCTION IN SUM OF SQUARES. RESCALE PARAMETERS
RESTRAINED CHANGE MECHANISM SETAT ( 0.5000E-01+ 0.0000) TIMES THE VALUE OF THE ORIGINAL PARAMETER
CYCLE  SUM OF SQUARES      ***** B(J) PARAMETERS *****
0 2      2.0672008E+02      2.0092500E+11      1.2397500E+03      1.8107582E+04
NO REDUCTION IN SUM OF SQUARES. RESCALE PARAMETERS
RESTRAINED CHANGE MECHANISM SETAT ( 0.2500E-01+ 0.0000) TIMES THE VALUE OF THE ORIGINAL PARAMETER
CYCLE  SUM OF SQUARES      ***** B(J) PARAMETERS *****
0 2      2.0671765E+02      2.0621251E+11      1.2723750E+03      1.8106831E+04
NO REDUCTION IN SUM OF SQUARES. RESCALE PARAMETERS
RESTRAINED CHANGE MECHANISM SETAT ( 0.1250E-01+ 0.0000) TIMES THE VALUE OF THE ORIGINAL PARAMETER
CYCLE  SUM OF SQUARES      ***** B(J) PARAMETERS *****
0 2      2.0671890E+02      2.0885625E+11      1.2886875E+03      1.8108155E+04
NO REDUCTION IN SUM OF SQUARES. RESCALE PARAMETERS
RESTRAINED CHANGE MECHANISM SETAT ( 0.8250E-02+ 0.0000) TIMES THE VALUE OF THE ORIGINAL PARAMETER
CYCLE  SUM OF SQUARES      ***** B(J) PARAMETERS *****
0 2      2.0671871E+02      2.1017813E+11      1.2988438E+03      1.8105917E+04
NO REDUCTION IN SUM OF SQUARES. RESCALE PARAMETERS
RESTRAINED CHANGE MECHANISM SETAT ( 0.3125E-02+ 0.0000) TIMES THE VALUE OF THE ORIGINAL PARAMETER
CYCLE  SUM OF SQUARES      ***** B(J) PARAMETERS *****
0 2      2.0671648E+02      2.1083908E+11      1.3009219E+03      1.8105799E+04
NO REDUCTION IN SUM OF SQUARES. RESCALE PARAMETERS
RESTRAINED CHANGE MECHANISM SETAT ( 0.1563E-02+ 0.0000) TIMES THE VALUE OF THE ORIGINAL PARAMETER

```

```

CYCLE  SUM OF SQUARES  ***** B(J) PARAMETERS *****
0 2    2.0671628E+02    2.1118954E+11  1.3028609E+03  1.6105739E+04
CYCLE  SUM OF SQUARES  ***** B(J) PARAMETERS *****
0 3    2.1690265E+02    4.2299998E+10  2.6100000E+02  1.6120897E+04
NO REDUCTION IN SUM OF SQUARES. RESCALE PARAMETERS
RESTRAINED CHANGE MECHANISM SETAT ( 0.2000E+00+ 0.4000) TIMES THE VALUE OF THE ORIGINAL PARAMETER
CYCLE  SUM OF SQUARES  ***** B(J) PARAMETERS *****
0 3    2.0848851E+02    8.4599998E+10  5.2200000E+02  1.6113283E+04
NO REDUCTION IN SUM OF SQUARES. RESCALE PARAMETERS
RESTRAINED CHANGE MECHANISM SETAT ( 0.1000E+00+ 0.4000) TIMES THE VALUE OF THE ORIGINAL PARAMETER
CYCLE  SUM OF SQUARES  ***** B(J) PARAMETERS *****
0 3    2.0768882E+02    1.0575000E+11  6.5250000E+02  1.6109484E+04
NO REDUCTION IN SUM OF SQUARES. RESCALE PARAMETERS
RESTRAINED CHANGE MECHANISM SETAT ( 0.8000E-01+ 0.4000) TIMES THE VALUE OF THE ORIGINAL PARAMETER
CYCLE  SUM OF SQUARES  ***** B(J) PARAMETERS *****
0 3    2.0731441E+02    1.3325000E+11  7.1776000E+02  1.6107582E+04
NO REDUCTION IN SUM OF SQUARES. RESCALE PARAMETERS
RESTRAINED CHANGE MECHANISM SETAT ( 0.2500E-01+ 0.4000) TIMES THE VALUE OF THE ORIGINAL PARAMETER
CYCLE  SUM OF SQUARES  ***** B(J) PARAMETERS *****
0 3    2.0721779E+02    1.2161250E+11  7.5037500E+02  1.6108631E+04
NO REDUCTION IN SUM OF SQUARES. RESCALE PARAMETERS
RESTRAINED CHANGE MECHANISM SETAT ( 0.1250E-01+ 0.4000) TIMES THE VALUE OF THE ORIGINAL PARAMETER
CYCLE  SUM OF SQUARES  ***** B(J) PARAMETERS *****
0 3    2.0717542E+02    1.2425626E+11  7.6688750E+02  1.6109155E+04
PARTITION LESS THAN MESH LIMIT - - - RECYCLE RESTRAINT MECHANISM
CYCLE  SUM OF SQUARES  ***** B(J) PARAMETERS *****
0 4    2.1380205E+02    -1.2890001E+11 -7.8300700E+02  1.6120887E+04
NO REDUCTION IN SUM OF SQUARES. RESCALE PARAMETERS
RESTRAINED CHANGE MECHANISM SETAT ( 0.4000E+00+ 0.8000) TIMES THE VALUE OF THE ORIGINAL PARAMETER
CYCLE  SUM OF SQUARES  ***** B(J) PARAMETERS *****
0 4    2.6721825E+02    -4.2300015E+10 -2.6100000E+02  1.6113288E+04

```

```

NO REDUCTION IN SUM OF SQUARES. RESCALE PARAMETERS
RESTRAINED CHANGE MECHANISM SETAT ( 0.2000E+00+ 0.8000) TIMES THE VALUE OF THE ORIGINAL PARAMETER
CYCLE SUM OF SQUARES ***** B(J) PARAMETERS *****
0 4 1.0302211E+03 0.0000000E+00 0.0000000E+00 1.8109484E+04

NO REDUCTION IN SUM OF SQUARES. RESCALE PARAMETERS
RESTRAINED CHANGE MECHANISM SETAT ( 0.1000E+00+ 0.8000) TIMES THE VALUE OF THE ORIGINAL PARAMETER
CYCLE SUM OF SQUARES ***** B(J) PARAMETERS *****
0 4 2.4509721E+02 2.1149991E+10 1.3050000E+02 1.8107582E+04

NO REDUCTION IN SUM OF SQUARES. RESCALE PARAMETERS
RESTRAINED CHANGE MECHANISM SETAT ( 0.5000E-01+ 0.8000) TIMES THE VALUE OF THE ORIGINAL PARAMETER
CYCLE SUM OF SQUARES ***** B(J) PARAMETERS *****
0 4 2.2527604E+02 3.1724995E+10 1.9575000E+02 1.8106831E+04

NO REDUCTION IN SUM OF SQUARES. RESCALE PARAMETERS
RESTRAINED CHANGE MECHANISM SETAT ( 0.2500E-01+ 0.8000) TIMES THE VALUE OF THE ORIGINAL PARAMETER
CYCLE SUM OF SQUARES ***** B(J) PARAMETERS *****
0 4 2.2040285E+02 3.7012505E+10 2.2837500E+02 1.8108155E+04

NO REDUCTION IN SUM OF SQUARES. RESCALE PARAMETERS
RESTRAINED CHANGE MECHANISM SETAT ( 0.1250E-01+ 0.8000) TIMES THE VALUE OF THE ORIGINAL PARAMETER
CYCLE SUM OF SQUARES ***** B(J) PARAMETERS *****
0 4 2.1859171E+02 3.856243E+10 2.4488750E+02 1.8105917E+04

PARTITION LESS THAN MESH LIMIT - - - RECYCLE RESTRAINT MECHANISM
CYCLE SUM OF SQUARES ***** B(J) PARAMETERS *****
0 5 2.0848578E+02 -2.2726895E+11 -1.4988198E+03 1.8120897E+04

NO REDUCTION IN SUM OF SQUARES. RESCALE PARAMETERS
RESTRAINED CHANGE MECHANISM SETAT ( 0.1200E+01+ 1.8000) TIMES THE VALUE OF THE ORIGINAL PARAMETER
CYCLE SUM OF SQUARES ***** B(J) PARAMETERS *****
0 5 4.7882354E+02 -7.8834729E+09 -8.8808814E+01 1.8113288E+04

NO REDUCTION IN SUM OF SQUARES. RESCALE PARAMETERS
RESTRAINED CHANGE MECHANISM SETAT ( 0.6000E+00+ 1.8000) TIMES THE VALUE OF THE ORIGINAL PARAMETER
CYCLE SUM OF SQUARES ***** B(J) PARAMETERS *****
0 5 2.0624091E+02 1.0180827E+11 6.0409509E+07 1.8109484E+04
NEW SOMIN= 2.082409E+02

```

```

I      B(I,3)      A(I,1)      A(I,2)      .....
0 1  5.124E-11    7.849E-20  -1.244E-11  5.951E-13
0 2  -8.402E-03    -1.244E-11  1.974E-03  -9.483E-05
0 3  5.035E-04     8.951E-13  -9.483E-05  5.984E-06
CYCLE  SUM OF SQUARES      ***** B(J) PARAMETERS *****
0 2      2.0624091E+02      1.0180827E+11  8.0409509E+02  1.81094L4E+04

```

```

I      B(I,3)      A(I,1)      A(I,2)      .....
0 1  -3.402E+10    2.231E+22  1.421E+14  4.317E+13
0 2  -2.185E+02    1.421E+14  8.112E+05  3.103E+05
0 3  4.741E+00     4.317E+13  3.103E+05  7.939E+05
S PARAMETERS
1.0181E+11 -4.0723E+10 -3.4021E+10 -1.0000E+00
6.0410E+02 -2.4184E+02 -2.1849E+02 -1.0000E+00
1.8109E+04 6.4438E+03 4.7408E+00 1.0000E+00
CYCLE  SUM OF SQUARES      ***** B(J) PARAMETERS *****
0 3      2.0620749E+02      6.7787812E+10  3.8500095E+02  1.8114225E+04
NEW SOMIN= 2.062075E+02

```

```

I      B(I,3)      A(I,1)      A(I,2)      .....
0 1  -4.098E-11    1.805E-19  -2.893E-11  9.185E-13
0 2  7.145E-03     -2.893E-11  4.841E-03  -1.480E-04
0 3  -3.134E-04     9.185E-13  -1.480E-04  6.124E-06
CYCLE  SUM OF SQUARES      ***** B(J) PARAMETERS *****
0 3      2.0620749E+02      6.7787812E+10  3.8500095E+02  1.8114225E+04

```

```

I      B(I,3)      A(I,1)      A(I,2)      .....
0 1  1.355E+10     4.249E+21  2.705E+13  1.803E+13
0 2  8.587E+01     2.705E+13  1.732E+05  1.375E+05
0 3  -3.422E+00     1.803E+13  1.375E+05  7.888E+05
S PARAMETERS
6.7788E+10 2.7115E+10 1.3549E+10 1.0000E+00
3.8500E+02 1.5424E+02 8.5872E+01 1.0000E+00
1.8114E+04 -6.1457E+03 -3.4224E+00 -1.0000E+00
CYCLE  SUM OF SQUARES      ***** B(J) PARAMETERS *****
0 4      2.0615884E+02      8.1338738E+10  4.7147275E+02  1.8110802E+04
NEW SOMIN= 2.061588E+02

```

```

I      B(I,3)      A(I,1)      A(I,2)      .....
0 1  -5.702E-12    1.247E-19  -1.992E-11  7.574E-13
0 2  8.928E-04     -1.992E-11  3.184E-03  -1.218E-04
0 3  -2.833E-05     7.574E-13  -1.218E-04  6.089E-06
CYCLE  SUM OF SQUARES      ***** B(J) PARAMETERS *****

```

0 4 2.0815884E+02 8.1338738E+10 4.7147275E+02 1.8110802E+04

I	B(I,3)	A(I,1)	A(I,2)	.....
0 1	-8.870E+08	8.838E+21	5.850E+13	2.654E+13
0 2	-5.212E+00	5.830E+13	3.598E+05	1.981E+05
0 3	1.486E+00	2.684E+13	1.981E+05	7.878E+05

S PARAMETERS

8.1337E+10 -3.2535E+10 -8.8895E+08 -1.0000E+00  
4.7147E+02 -1.8858E+02 -5.2117E+00 -1.0000E+00  
1.8111E+04 8.4443E+03 1.4581E+00 1.0000E+00

CYCLE SUM OF SQUARES \*\*\*\*\* B(J) PARAMETERS \*\*\*\*\*

0 5 2.0815882E+02 8.0449782E+10 4.8828105E+02 1.8112258E+04  
NEW SOMIN= 2.081588E+02

I	B(I,3)	A(I,1)	A(I,2)	.....
0 1	8.830E-14	1.273E-19	-2.032E-11	7.851E-13
0 2	-5.780E-08	-2.032E-11	3.247E-03	-1.228E-04
0 3	-1.282E-03	7.851E-13	-1.228E-04	8.064E-08

CYCLE SUM OF SQUARES \*\*\*\*\* B(J) PARAMETERS \*\*\*\*\*

0 5 2.0815882E+02 8.0449782E+10 4.8828105E+02 1.8112258E+04

I	B(I,3)	A(I,1)	A(I,2)	.....
0 1	2.173E+08	8.481E+21	5.408E+13	2.598E+13
0 2	1.343E+00	5.408E+13	3.480E+05	1.925E+05
0 3	-4.953E-01	2.598E+13	1.925E+05	7.890E+05

S PARAMETERS

8.0450E+10 3.2180E+10 2.1732E+08 1.0000E+00  
4.8828E+02 1.8850E+02 1.3430E+00 1.0000E+00  
1.8112E+04 -8.4449E+03 -4.0542E-01 -1.0000E+00

CYCLE SUM OF SQUARES \*\*\*\*\* B(J) PARAMETERS \*\*\*\*\*

0 5 2.0815887E+02 8.0687098E+10 4.8760410E+02 1.8111853E+04

C. Termination Code

NEGLIGIBLE CHANGE IN SUM OF SQUARES

C. Document number of iterations and fit

AFTER 6 ITERATIONS  
THE MINIMIZING VALUES OF THE PARAMETERS ARE:  
8.0687098E+10 4.8760410E+02 1.8111853E+04

WITH THE FOLLOWING STD. DEVIATIONS:  
9.8831018E+10 8.3123511E+02 9.5323285E+02

THE SUM OF SQUARES, VARIANCE AND SAMPLE STD. DEVIATION FOR THIS FIT ARE 2.08158E+02 1.15172E+00 1.07318E+00



C. Pointwise Comparisons

NUMBER	LABEL	Y OBSERVED	Y CALCULATED	OBS-CALC	(OBS-CALC)/OBS
1	AGC P530	2.08200E+01	1.84908E+02	-1.84289E+02	-7.98748E+00
2	AGC P531	1.1100E+01	1.88320E+02	-1.87210E+02	-1.41503E+01
3	AGC P532	1.26500E+01	1.88320E+02	-1.87035E+02	-1.23059E+01
4	AGC P533	1.03800E+01	1.88320E+02	-1.87210E+02	-1.52471E+01
5	AGC P534	1.21500E+01	1.88320E+02	-1.86705E+02	-1.28535E+01
6	AGC P535	1.33200E+01	1.88320E+02	-1.85000E+02	-1.16387E+01
7	AGC P536	1.82500E+01	1.75178E+02	-1.56928E+02	-1.04870E+01
8	AGC P537	1.88100E+01	1.68981E+02	-1.52171E+02	-8.05240E+00
9	AGC P538	1.62300E+01	1.68981E+02	-1.52751E+02	-9.41183E+00
10	AGC P539	1.67100E+01	1.68981E+02	-1.52271E+02	-9.11255E+00
11	AGC P540	1.89400E+01	1.34908E+02	-1.65969E+02	-8.76288E+00
12	AGC P541	1.84500E+01	1.68981E+02	-1.50531E+02	-8.15888E+00
13	AGC P542	1.59900E+01	1.68981E+02	-1.55891E+02	-1.19092E+01
14	AGC P543	1.30200E+01	1.75178E+02	-1.62158E+02	-1.24545E+01
15	AGC P544	1.68700E+01	1.68981E+02	-1.50101E+02	-7.85025E+00
16	DGC P545	2.85300E+01	1.68981E+02	-1.42316E+02	-5.35436E+00
17	DGC P546	2.17400E+01	1.68981E+02	-1.47108E+02	-6.76662E+00
18	DGC P547	2.76000E+01	1.75143E+02	-1.47535E+02	-5.34577E+00
19	DGC P548	2.81800E+01	1.84630E+02	-1.56450E+02	-5.55180E+00
20	DGC P549	2.85500E+01	1.68981E+02	-1.42288E+02	-5.35956E+00
21	DGC P550	3.03400E+01	1.68981E+02	-1.78508E+02	-4.58514E+00
22	DGC P551	3.41100E+01	1.68981E+02	-1.44738E+02	-8.00317E+00
23	DGC P552	1.48400E+01	1.75143E+02	-1.60203E+02	-1.07231E+01
24	DGC P553	2.12800E+01	1.68981E+02	-1.47556E+02	-6.93079E+00
25	DGC P554	2.63100E+01	1.84630E+02	-1.58320E+02	-6.01748E+00
26	DGC P555	2.34300E+01	1.68981E+02	-1.45416E+02	-6.20642E+00
27	DGC P556	2.17900E+01	1.68981E+02	-1.47058E+02	-7.4880E+00
28	DGC P557	2.88800E+01	1.68981E+02	-1.40158E+02	-4.88520E+00
29	P515	2.84100E+01	1.84412E+02	-1.55002E+02	-5.27039E+00
30	IC1 P516	1.63135E+01	1.77607E+02	-1.61297E+02	-9.88947E+00
31	IC1 P517	1.43600E+01	1.72135E+02	-1.57775E+02	-1.09871E+01
32	IC1 P519	1.54400E+01	1.68483E+02	-1.54023E+02	-1.24903E+01
33	IC1 P520	1.8000E+01	1.72135E+02	-1.60535E+02	-9.97558E+00
34	IC1 P521	1.25300E+01	1.68483E+02	-1.58932E+02	-1.38392E+01
35	IC1 P522	1.02300E+01	1.72135E+02	-1.61965E+02	-1.25246E+01
36	IC1 P523	1.26600E+01	1.68483E+02	-1.56803E+02	-1.58285E+01
37	IC1 P529	1.36700E+01	1.84412E+02	-1.70742E+02	-1.23857E+01
38	X52A P850	4.87300E+02	2.07835E+02	2.7605E+02	5.70735E-01
39	X52A P852	4.29300E+02	2.07835E+02	2.21665E+02	5.16340E-01
40	X52A P853	4.88100E+02	2.07835E+02	2.80465E+02	5.74605E-01
41	X52A P855	4.89000E+02	2.07835E+02	2.91385E+02	5.83897E-01
42	X52A P870	4.68600E+02	2.07835E+02	2.61965E+02	5.57848E-01
43	X52A P874	4.42200E+02	2.07835E+02	2.34565E+02	5.30449E-01
44	X52B P839	4.86900E+02	2.40888E+02	2.56012E+02	5.15219E-01
45	X52B P848	5.65800E+02	2.40888E+02	3.24712E+02	5.74102E-01
46	X52B P858	3.37700E+02	2.40888E+02	2.96012E+02	5.52003E-01
47	X52B P880	5.89250E+02	2.40888E+02	3.48312E+02	5.91161E-01
48	X52B P873	4.82800E+02	2.40888E+02	2.41912E+02	5.01061E-01
49	X52B P887	5.34000E+02	2.40888E+02	2.93112E+02	5.48898E-01
50	X52C P835	8.87300E+02	3.38085E+02	3.49205E+02	5.08082E-01
51	X52C P844	6.46300E+02	3.38085E+02	3.08205E+02	4.76878E-01
52	X52C P862	6.56300E+02	3.38085E+02	3.18205E+02	4.84847E-01
53	X52C P868	6.69400E+02	3.38085E+02	3.31305E+02	4.94928E-01
54	X52C P867	6.60500E+02	3.38085E+02	3.22405E+02	4.88122E-01

55	XS2C	P672	8.91200E+02	3.38095E+02	3.52205E+02	5.10929E-01
56	XS2D	P642	8.64800E+02	4.08023E+02	2.55575E+02	3.84555E-01
57	XS2D	P645	7.39200E+02	4.08023E+02	3.30175E+02	4.48665E-01
58	XS2D	P651	8.15100E+02	4.08025E+02	2.06075E+02	3.35027E-01
59	XS2D	P659	8.19800E+02	4.08025E+02	1.10475E+02	2.12657E-01
60	XS2D	P669	8.22700E+02	4.08025E+02	2.17675E+02	3.47335E-01
61	XS2D	P668	8.22200E+02	4.08025E+02	2.13175E+02	3.42815E-01
62	XS2E	P643	8.21400E+02	4.84834E+02	1.26566E+02	2.03878E-01
63	XS2E	P654	7.74000E+02	4.84834E+02	2.52566E+02	3.37928E-01
64	XS2E	P661	8.96300E+02	4.84834E+02	1.01468E+02	1.70159E-01
65	XS2E	P668	8.68800E+02	4.84834E+02	9.40658E+01	1.59731E-01
66	XS2E	P678	8.15800E+02	4.84834E+02	1.20968E+02	1.96437E-01
67	XS2E	P685	8.06500E+02	4.84834E+02	3.11888E+02	3.86442E-01
68	XS3EE	P637	4.15800E+02	3.15299E+02	1.00801E+02	2.41888E-01
69	XS3EE	P641	4.07800E+02	3.15299E+02	9.26010E+01	2.27018E-01
70	XS3EE	P654	4.20800E+02	3.15299E+02	1.05501E+02	2.50715E-01
71	XS3EE	P655	4.63700E+02	3.15299E+02	1.48401E+02	3.20037E-01
72	XS3EE	P671	4.05200E+02	3.15299E+02	8.99011E+01	2.21888E-01
73	XS3EE	P678	4.26300E+02	3.15299E+02	1.11001E+02	2.80382E-01
74	XS3F	P638	7.77000E+02	5.00615E+02	2.76385E+02	3.55708E-01
75	XS3F	P647	7.93300E+02	5.00615E+02	2.92885E+02	3.88948E-01
76	XS3F	P648	8.98800E+02	5.00615E+02	1.89865E+02	2.86948E-01
77	XS3F	P676	8.26800E+02	5.00615E+02	1.24885E+02	2.8427E-01
78	XS3F	P688	8.26800E+02	5.00615E+02	5.53853E+01	1.99785E-01
79	XS3F	P990	8.92200E+02	5.00615E+02	1.91588E+02	9.96138E-02
80	XS3G	P636	8.41800E+02	3.51047E+02	1.90553E+02	2.7877E-01
81	XS3G	P640	8.68300E+02	3.51047E+02	3.17253E+02	3.51833E-01
82	XS3G	P663	8.82200E+02	3.51047E+02	2.17153E+02	4.74718E-01
83	XS3G	P664	7.21800E+02	3.51047E+02	3.70553E+02	3.8217E-01
84	XS3G	P180	8.54000E+02	3.51047E+02	3.02953E+02	5.13518E-01
85	XS3G	P682	8.37800E+02	3.51047E+02	1.86753E+02	3.47253E-01
86	XS3H	P648	8.21200E+02	5.13791E+02	3.07409E+02	3.74342E-01
87	XS3H	P675	8.53800E+02	5.13791E+02	1.98809E+02	2.13908E-01
88	XS3H	P677	8.28200E+02	5.13791E+02	1.44093E+02	2.72800E-02
89	XS3H	P683	8.07900E+02	5.13791E+02	2.94108E+02	3.64042E-01
90	XS3H	P854	8.94200E+02	5.13791E+02	8.04093E+01	1.35324E-01
91	XS3H	P689	8.81000E+02	5.13791E+02	7.43093E+01	1.26355E-01
92	XS4E	Q433	1.20700E+01	1.86593E+02	-1.74523E+02	-1.44597E+01
93	XS4E	Q489	1.25800E+01	1.86593E+02	-1.74033E+02	-1.38581E+01
94	XS4E	Q483	1.08000E+01	1.83593E+02	-1.75793E+02	-1.82771E+01
95	XS4E	Q505	8.35500E+00	1.86593E+02	-1.78238E+02	-2.13331E+01
96	XS4H	Q369	7.27800E+02	3.51137E+02	3.78463E+02	5.17404E-01
97	XS4H	Q525	5.53800E+02	3.51137E+02	2.02863E+02	3.65950E-01
98	XS4H	Q598	4.91100E+02	3.51137E+02	1.39863E+02	3.84899E-01
99	XS4H	Q609	5.38300E+02	3.51137E+02	1.85183E+02	3.45280E-01
100	GC1	Q387	8.11600E+02	1.09244E+03	-2.80841E+02	-3.46034E-01
101	GC1	Q329	8.46000E+02	1.09244E+03	-2.49441E+02	-2.91301E-01
102	GC1	Q320	7.97800E+02	1.05188E+03	-2.54077E+02	-3.18472E-01
103	GC1	Q391	7.57800E+02	1.05188E+03	-2.94077E+02	-3.88087E-01
104	GC2	Q363	1.15700E+03	1.09820E+03	5.88018E+01	5.08227E-02
105	GC2	Q364	1.13300E+03	1.09820E+03	3.48018E+01	3.07186E-02
106	GC2	Q385	1.04800E+03	1.04838E+03	-3.56078E-01	-3.39770E-04
107	GC2	Q388	1.04200E+03	1.04838E+03	-3.56078E-01	-3.39770E-04
108	GC2	Q370	9.37300E+02	1.01880E+03	-8.35808E+00	-6.08986E-03
109	GC2	Q371	9.47800E+02	1.01880E+03	-8.13040E+01	-8.87437E-02
110	GC3	Q398	4.52500E+01	1.50578E+02	-7.07038E+01	-7.45801E-02
111	GC3	Q399	8.82400E+01	1.50578E+02	-1.05328E+02	-2.32789E+00
112	GC3	Q398	5.72900E+01	1.44850E+02	-8.23379E+01	-1.20659E+00
113	GC3	Q397	3.80600E+01	1.44850E+02	-8.78605E+01	-1.53012E+00
114	GC3	Q394	5.62800E+01	1.39521E+02	-1.05890E+02	-2.71097E+00
115	GC3	Q395	5.63800E+01	1.39521E+02	-8.32614E+01	-1.47894E+00
116	GC4	Q405	8.79700E+02	7.08080E+02	-8.31314E+01	-1.47422E+00
					-2.63804E+01	-3.87824E-02

117	GC4	Q406	8.95500E+02	7.06800E+02	-1.05604E+01	-1.51839E-02
118	GC4	Q403	9.42100E+02	6.79598E+02	2.82504E+02	2.78637E-01
119	GC4	Q404	9.18500E+02	6.70596E+02	2.38904E+02	2.58488E-01
120	GC5	Q497	2.80200E+01	8.18378E+01	-5.38178E+01	-1.92089E+00
121	GC5	Q499	3.37300E+01	8.18378E+01	-4.81078E+01	-1.42628E+00
122	GC5	Q495	2.95500E+01	7.86338E+01	-4.80838E+01	-1.68104E+00
123	GC5	Q498	2.80200E+01	7.86338E+01	-5.25538E+01	-2.01510E+00
124	GC8	Q517	1.64800E+02	1.80770E+02	-2.59700E+01	-1.57595E-01
125	GC8	Q519	1.52100E+02	1.80770E+02	-3.86700E+01	-2.54241E-01
126	GC7	Q513	4.21200E+02	2.70885E+02	1.50318E+02	3.58874E-01
127	GC7	Q514	4.14500E+02	2.70885E+02	1.43815E+02	3.48478E-01
128	GC8	Q512	7.93300E+02	1.12798E+03	-3.34685E+02	-4.21888E-01
129	GC8	Q490	5.88000E+02	1.11387E+03	-5.25867E+02	-8.93991E-01
130	GC9	Q520	2.24400E+02	2.11342E+03	2.85303E+00	1.27228E-02
131	GC9	Q522	2.45900E+02	2.21545E+02	2.43550E+01	9.80444E-02
132	GC10	Q509	5.64900E+02	1.11335E+03	-5.48453E+02	-8.70885E-01
133	GC12	Q503	1.45700E+03	1.11335E+03	3.43647E+02	2.35859E-01
134	GC13X	Q533	5.40900E+02	1.11323E+03	-5.72328E+02	-1.05810E+00
135		Q539	1.82600E+03	1.11322E+03	8.12710E+02	4.21988E-01
136		Q525	1.30000E+01	1.87973E+02	-1.74973E+02	-1.34594E+01
137		T502	5.97900E+01	1.87973E+02	-1.28183E+02	-2.14388E+00
138		Q536	1.11700E+01	1.87973E+02	-1.78803E+02	-1.58284E+01
139		T515	5.69400E+01	1.87973E+02	-1.31033E+02	-2.30124E+00
140		Q537	2.87800E+01	1.87973E+02	-1.59193E+02	-5.53137E+00
141		T517	6.14000E+01	1.87573E+02	-1.26573E+02	-2.64145E+00
142		Q584	7.32000E+00	1.77541E+02	-1.70221E+02	-2.32542E+01
143	ES1	Q385	1.01800E+01	1.77541E+02	-1.67381E+02	-1.84745E+01
144	ES1	Q386	1.03100E+01	1.77541E+02	-1.67231E+02	-1.82203E+01
145	ES2	Q410	5.35000E+01	3.33284E+01	-2.01718E+01	3.77040E-01
146	ES2	Q411	5.54800E+01	3.33284E+01	-2.21318E+01	3.89058E-01
147	ES2	Q426	6.78800E+01	3.33284E+01	3.43517E+01	5.07580E-01
148	ES2	R967	4.34400E+01	3.33284E+01	1.01118E+01	2.32773E-01
149	ES2	R972	4.54800E+01	3.33284E+01	1.21318E+01	2.68864E-01
150	ES2	R979	2.88200E+01	3.33284E+01	-4.50835E+00	-1.86431E-01
151	ES8	Q414	4.89100E+02	2.84787E+02	1.94333E+02	3.87328E-01
152	ES8	Q416	5.58600E+02	2.84787E+02	2.64833E+02	4.73254E-01
153	ES8	Q422	3.88300E+02	2.84787E+02	9.35330E+01	2.40878E-01
154	ES8	Q431	2.47500E+01	1.77811E+02	-1.52881E+02	-8.11820E+00
155	ES8	Q432	2.07800E+01	1.77811E+02	-1.58840E+02	-8.42208E+00
156	ES8	Q436	4.43000E+00	1.77811E+02	-1.56851E+02	-7.55544E+00
157	ES8A	Q452	1.78900E+01	1.77700E+02	-1.73181E+02	-3.80928E+01
158	ES8A	Q481	2.51800E+01	1.77700E+02	-1.60010E+02	-9.04522E+00
159	ES8A	Q469	1.88800E+01	1.77700E+02	-1.52540E+02	-8.06280E+00
160	ES10	Q434	7.83000E+00	1.84873E+01	-1.58840E+02	-8.42208E+00
161	ES10	Q435	8.78000E+00	1.84873E+01	-1.08573E+01	-1.38108E+00
162	ES10	Q438	8.37000E+00	1.84873E+01	-9.70730E+00	-1.10581E+00
163	ES14	Q455	6.33000E+00	1.77700E+02	-1.01173E+01	-1.20876E+00
164	ES14	Q460	6.67000E+00	1.77700E+02	-1.71370E+02	-2.70727E+01
165	ES14	Q467	8.15000E+00	1.77700E+02	-1.71030E+02	-2.58417E+01
166	ES18	Q444	3.09000E+00	1.84873E+01	-1.89550E+02	-2.08037E+01
167	ES18	Q458	3.08000E+00	1.84873E+01	-1.53973E+01	-4.98294E+00
168	ES18	Q483	2.80000E+00	1.84873E+01	-1.54073E+01	-5.00237E+00
169	ES18	Q450	1.07800E+02	7.55494E+02	-1.55873E+01	-5.37493E+00
170	ES18	Q451	8.94300E+01	7.55494E+02	-6.47894E+02	-8.00829E+00
171	ES18	Q459	6.08300E+01	7.55494E+02	-6.66084E+02	-7.44788E+00
172	ES20	Q472	4.22000E+02	2.01500E+02	-6.74684E+02	-8.24870E+00
173	ES20	Q473	3.35000E+02	2.01500E+02	2.20500E+02	5.22511E-01
174	ES20	Q478	3.20300E+02	2.01500E+02	1.33500E+02	3.88507E-01
175	ES22	Q481	1.18300E+01	2.14035E+01	-1.18600E+02	-3.70901E-01
176	ES22	Q484	1.65100E+01	2.14035E+01	-9.57351E+00	-8.09257E-01
177	ES22	Q485	1.09000E+01	2.14035E+01	-4.89351E+00	-2.98397E-01
178	ES24	Q489	3.81700E+02	8.48374E+02	-1.05035E+01	-9.83625E-01
					3.83257E+01	4.11986E-02

179	ES24	Q480	8.83200E+02	8.45374E+02	3.78257E+01	4.28280E-02
180	ES24	Q480	9.50000E+02	8.45374E+02	1.04626E+02	1.10132E-01
181	ES24	Q880	6.25000E+02	8.45374E+02	-2.13474E+02	-3.50654E-01
182	ES24	T 53	6.68800E+02	8.45374E+02	-1.76774E+02	-2.84395E-01

AVERAGE DEVIATION 2.09539E+00  
 AVERAGE REL DEV -3.82953E+00  
 AVE ABS REL DEV 4.13689E+00  
 MAXIMUM DEVIATION 8.12710E+02 AT POINT 135  
 MAXIMUM REL DEV 3.90928E+01 AT POINT 158  
 ROOT MEAN SQUARE DEVIATION 1.07318E+00

CAUCHY CONVERGENCE OF SUM OF SQUARES. FRACTIONAL REDUCTION IN MINIMUM SUMSQ IS LESS THAN 5.000E-07

C. Output from the uncertainty propagation routine ERPROP  
 C. Zero in fourth column indicates benchmark (M8D only) fit.

TIME	DEPTH	UNCERTAINTY		
YRS	MICROMS	MICROMS		
1.000E+00	7.332791E+02	7.393943E+01	0.000000E+00	
2.000E+00	1.411601E+03	2.010527E+02	0.000000E+00	
5.000E+00	3.227600E+03	7.234831E+02	0.000000E+00	
1.000E+01	5.829428E+03	1.678392E+03	0.000000E+00	
2.000E+01	9.084351E+03	3.438128E+03	0.000000E+00	
5.000E+01	1.376238E+04	6.495665E+03	0.000000E+00	
1.000E+02	1.709013E+04	9.091291E+03	0.000000E+00	
2.000E+02	2.010962E+04	1.176257E+04	0.000000E+00	
3.000E+02	2.229156E+04	1.38387E+04	0.000000E+00	
5.000E+02	2.511629E+04	1.688513E+04	0.000000E+00	
1.000E+03	2.826119E+04	2.111937E+04	0.000000E+00	

C. Begin Sequential Evaluations. proceed in originally-generated order through the ESS, 1-32

PHASE 2 \*\* EVALUATING EXPERIMENT NUMBER: 1

ADDED VIRTUAL DATA POINT: [ V 1- 11111]  
 Y.E= 4.783800 81.92543

C. The iterations and pointwise comparisons appear here  
 C.

AVERAGE DEVIATION 2.09887E+00  
 AVERAGE REL DEV -3.80864E+00  
 AVE ABS REL DEV 4.11435E+00  
 MAXIMUM DEVIATION 8.12831E+02 AT POINT 135  
 MAXIMUM REL DEV 3.90935E+01 AT POINT 158  
 ROOT MEAN SQUARE DEVIATION 1.07020E+00

CAUCHY CONVERGENCE OF SUM OF SQUARES. FRACTIONAL REDUCTION IN MINIMUM SUMSQ IS LESS THAN 5.000E-07

TIME	DEPTH	UNCERTAINTY		
YRS	MICROMS	MICROMS		
1.000E+00	7.331759E+02	7.391483E+01	2.458717E-02	
2.000E+00	1.411383E+03	2.012343E+02	-1.815948E-01	
5.000E+00	3.227085E+03	7.247404E+02	-1.257203E+00	
1.000E+01	5.828497E+03	1.681752E+03	-3.358619E+00	
2.000E+01	9.082882E+03	3.445465E+03	-7.337156E+00	
5.000E+01	1.375963E+04	6.509928E+03	-1.426172E+01	
1.000E+02	1.708657E+04	9.111385E+03	-2.009888E+01	
2.000E+02	2.010517E+04	1.178880E+04	-2.603418E+01	

3.000E+02 2.22848E+04 1.387051E+04 -3.063885E+01  
 5.000E+02 2.511038E+04 1.872204E+04 -3.890820E+01  
 1.000E+03 2.925388E+04 2.116597E+04 -4.680742E+01

PHASE 2 \*\* EVALUATING EXPERIMENT NUMBER: 2

ADDED VIRTUAL DATA POINT: [ V 2- 21111]  
 Y,E= 1327.772 285.7686

C.  
 C. This continues to virtual data point [ V 32- 22222]  
 C.  
 C.

PHASE 2 \*\* EVALUATING EXPERIMENT NUMBER: 32

ADDED VIRTUAL DATA POINT: [ V 32- 22222]  
 Y,E= 7420.588 278.1801

NEGLECTIBLE CHANGE IN SUM OF SQUARES

AFTER 1 ITERATIONS  
 THE MINIMIZING VALUES OF THE PARAMETERS ARE:  
 8.0608428E+10 4.8725601E+02 1.6112378E+04

WITH THE FOLLOWING STD. DEVIATIONS:  
 3.0414789E+10 1.8115343E+02 8.1524707E+02

THE SUM OF SQUARES, VARIANCE AND SAMPLE STD. DEVIATION FOR THIS FIT ARE 2.06158E+02 1.14532E+00 1.07020E+00

2.000E+00	1.411548E+03	4.715290E+01	1.538998E+02
5.000E+00	3.227325E+03	1.211424E+02	6.023407E+02
1.000E+01	5.628716E+03	2.908677E+02	1.3875225E+03
2.000E+01	9.082798E+03	6.447813E+02	2.783338E+03
5.000E+01	1.375934E+04	1.305315E+03	5.190349E+03
1.000E+02	1.708586E+04	1.88223E+03	7.205088E+03
2.000E+02	2.010388E+04	2.485871E+03	9.268888E+03
3.000E+02	2.28488E+04	2.878818E+03	1.086305E+04
5.000E+02	2.510820E+04	3.840922E+03	1.304421E+04
1.000E+03	2.925088E+04	4.684534E+03	1.643483E+04

C. Now the ESS data is reordered by greatest-to-least uncertainty reduction

C. Point Delta Uncert. Delta Unc./BMark Unc.

32- 22222	1.086305E+04	7.849100E-01
24- 22212	1.078574E+04	7.800467E-01
30- 21222	1.068224E+04	7.718457E-01
22- 21212	1.061622E+04	7.670755E-01
28- 22122	2.811241E+03	1.888753E-01
20- 22112	2.462118E+03	1.778004E-01
28- 21122	2.237070E+03	1.616386E-01
18- 21112	2.14595E+03	1.527801E-01
12- 22121	3.985605E+02	2.887626E-02
4- 22111	3.806420E+02	2.750334E-02

10-	21121	3.24887E+02	2.347484E-02
2-	21111	3.002852E+02	2.189711E-02
31-	12222	2.953808E+02	2.134275E-02
23-	12212	2.078959E+02	1.501430E-02
28-	11222	1.266318E+02	9.148788E-03
21-	11212	1.142002E+02	8.251539E-03
8-	22211	3.544922E-01	2.581384E-05
16-	22221	-4.587500E-01	-3.386955E-05
14-	21221	-1.598809E+00	-1.155788E-04
6-	21211	-1.644531E+00	-1.188257E-04
15-	12221	-2.449023E+01	-1.789543E-03
13-	11221	-2.829888E+01	-2.044592E-03
27-	12122	-2.833887E+01	-2.047626E-03
25-	11122	-2.861328E+01	-2.087454E-03
18-	12112	-2.878492E+01	-2.080578E-03
3-	12111	-2.978320E+01	-2.151980E-03
17-	11112	-3.009277E+01	-2.174354E-03
11-	12121	-3.048828E+01	-2.202932E-03
9-	11121	-3.081718E+01	-2.212248E-03
1-	11111	-3.083985E+01	-2.213889E-03
7-	12211	-3.549219E+01	-2.584489E-03
5-	11211	-3.737402E+01	-2.700481E-03

C. In phase 3 the previously ordered ESS is accumulated hence "added" versus "evaluated"  
C.

PHASE 3 \*\*\* ADDING EXPERIMENT NUMBER: 1  
ADDED VIRTUAL DATA POINT: [ V 32- 22222 ]  
Y,E= 7420.582 276.1801

1.000E+00	7.332707E+02	2.819351E+01	4.574592E+01
2.000E+00	1.411548E+03	4.715280E+01	1.539001E+02
5.000E+00	3.227324E+03	1.211432E+02	8.023398E+02
1.000E+01	5.628714E+03	2.908890E+02	1.387523E+03
2.000E+01	9.082793E+03	6.447934E+02	2.789334E+03
5.000E+01	1.375933E+04	1.305322E+03	5.180342E+03
1.000E+02	1.708584E+04	1.888228E+03	7.205083E+03
2.000E+02	2.010398E+04	2.485881E+03	9.286887E+03
3.000E+02	2.228486E+04	2.978828E+03	1.086304E+04
5.000E+02	2.510817E+04	3.840937E+03	1.304420E+04
1.000E+03	2.925084E+04	4.884550E+03	1.643481E+04

PHASE 3 \*\*\* ADDING EXPERIMENT NUMBER: 2  
ADDED VIRTUAL DATA POINT: [ V 24- 22212 ]  
Y,E= 7420.580 288.9709

878787887  
CAUCHY CONVERGENCE OF SUM OF SQUARES. FRACTIONAL REDUCTION IN MINIMUM SUMSQ IS LESS THAN 5.000E-07

PHASE 3 \*\*\* ADDING EXPERIMENT NUMBER: 32  
ADDED VIRTUAL DATA POINT: [ V 5- 11211 ]  
Y,E= 82.71986 117.0323

NEGLECTIBLE CHANGE IN SUM OF SQUARES  
AFTER 1 ITERATIONS

THE MINIMIZING VALUES OF THE PARAMETERS ARE:

8.068587E+10 4.6758340E+02 1.6110374E+04  
 WITH THE FOLLOWING STD. DEVIATIONS:  
 1.0923619E+10 6.4830513E+01 4.3218503E+02

THE SUM OF SQUARES, VARIANCE AND SAMPLE STD. DEVIATION FOR THIS FIT ARE 2.06158E+02 9.77054E-01 9.88460E-01

.....

AVERAGE DEVIATION 1.81560E+00  
 AVERAGE REL DEV -3.25693E+00  
 AVE ABS REL DEV 3.51837E+00  
 MAXIMUM DEVIATION 8.12882E+02 AT POINT 135  
 MAXIMUM REL DEV 3.90937E+01 AT POINT 156  
 ROOT MEAN SQUARE DEVIATION 9.88460E-01

CAUCHY CONVERGENCE OF SUM OF SQUARES. FRACTIONAL REDUCTION IN MINIMUM SUMSQ IS LESS THAN 5.000E-07

TIME	DEPTH	UNCERTAINTY
YRS	MICROMS	MICROMS
1- 000E+00	7.331828E+02	8.987084E+00
2- 000E+00	1.411375E+03	1.884575E+01
5- 000E+00	3.227074E+03	5.954769E+01
1- 000E+01	5.628485E+03	1.398898E+02
2- 000E+01	9.082808E+03	2.938950E+02
5- 000E+01	1.375985E+04	5.885852E+02
1- 000E+02	1.708707E+04	8.079352E+02
2- 000E+02	2.010588E+04	1.055910E+03
5- 000E+02	2.228732E+04	1.249933E+03
1- 000E+03	2.925538E+04	1.518995E+03
2- 2222	1.086304E+04	1.935039E+03
24- 2212	1.131993E+04	7.849082E-01
30- 2122	1.149219E+04	8.179219E-01
22- 2121	1.158825E+04	8.303883E-01
28- 2212	1.165575E+04	8.373095E-01
20- 2212	1.170498E+04	8.421863E-01
26- 2112	1.174144E+04	8.457439E-01
18- 2211	1.177105E+04	8.483779E-01
12- 2211	1.178242E+04	8.505175E-01
4- 2211	1.178848E+04	8.513389E-01
2- 2111	1.179595E+04	8.517753E-01
31- 1222	1.180579E+04	8.523167E-01
23- 1221	1.180631E+04	8.530277E-01
29- 1122	1.181358E+04	8.532102E-01
21- 1121	1.181833E+04	8.535908E-01
8- 2211	1.182405E+04	8.539899E-01
16- 2221	1.182524E+04	8.543470E-01
14- 2121	1.182427E+04	8.54370E-01
15- 1211	1.182427E+04	8.54370E-01
13- 1121	1.182427E+04	8.54370E-01
27- 1212	1.182427E+04	8.54370E-01
25- 1112	1.182427E+04	8.54370E-01
19- 1211	1.182427E+04	8.54370E-01
3- 1211	1.182427E+04	8.54370E-01
17- 1112	1.182427E+04	8.54370E-01

TIME YRS	DEPTH MICROMS	UNCERTAINTY MICROMS
11- 12121	1.257747E+04	9.087858E-01
9- 11121	1.258051E+04	9.080051E-01
1- 11111	1.258390E+04	9.082500E-01
7- 12211	1.258680E+04	9.094667E-01
5- 11211	1.258988E+04	9.098824E-01
* * * * * JADD * * * * *		
1- 12121	7.332684E+02	1.920632E+01
2- 000E+00	1.411543E+03	2.850878E+01
5- 000E+00	3.227324E+03	6.160953E+01
1- 000E+01	5.628732E+03	1.512225E+02
2- 000E+01	9.082851E+03	3.512112E+02
5- 000E+01	1.375947E+04	5.692982E+02
1- 000E+02	1.708604E+04	8.075104E+02
2- 000E+02	2.010423E+04	1.055301E+03
3- 000E+02	2.228518E+04	1.249218E+03
5- 000E+02	2.510858E+04	1.516004E+03
1- 000E+03	2.925135E+04	1.933671E+03
17- 22211	4.913547E+02	1.650598E-01
18- 22211	5.716572E+02	1.920357E-01
18- 21221	6.071611E+02	2.039824E-01
1- 22212	1.207370E+03	4.055886E-01
18- 21211	1.233710E+03	4.144377E-01
2- 21222	1.485111E+03	4.988904E-01
3- 21212	1.633325E+03	5.486798E-01
4- 23122	1.839454E+03	5.507385E-01
5- 22112	1.844844E+03	5.525223E-01
6- 21122	1.849941E+03	5.542613E-01
7- 21112	1.854635E+03	5.558383E-01
20- 12221	1.858078E+03	5.569978E-01
30- 12211	1.861498E+03	5.581438E-01
21- 11221	1.864896E+03	5.592852E-01
31- 11211	1.868277E+03	5.604210E-01
9- 22111	1.874405E+03	5.624797E-01
8- 22121	1.880247E+03	5.644421E-01
10- 21121	1.885242E+03	5.661200E-01
11- 21111	1.889924E+03	5.676929E-01
12- 12222	1.893355E+03	5.688455E-01
13- 12212	1.896715E+03	5.699741E-01
14- 11222	1.899955E+03	5.710759E-01
15- 11212	1.703232E+03	5.721634E-01
24- 12112	1.708352E+03	5.732115E-01
28- 11111	1.708454E+03	5.742536E-01
28- 11121	1.712535E+03	5.752694E-01
25- 12111	1.715592E+03	5.763155E-01
22- 12122	1.718628E+03	5.773352E-01
27- 12121	1.721648E+03	5.783497E-01
26- 11112	1.724634E+03	5.793528E-01
23- 11122	1.727610E+03	5.803527E-01
* * * * * JADD * * * * *		
1- 000E+00	7.332684E+02	8.178672E+00
2- 000E+00	1.411543E+03	1.810906E+01
5- 000E+00	3.227324E+03	6.060882E+01
1- 000E+01	5.628732E+03	1.422246E+02
2- 000E+01	9.082853E+03	2.988163E+02





10- 1212	5.042418E+01	3.753198E-02
11- 11222	8.372473E+01	3.988866E-02
12- 11212	8.705948E+01	4.247078E-02
19- 11121	8.028532E+01	4.487203E-02
23- 12111	8.347846E+01	4.724638E-02
24- 12121	8.668405E+01	4.861228E-02
22- 11122	8.978736E+01	5.195193E-02
20- 11111	7.282334E+01	5.427867E-02
17- 11112	7.603174E+01	5.659233E-02
13- 12221	7.812524E+01	5.889490E-02
18- 12112	8.235342E+01	6.122328E-02
15- 12211	8.528826E+01	6.348815E-02
16- 11211	8.823401E+01	6.567478E-02
14- 11221	9.132251E+01	6.797364E-02
21- 12122	9.428259E+01	7.018416E-02

\* \* \* \* \* JADO \* \* \* \* \*  
 \* \* \* \* \* 23 \* \* \* \* \*